Supplementary File
"Improved Estimates of Child Malnutrition Trends in Bangladesh Using Remote-Sensed Data"

In this supplementary file, we provide detailed descriptions of the direct estimates, remote-sensed data, and detailed results of trend estimates at different levels of disaggregation. Section S.1 discusses how the direct estimates are obtain and what are the inputs for the developed models. Section S.2 illustrate various remote-sense data and their association with child undernutrition over the space and time.

Sections S.3 and S.4 provide exhaustive information about the results, discussing the trend estimation of child undernutrition at various levels of aggregation, to complement the results given in the main manuscript. Information related to posterior predictive check are shown in Section S.5. Finally, Gaussian and binomial based models are compared to understand why the binomial models are chosen when the time-series models are developed at the sub-district level in Section S.6. These detail information in tabular and graphical format are provided to aid researchers interested in additional details necessary for replicating our work.

S.1 Direct Estimates

As a first step, direct estimates of stunting along with their variances and the number of stunted children are calculated from each survey year's unit-level data using the standard design-based estimator (denoted by DIR). This direct estimator uses the survey sampling weights to account for the sampling design and differential non-response. The survey sampling weights given in the survey datasets are normalized to equalize the total number of unweighted cases to the total number of weighted cases at the national level. Suppose y is the response variable of interest, s_{it} is the set of under-five children belongs to sub-districts i $(i = 1, .., 544)$ for which y is observed in year t $(t = 1, .., 19)$, and w_{ikt} is the corresponding normalized survey weight for k^{th} children. The number of children observed in domain i at the survey year t is defined by n_{it}. The sampling variance $var(\hat{Y}_{it})$ can be estimated considering the sampling design and sampling weight following the Demographic Health Survey (DHS) standard (Appendix in NIPORT and ICF (2020)). However, it provided zero variances for many domains though they had reasonable sample size and so only the sampling weights are considered in the calculation of sampling variances. The normalized weights are utilized to calculate the proportions and their sampling variances as below.

$$\hat{y}_{it} = \frac{\sum_{k \in s_{it}} w_{ikt} y_{ikt}}{\sum_{k \in s_{it}} w_{ikt}}$$

$$var(\hat{y}_{it}) = \frac{1}{n_{it}(n_{it} - 1)} \sum_{k \in s_{it}} w_{ikt} (y_{ikt} - \hat{y}_{it})^2$$

The estimated stunting prevalence with their estimated variances computed for the six surveys 1999-2000, 2004, 2007, 2011, 2014, and 2017-18 are used as the direct estimates. Since direct estimates are considered as annual in frequency, survey years are referred to as 2000, 2004, 2007, 2011, 2013, 2014, and 2018 in the time-series model. The number of stunted children along with the total number of sampled children in each of the considered domains are used for developing multilevel time-series models assuming the response variable follows a binomial distribution. The stunting prevalence estimated with and without consideration of sampling weight shown in Figure S.1.1 indicates estimates are unbiased with some differences. However, the relationship between the observed sample size and effective (weighted) sample size shown in Figure S.1.1 indicates the sampling design is non-informative. The weighted number of stunted children and the effective sample sizes are used in the development of multilevel time series models to account for the sampling design in the model development.

Table S.1.1 shows the distribution of sampled number of children for the observed sub-districts in the six survey years. Summary statistics of the design-based direct estimates of stunting and the associated standard errors are also given. The values of n under "NA" indicates the uncovered sub-districts in the survey years. Overall 46 domains had zero stunting estimate, while 2 domains had a stunting value of 1. There were more than 100 sub-districts with 5 or fewer children for which the stunting levels and standard errors are too noisy. On the other hand, the statistics at the district level shown in Table S.1.2 reveals less sparsity in the direct estimates of stunting and their standard errors. A few districts had sample size less than 10 and so there are no domains have zero or one stunting level.

	Statistic	Year	Min	Q1	Q2	Mean	Q3	Max	NA
1	n	2000	2	12	17	20	23	86	269
2	n	2004	5	14	18	22	25	143	266
3	n	2007	4	12	16	19	23	64	268
4	n	2011	2	11	16	20	26	188	164
5	n	2014	1	10	15	19	24	173	177
6	n	2018	1	11	16	20	25	128	150
7	Estimate	2000	0	0.38	0.5	0.49	0.61	0.9	269
8	Estimate	2004	0	0.37	0.48	0.48	0.59	0.88	266
9	Estimate	2007	0	0.3	0.41	0.41	0.53	0.86	268
10	Estimate	2011	0	0.29	0.4	0.39	0.5	1	164
11	Estimate	2014	0	0.23	0.33	0.34	0.45	1	177
12	Estimate	2018	0	0.21	0.29	0.31	0.4	0.83	150
13	SE	2000	0	0.1	0.11	0.12	0.14	0.29	269
14	SE	2004	0	0.09	0.11	0.11	0.13	0.24	266
15	SE	2007	0	0.1	0.12	0.12	0.14	0.29	268
16	SE	2011	0	0.09	0.11	0.12	0.14	0.5	164
17	SE	2014	0	0.09	0.11	0.12	0.14	0.29	178
18	SE	2018	0	0.08	0.11	0.11	0.14	0.5	151

Table S.1.1: Distribution of the number of observed (unweighted) children (n), the direct estimate of stunting (est) and the corresponding standard error (se) for the 544 sub-districts in Bangladesh Demographic Health Surveys 1999-2000, 2004, 2007, 2011, 2014, 2017-18.

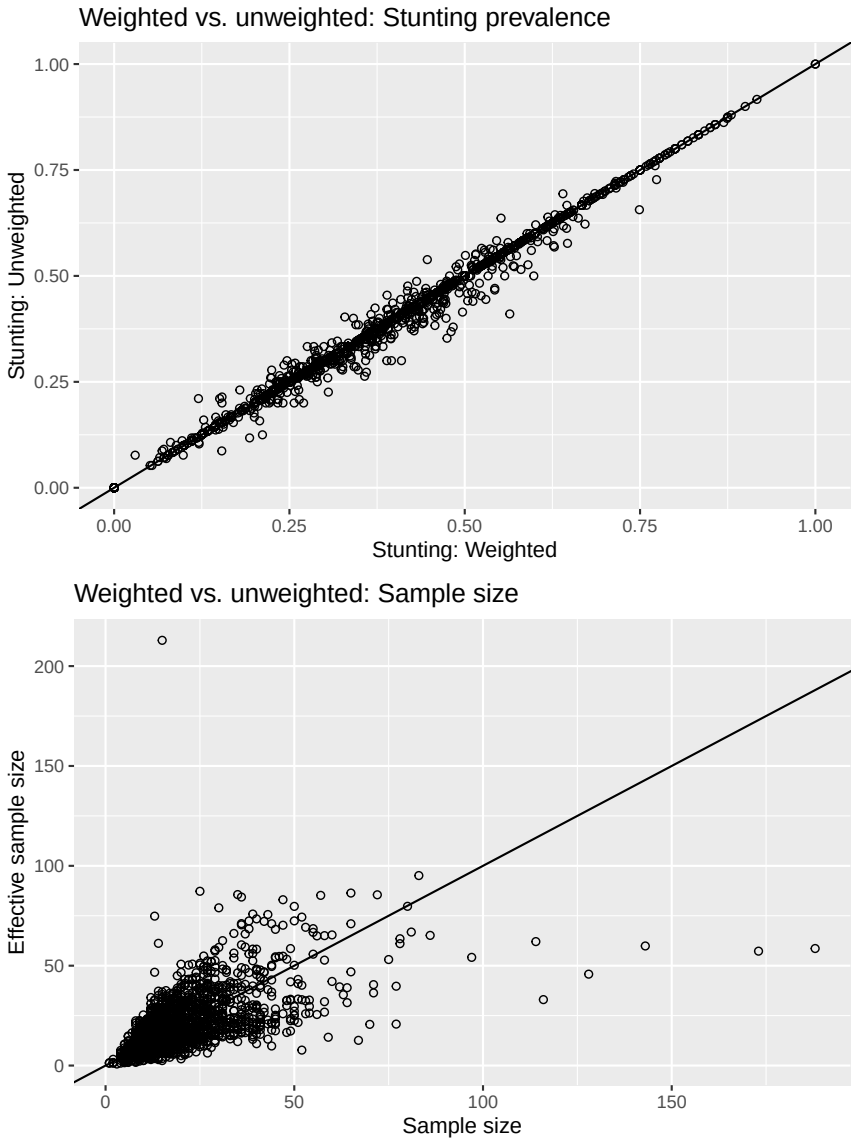


Figure S.1.1: Stunting prevalence and sample size estimated with and without sampling weight.

	Statistic	Year	Min	Q1	Q2	Mean	Q3	Max	NA
1	n	2000	17	55	70	85	93	247	
2	n	2004	18	48	80	95	105	413	1
3	n	2007	5	49	66	85	92	349	2
4	n	2011	15	64	92	119	164	538	
5	n	2014	7	49	78	109	141	489	
6	n	2018	23	61	104	123	150	433	
7	Estimate	2000	0.32	0.45	0.5	0.5	0.55	0.71	
8	Estimate	2004	0.21	0.41	0.49	0.48	0.55	0.74	1
9	Estimate	2007	0.18	0.36	0.44	0.43	0.5	0.6	2
10	Estimate	2011	0.23	0.35	0.39	0.41	0.46	0.69	
11	Estimate	2014	0.14	0.29	0.35	0.35	0.4	0.64	
12	Estimate	2018	0.09	0.25	0.31	0.3	0.37	0.45	
13	SE	2000	0.03	0.05	0.06	0.06	0.07	0.13	
14	SE	2004	0.02	0.04	0.06	0.06	0.07	0.11	1
15	SE	2007	0.03	0.05	0.06	0.07	0.07	0.2	2
16	SE	2011	0.02	0.04	0.05	0.06	0.06	0.12	
17	SE	2014	0.02	0.04	0.05	0.06	0.07	0.18	
18	SE	2018	0.02	0.04	0.05	0.05	0.06	0.1	

Table S.1.2: Distribution of the number of observed (unweighted) children (n), the direct estimate of stunting (est) and the corresponding standard error (se) for the 64 districts in Bangladesh Demographic Health Surveys 1999-2000, 2004, 2007, 2011, 2014, 2017-18.

S.2 Remote-sensed Data

In this study, we have used night-time light intensity data as local-level socio-economic indicators and some environmental variables like vegetation index, land surface temperature and rainfall (precipitation). The sub-district level stunting prevalence is found negatively and positively associated with NTL intensity and total annual rainfall. Figures S.2.2 and S.2.3 show how the stunting level is correlated with the considered remote-sensed data. Vegetation condition index (VCI), temperature condition index (TCI), and precipitation condition index (PCI) are also calculated following (Du et al., 2013) using the remote-sensed data of NDVI, LST, and rainfall. Figures S.2.4 and S.2.5 show that both district and sub-district level VCI and PCI are negatively and positively correlated respectively with the sub-district level stunting prevalence.

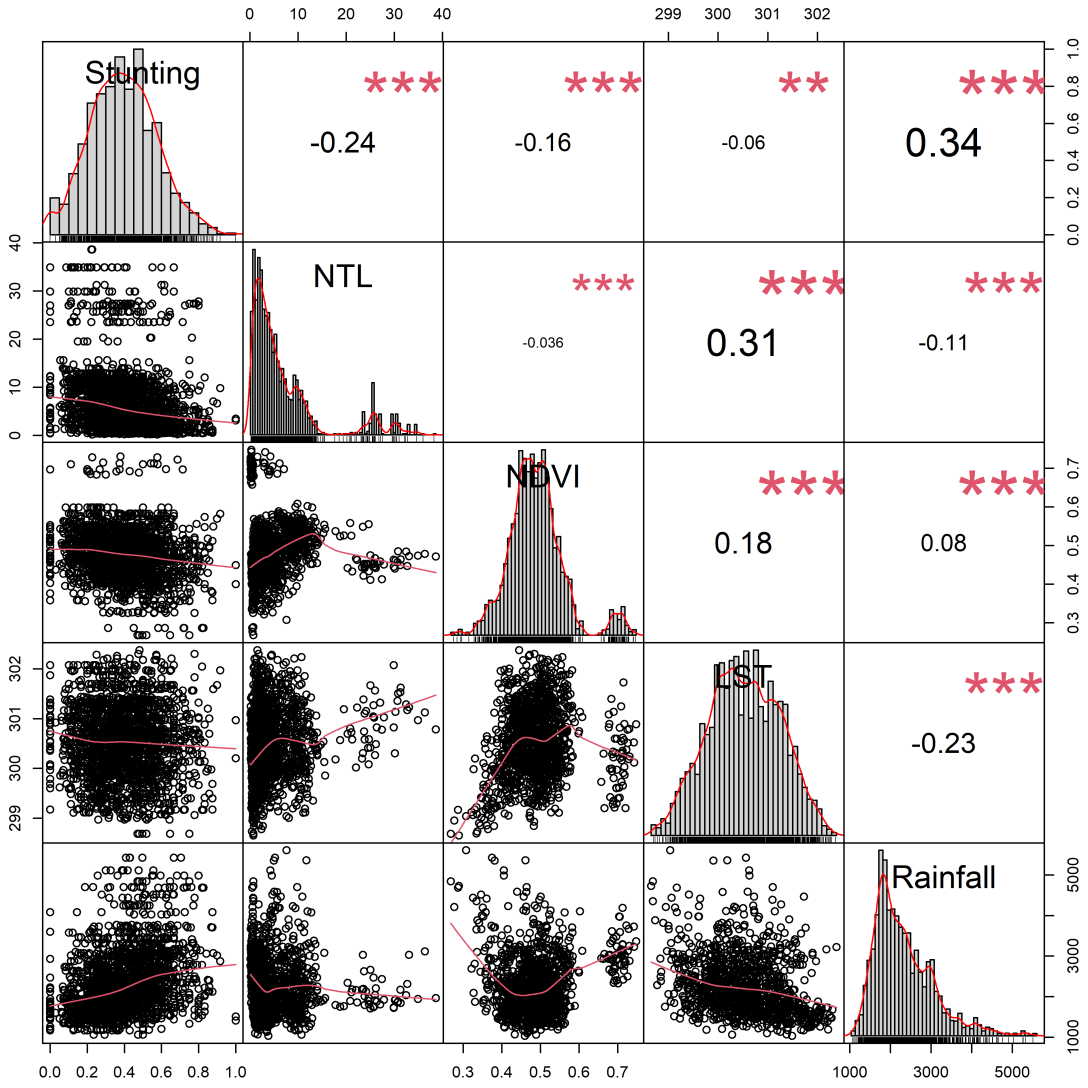


Figure S.2.2: Correlation of sub-district level stunting prevalence with district level NTL, mean NDVI, mean LST, and total rainfall.

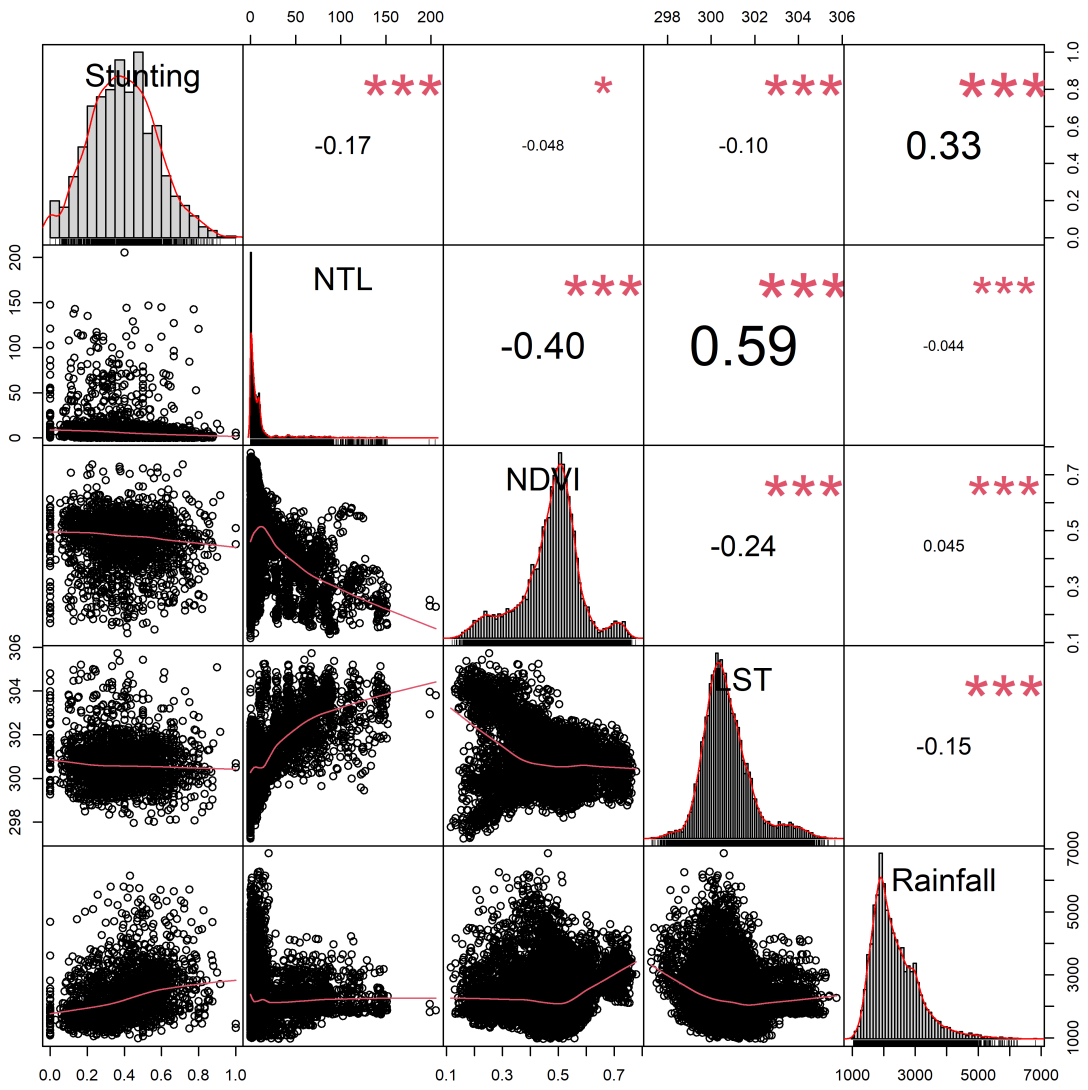


Figure S.2.3: Correlation of sub-district level stunting prevalence with sub-district level NTL, mean NDVI, mean LST, and total rainfall.

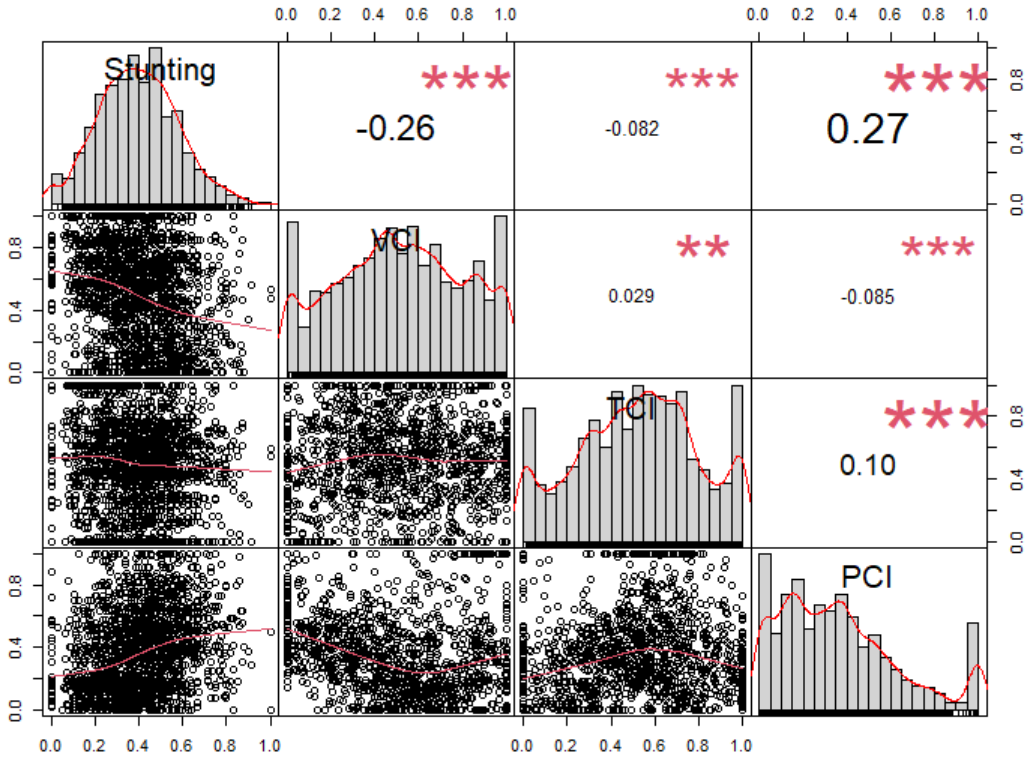


Figure S.2.4: Correlation of sub-district level stunting prevalence with district level VCI, TCI and PCI.

S.2.1 Night-time light data

Figure S.2.8 shows the change in the district-level night-time light intensity at the survey time points over the reference time period 2000-2018, while the same is shown at sub-district level in Figure S.2.9 along the stunting prevalence at the corresponding level. Though changes are clear at the district-level, the pattern is not consistent at the sub-district level. Even the highest amount of NTL is not found in the sub-districts under Dhaka district. These inconsistencies can be due to very small areas (raster) of the sub-districts in the capital city part of Dhaka district. The NTL trends at district and sub-district level over the whole reference period 2000-2018 shown in Figures S.2.6 and S.2.7 also shows that trends at district level is consistent compared to sub-district level. Also, the correlation between NTL and stunting is higher at district level than that at the sub-district level. The negative correlation between stunting and NTL exists mainly in the central (Dhaka Division) and north-eastern (Sylhet and Mymensingh divisions) parts of the country. The higher intensity level relates to lower stunting in Dhaka, Gazipur and Narayanganj district or lower intensity related to higher stunting level in Netroka, Sunamgonj and Sylhet districts. So the district level NTL data have been used in the model development rather than the sub-district level.

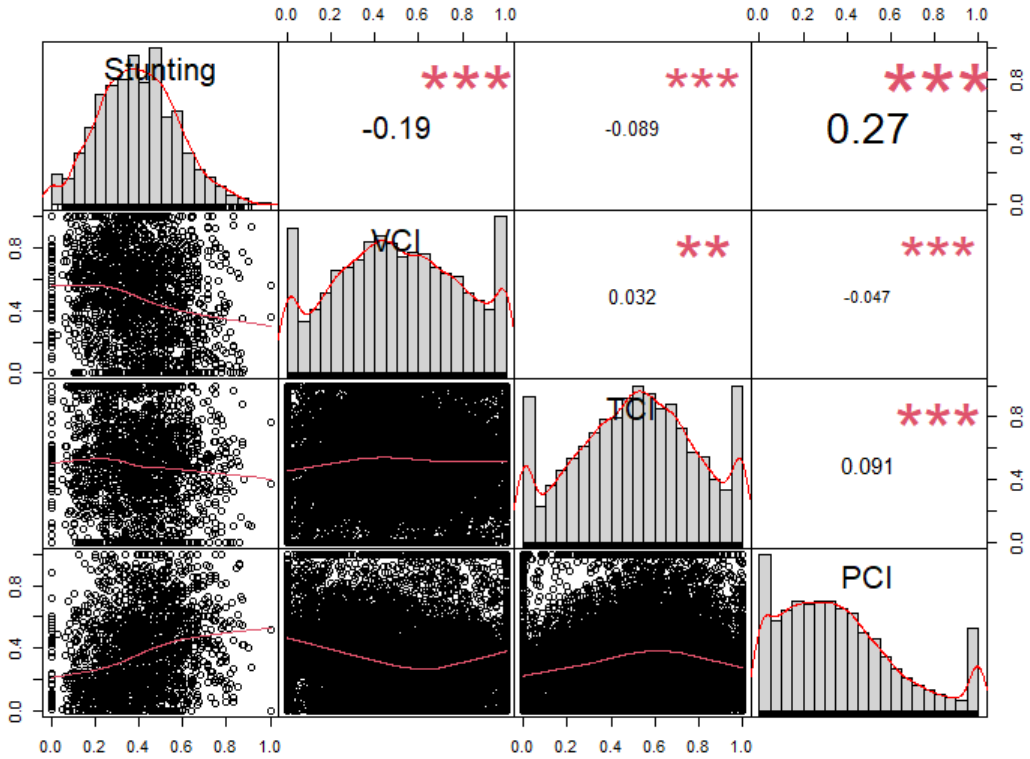


Figure S.2.5: Correlation of sub-district level stunting prevalence with sub-district level VCI, TCI and PCI.

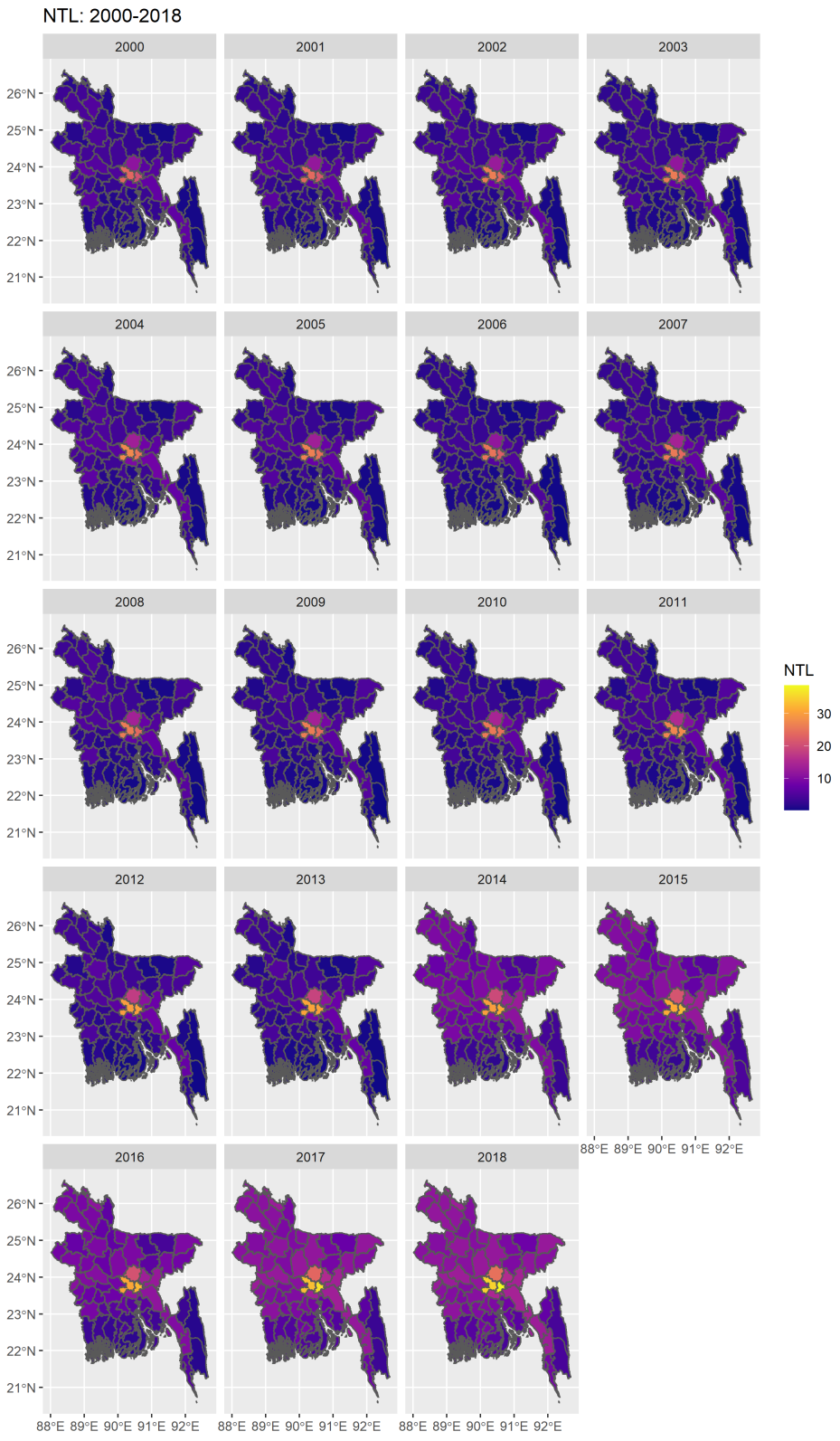


Figure S.2.6: District level annual night-time light intensity during 2000-2018.

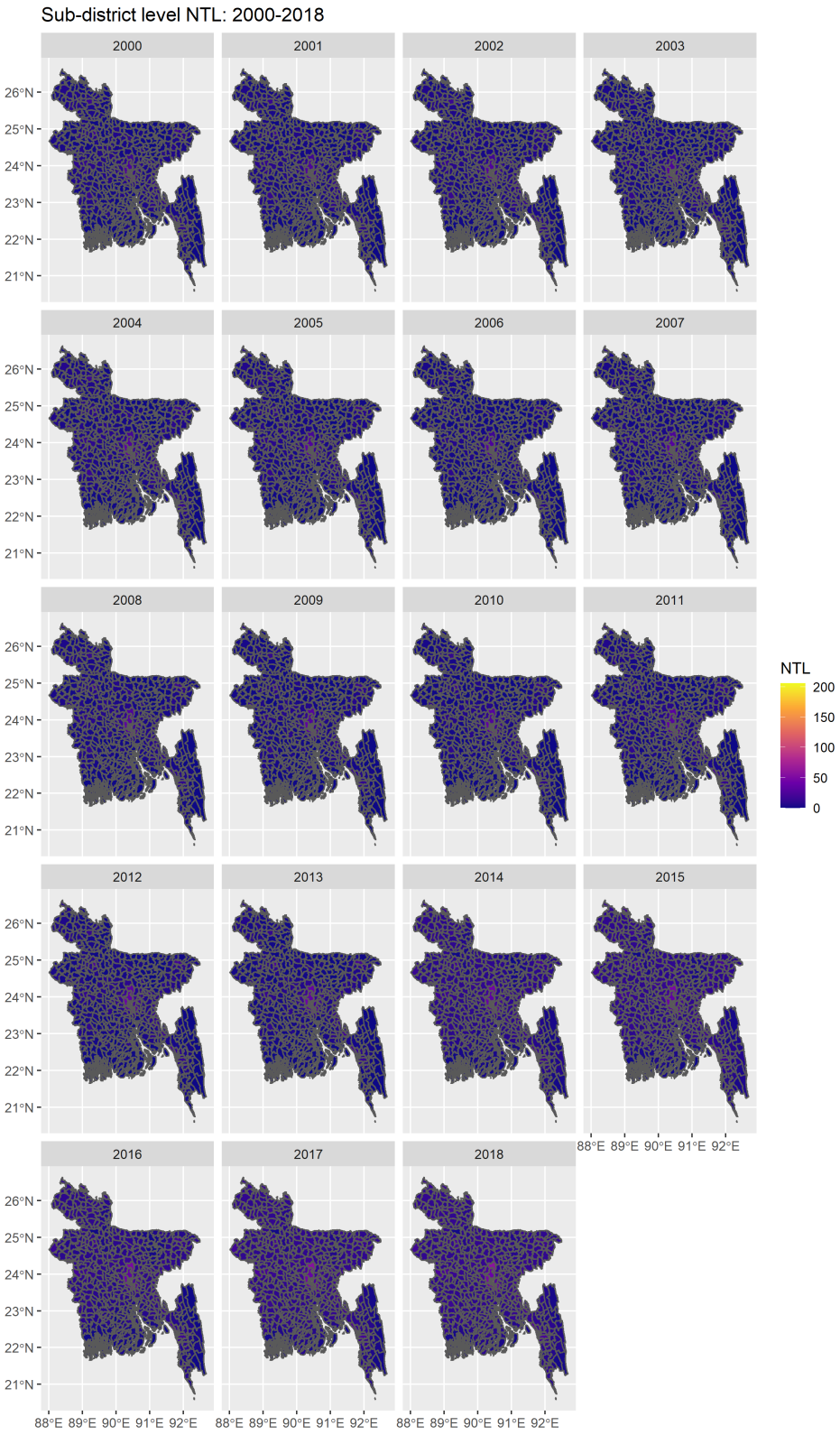


Figure S.2.7: Sub-district level night-time light intensity in survey years 2000, 2004, 2007, 2011, 2014 and 2018.

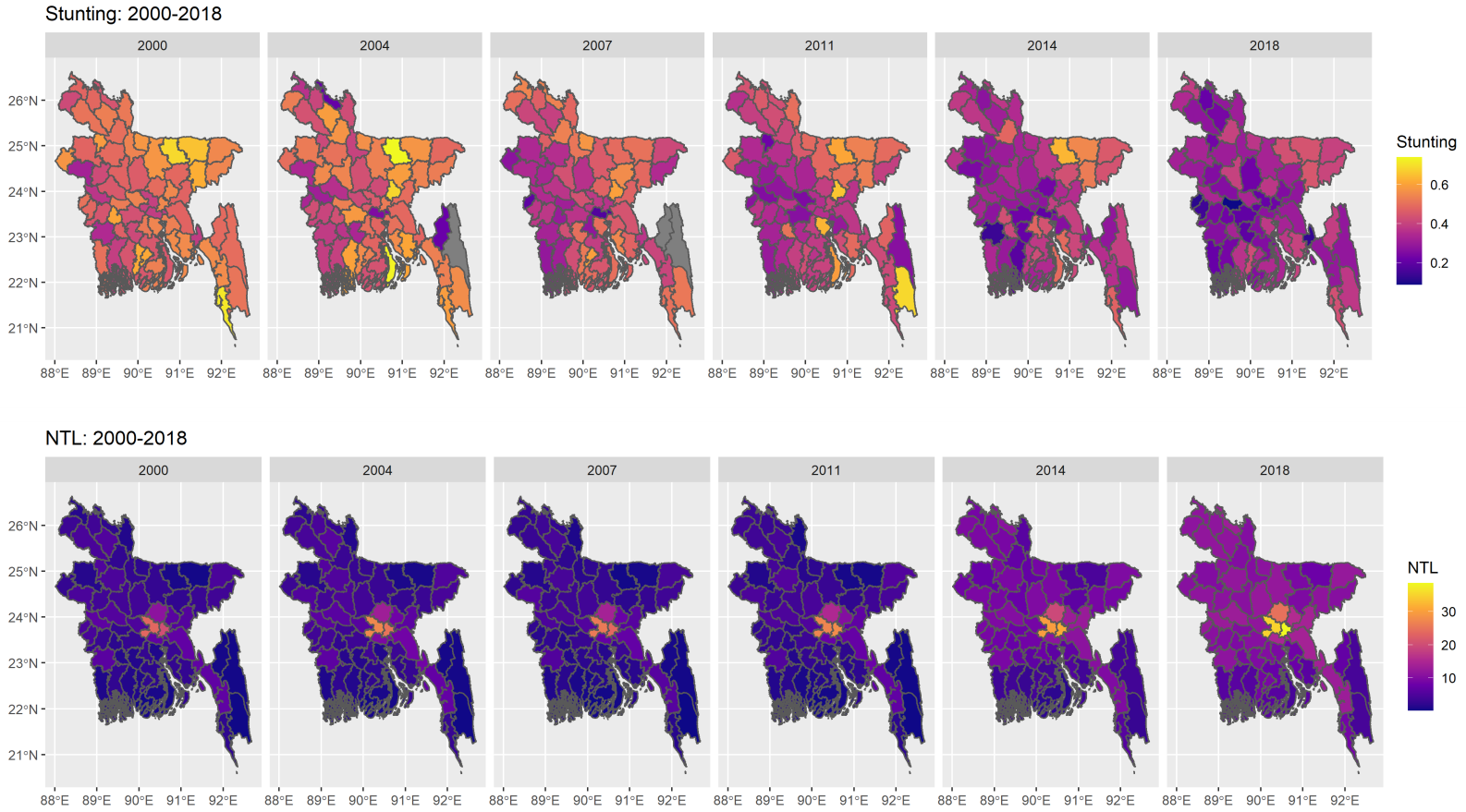


Figure S.2.8: District level night-time light (NTL) intensity and stunting prevalence in survey years 2000, 2004, 2007, 2011, 2014 and 2018.

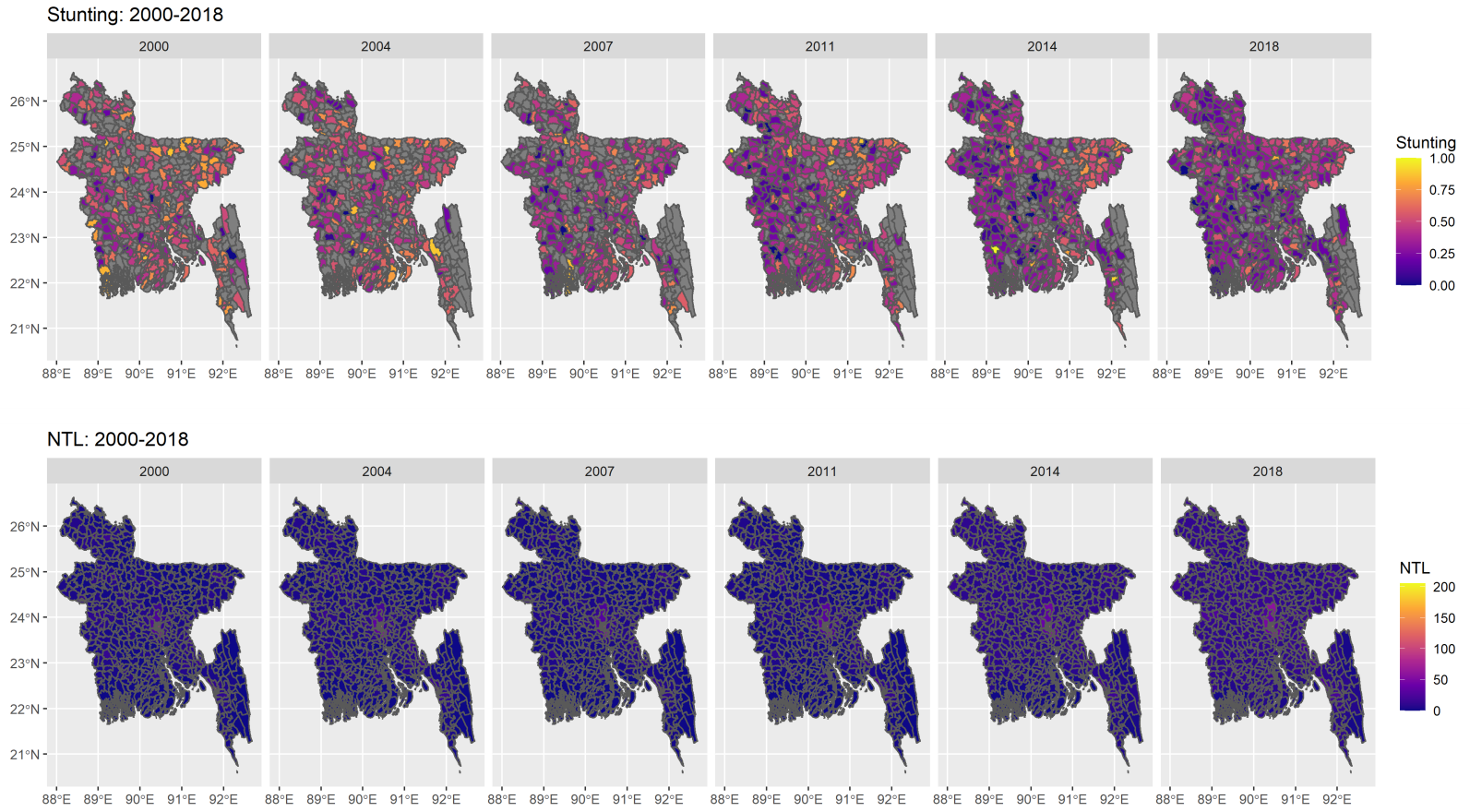


Figure S.2.9: Sub-district level night-time light (NTL) intensity and stunting prevalence in survey years 2000, 2004, 2007, 2011, 2014 and 2018.

S.2.2 Normalized Difference Vegetation Index (NDVI) and Vegetation Condition Index (VCI)

The normalized difference vegetation index (NDVI), which is derived from remote-sensing (satellite) data, is closely linked to drought conditions. To determine the density of green on a patch of land, the distinct colors (wavelengths) of visible and near-infrared sunlight reflected by the plants are observed. The NDVI helps to differentiate vegetation from other types of land cover (artificial) and determine its overall state. It also allows to define and visualize vegetated areas on the map as well as detect abnormal changes in the growth process. For vegetation regions, the weather-related NDVI changes are smaller than the ecosystem related one and the drought impacts on vegetation cannot be easily detected from NDVI data directly. The vegetation condition index (VCI) developed in Kogan (1995) is to control local differences in ecosystem productivity. The VCI compares the current NDVI to the range of NDVI values observed in the same period. The VCI is expressed in percentage of the range of NDVI values and gives an idea where the observed value is situated between the extreme values (minimum and maximum) in the previous years. The values of VCI is calculated as

$$VCI_{dt} = \frac{\text{NDVI}_{dt} - \text{NDVI}^{(d)}_{\text{min}}}{\text{NDVI}^{(d)}_{\text{max}} - \text{NDVI}^{(d)}_{\text{min}}} \tag{1}$$

where NDVI_{dt} is the value for domain d in year t, $NDVI^{(d)}_{max}$ and $NDVI^{(d)}_{min}$ are maximum and minimum values for domain d during the period 2000-2018. The range of VCI is from 0 (if NDVI_{dt} equals to $\text{NDVI}^{(d)}_{\text{min}}$) to 1 (if NDVI_{dt} equals to $\text{NDVI}^{(d)}_{\text{max}}$), corresponding to the changes in vegetation condition from extremely unfavorable to optimal. In case of an extremely dry month with the lowest NDVI value for a reference period and a place, the vegetation condition is poor and the VCI is close or equal to 0, while the VCI is close or equal to 1 indicates at optimal conditions of vegetation (Jain et al., 2009). Since we are studying using annual data, we calculated annual VCI values for each of the districts or sub-districts during 2000–2018 (note that NDVI data are available from February 2000 in MODIS).

Figures S.2.10 and S.2.11 shows the spatial distribution of NDVI values at the district and sub-district levels respectively. Both the Figures show that the change is very slow over the 19 years period. However, it shows that some districts like Sunamganj, Netrokona, Kishoregonj (wet land areas), Khulna and Shatkhira (Mangrove areas) have lower values of NDVI. To understand the change in the vegetation of a particular district over a time period, the VCI score provides a good understanding at which year or month the vegetation was low and high compared to the corresponding range of NDVI. Figures S.2.12 and S.2.13 shows how the VCI values over the time period compared to minimum and maximum value of NDVI. For Sunamgonj district, as for example, the minimum NDVI was in 2004 (which may indicate maximum time was under water) and maximum was in 2018 (which may indicate minimum time was under water). The time series of VCI values at both district and sub-district level shows the VCI values increases from the initial point to the end of the time-period. But it is clear that in Chittagong hill tracts area, the VCI values going down at the end of the time-period.

Though the NDVI values does not change substantially, the distribution at the sub-district

level in Figure S.2.11 shows that the south-eastern part including the Chittagong Hill Tracts areas have the highest level of NDVI values over the whole time period. On the other hand, the mean NDVI values are found lowest in the areas close to the four major river systems: the Brahmaputra-Jamuna flows from the north, the Ganges-Padma flows from the mid-western part, the Surma-Meghna flows from the north-eastern part and the Chittagong Region river system in which way the whole river system meets with the Bay of Bengal. The comparison of NDVI distribution at district level with the distribution of stunting prevalence doe not show any particularly pattern. However, a general pattern between the stunting and VCI distribution is that the stunting prevalence decreased and VCI values increased over the time period. However, this negative correlation is not evident statistically.

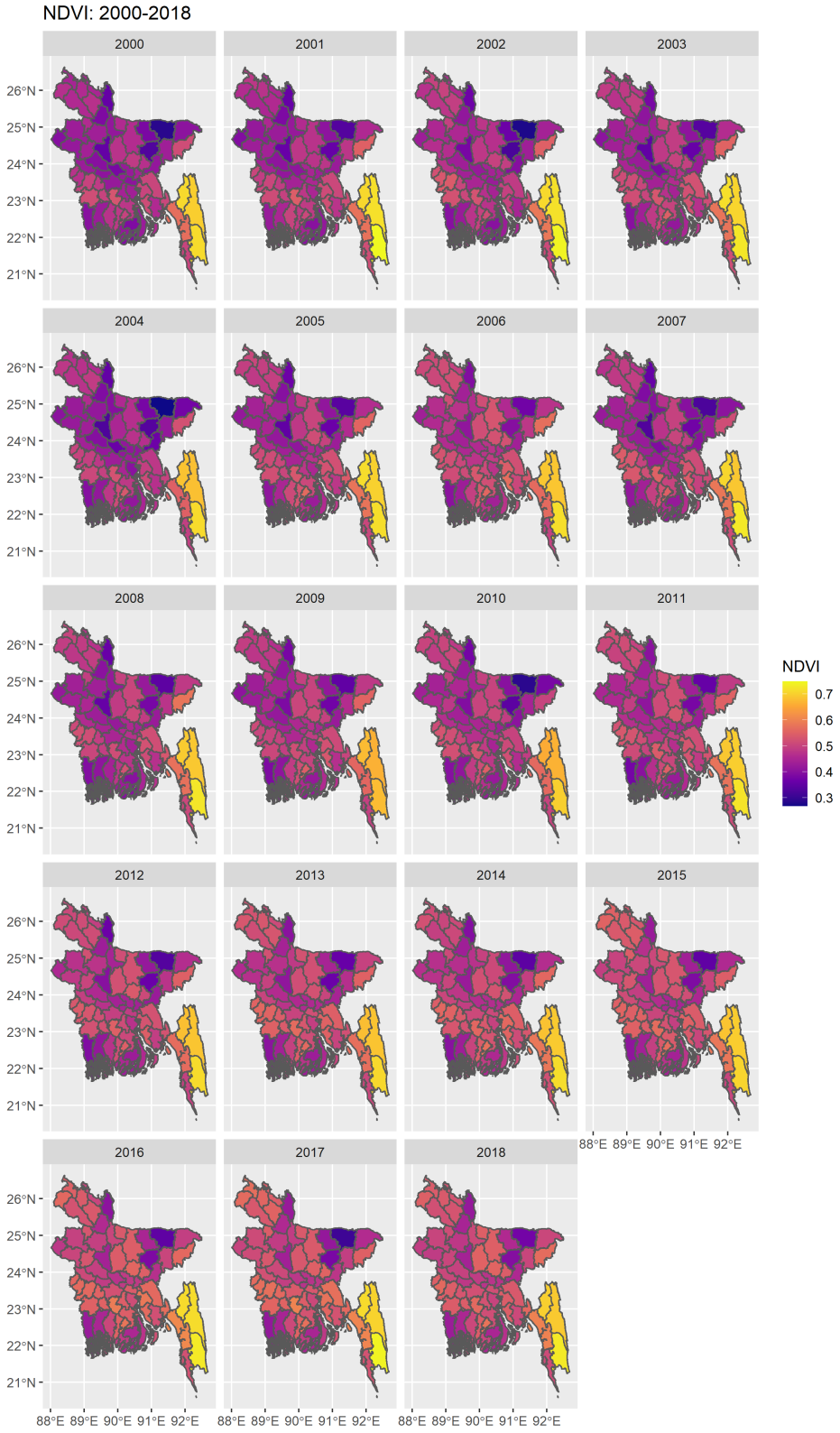


Figure S.2.10: District level mean normalized deviance vegetation index (NDVI) values during 2000-2018.

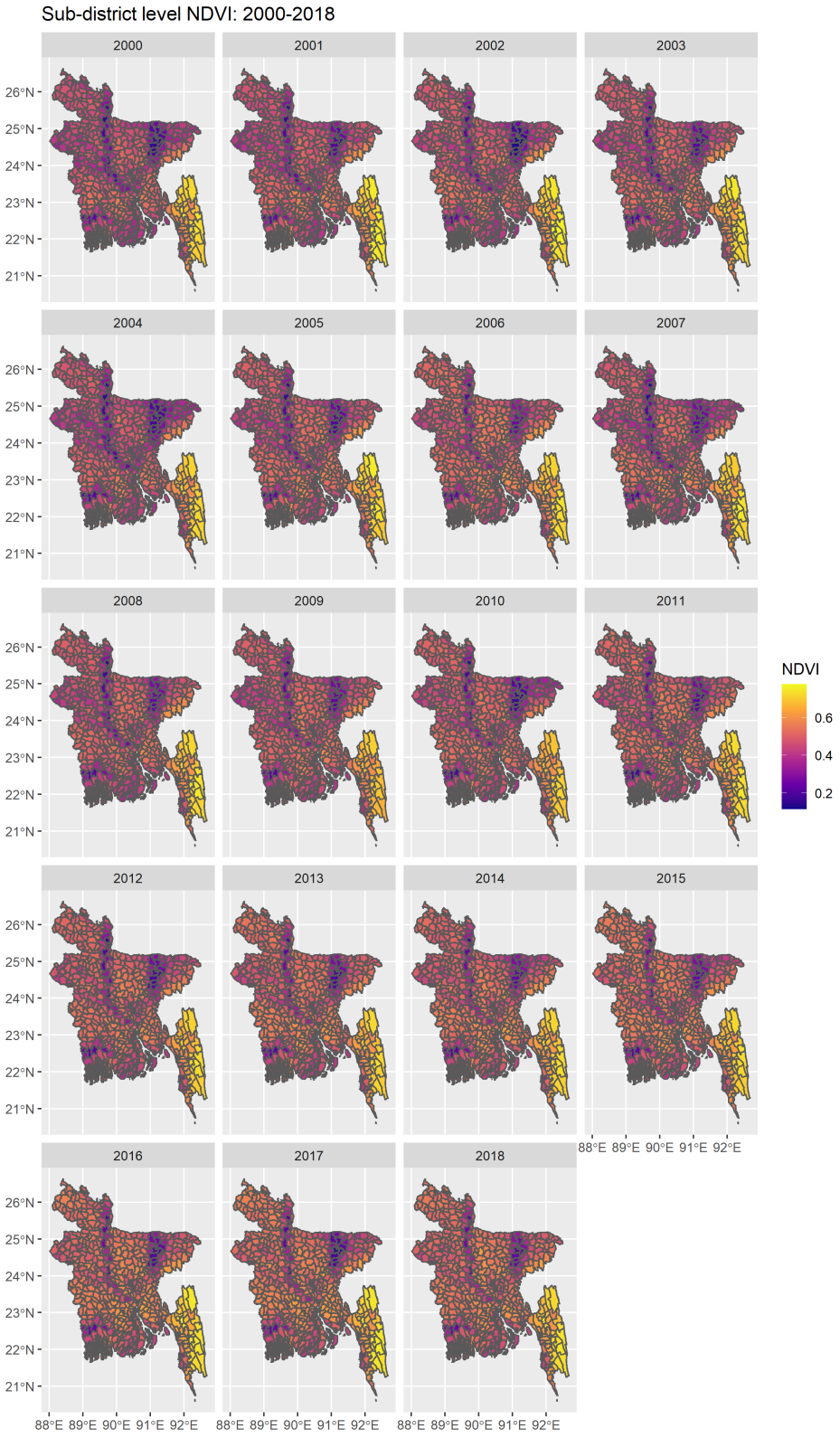


Figure S.2.11: Sub-district level mean normalized deviance vegetation index (NDVI) values during 2000-2018.

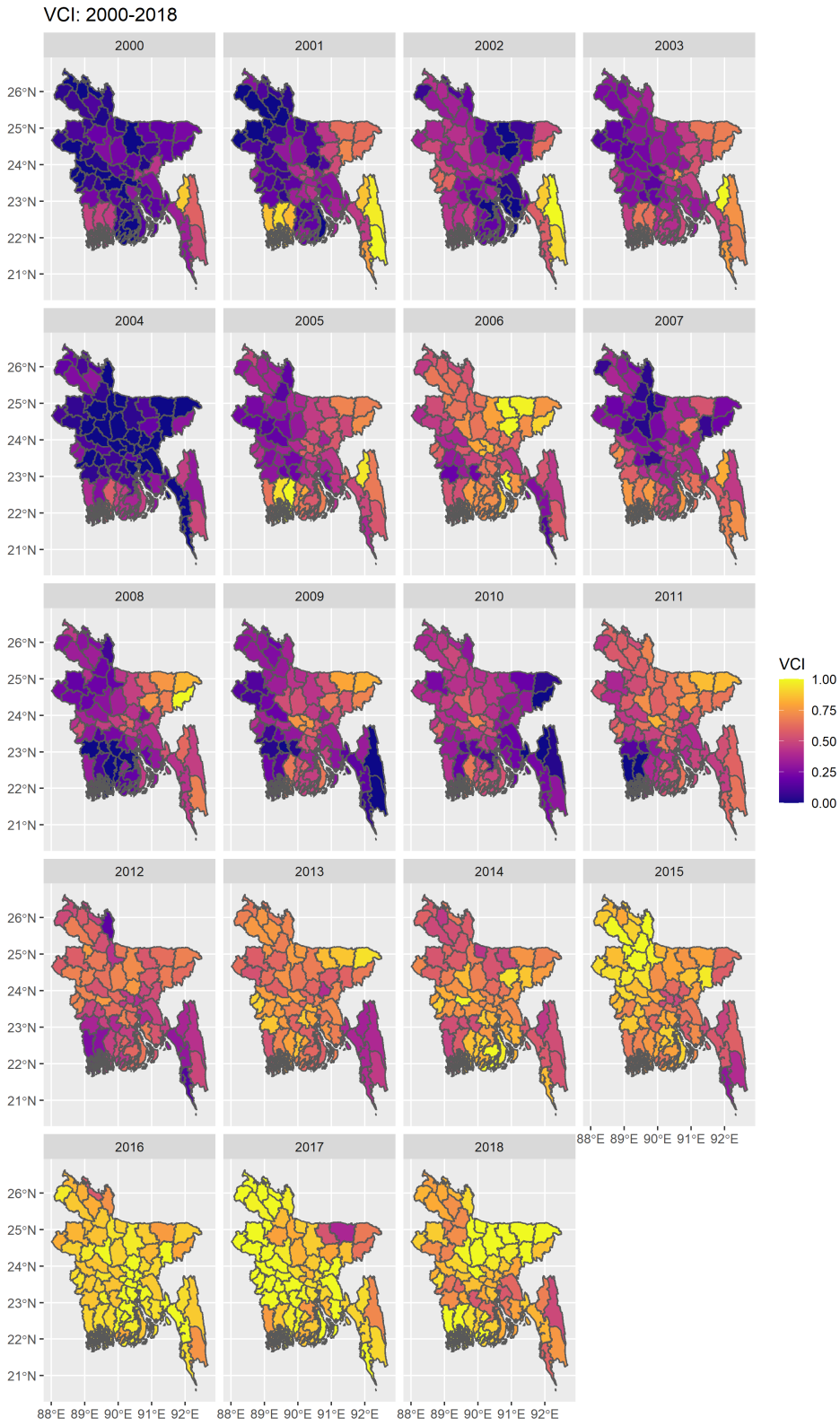


Figure S.2.12: District level Vegetation Condition Index (VCI) values during 2000-2018.

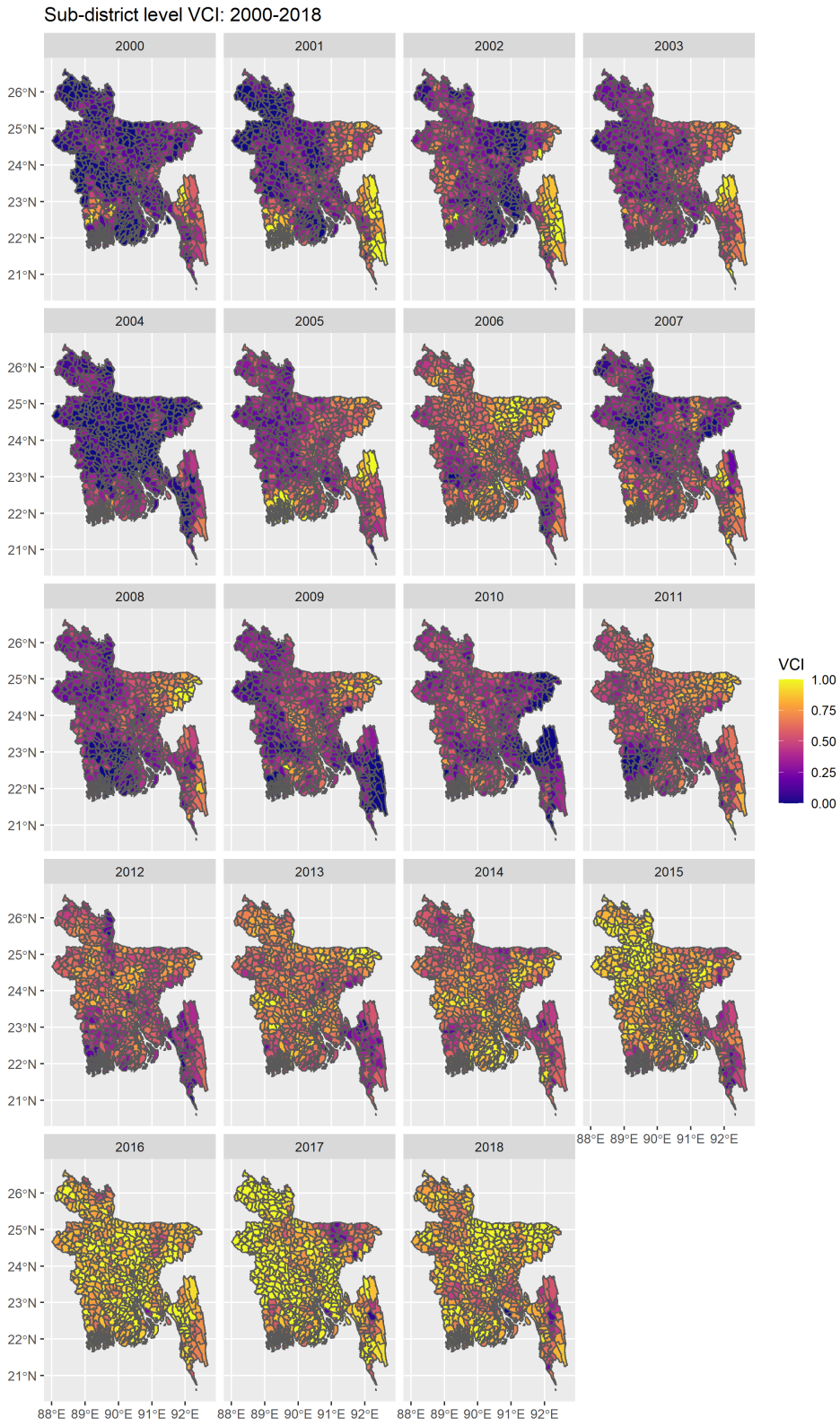


Figure S.2.13: Sub-district level Vegetation Condition Index (VCI) values during 2000-2018.

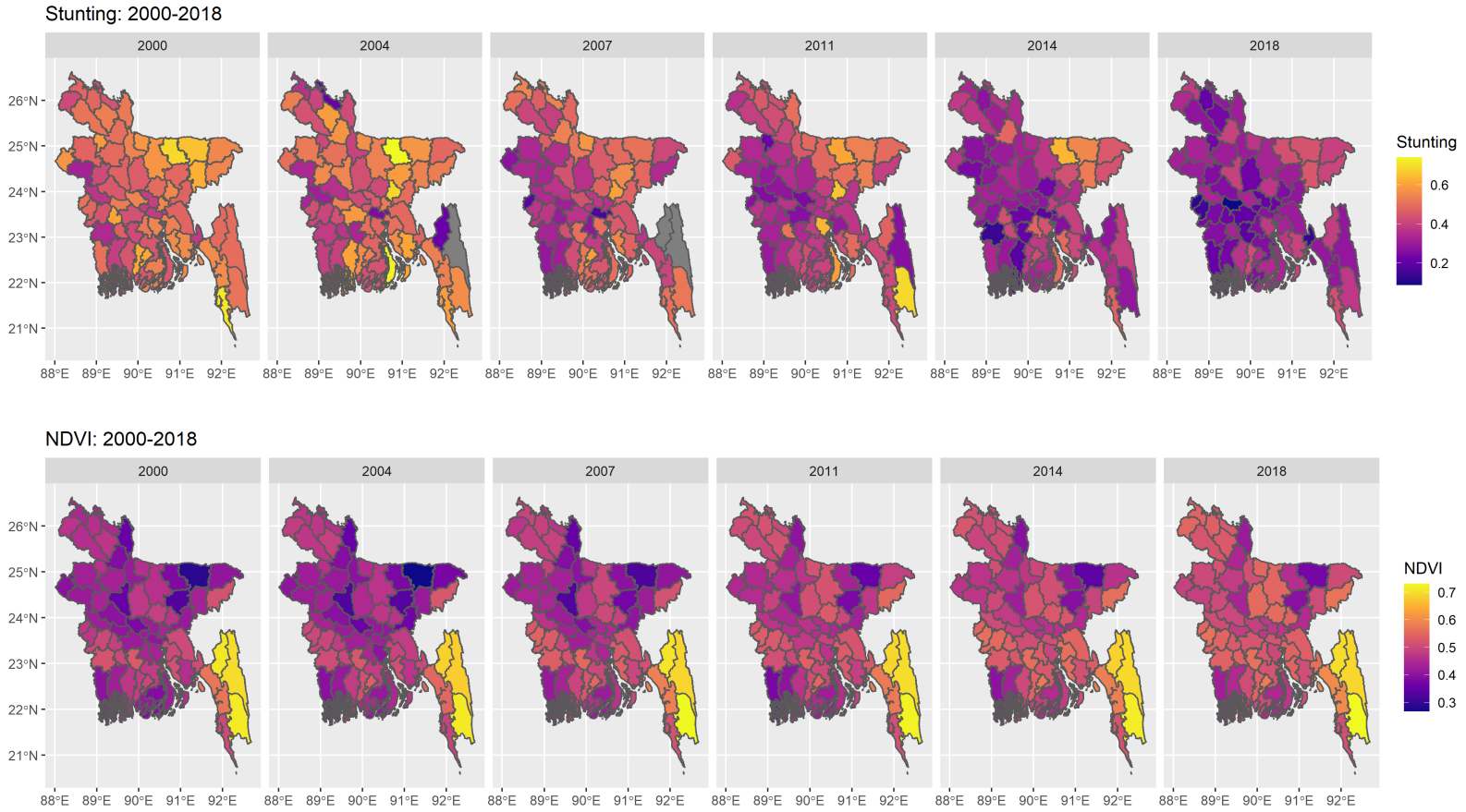


Figure S.2.14: District level VCI and stunting prevalence in survey years 2000, 2004, 2007, 2011, 2014 and 2018.

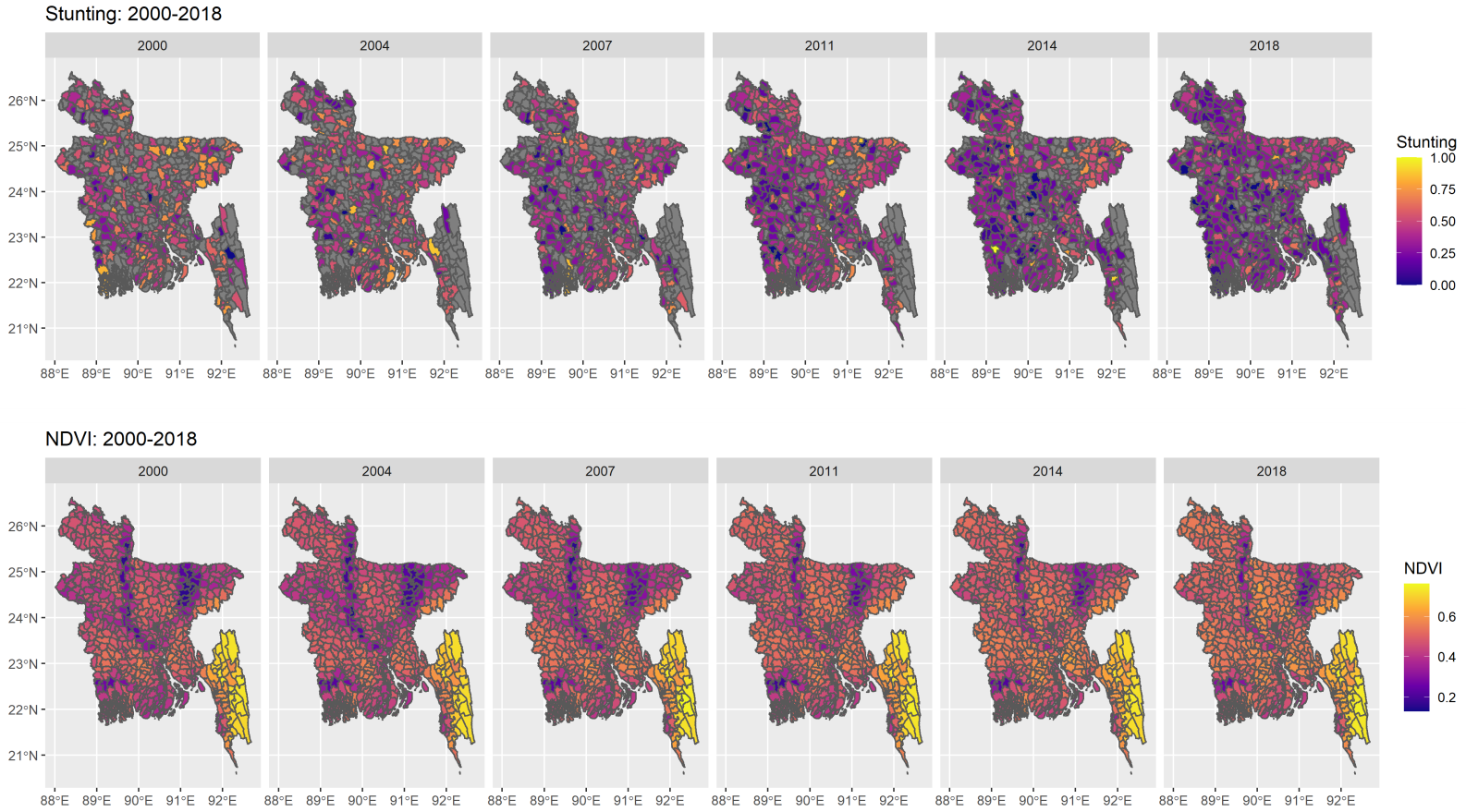


Figure S.2.15: Sub-district level NDVI and stunting prevalence in survey years 2000, 2004, 2007, 2011, 2014 and 2018.

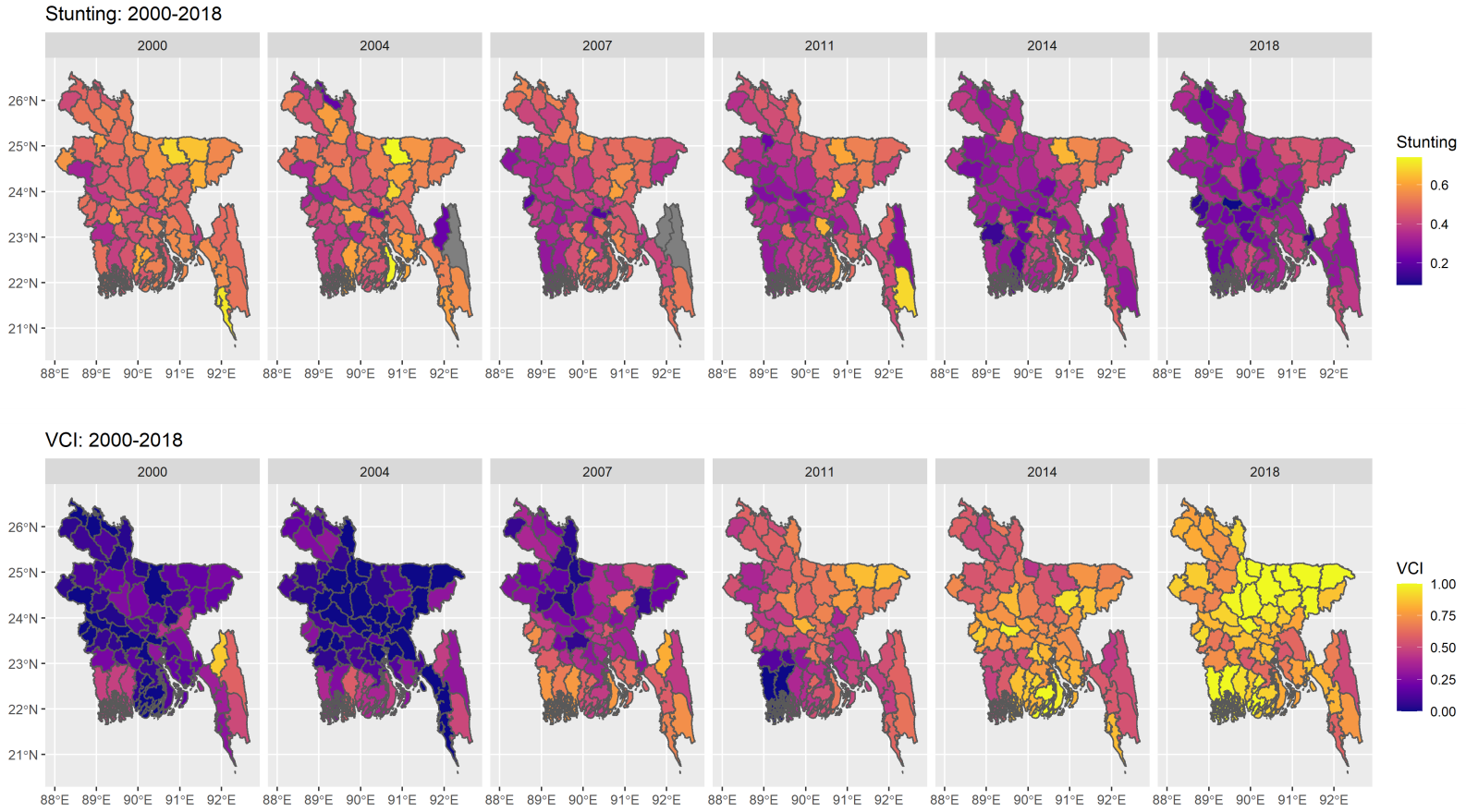


Figure S.2.16: District level VCI and stunting prevalence in survey years 2000, 2004, 2007, 2011, 2014 and 2018.

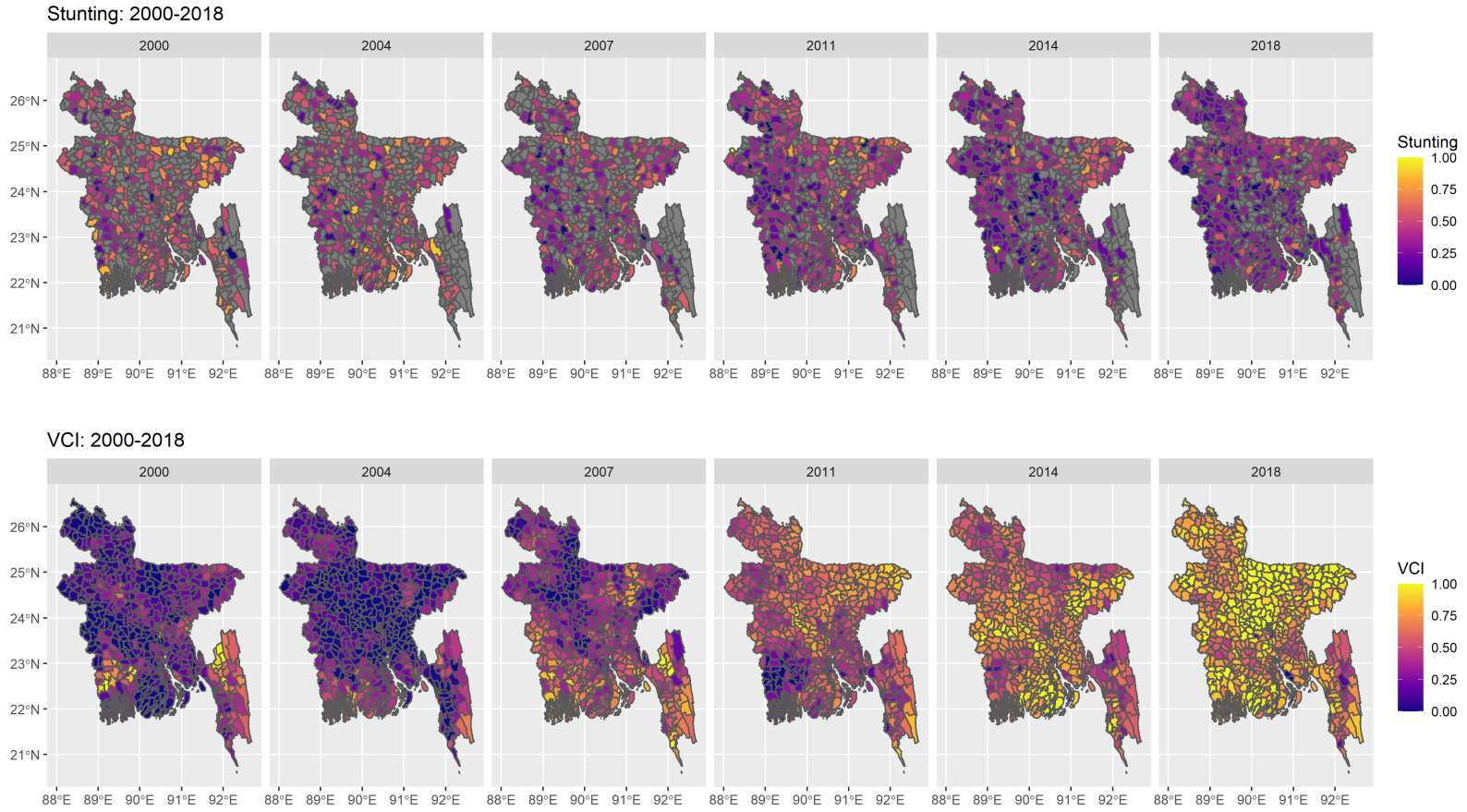


Figure S.2.17: Sub-district level VCI and stunting prevalence in survey years 2000, 2004, 2007, 2011, 2014 and 2018.

S.2.3 Land surface temperature

$$VCI_{dt} = \frac{\text{NDVI}_{dt} - \text{NDVI}_{\text{min}}^{(d)}}{\text{NDVI}_{\text{max}}^{(d)} - \text{NDVI}_{\text{min}}^{(d)}} \tag{2}$$

where NDVI_{dt} is the value for domain d in year t, $NDVI_{max}^{(d)}$ and $NDVI_{min}^{(d)}$ are maximum and minimum values for domain d during the period 2000-2018. The range of VCI is from 0 (if NDVI_{dt} equals to $\text{NDVI}_{\text{min}}^{(d)}$) to 1 (if NDVI_{dt} equals to $\text{NDVI}_{\text{max}}^{(d)}$), corresponding to the changes in vegetation condition from extremely unfavorable to optimal.

Figures S.2.18 and S.2.19 shows the spatial distribution of land surface temperature (LST) values at the district and sub-district level. The Figure shows the mean values of LST seem comparatively higher in the south-western part compared to the eastern part. The lowest temperature is in the middle parts of the north-eastern region, where the lands remain under water half of the year. In the similar way, the Chittagong hilly areas have lower LST values compared to the coastal areas of the south-eastern region. Like NDVI values, the spatial distribution of LST remains same but the change over time is tough to recognize.

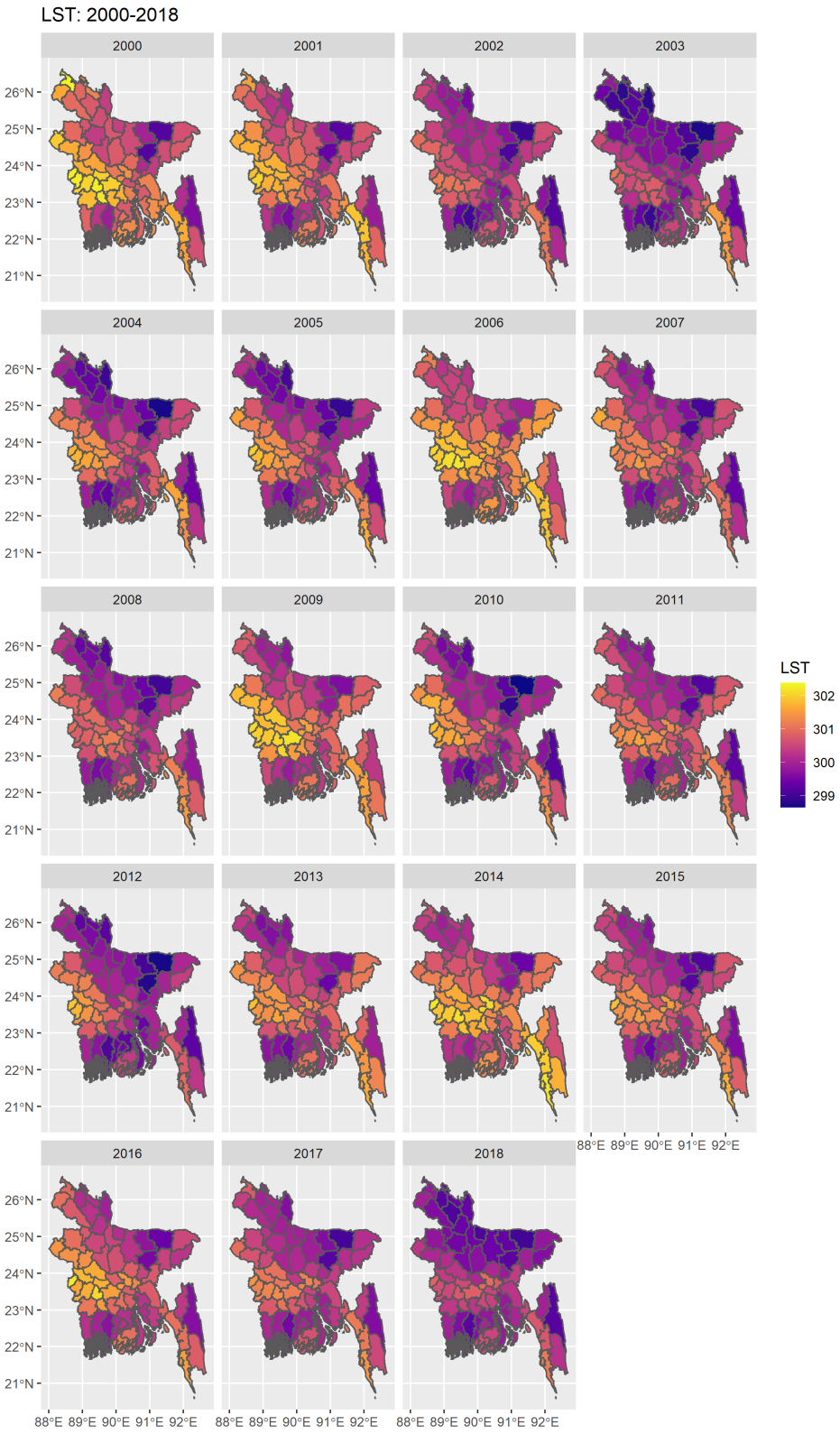


Figure S.2.18: District level land surface temperature (LST) values during 2000-2018.

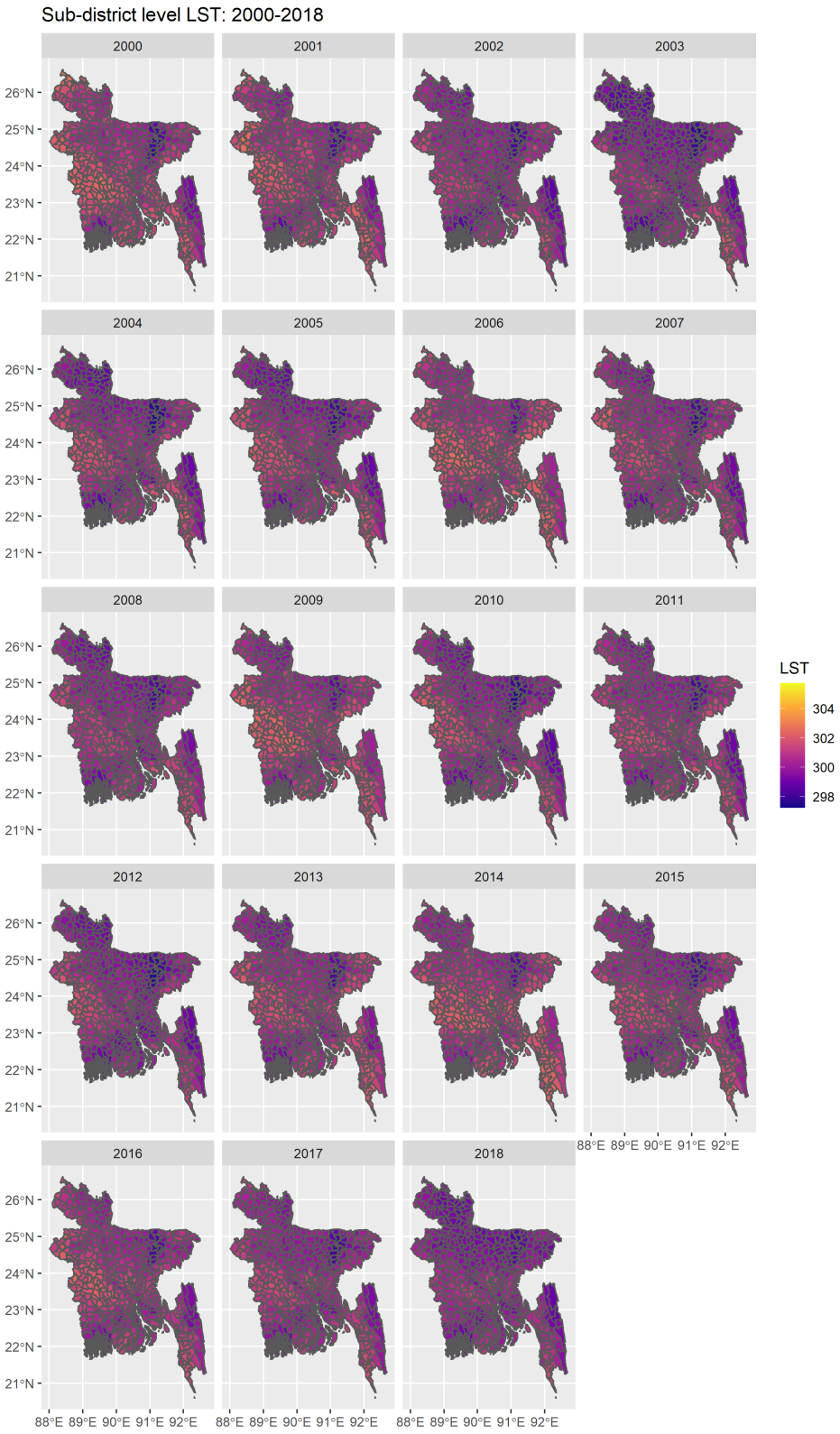


Figure S.2.19: District level land surface temperature (LST) values during 2000-2018.

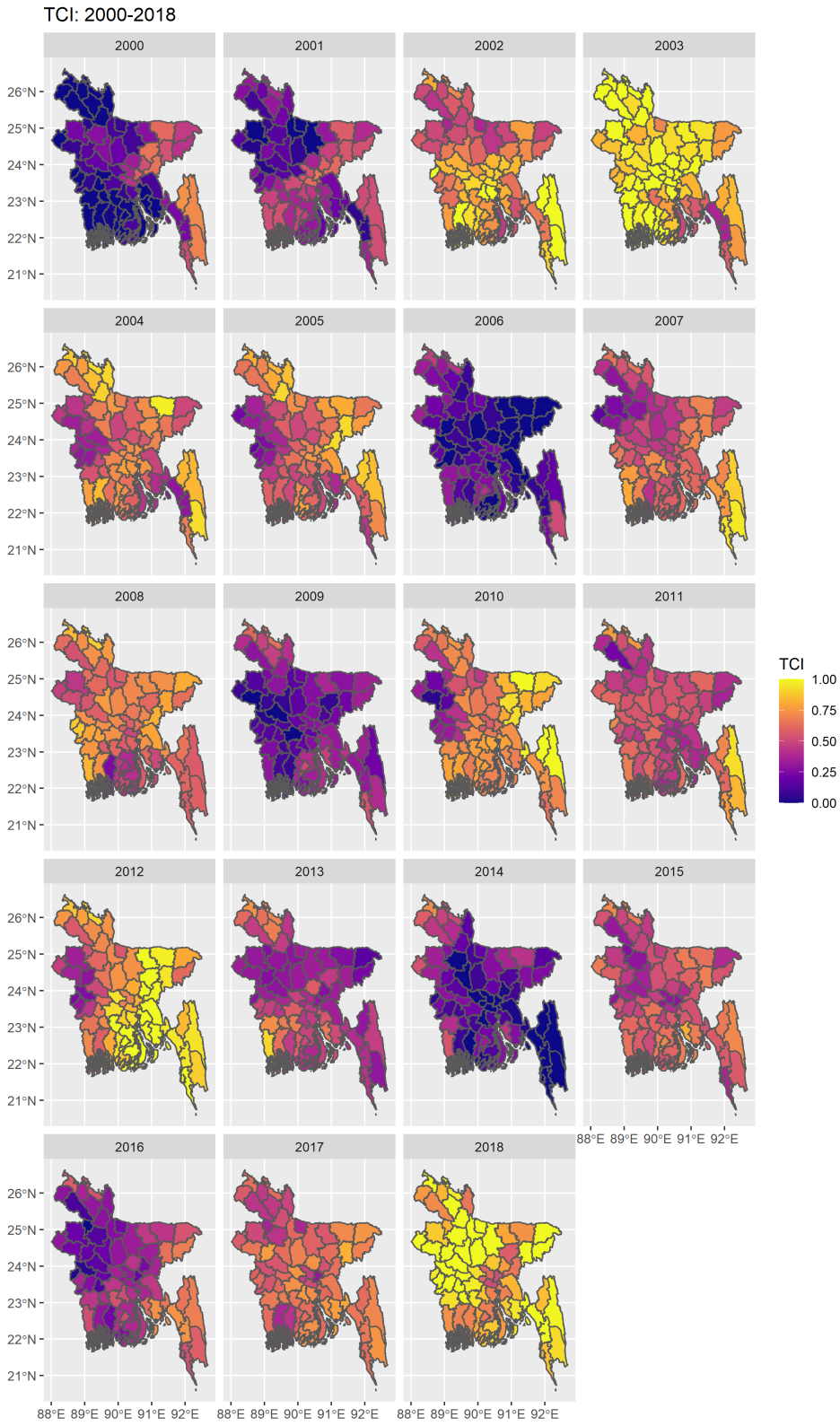


Figure S.2.20: District level Temperature Condition Index (TCI) values during 2000-2018.

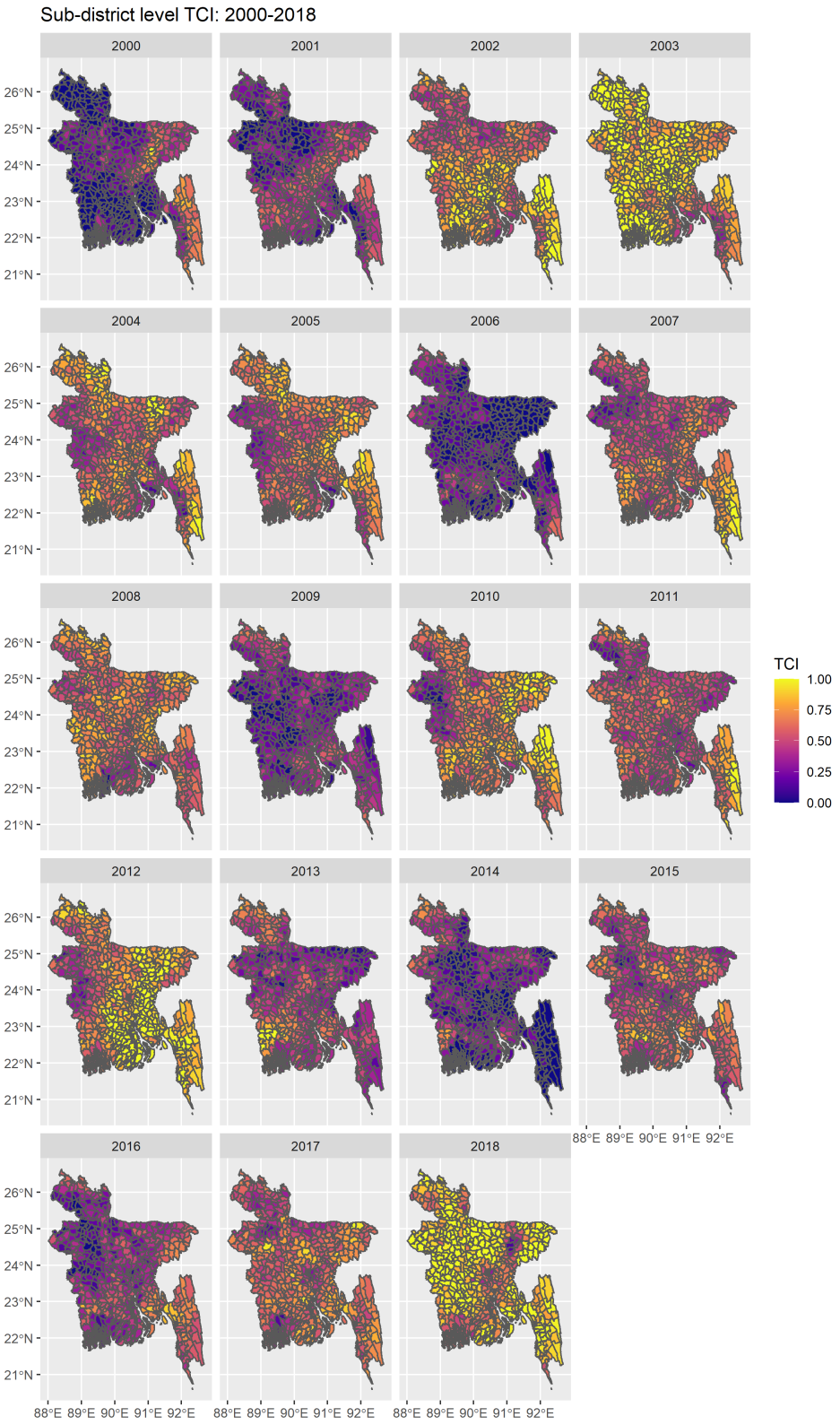


Figure S.2.21: Sub-district level Temperature Condition Index (TCI) values during 2000-2018.

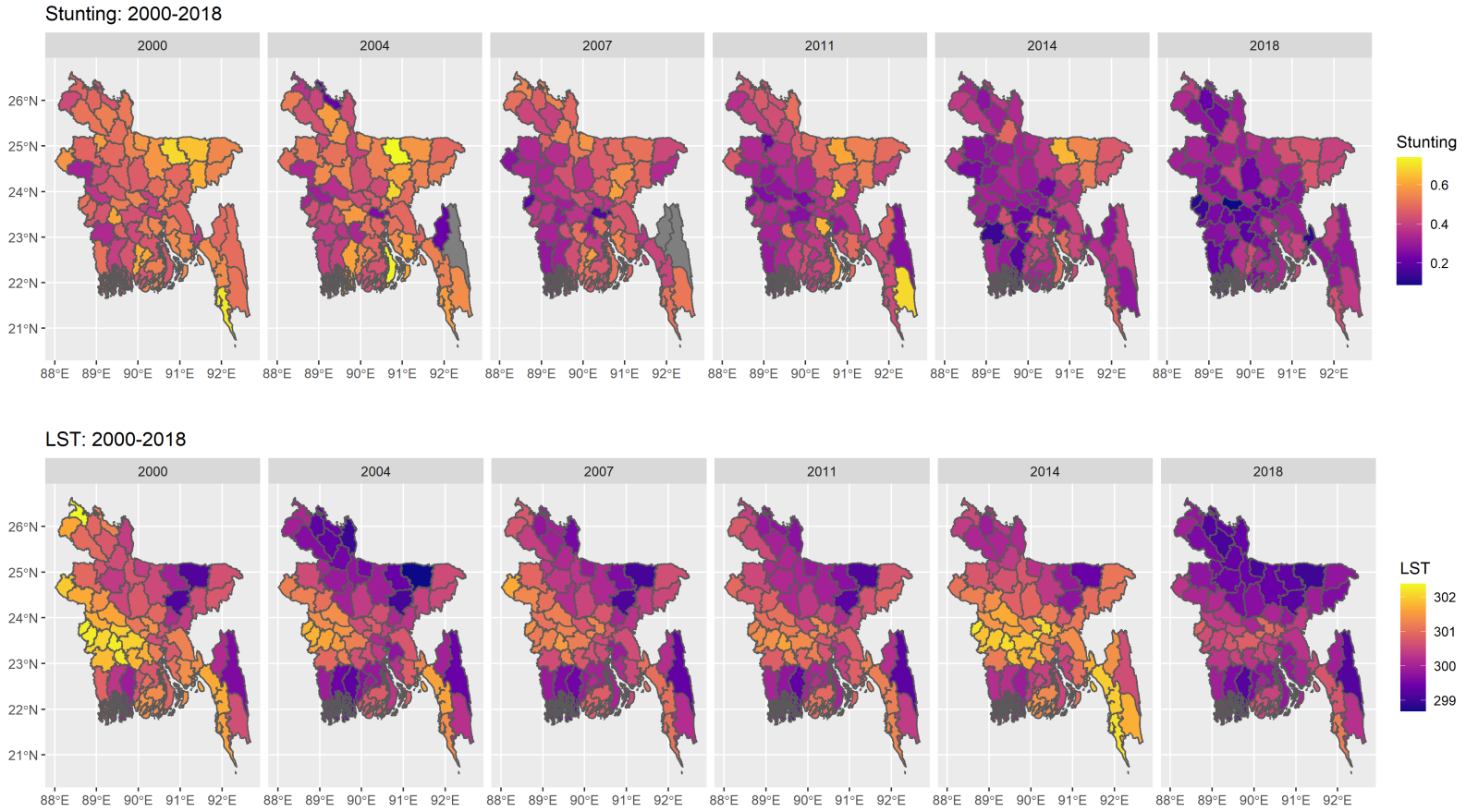


Figure S.2.22: District level LST and stunting prevalence in survey years 2000, 2004, 2007, 2011, 2014 and 2018.

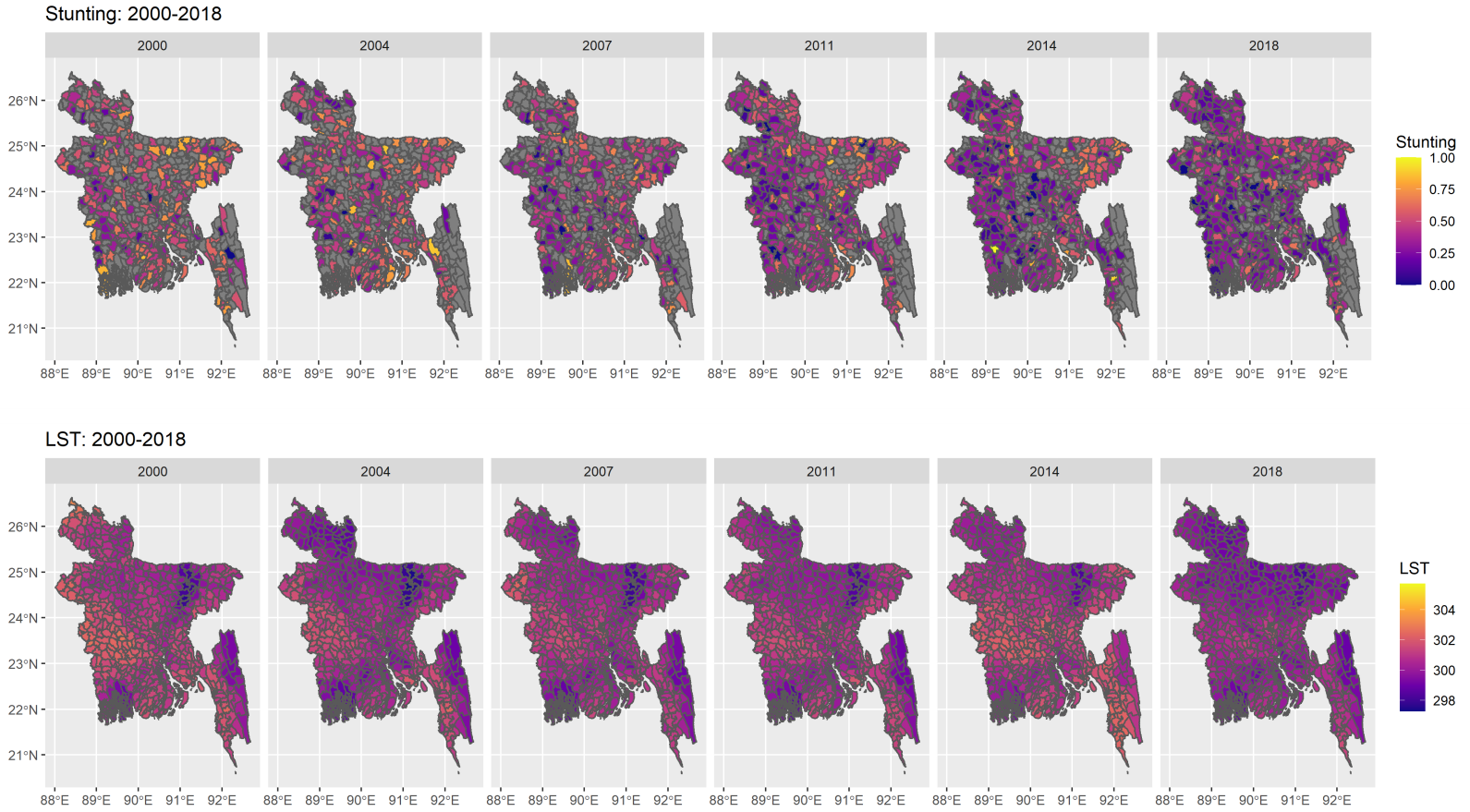


Figure S.2.23: Sub-district level LST and stunting prevalence in survey years 2000, 2004, 2007, 2011, 2014 and 2018.

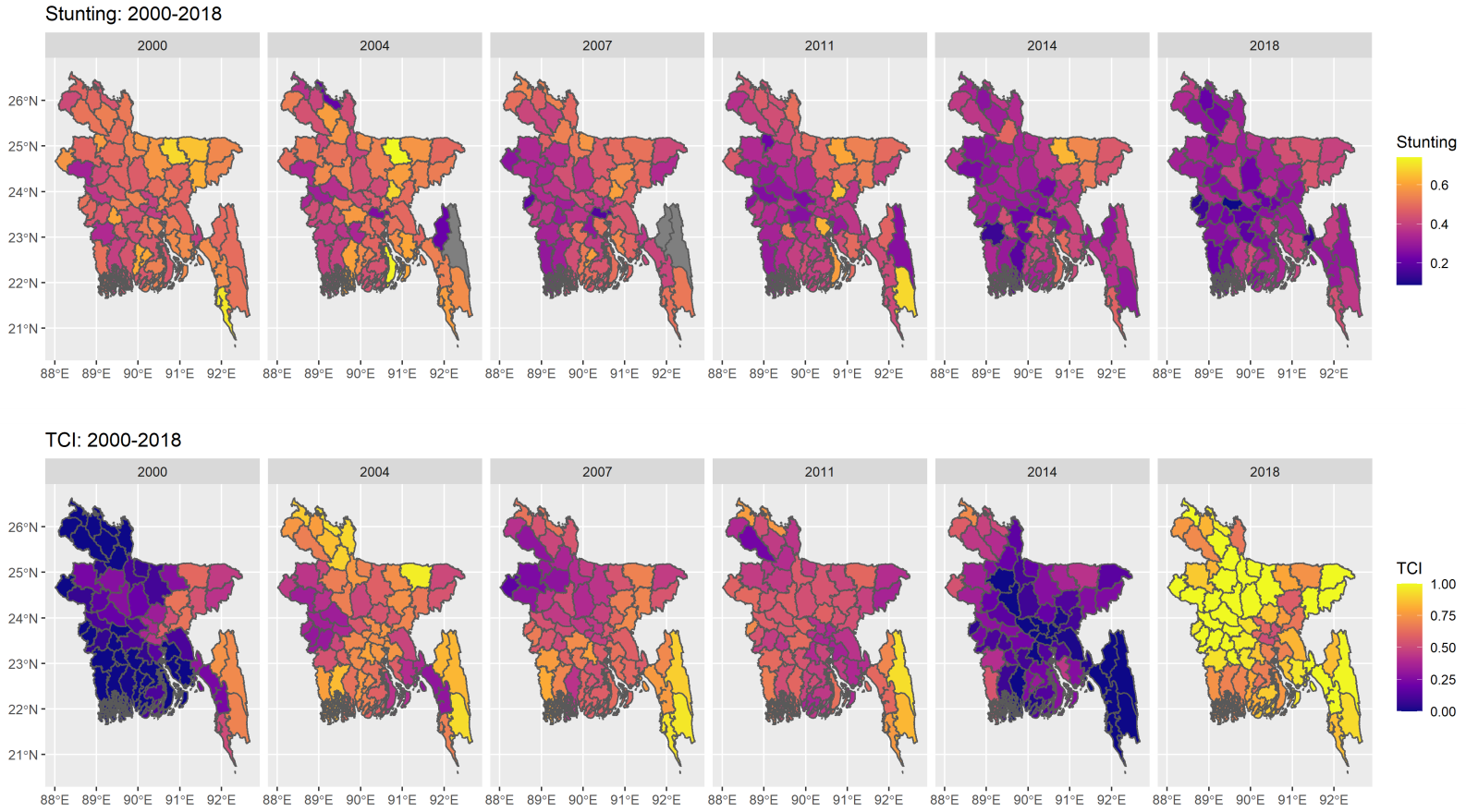


Figure S.2.24: District level TCI and stunting prevalence in survey years 2000, 2004, 2007, 2011, 2014 and 2018.

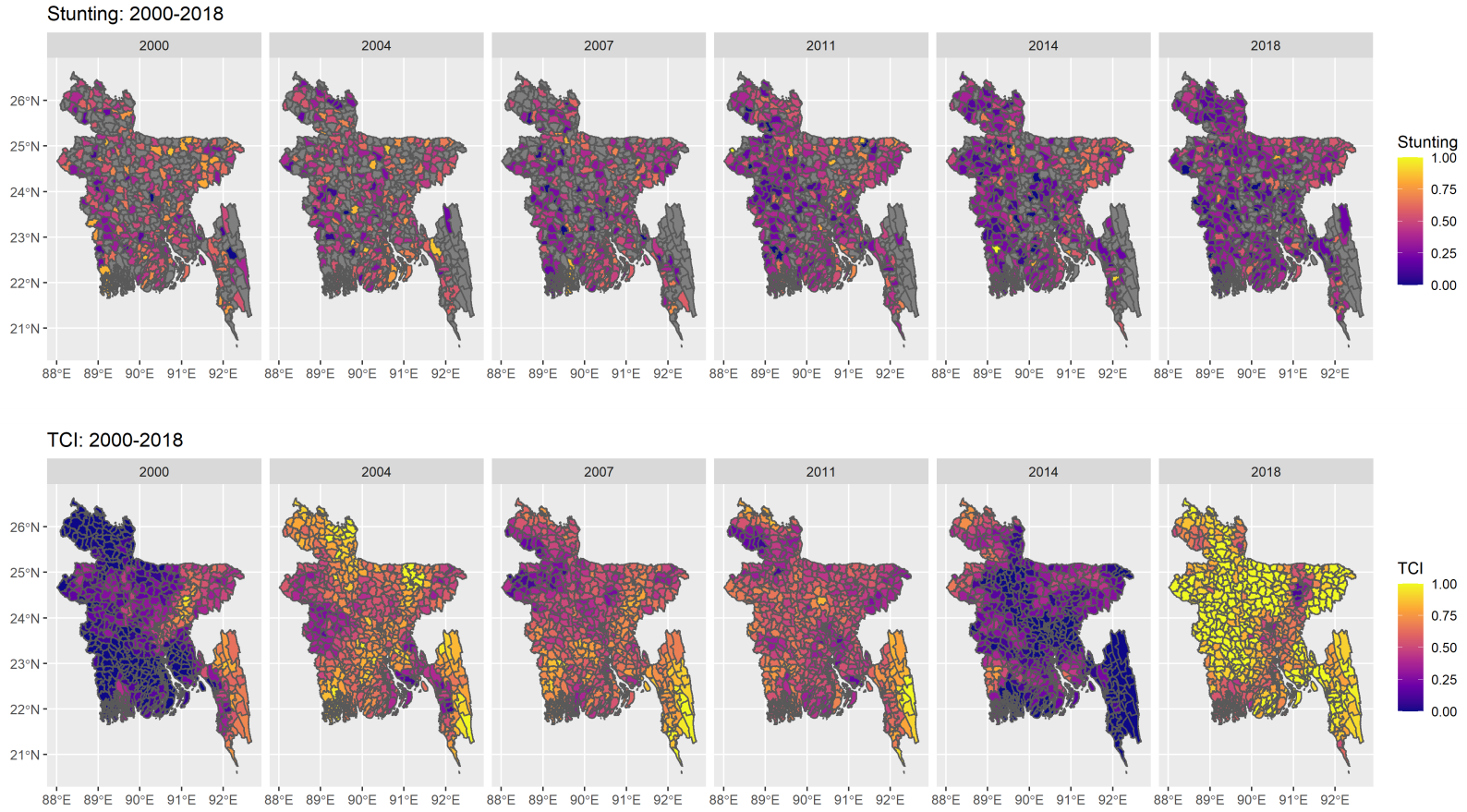


Figure S.2.25: Sub-district level TCI and stunting prevalence in survey years 2000, 2004, 2007, 2011, 2014 and 2018.

S.2.4 Annual rainfall

$$VCI_{dt} = \frac{\text{NDVI}_{dt} - \text{NDVI}_{\text{min}}^{(d)}}{\text{NDVI}_{\text{max}}^{(d)} - \text{NDVI}_{\text{min}}^{(d)}} \tag{3}$$

where NDVI_{dt} is the value for domain d in year t, $NDVI_{max}^{(d)}$ and $NDVI_{min}^{(d)}$ are maximum and minimum values for domain d during the period 2000-2018. The range of VCI is from 0 (if NDVI_{dt} equals to $\text{NDVI}_{\text{min}}^{(d)}$) to 1 (if NDVI_{dt} equals to $\text{NDVI}_{\text{max}}^{(d)}$), corresponding to the changes in vegetation condition from extremely unfavorable to optimal.

Figure S.2.31 shows the spatial distribution of annual total rainfall (or precipitation) at the sub-district level. This Figure shows some changes in the distribution of rainfall over space and time. As for example, total annual rainfall is found highest in the Sylhet region (the very north-eastern part) and consistently lower in a larger part of the western part of the country. With respect to 2000, the total rainfall seems lower after 2011. The summary statistics of total rainfall shows the highest rainfall is recorded in 2017. There is also pattern of lower to higher amount of rainfall from south-western (Khulna) region to north-eastern (Sylhet) region and this pattern roughly remain same.

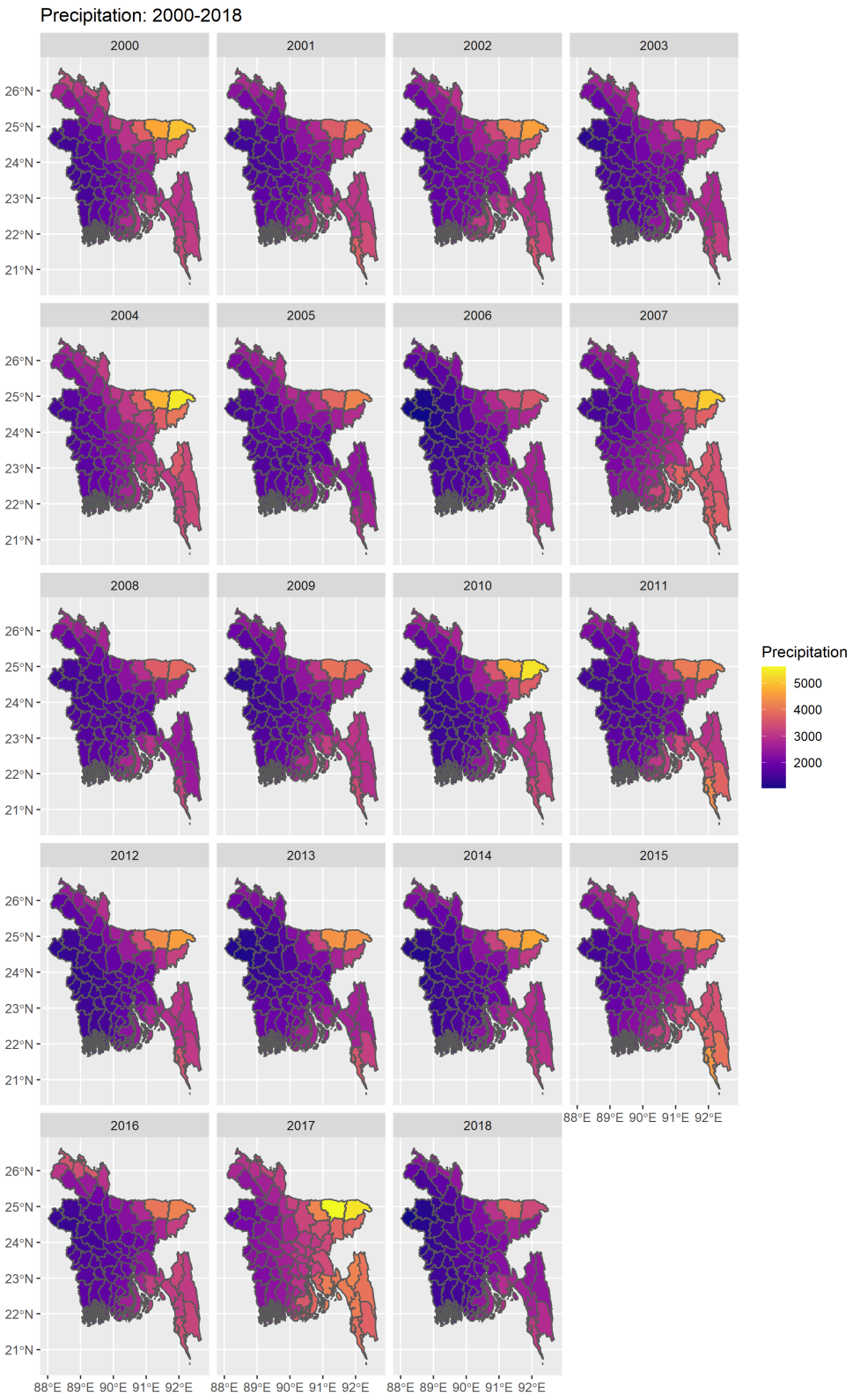


Figure S.2.26: District level Precipitation during 2000-2018.

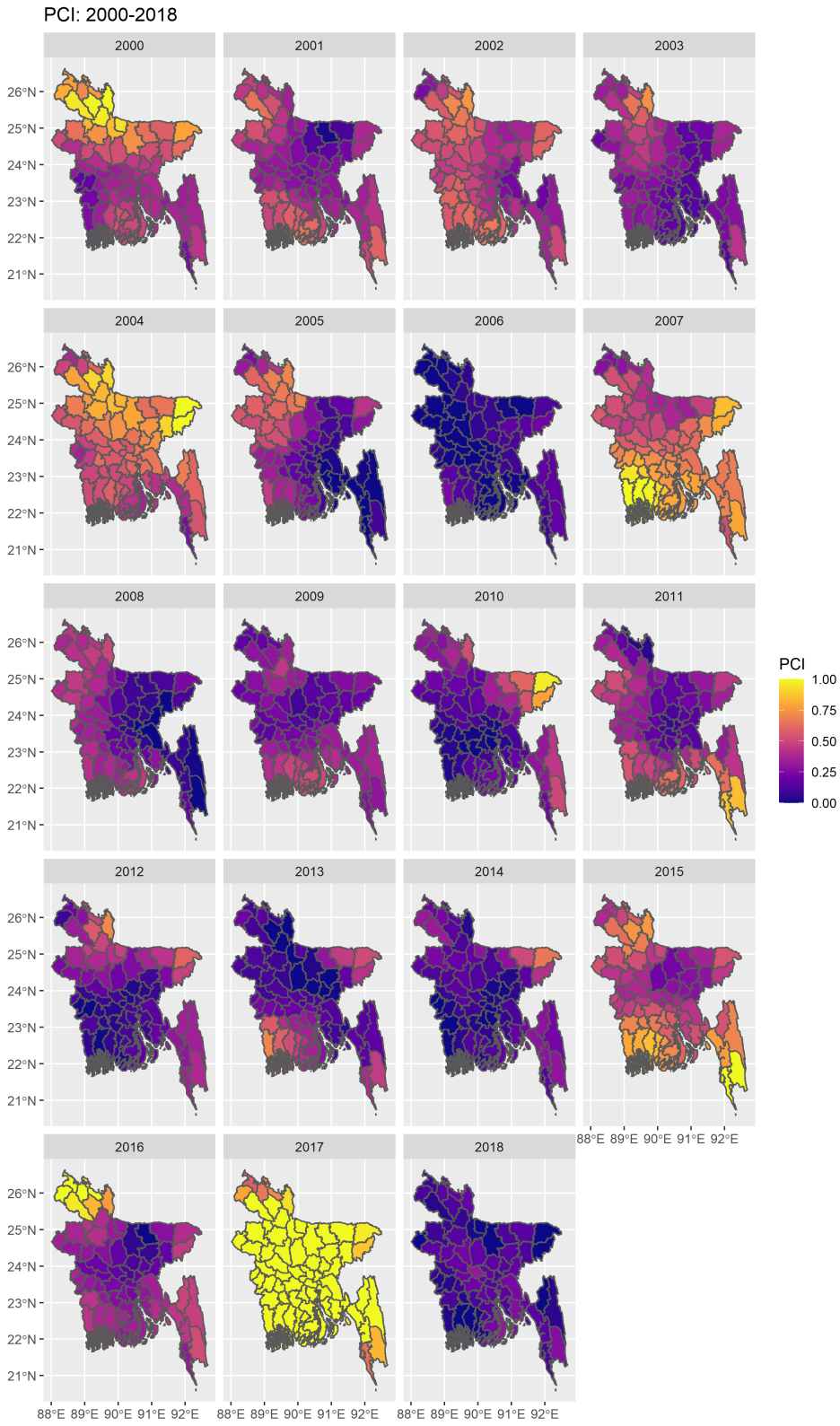


Figure S.2.27: District level Precipitation Condition Index (PCI) values during 2000-2018.

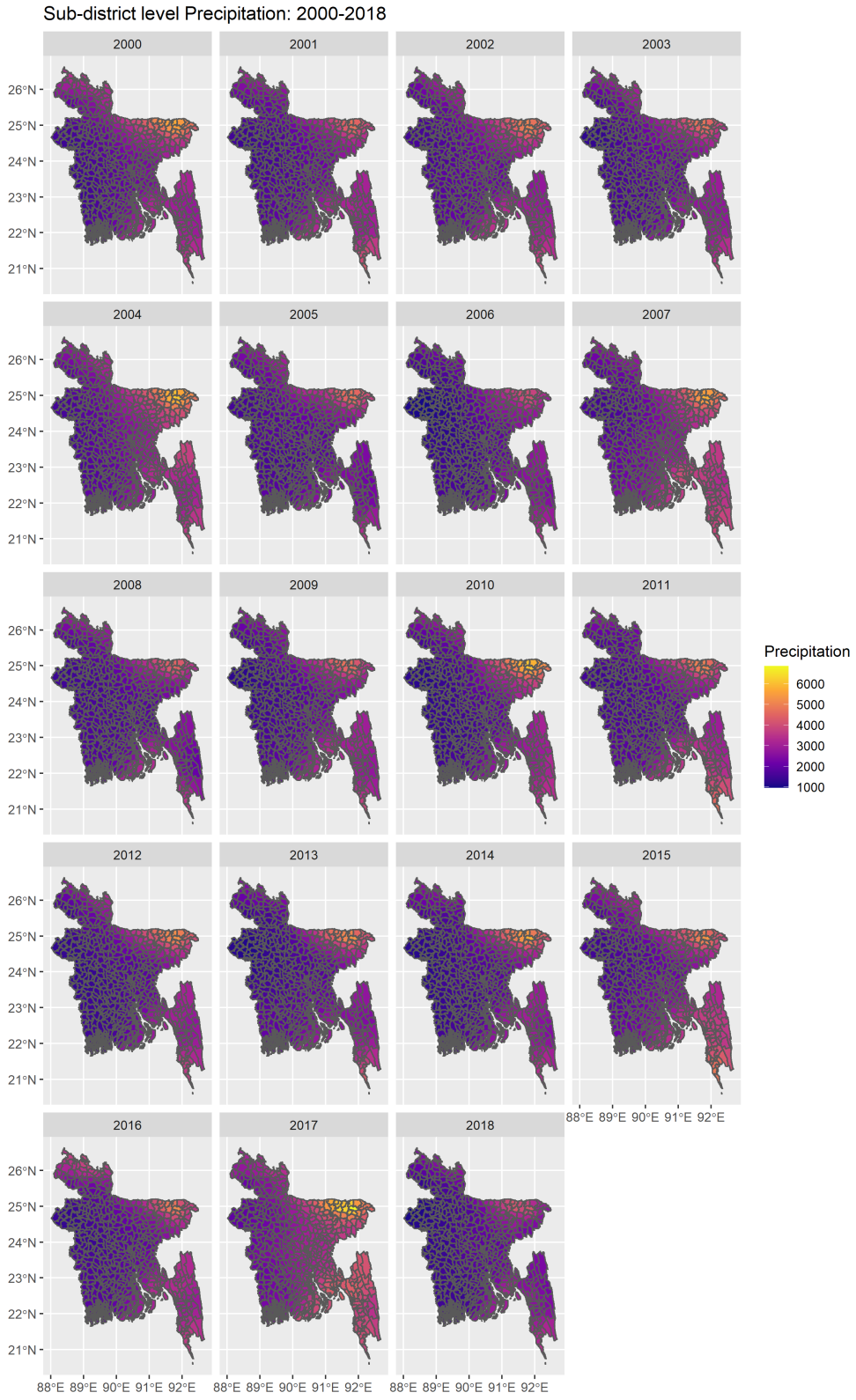


Figure S.2.28: Sub-district level annual (total) precipitation in survey years 2000, 2004, 2007, 2011, 2014 and 2018.

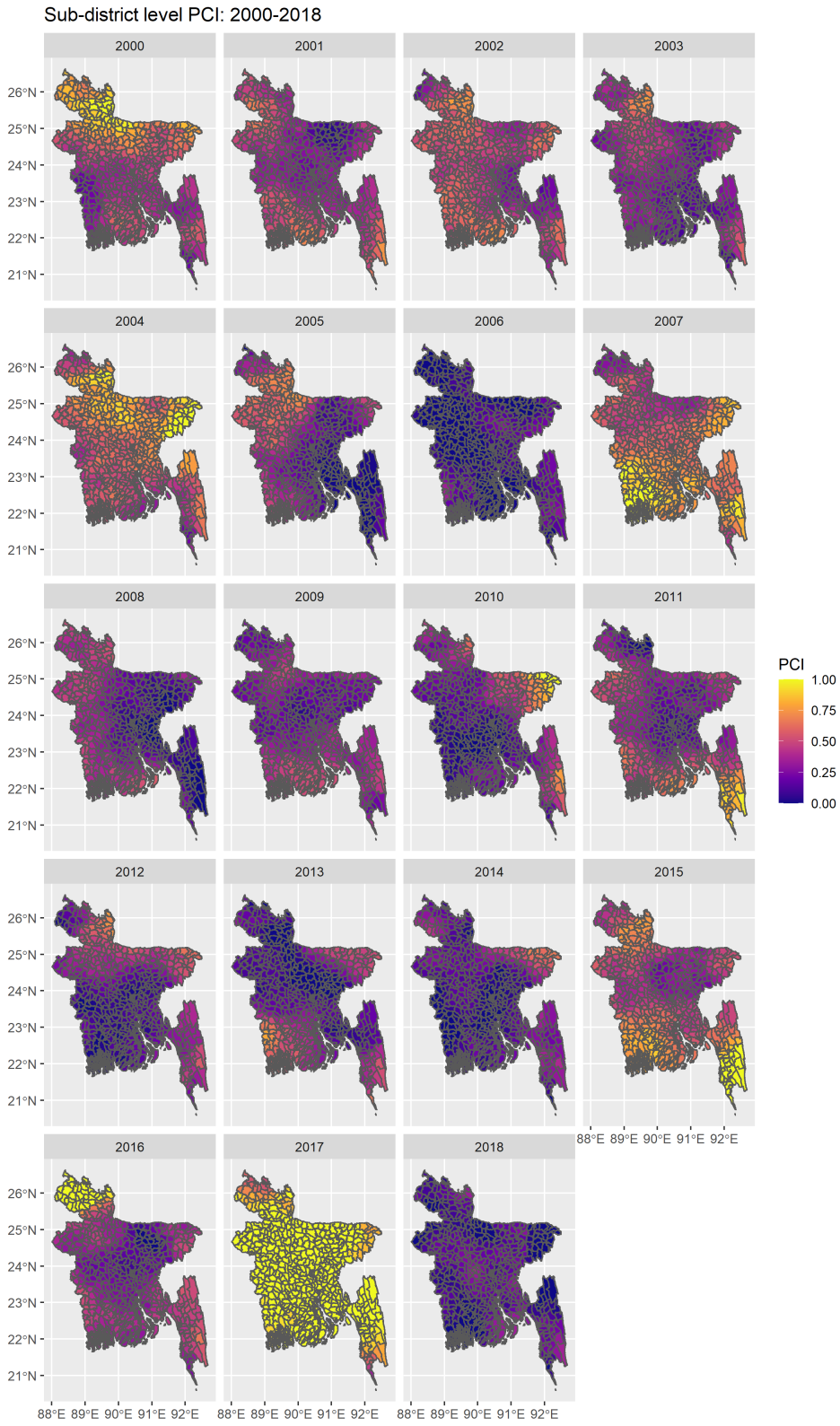


Figure S.2.29: Sub-district level Precipitation Condition Index (PCI) values during 2000-2018.

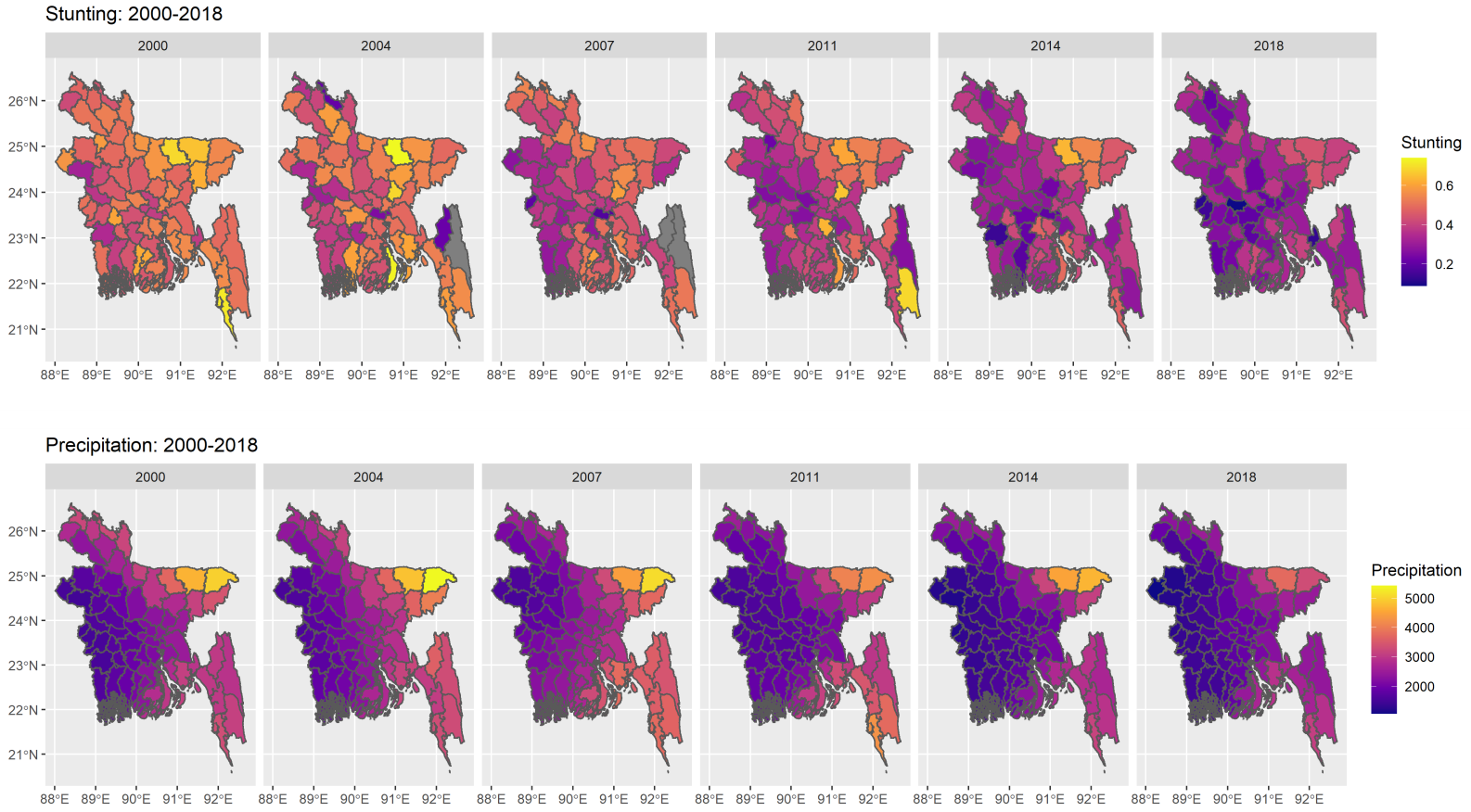


Figure S.2.30: District level Precipitation and stunting prevalence in survey years 2000, 2004, 2007, 2011, 2014 and 2018.

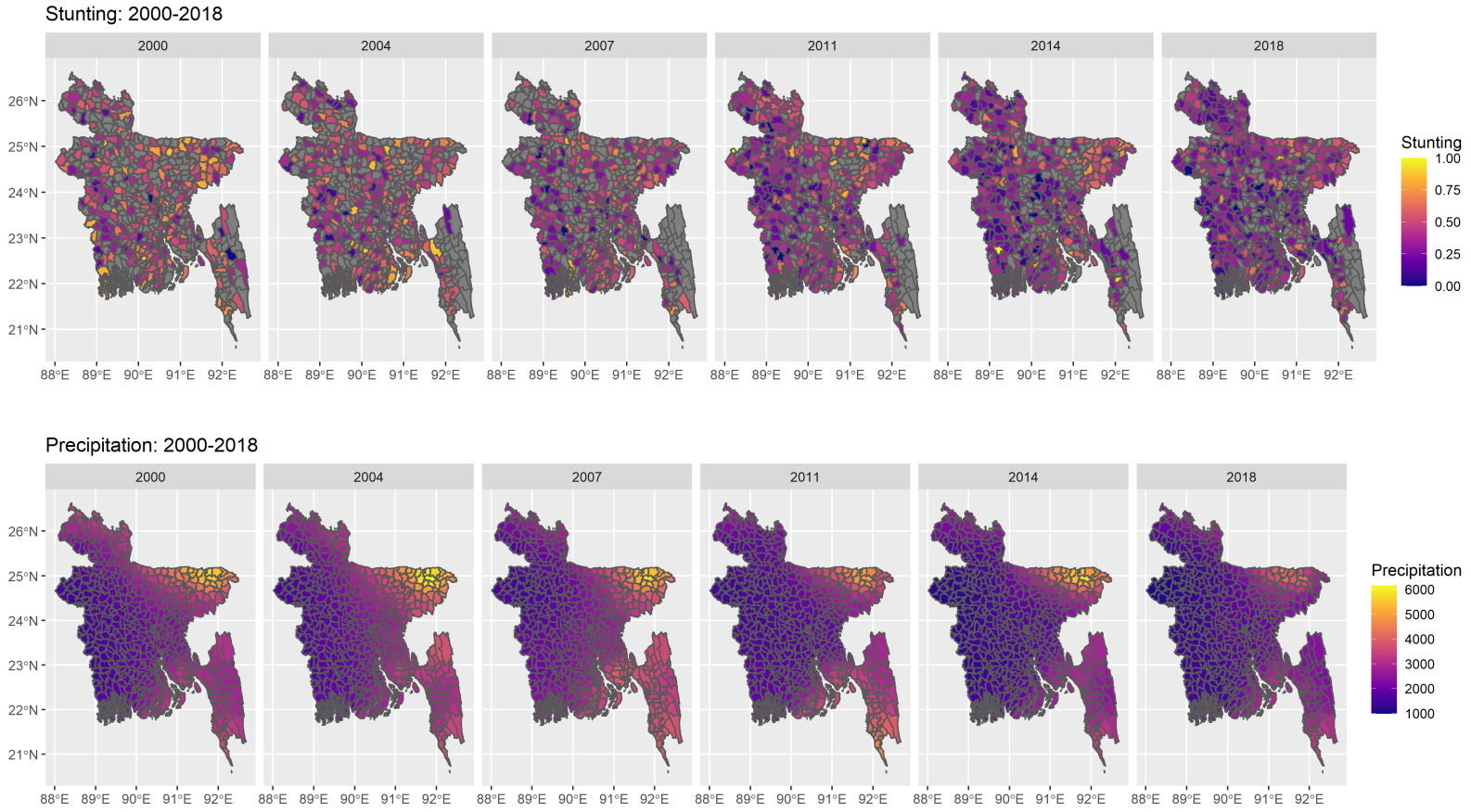


Figure S.2.31: Sub-district level Precipitation and stunting prevalence in survey years 2000, 2004, 2007, 2011, 2014 and 2018.

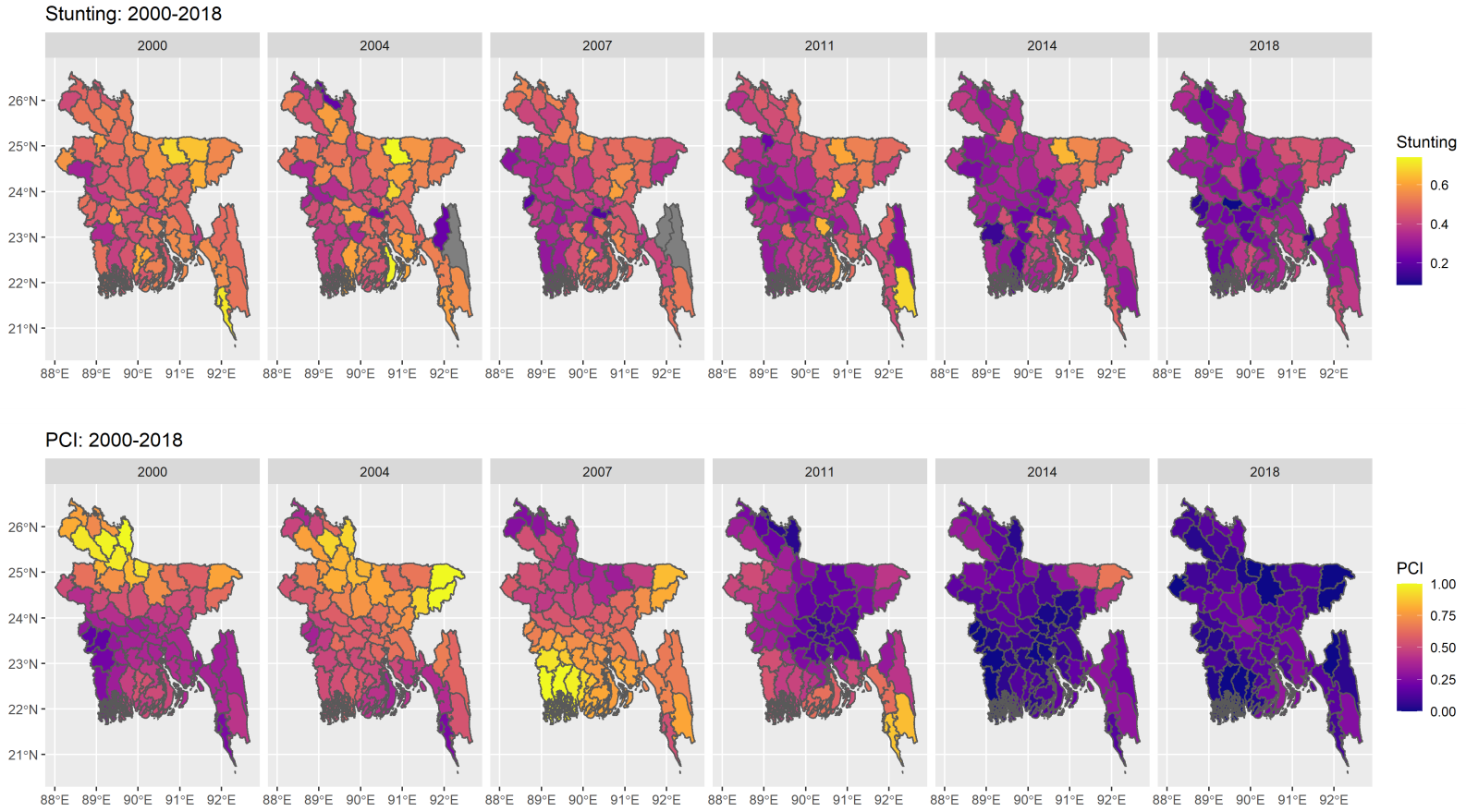


Figure S.2.32: District level PCI and stunting prevalence in survey years 2000, 2004, 2007, 2011, 2014 and 2018.

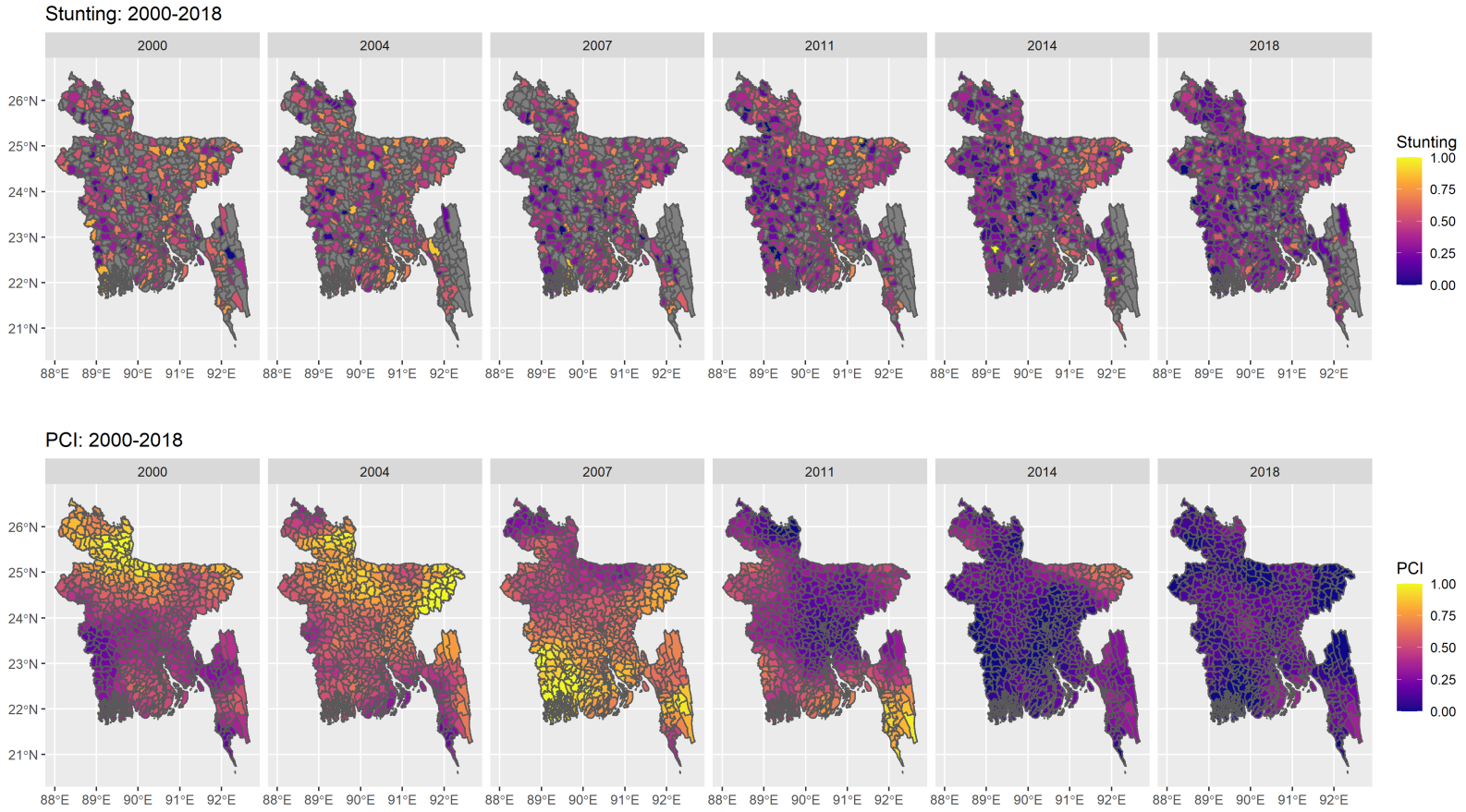


Figure S.2.33: Sub-district level PCI and stunting prevalence in survey years 2000, 2004, 2007, 2011, 2014 and 2018.

S.3 Trends of Stunting at district levels

Multilevel time-series models are developed at the sub-district level assuming the number of stunted children follows a binomial model instead of stunting level follows a Gaussian distribution. The model-based trends at the sub-district level are aggregated to estimate district level trends. Three models are developed based on different model components explained in the main manuscript. District level trends of stunting among under-5 children for the reference period 2000-2018 estimated by DIR estimator (black error-bar line), MTS-1 model (blue line), MTS-2 model (green line) and MTS-3 model (red line) with 95% confidence band are shown by division in the following pages.

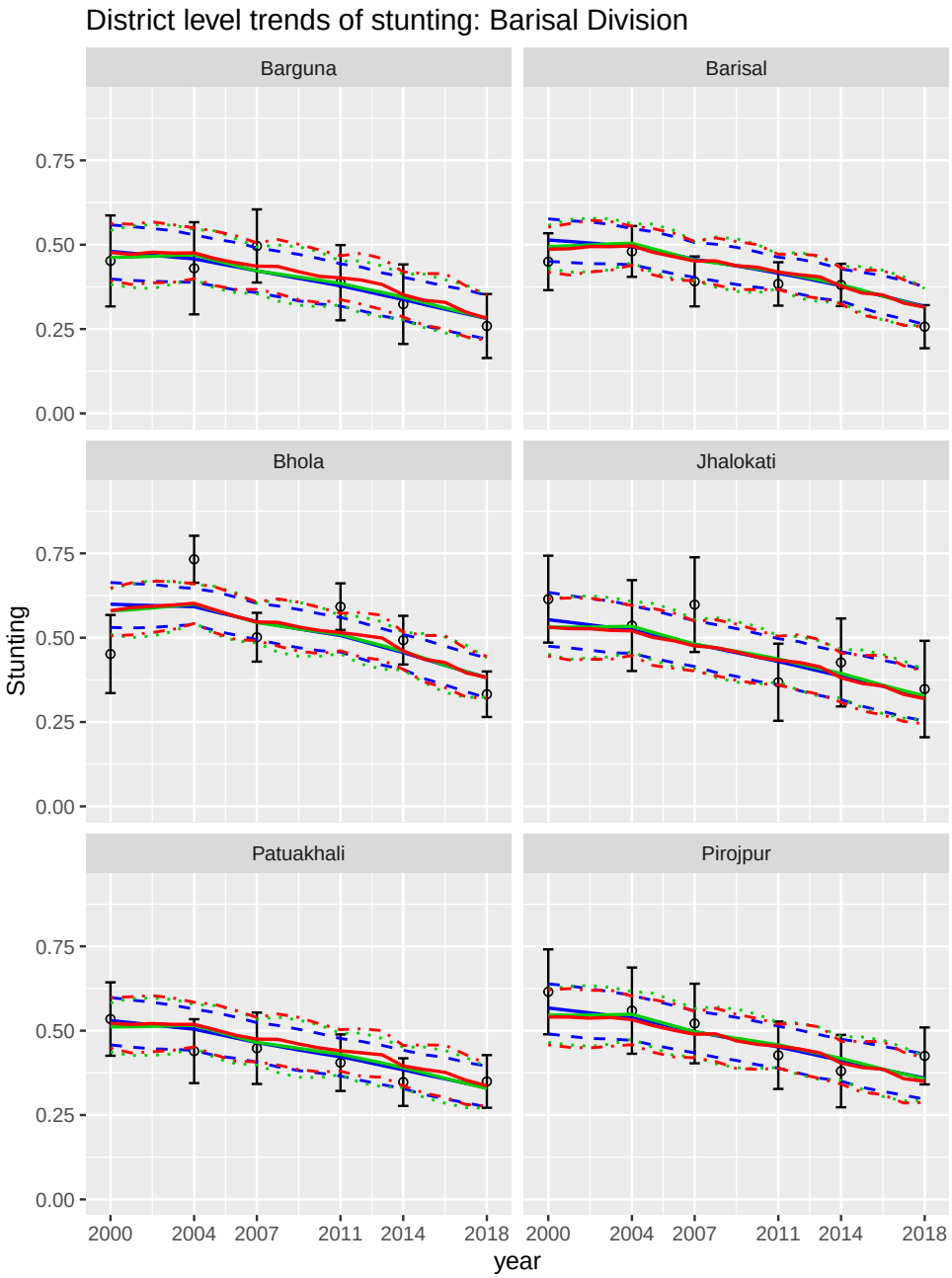


Figure S.3.34: District level trends of stunting among under-5 children in Barisal division during 2000-2018 estimated by DIR estimator (black error-bar line), MTS-1 model (blue line), MTS-2 model (green line) and MTS-3 model (red line) with 95% confidence band. Models are developed at sub-district level.

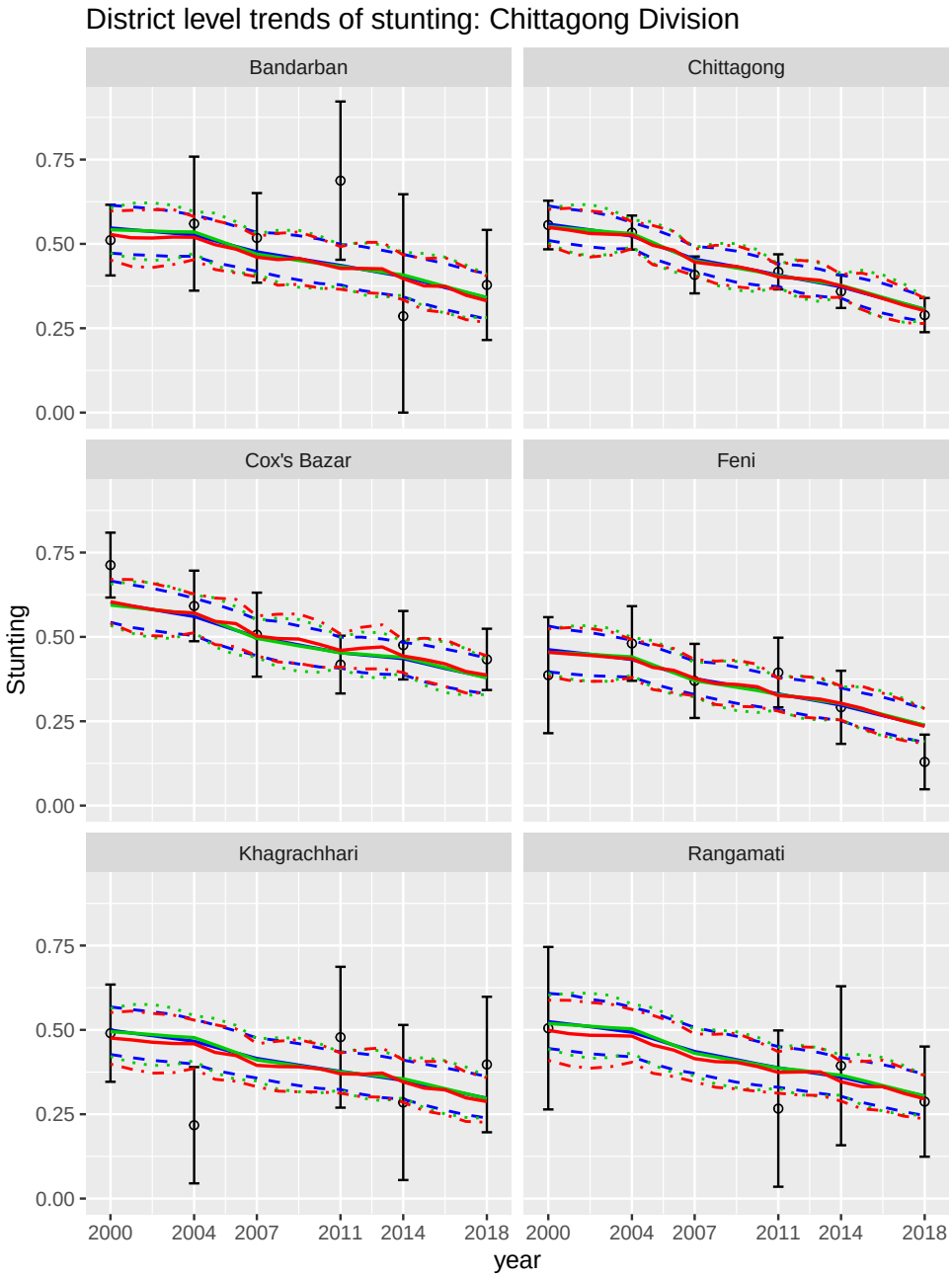


Figure S.3.35: District level trends of stunting among under-5 children in Chittagong division during 2000-2018 estimated by DIR estimator (black error-bar line), MTS-1 model (blue line), MTS-2 model (green line) and MTS-3 model (red line) with 95% confidence band. Models are developed at sub-district level.

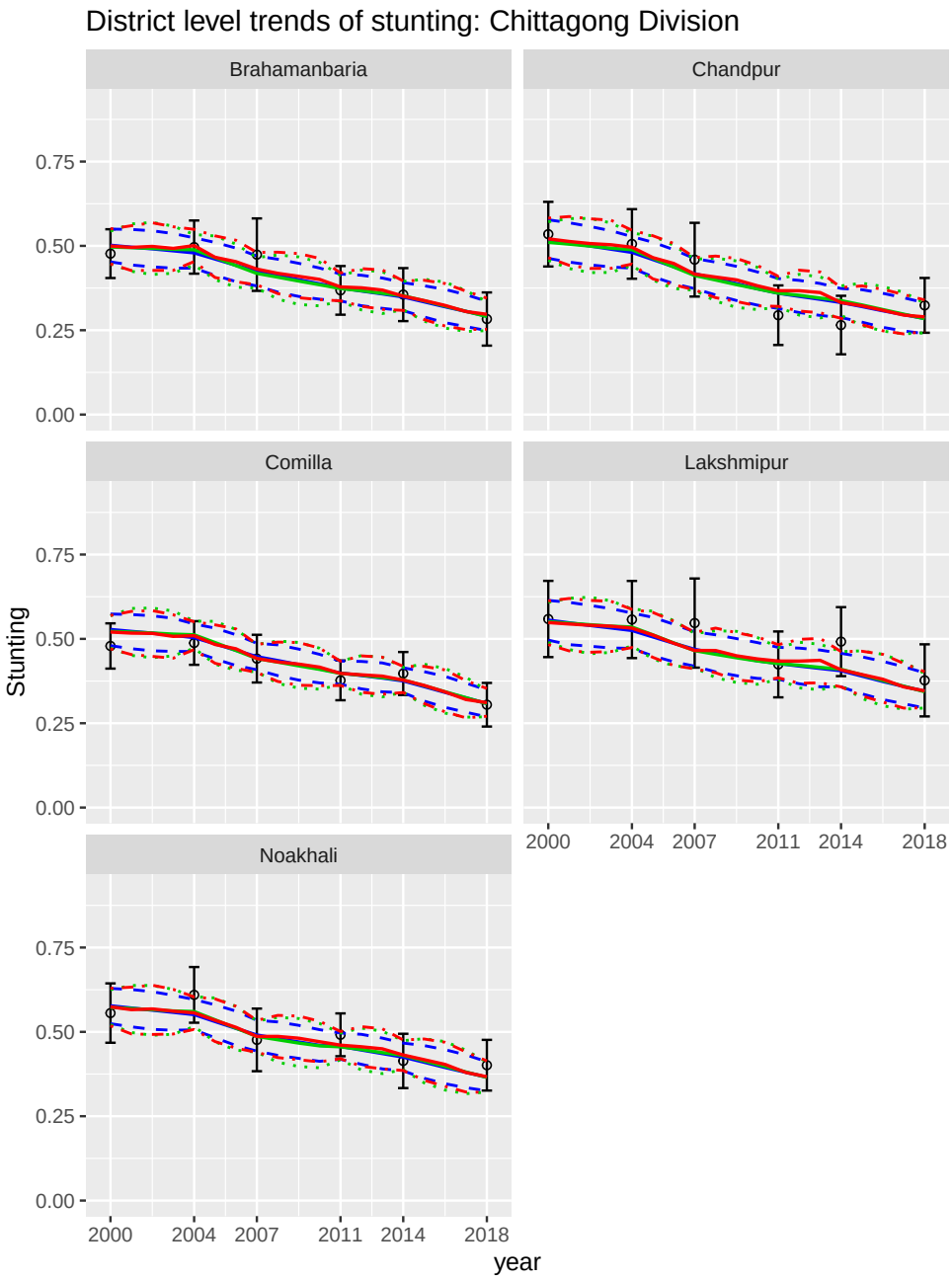


Figure S.3.36: District level trends of stunting among under-5 children in Chittagong division during 2000-2018 estimated by DIR estimator (black error-bar line), MTS-1 model (blue line), MTS-2 model (green line) and MTS-3 model (red line) with 95% confidence band. Models are developed at sub-district level.

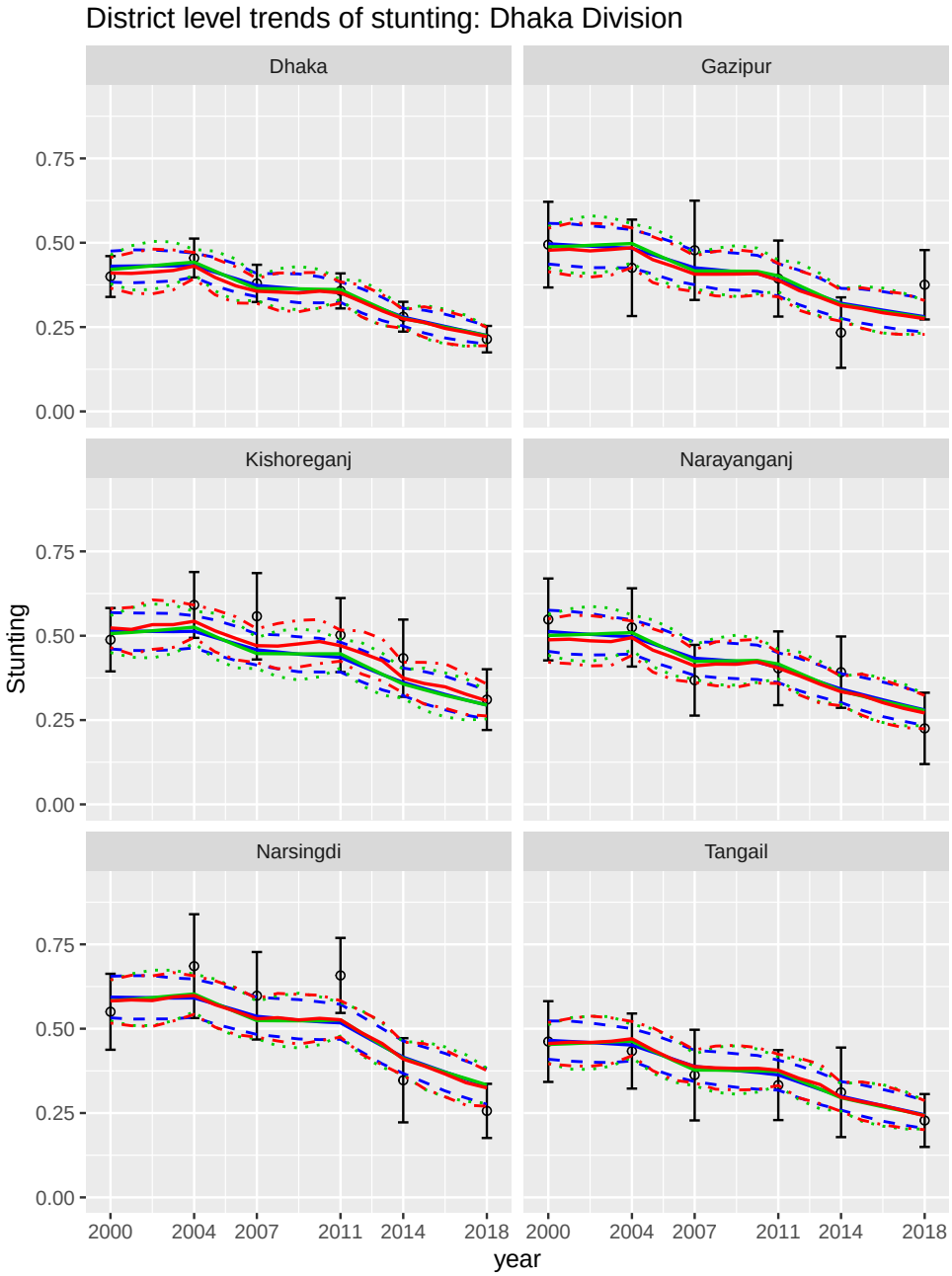


Figure S.3.37: District level trends of stunting among under-5 children in Dhaka division during 2000-2018 estimated by DIR estimator (black error-bar line), MTS-1 model (blue line), MTS-2 model (green line) and MTS-3 model (red line) with 95% confidence band. Models are developed at sub-district level.

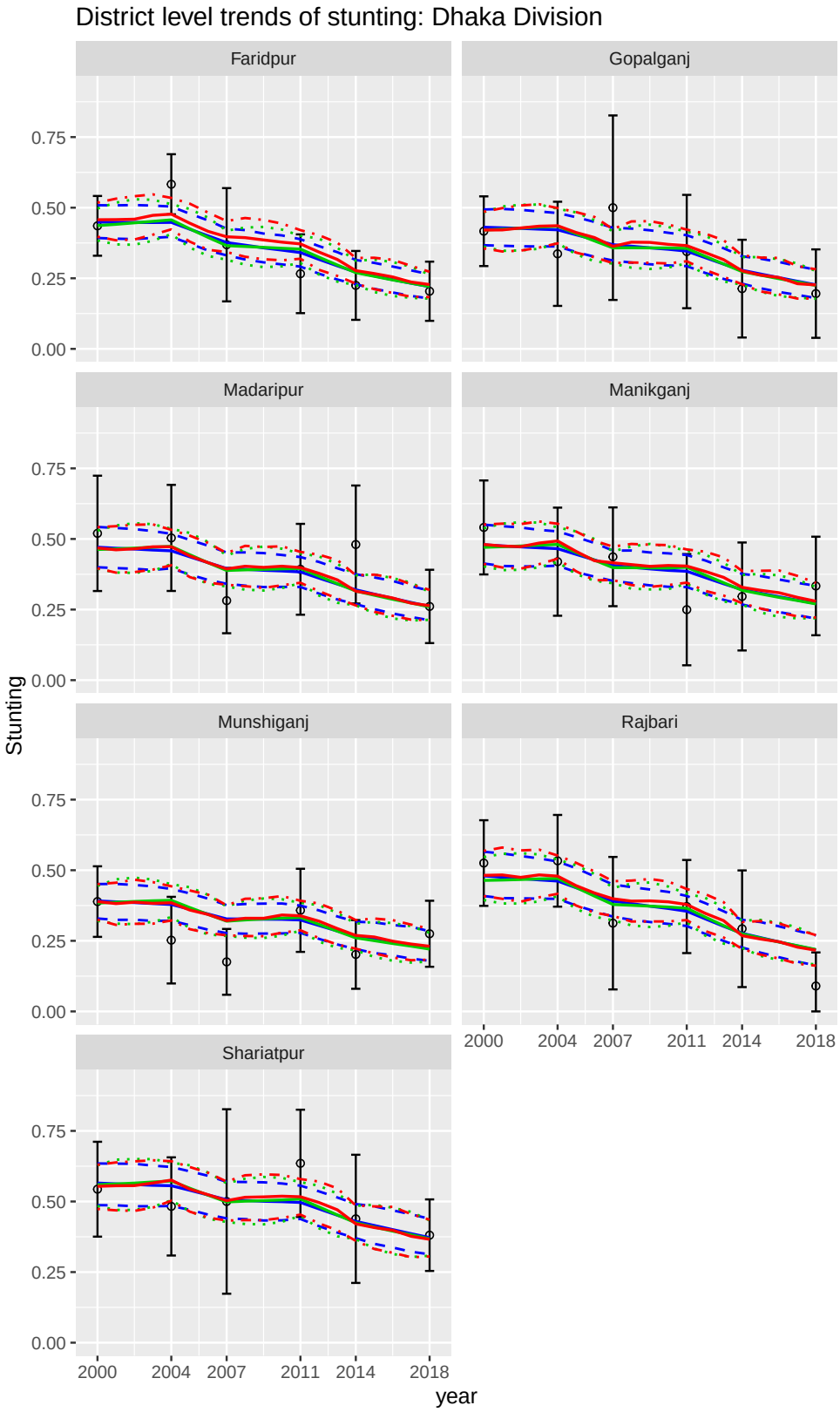


Figure S.3.38: District level trends of stunting among under-5 children in Dhaka division during 2000-2018 estimated by DIR estimator (black error-bar line), MTS-1 model (blue line), MTS-2 model (green line) and MTS-3 model (red line) with 95% confidence band. Models are developed at sub-district level.

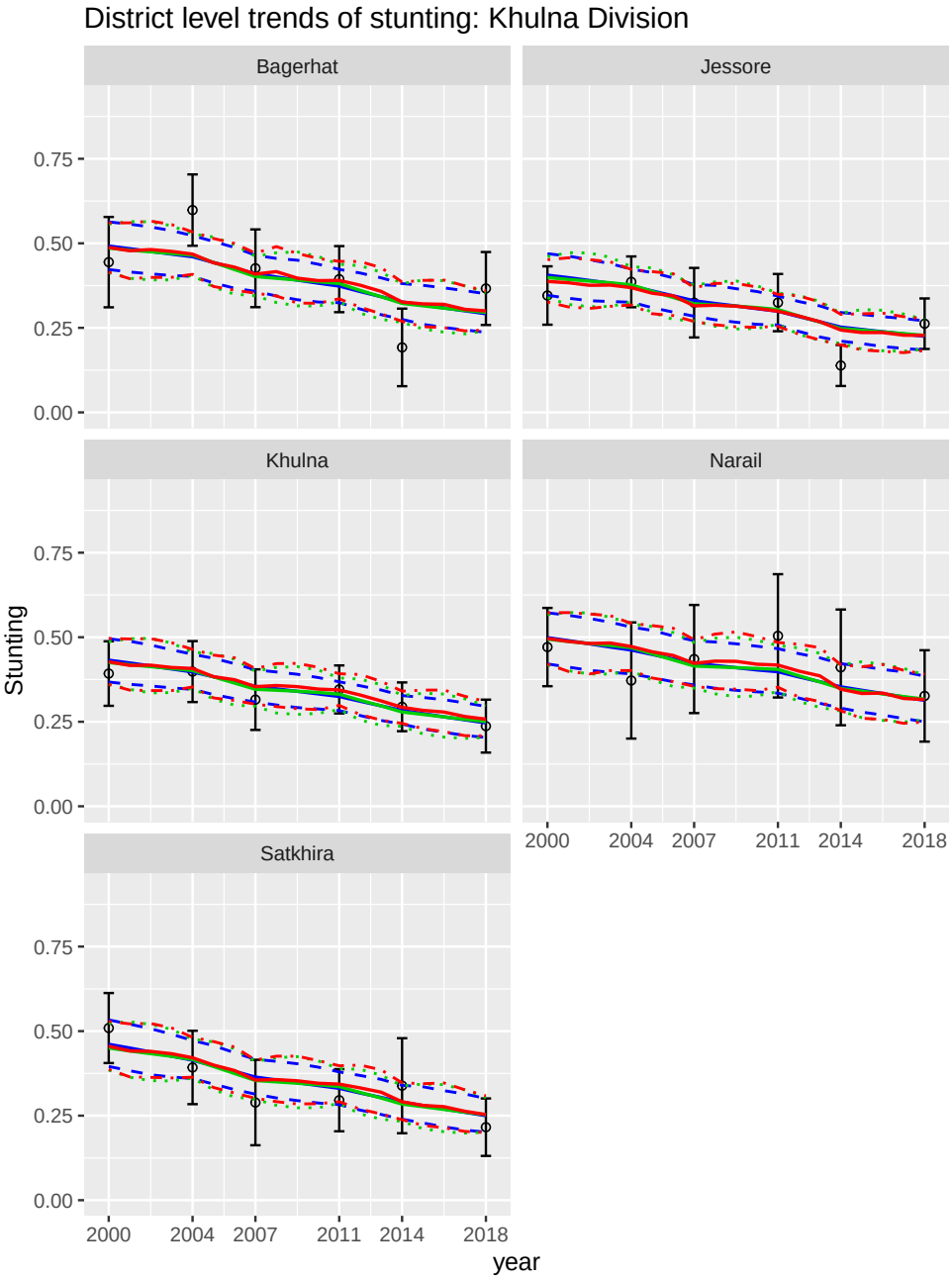


Figure S.3.39: District level trends of stunting among under-5 children in Khulna division during 2000-2018 estimated by DIR estimator (black error-bar line), MTS-1 model (blue line), MTS-2 model (green line) and MTS-3 model (red line) with 95% confidence band. Models are developed at sub-district level.

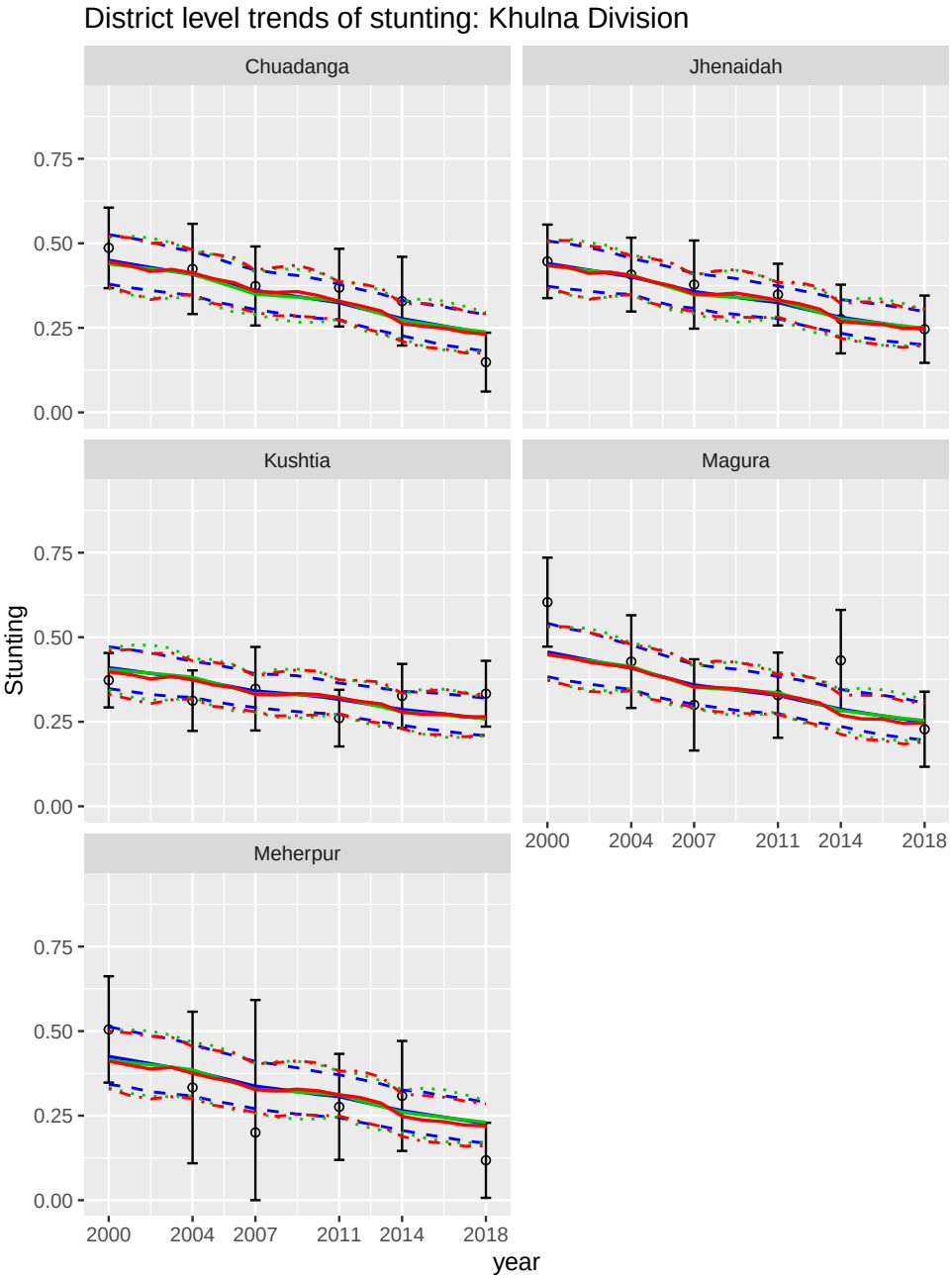


Figure S.3.40: District level trends of stunting among under-5 children in Khulna division during 2000-2018 estimated by DIR estimator (black error-bar line), MTS-1 model (blue line), MTS-2 model (green line) and MTS-3 model (red line) with 95% confidence band. Models are developed at sub-district level.

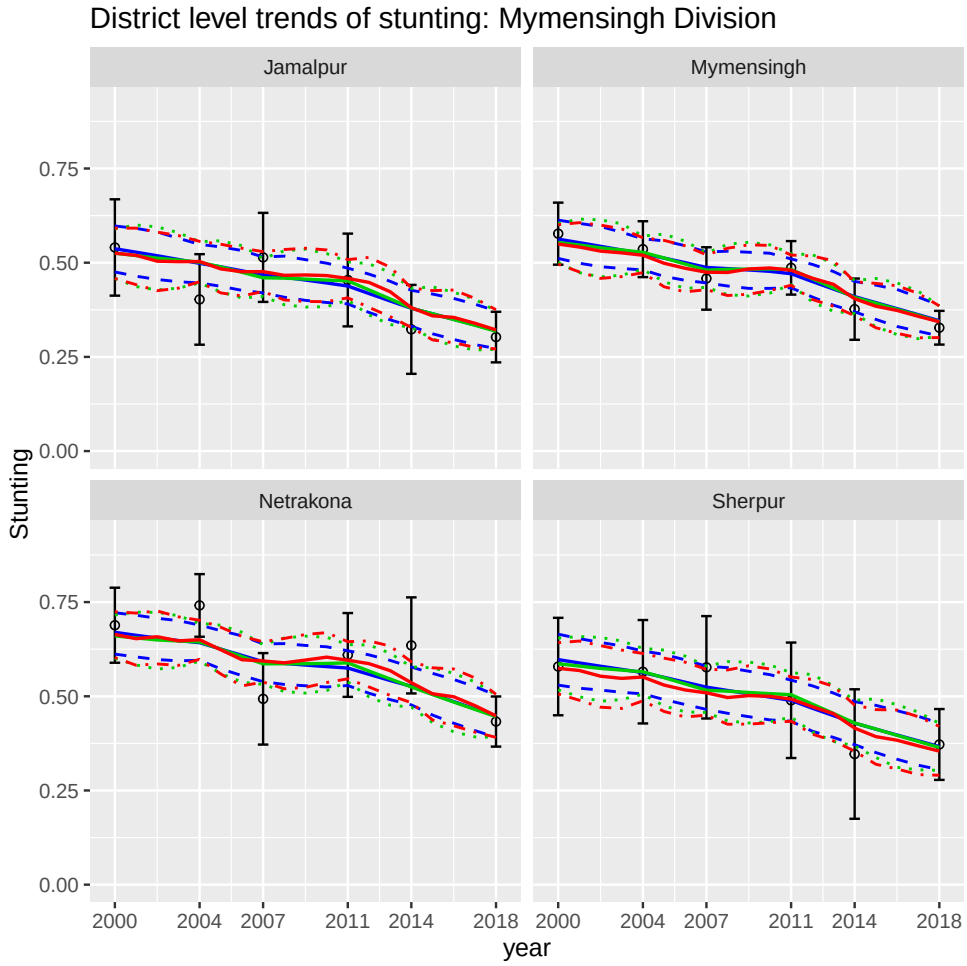


Figure S.3.41: District level trends of stunting among under-5 children in Mymensingh division during 2000-2018 estimated by DIR estimator (black error-bar line), MTS-1 model (blue line), MTS-2 model (green line) and MTS-3 model (red line) with 95% confidence band. Models are developed at sub-district level.

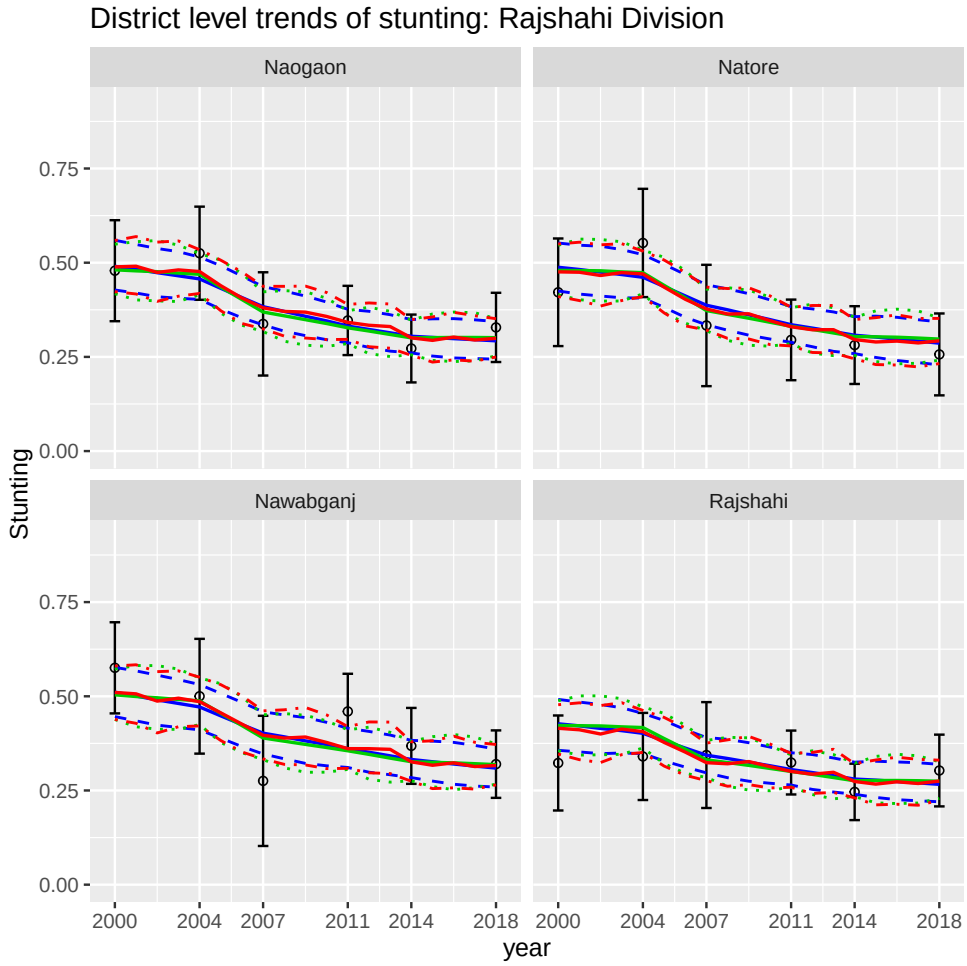


Figure S.3.42: District level trends of stunting among under-5 children in Rajshahi division during 2000-2018 estimated by DIR estimator (black error-bar line), MTS-1 model (blue line), MTS-2 model (green line) and MTS-3 model (red line) with 95% confidence band. Models are developed at sub-district level.

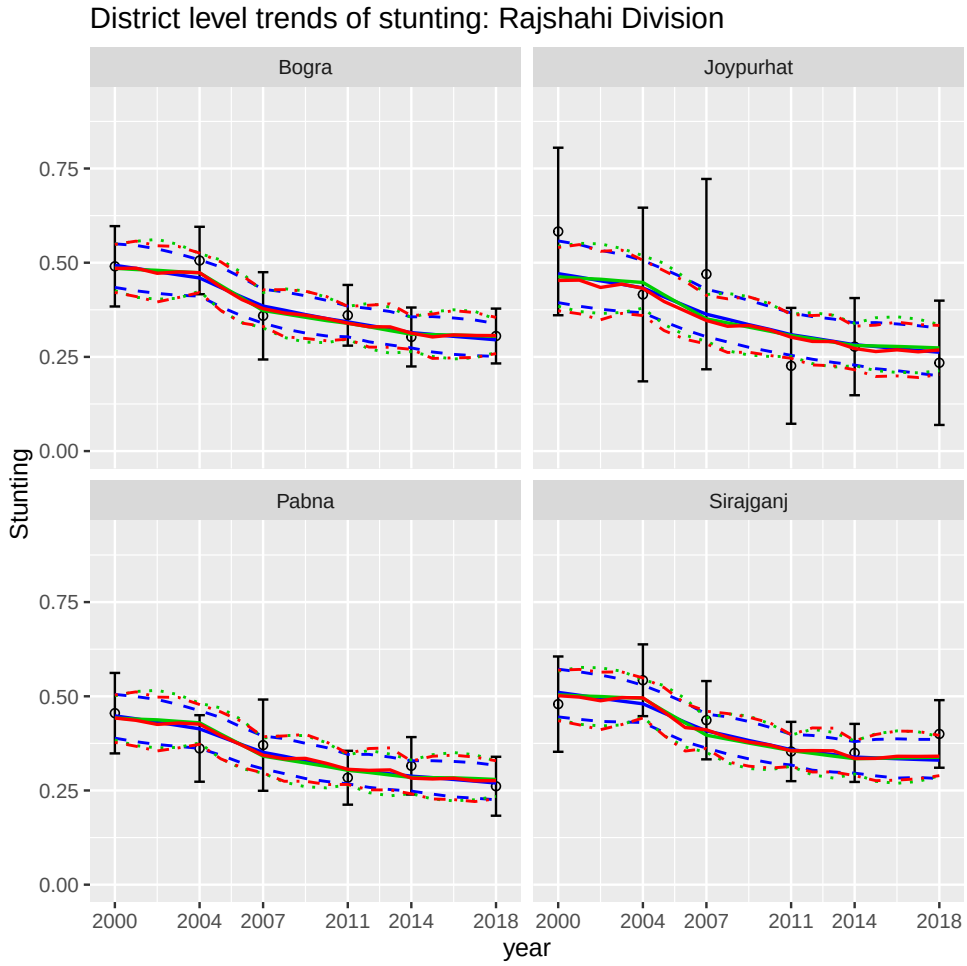


Figure S.3.43: District level trends of stunting among under-5 children in Rajshahi division during 2000-2018 estimated by DIR estimator (black error-bar line), MTS-1 model (blue line), MTS-2 model (green line) and MTS-3 model (red line) with 95% confidence band. Models are developed at sub-district level.

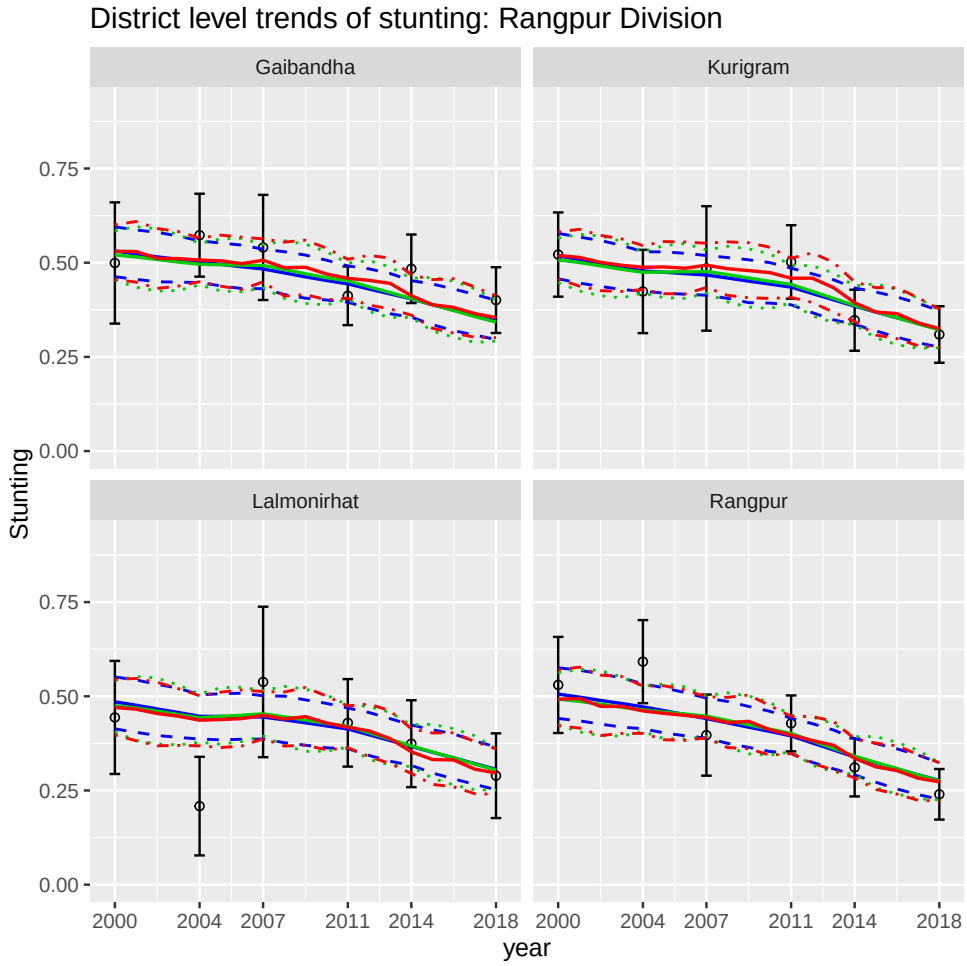


Figure S.3.44: District level trends of stunting among under-5 children in Rangpur division during 2000-2018 estimated by DIR estimator (black error-bar line), MTS-1 model (blue line), MTS-2 model (green line) and MTS-3 model (red line) with 95% confidence band. Models are developed at sub-district level.

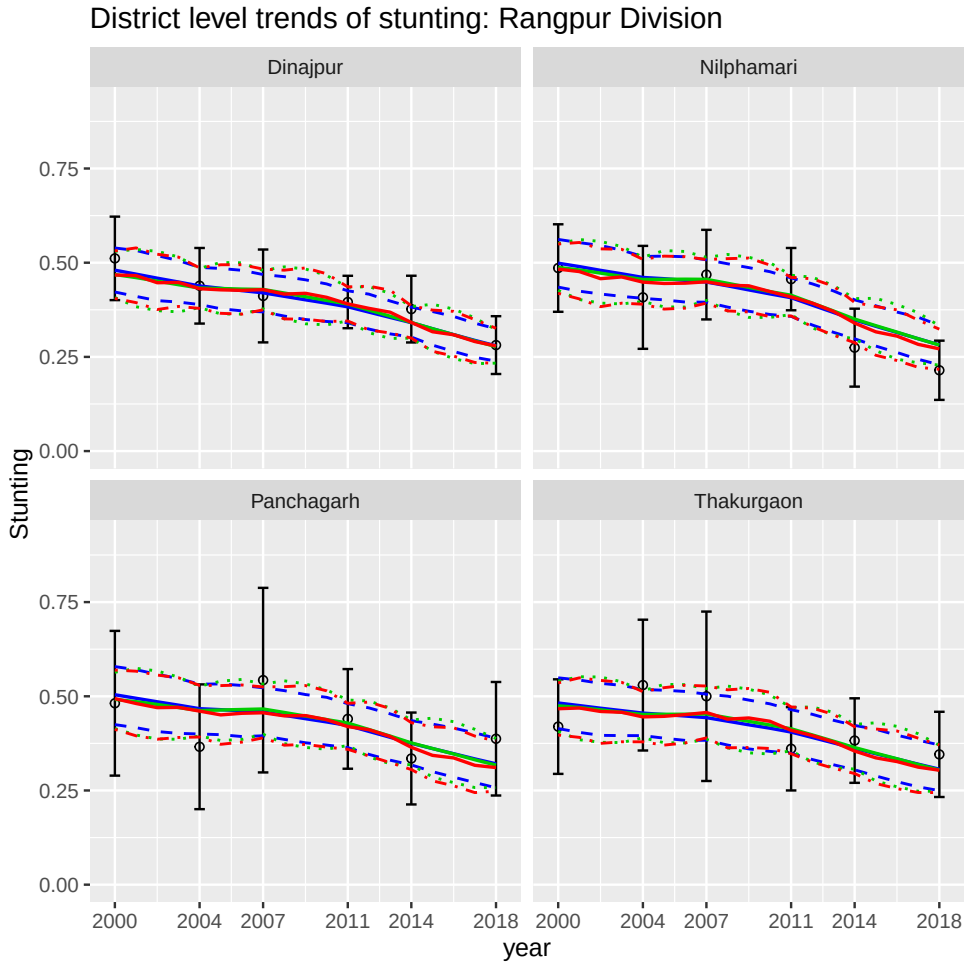


Figure S.3.45: District level trends of stunting among under-5 children in Rangpur division during 2000-2018 estimated by DIR estimator (black error-bar line), MTS-1 model (blue line), MTS-2 model (green line) and MTS-3 model (red line) with 95% confidence band. Models are developed at sub-district level.



Figure S.3.46: District level trends of stunting among under-5 children in Sylhet division during 2000-2018 estimated by DIR estimator (black error-bar line), MTS-1 model (blue line), MTS-2 model (green line) and MTS-3 model (red line) with 95% confidence band. Models are developed at sub-district level.

S.4 Trends of Stunting at sub-district level

Sub-district level trends of stunting among under-5 children for the reference period 2000-2018 estimated by DIR estimator (black error-bar line), MTS-1 model (blue line), MTS-2 model (green line) and MTS-3 model (red line) with 95% confidence band are shown by district as per their division in the following pages.

S.4.1 sub-district level trends: Barisal division

There are 6 districts and 40 sub-districts under Barisal division. The trends estimates of stunting for each of the sub-districts are shown under their respective districts in Figures from S.4.47 to S.4.53.

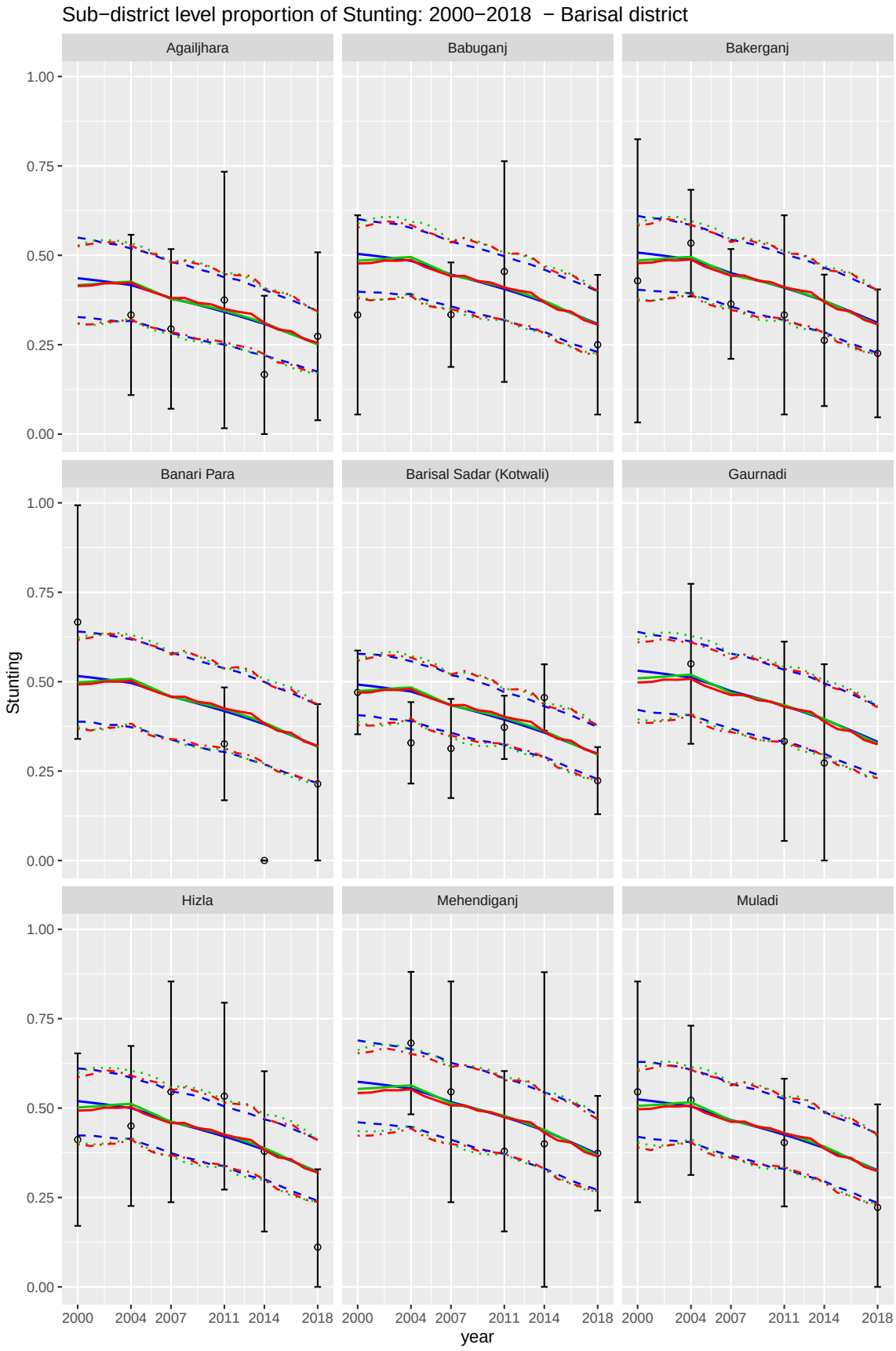


Figure S.4.47: Sub-district level trends of stunting in Barisal district during 2000-2018 by DIR estimator (black error-bar line), MTS-1 model (blue line), MTS-2 model (green line) and MTS-3 model (red line) with 95% confidence band. Models are developed at sub-district level.

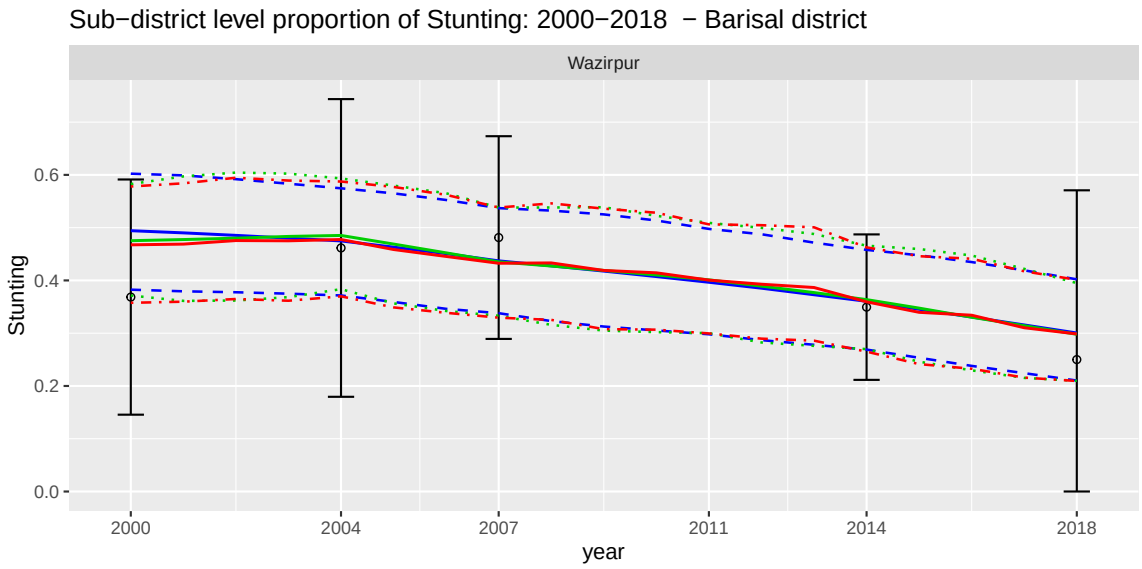


Figure S.4.48: Sub-district level trends of stunting in Barisal district during 2000-2018 by DIR estimator (black error-bar line), MTS-1 model (blue line), MTS-2 model (green line) and MTS-3 model (red line) with 95% confidence band. Models are developed at sub-district level.

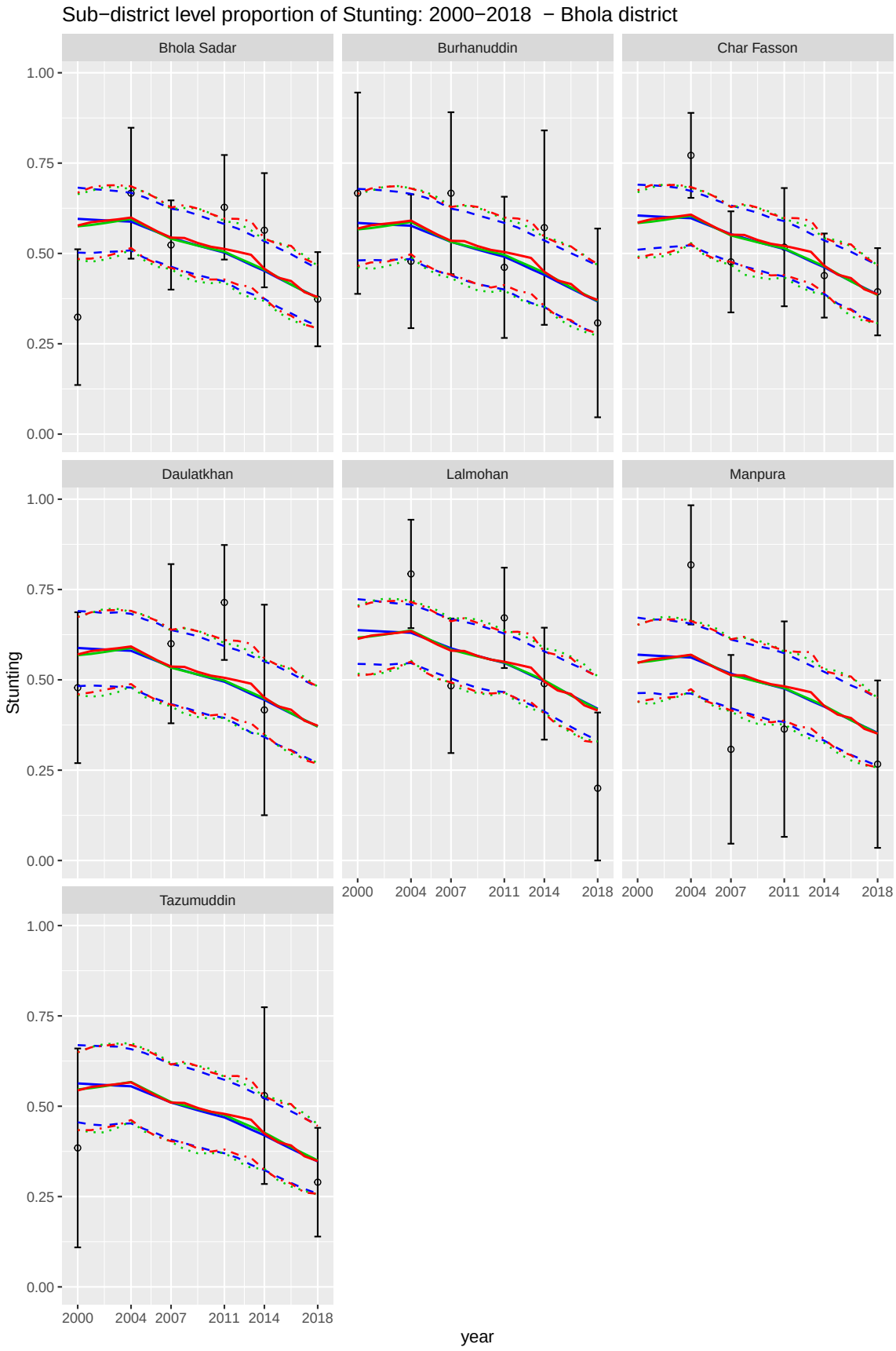


Figure S.4.49: Sub-district level trends of stunting in Bhola district during 2000-2018 by DIR estimator (black error-bar line), MTS-1 model (blue line), MTS-2 model (green line) and MTS-3 model (red line) with 95% confidence band. Models are developed at sub-district level.

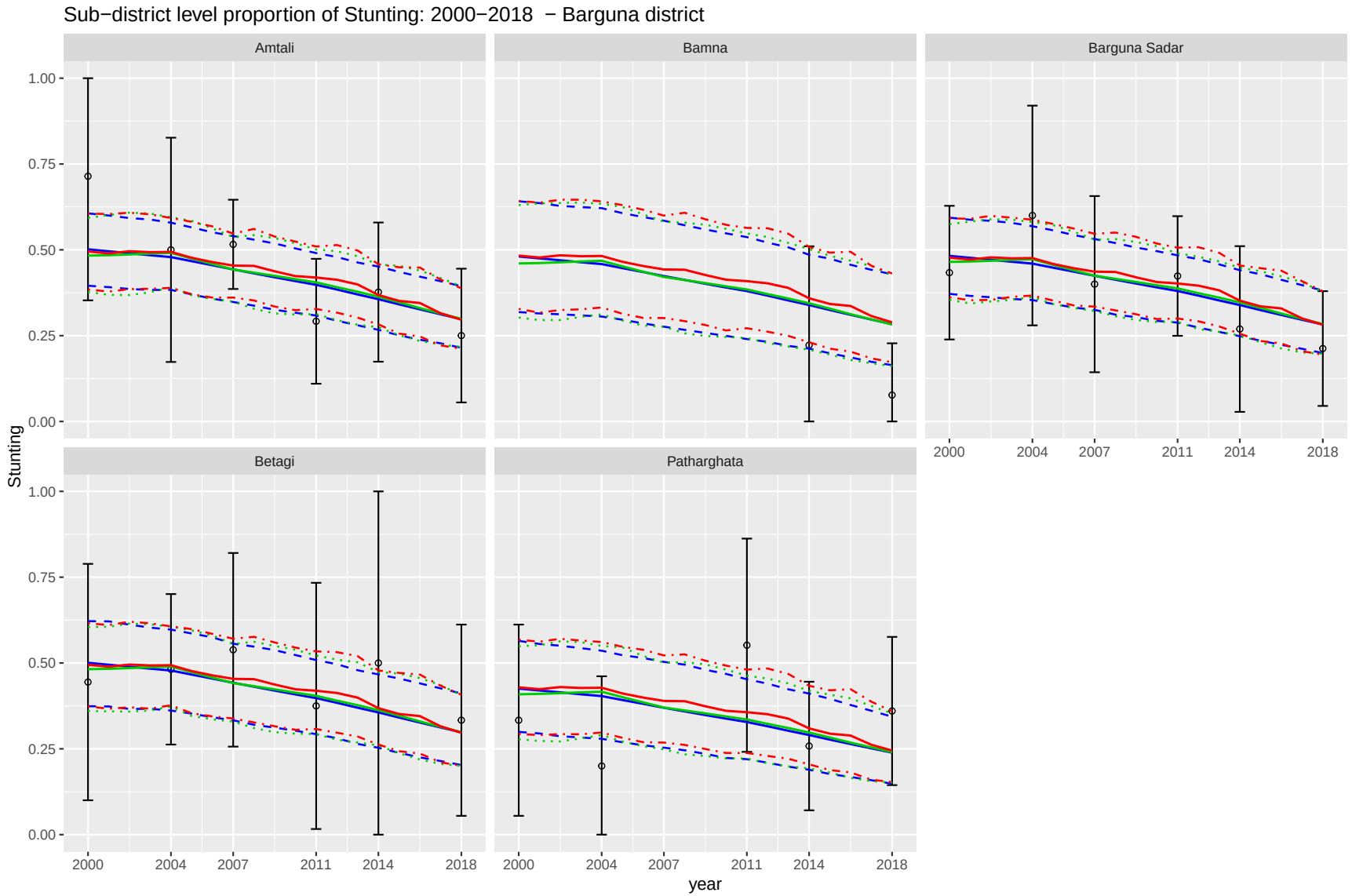


Figure S.4.50: Sub-district level trends of stunting in Barguna district during 2000-2018 by DIR estimator (black error-bar line), MTS-1 model (blue line), MTS-2 model (green line) and MTS-3 model (red line) with 95% confidence band. Models are developed at sub-district level.

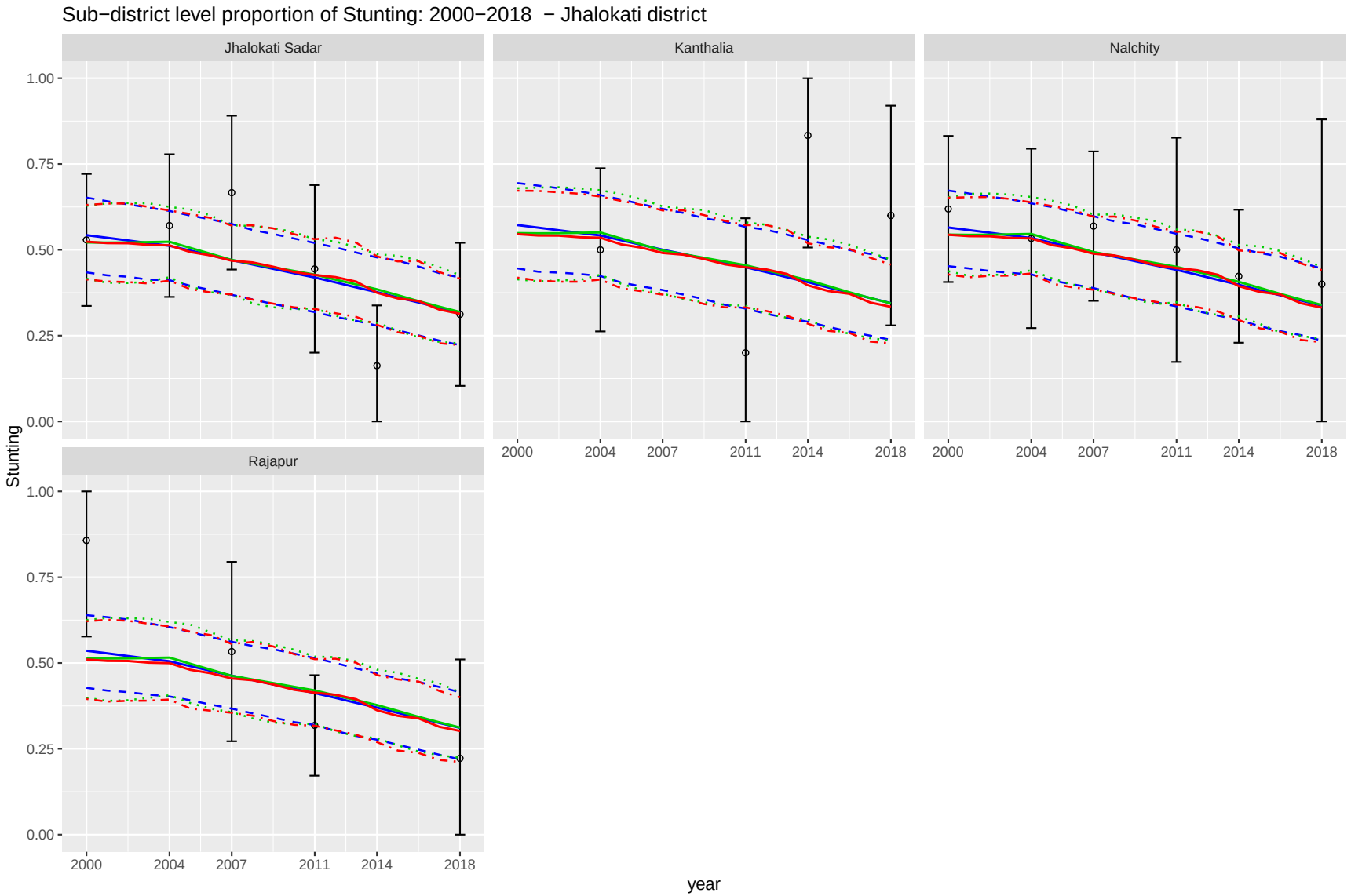


Figure S.4.51: Sub-district level trends of stunting in Jhalokati district during 2000-2018 by DIR estimator (black error-bar line), MTS-1 model (blue line), MTS-2 model (green line) and MTS-3 model (red line) with 95% confidence band. Models are developed at sub-district level.

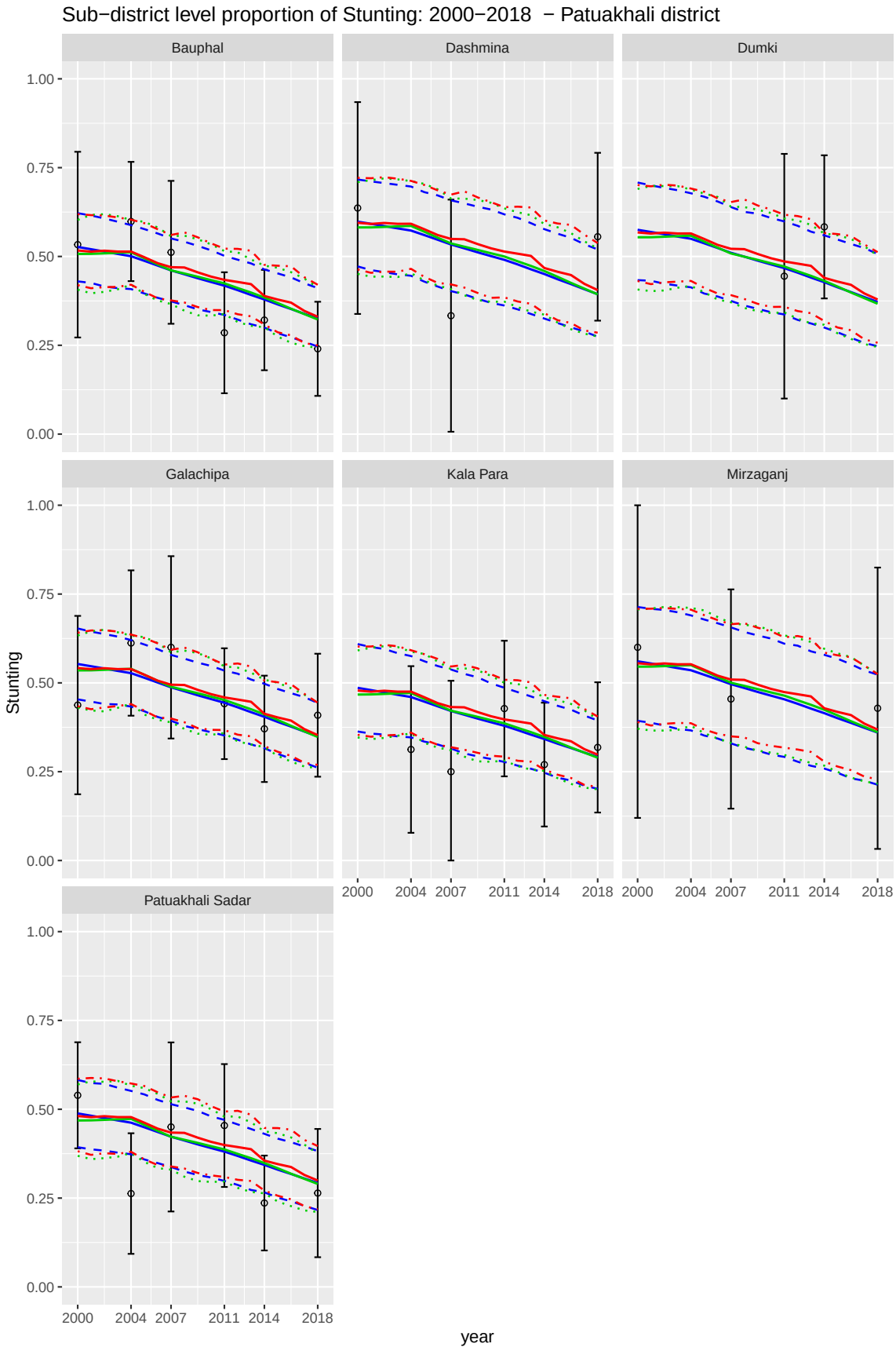


Figure S.4.52: Sub-district level trends of stunting in Patuakhali district during 2000-2018 by DIR estimator (black error-bar line), MTS-1 model (blue line), MTS-2 model (green line) and MTS-3 model (red line) with 95% confidence band. Models are developed at sub-district level.

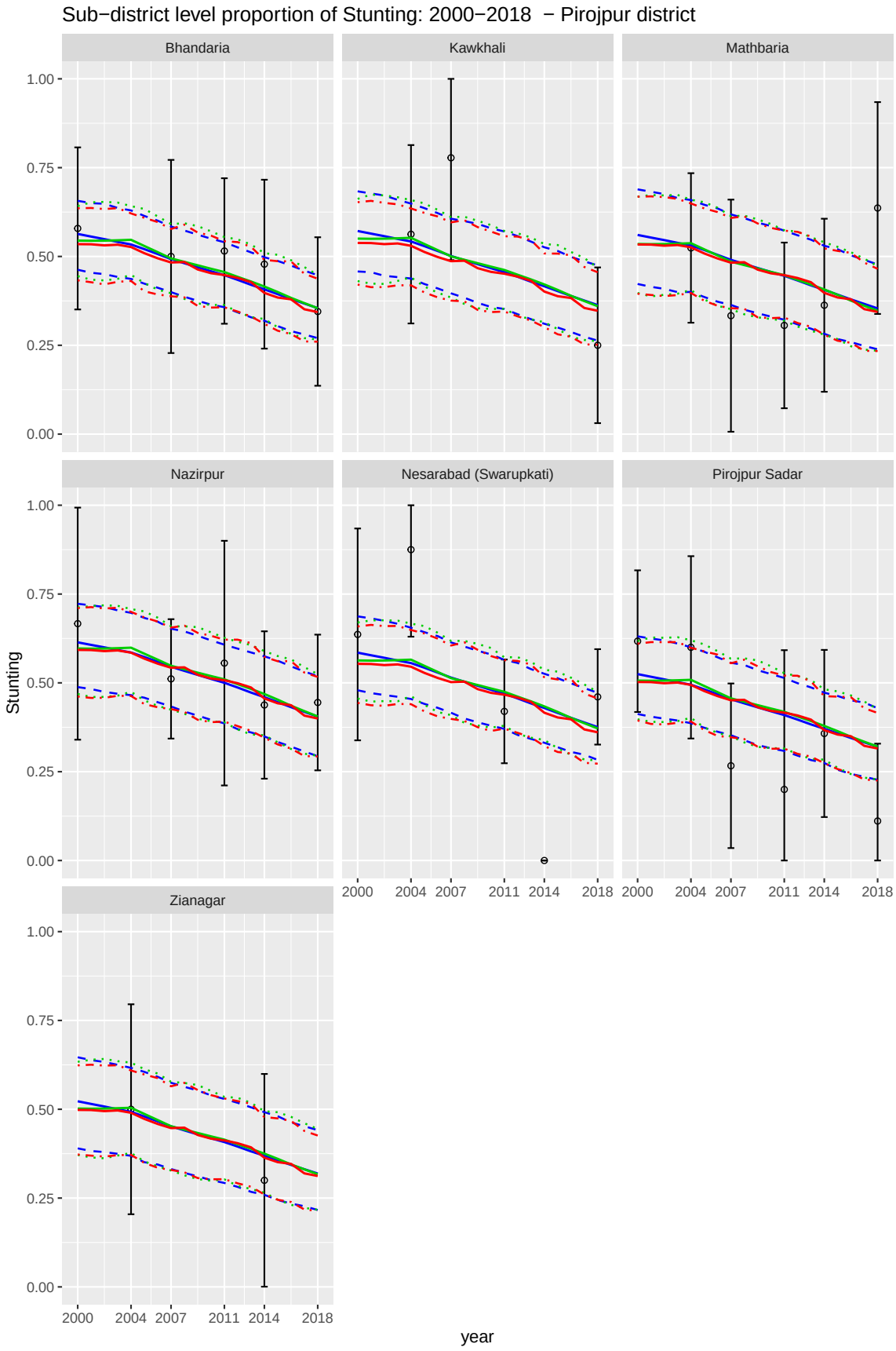


Figure S.4.53: Sub-district level trends of stunting in Pirojpur district during 2000-2018 by DIR estimator (black error-bar line), MTS-1 model (blue line), MTS-2 model (green line) and MTS-3 model (red line) with 95% confidence band. Models are developed at sub-district level.

S.4.2 sub-district level trends: Chittagong division

There are 11 districts and 111 sub-districts under Chittagong division. Chittagong district consists of 25 sub-districts, among which many of them are urban. The trends estimates of stunting for each of the sub-districts are shown under their respective districts in Figures from S.4.54 to S.4.67.

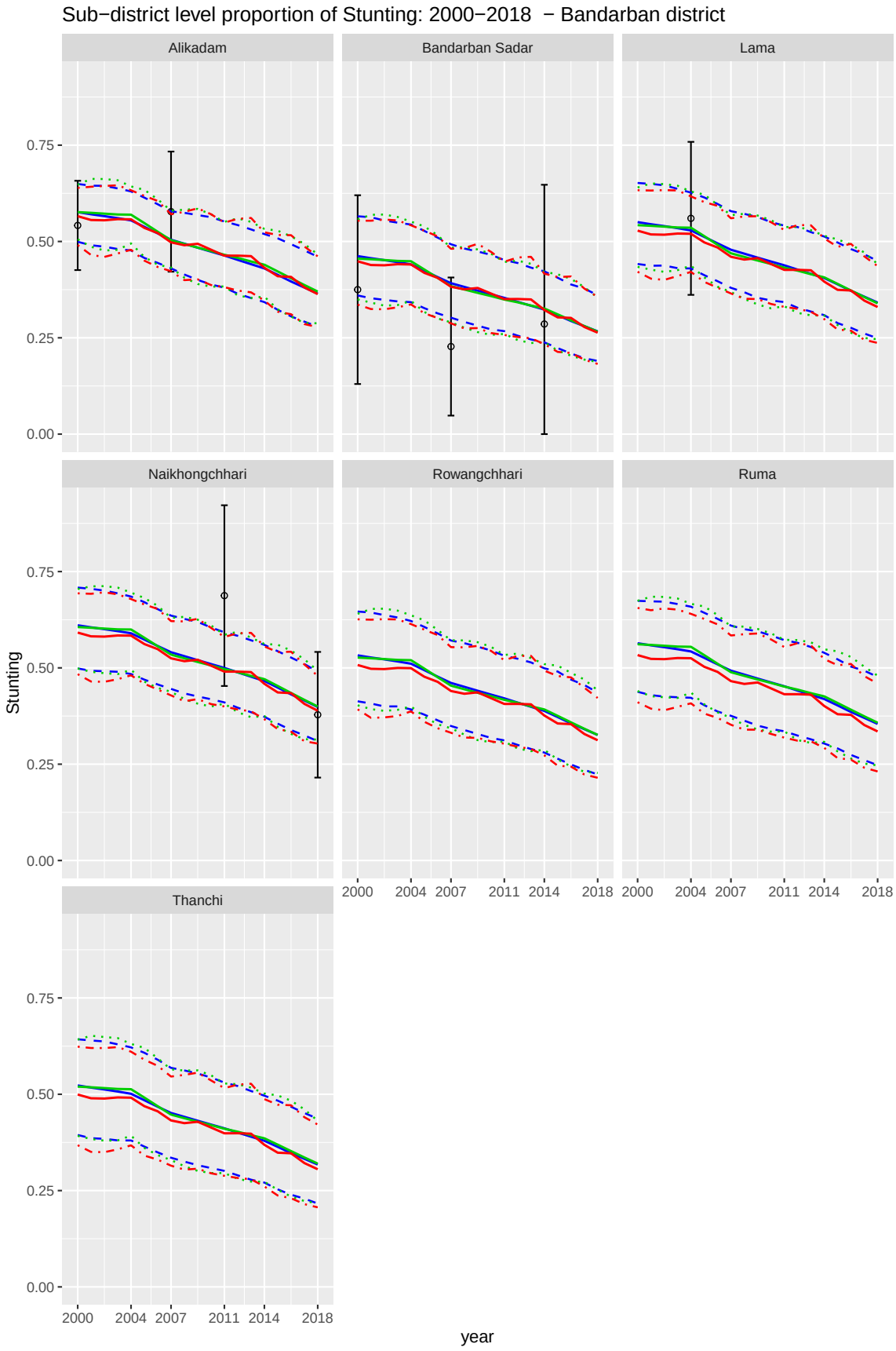


Figure S.4.54: Sub-district level trends of stunting in Chittagong district during 2000-2018 by DIR estimator (black error-bar line), MTS-1 model (blue line), MTS-2 model (green line) and MTS-3 model (red line) with 95% confidence band. Models are developed at sub-district level.

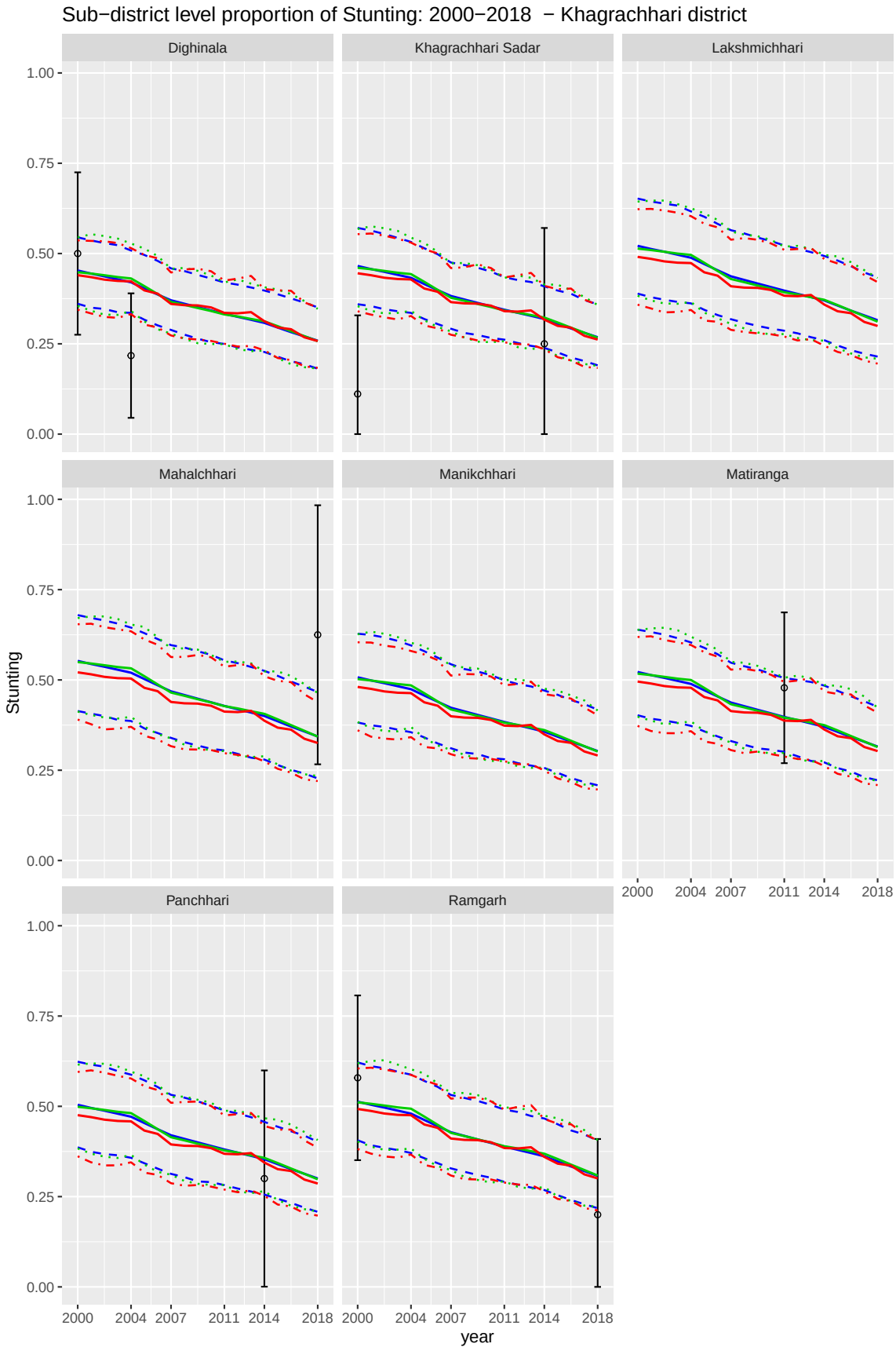


Figure S.4.55: Sub-district level trends of stunting in Chittagong district during 2000-2018 by DIR estimator (black error-bar line), MTS-1 model (blue line), MTS-2 model (green line) and MTS-3 model (red line) with 95% confidence band. Models are developed at sub-district level.

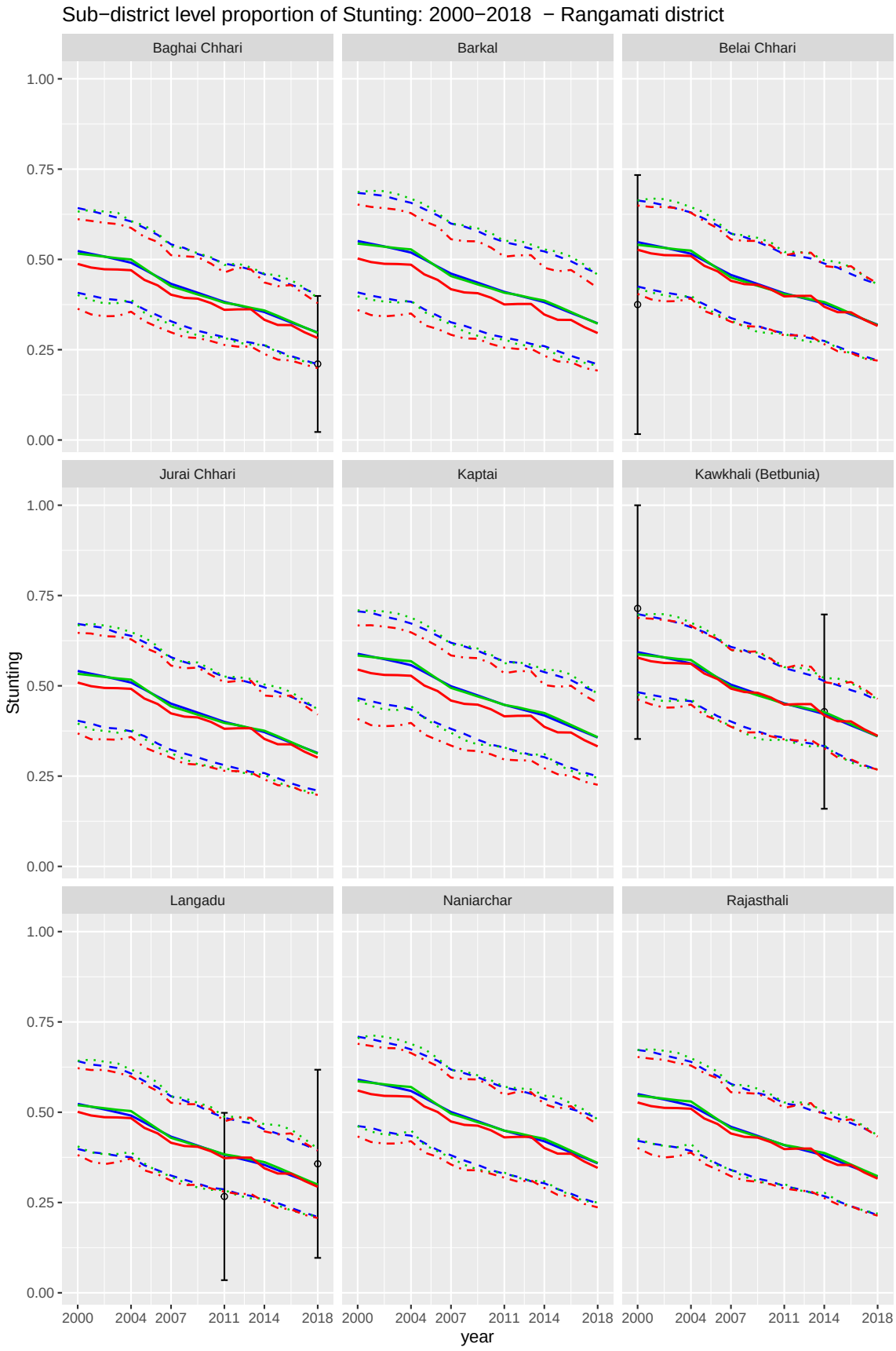


Figure S.4.56: Sub-district level trends of stunting in Chittagong district during 2000-2018 by DIR estimator (black error-bar line), MTS-1 model (blue line), MTS-2 model (green line) and MTS-3 model (red line) with 95% confidence band. Models are developed at sub-district level.

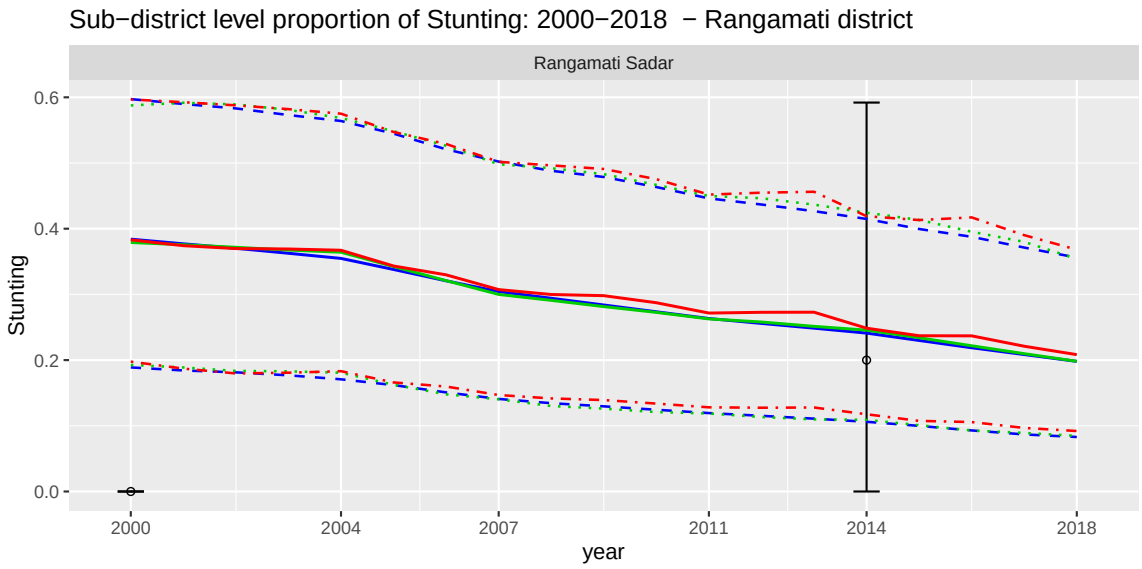


Figure S.4.57: Sub-district level trends of stunting in Chittagong district during 2000-2018 by DIR estimator (black error-bar line), MTS-1 model (blue line), MTS-2 model (green line) and MTS-3 model (red line) with 95% confidence band. Models are developed at sub-district level.

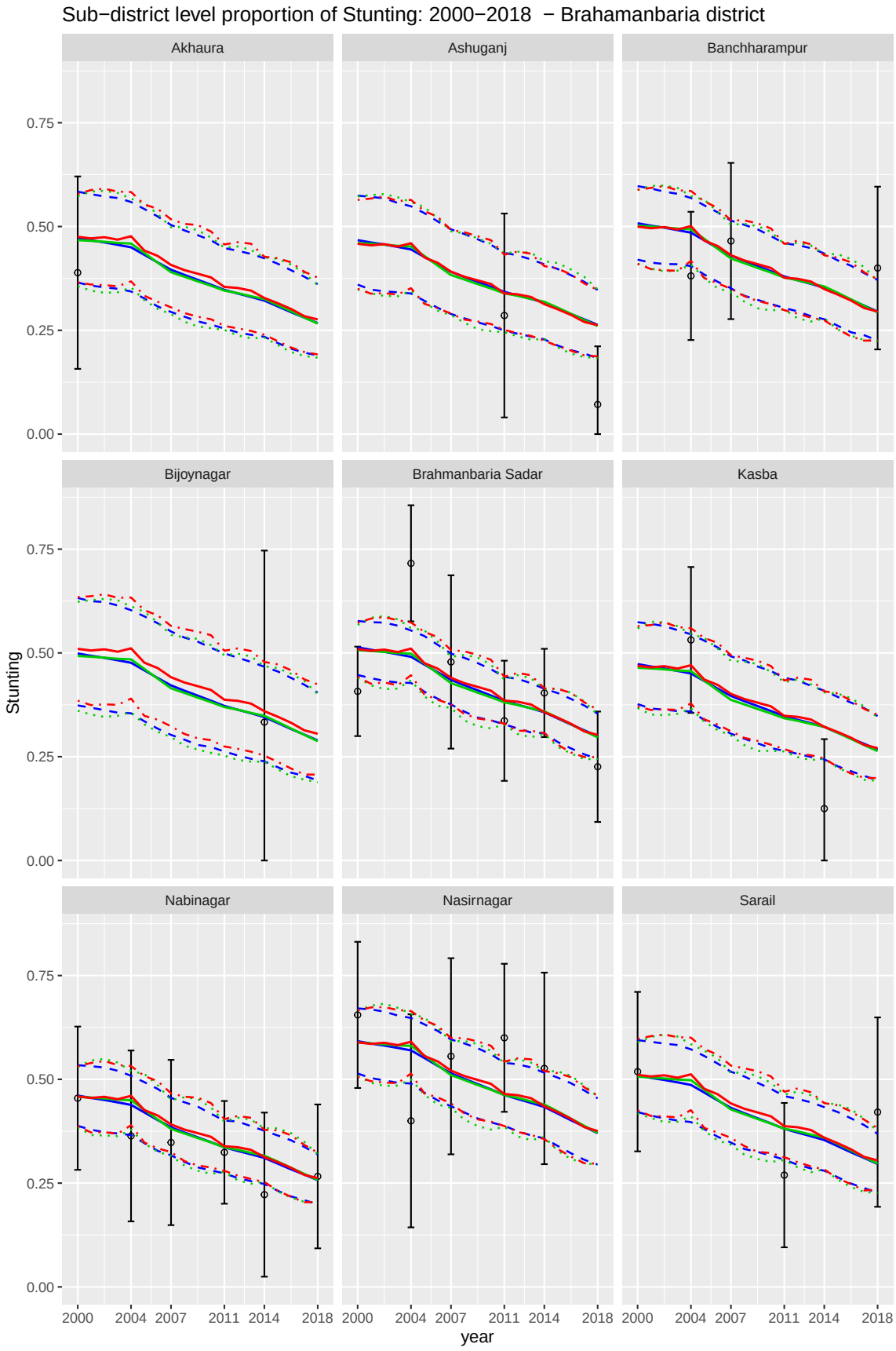


Figure S.4.58: Sub-district level trends of stunting in Chittagong district during 2000-2018 by DIR estimator (black error-bar line), MTS-1 model (blue line), MTS-2 model (green line) and MTS-3 model (red line) with 95% confidence band. Models are developed at sub-district level.

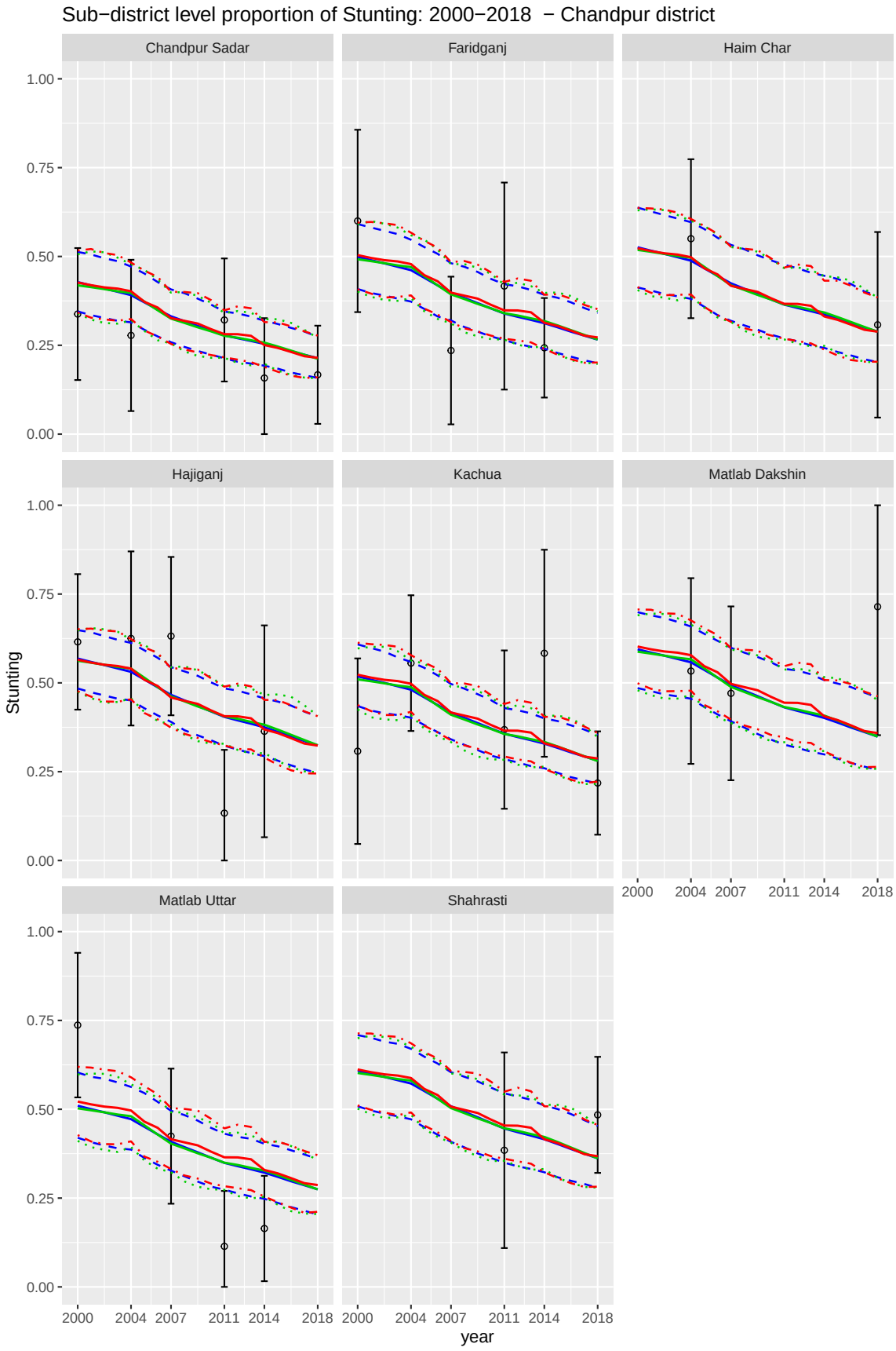


Figure S.4.59: Sub-district level trends of stunting in Chittagong district during 2000-2018 by DIR estimator (black error-bar line), MTS-1 model (blue line), MTS-2 model (green line) and MTS-3 model (red line) with 95% confidence band. Models are developed at sub-district level.

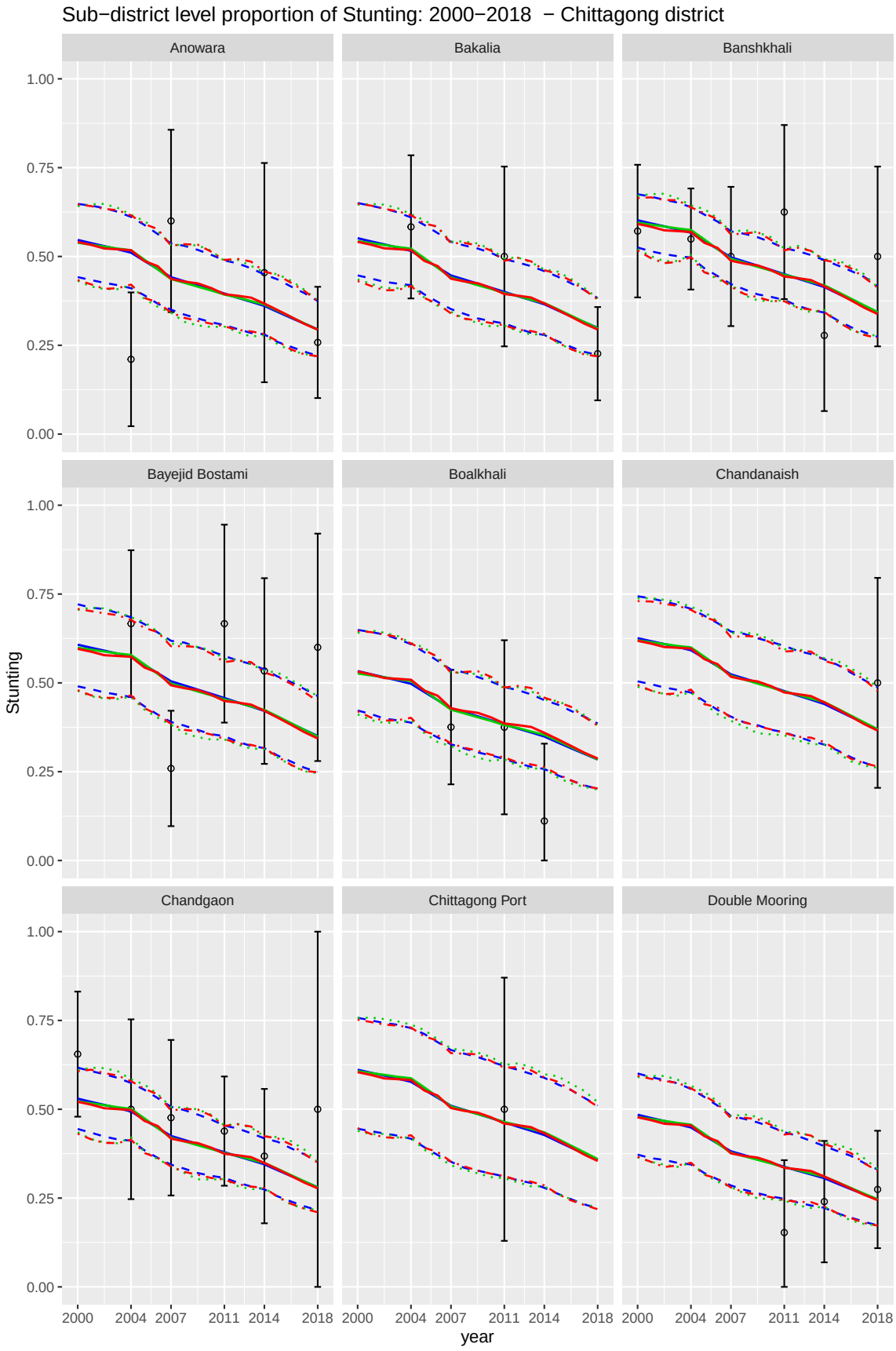


Figure S.4.60: Sub-district level trends of stunting in Chittagong district during 2000-2018 by DIR estimator (black error-bar line), MTS-1 model (blue line), MTS-2 model (green line) and MTS-3 model (red line) with 95% confidence band. Models are developed at sub-district level.

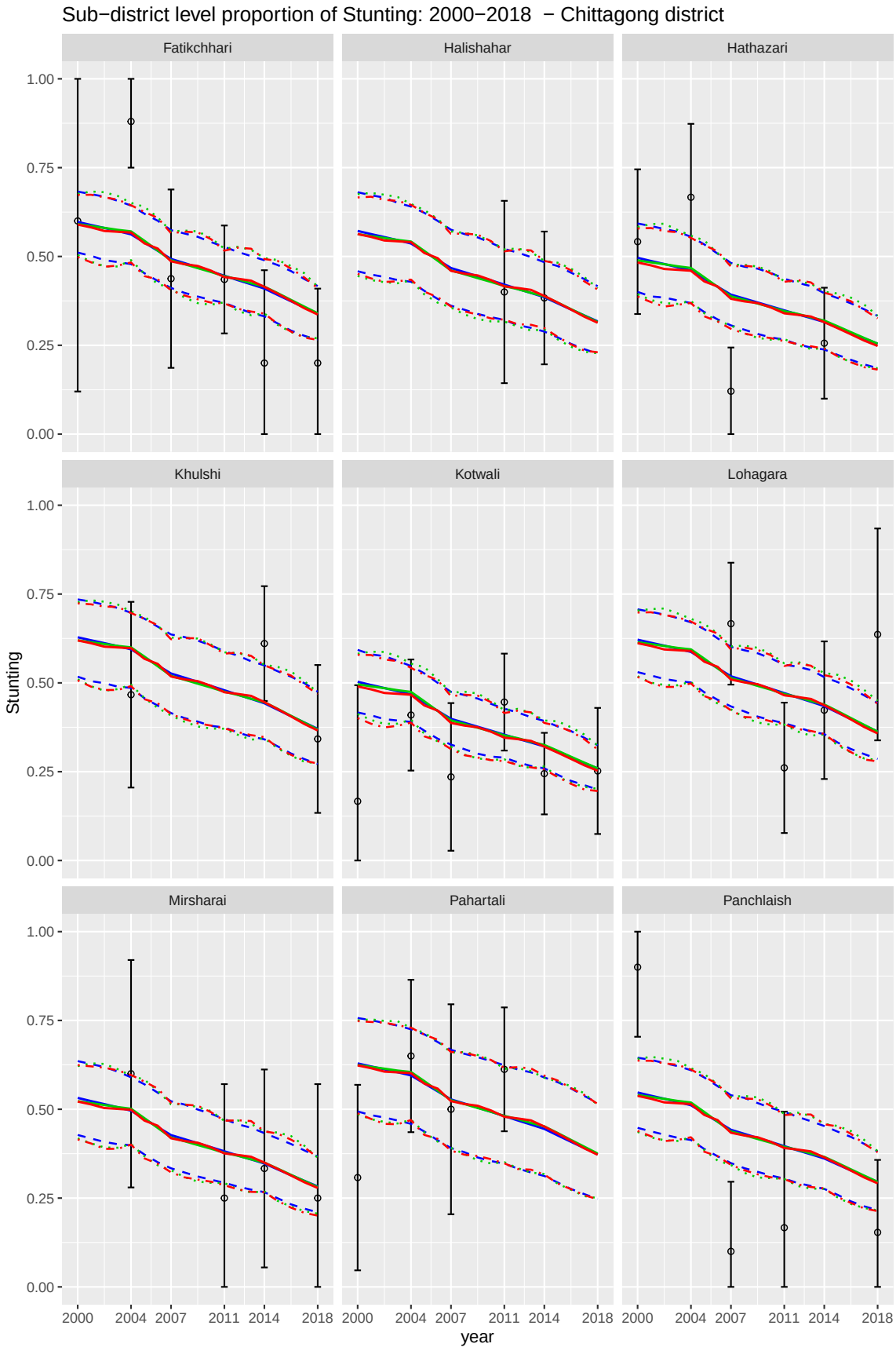


Figure S.4.61: Sub-district level trends of stunting in Chittagong district during 2000-2018 by DIR estimator (black error-bar line), MTS-1 model (blue line), MTS-2 model (green line) and MTS-3 model (red line) with 95% confidence band. Models are developed at sub-district level.

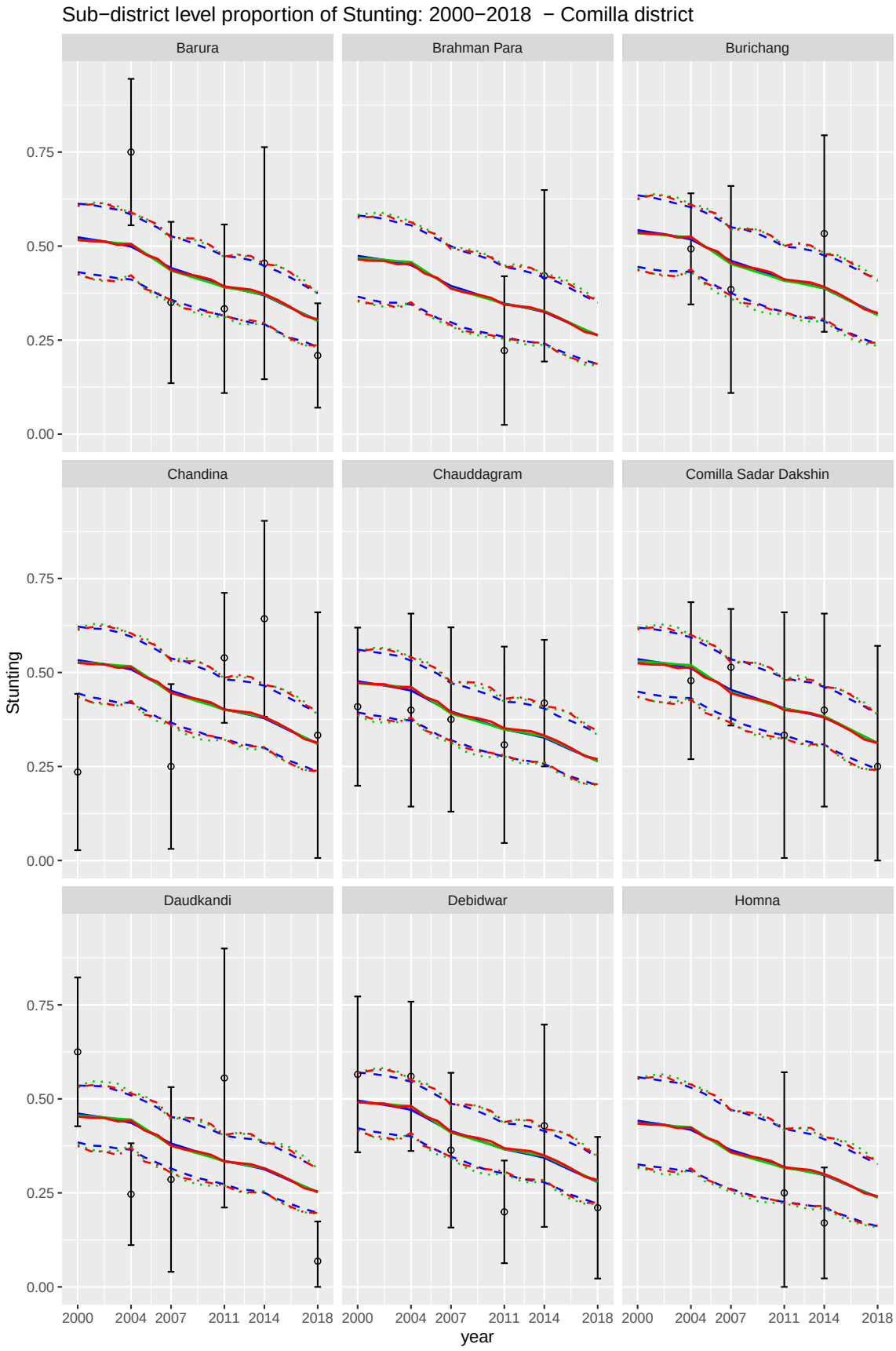


Figure S.4.62: Sub-district level trends of stunting in Chittagong district during 2000-2018 by DIR estimator (black error-bar line), MTS-1 model (blue line), MTS-2 model (green line) and MTS-3 model (red line) with 95% confidence band. Models are developed at sub-district level.

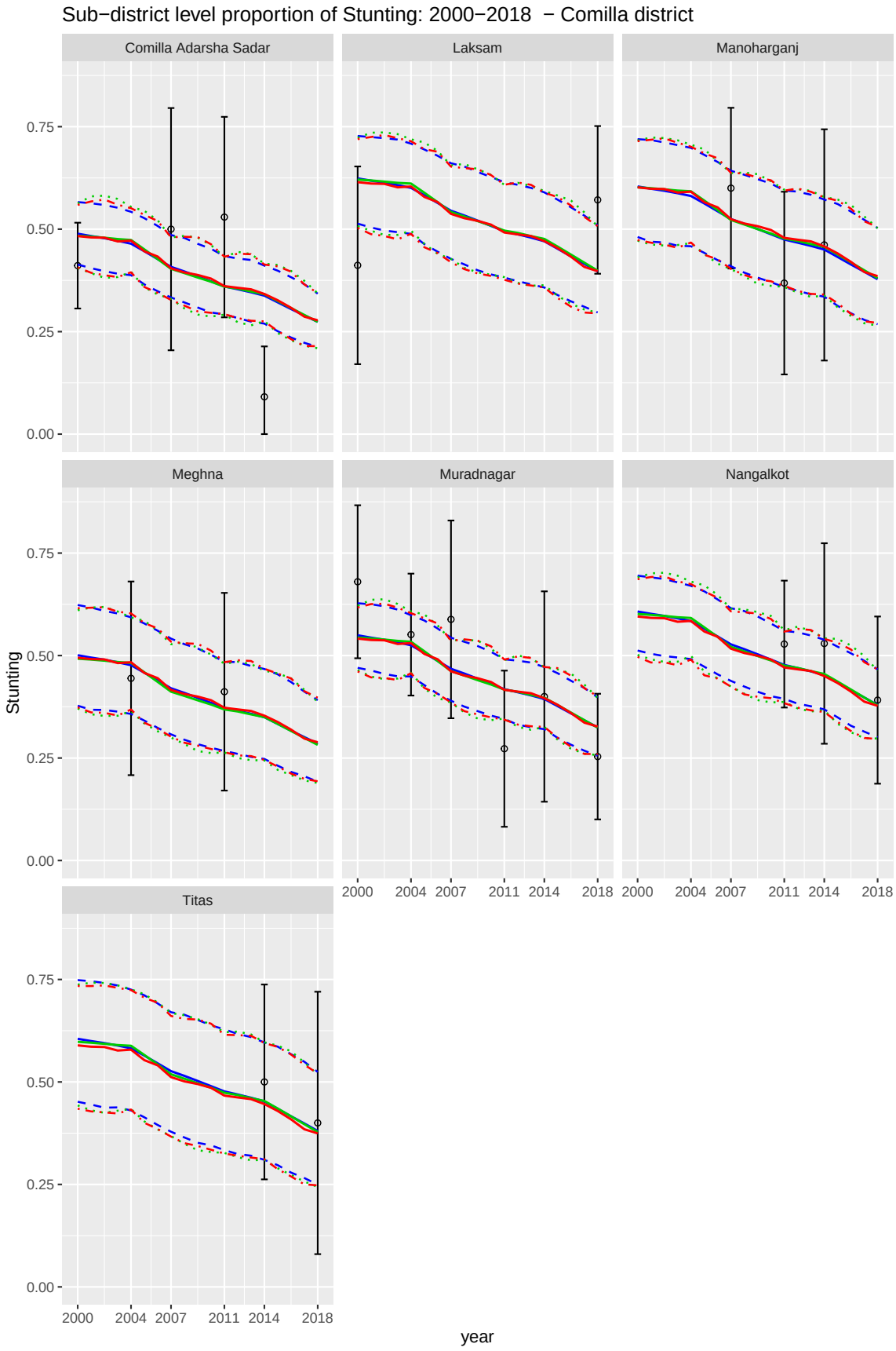


Figure S.4.63: Sub-district level trends of stunting in Chittagong district during 2000-2018 by DIR estimator (black error-bar line), MTS-1 model (blue line), MTS-2 model (green line) and MTS-3 model (red line) with 95% confidence band. Models are developed at sub-district level.

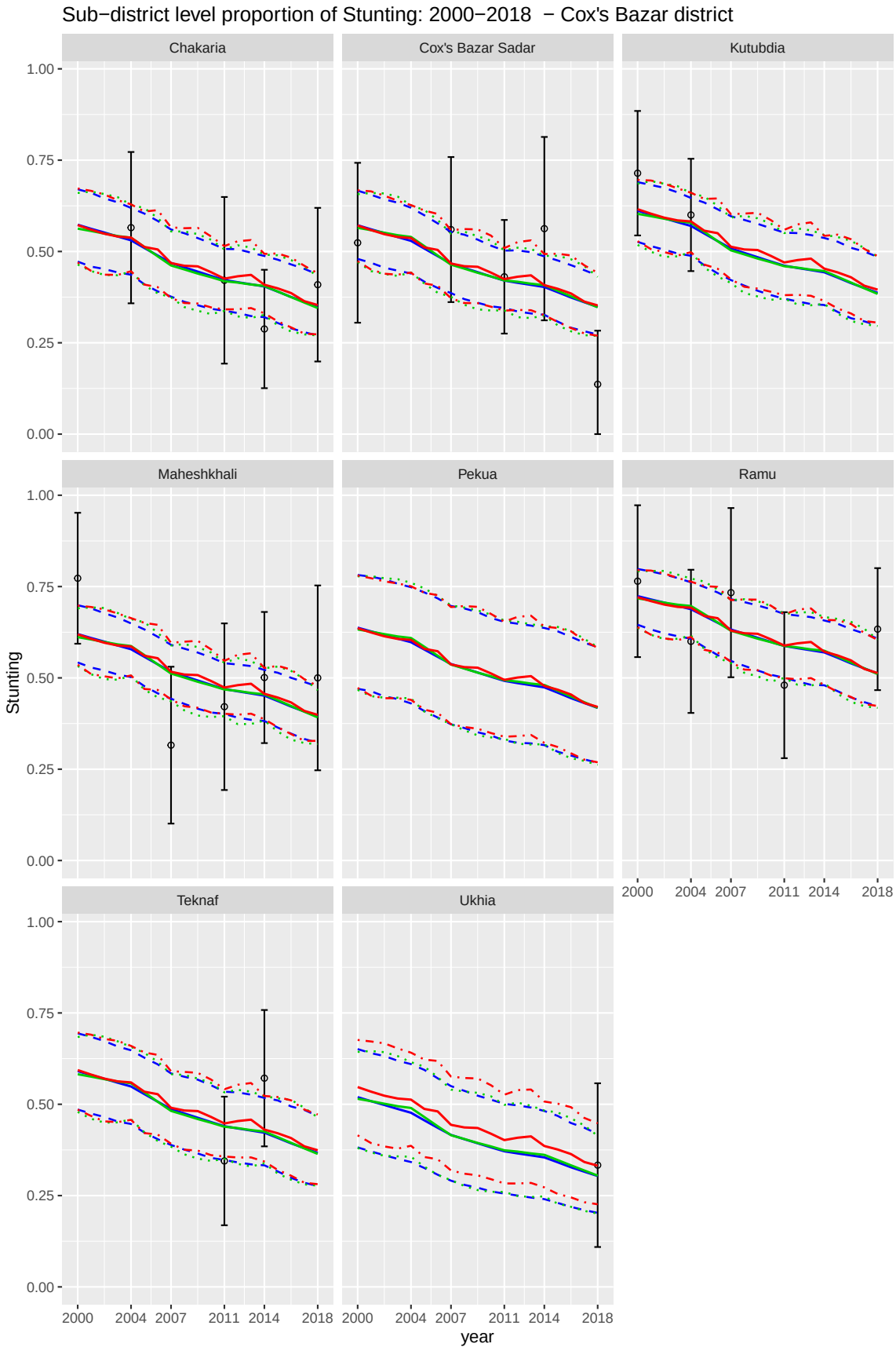


Figure S.4.64: Sub-district level trends of stunting in Chittagong district during 2000-2018 by DIR estimator (black error-bar line), MTS-1 model (blue line), MTS-2 model (green line) and MTS-3 model (red line) with 95% confidence band. Models are developed at sub-district level.

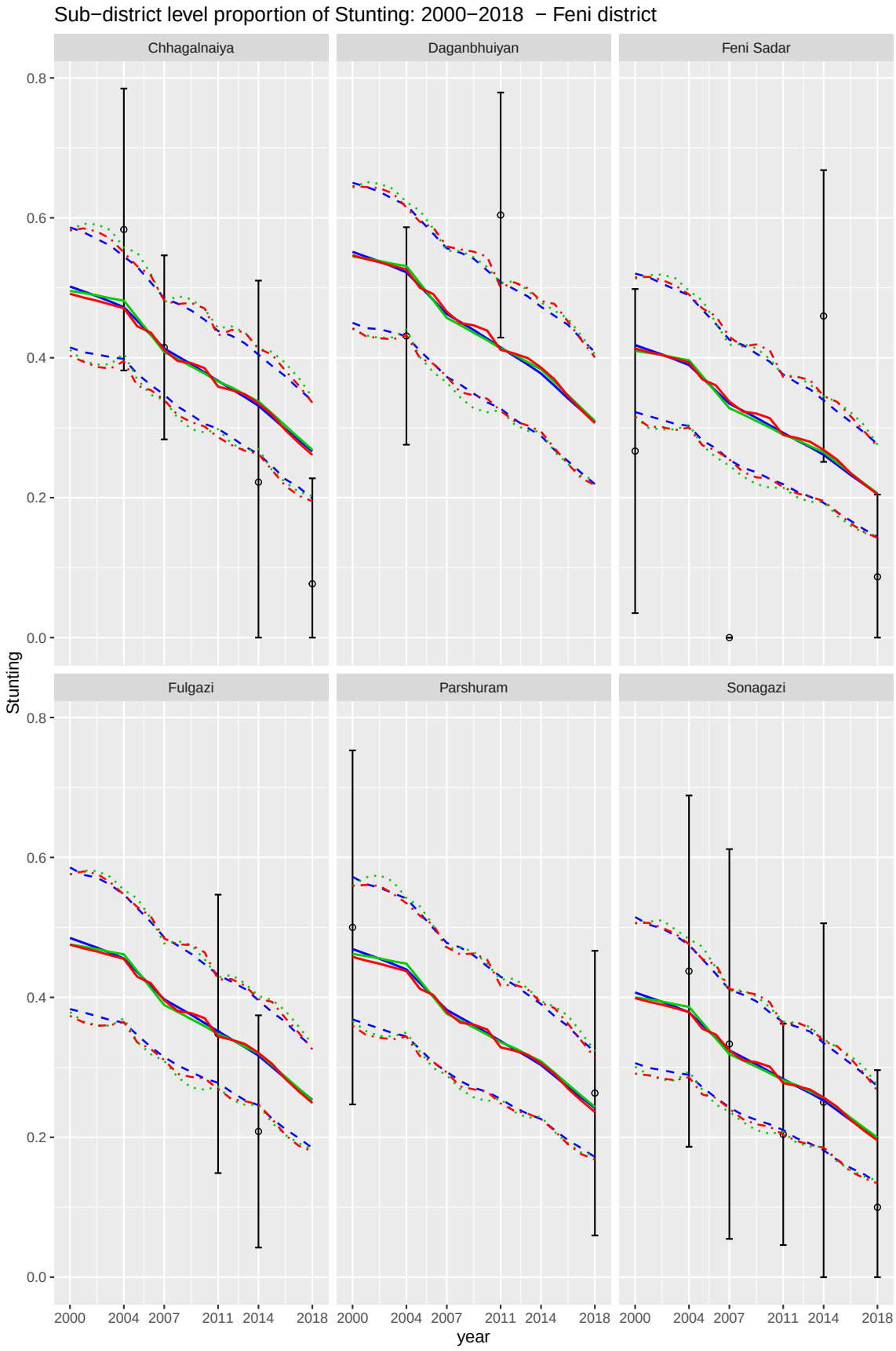


Figure S.4.65: Sub-district level trends of stunting in Chittagong district during 2000-2018 by DIR estimator (black error-bar line), MTS-1 model (blue line), MTS-2 model (green line) and MTS-3 model (red line) with 95% confidence band. Models are developed at sub-district level.

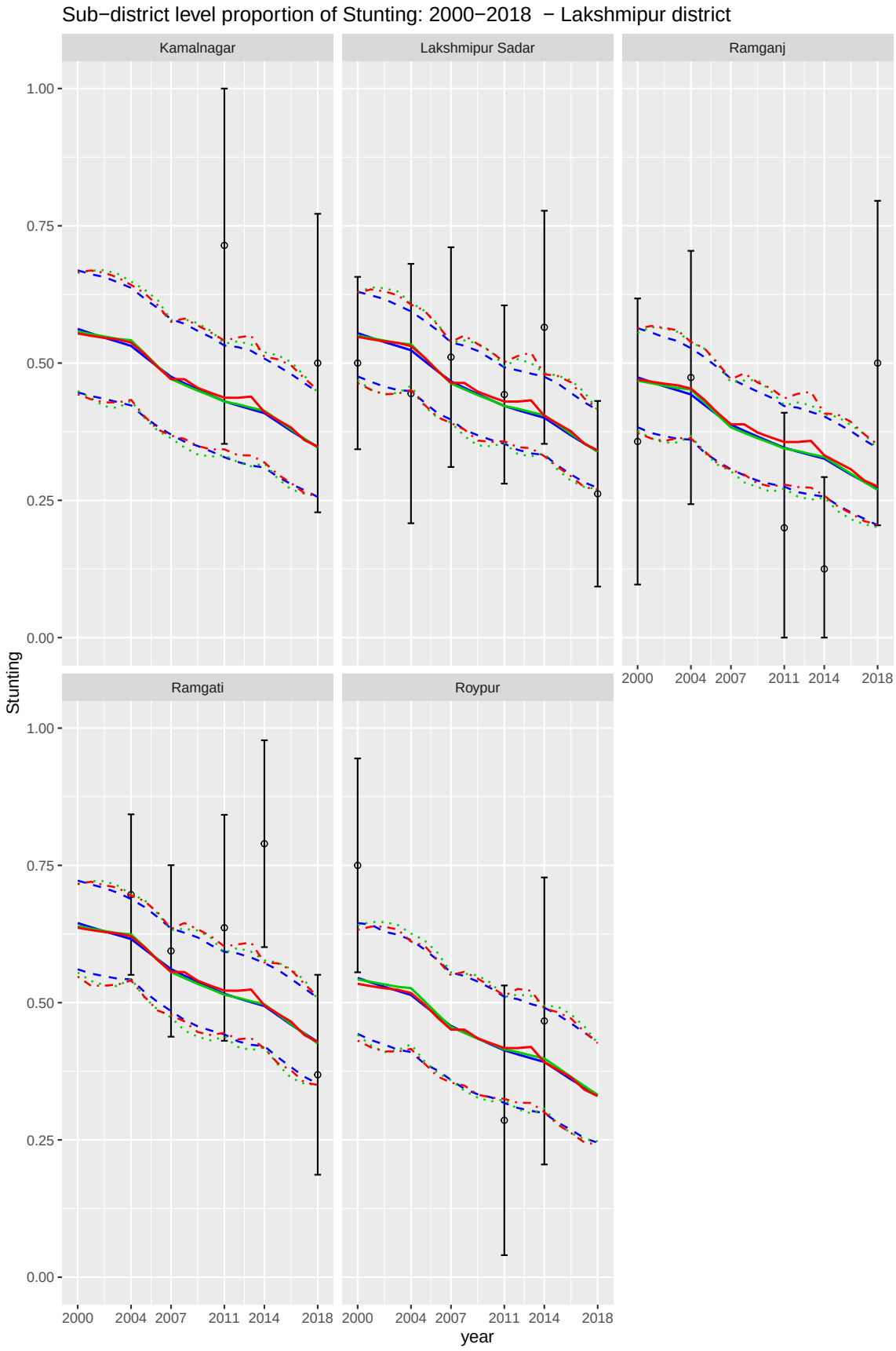


Figure S.4.66: Sub-district level trends of stunting in Chittagong district during 2000-2018 by DIR estimator (black error-bar line), MTS-1 model (blue line), MTS-2 model (green line) and MTS-3 model (red line) with 95% confidence band. Models are developed at sub-district level.

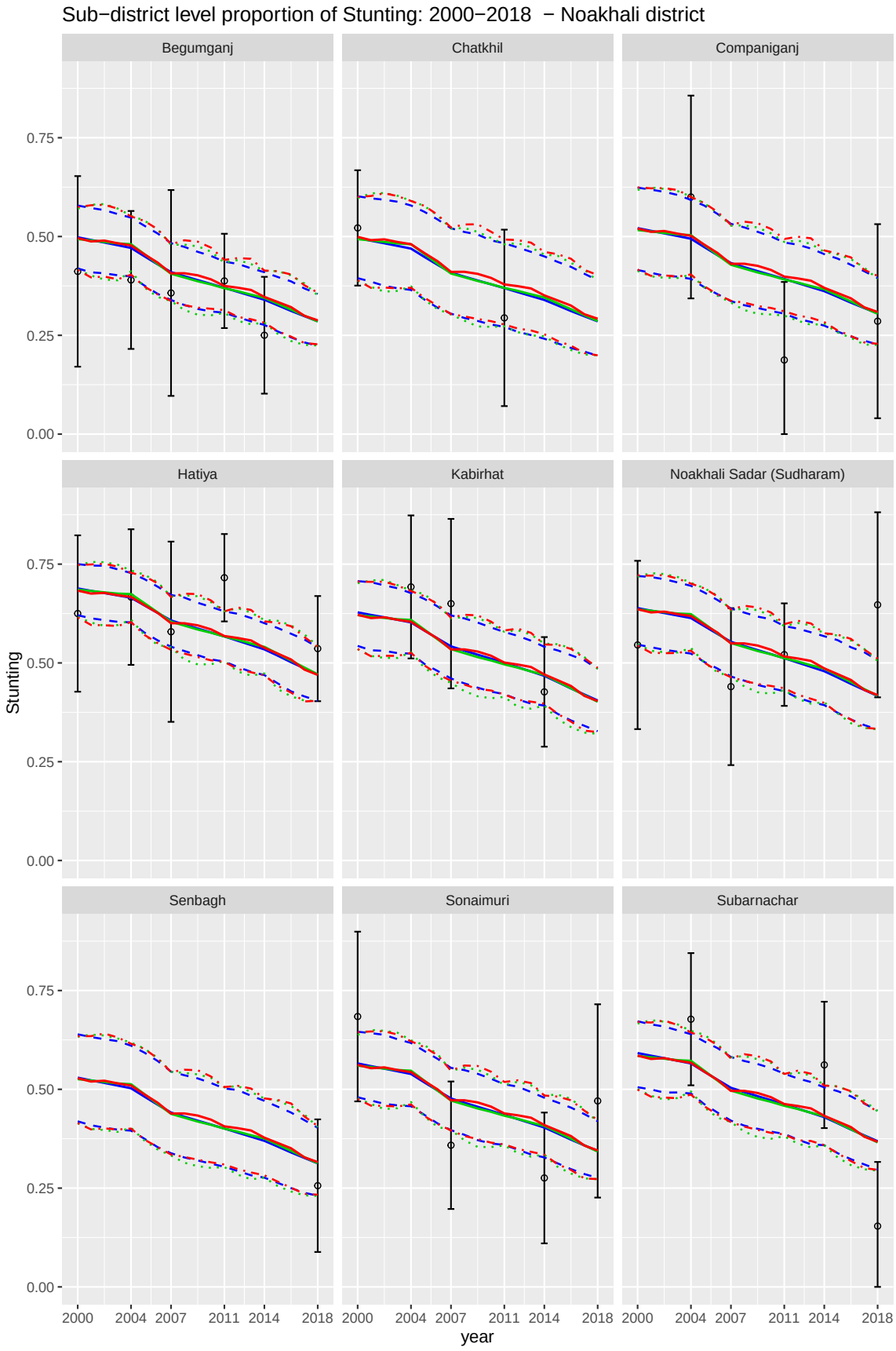


Figure S.4.67: Sub-district level trends of stunting in Chittagong district during 2000-2018 by DIR estimator (black error-bar line), MTS-1 model (blue line), MTS-2 model (green line) and MTS-3 model (red line) with 95% confidence band. Models are developed at sub-district level.

S.4.3 Sub-district level trends: Dhaka division

There are 13 districts and 129 sub-districts under Dhaka division. Dhaka district consists of the most sub-districts (46), among which many of them are urban and smaller than the rural ones. The trends estimates of stunting for each of the sub-districts are shown under their respective districts in Figures from S.4.68 to S.4.86.

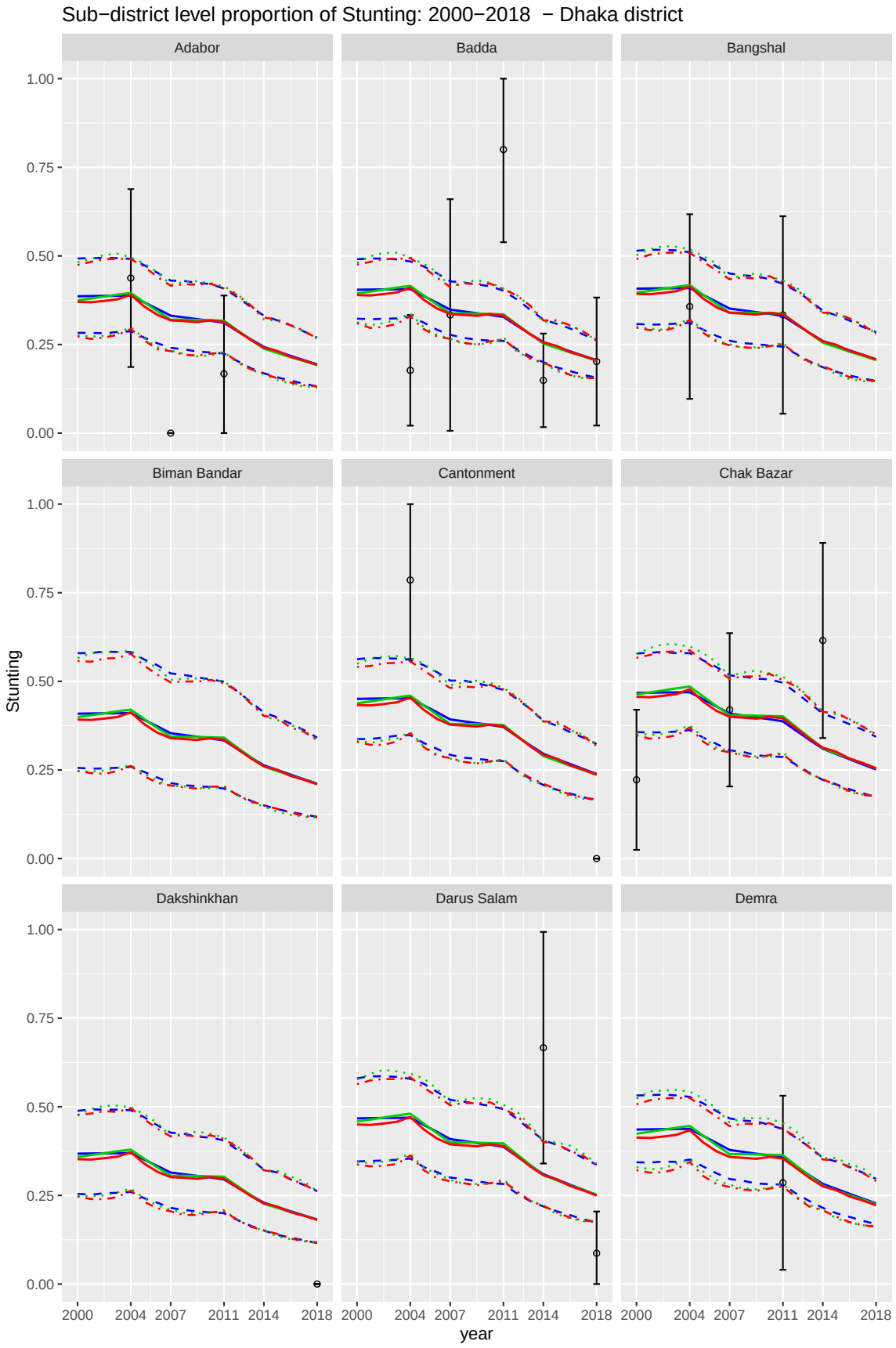


Figure S.4.68: Sub-district level trends of stunting in Dhaka district during 2000-2018 by DIR estimator (black error-bar line), MTS-1 model (blue line), MTS-2 model (green line) and MTS-3 model (red line) with 95% confidence band. Models are developed at sub-district level.

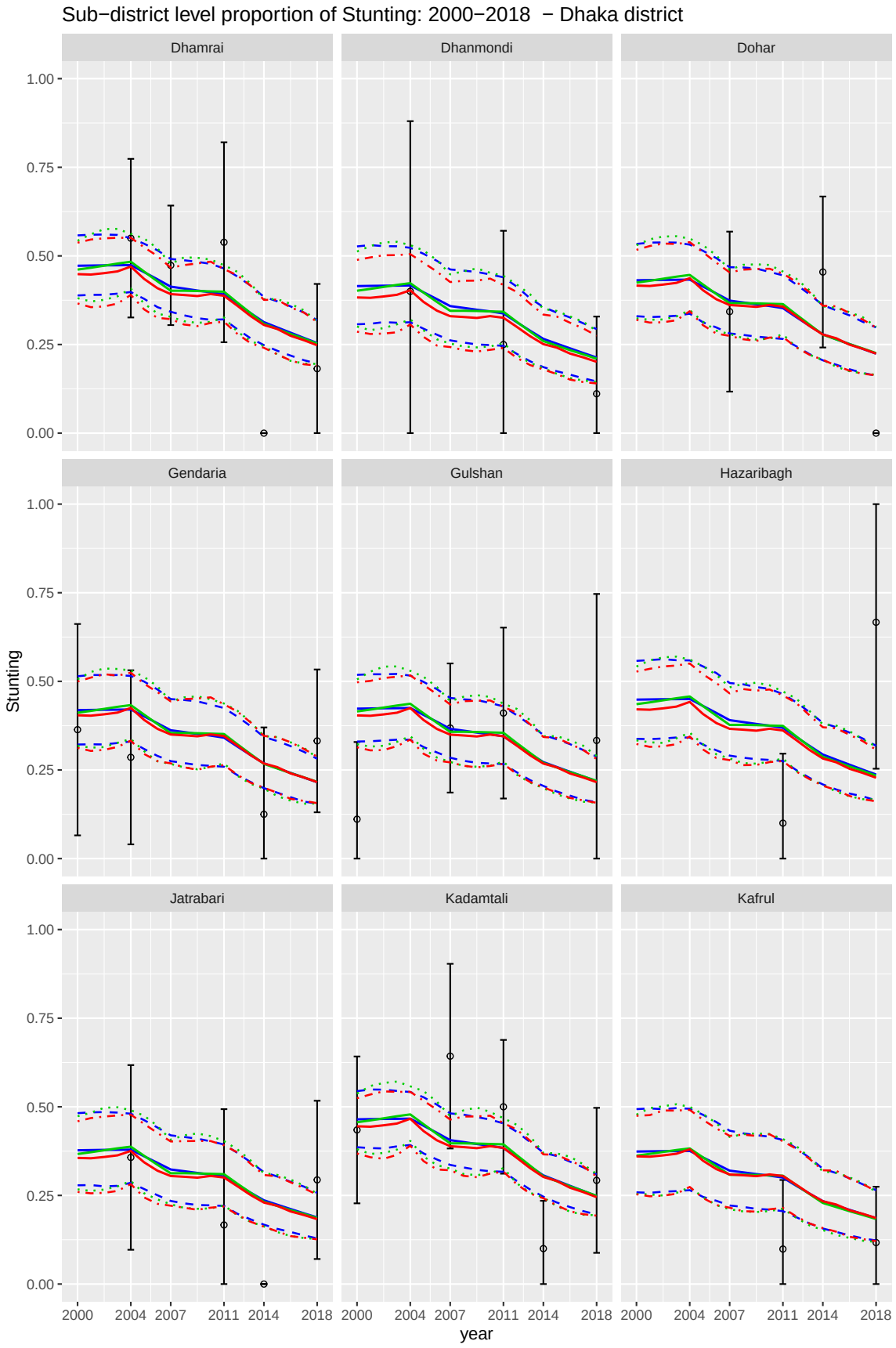


Figure S.4.69: Sub-district level trends of stunting in Dhaka district during 2000-2018 by DIR estimator (black error-bar line), MTS-1 model (blue line), MTS-2 model (green line) and MTS-3 model (red line) with 95% confidence band. Models are developed at sub-district level.

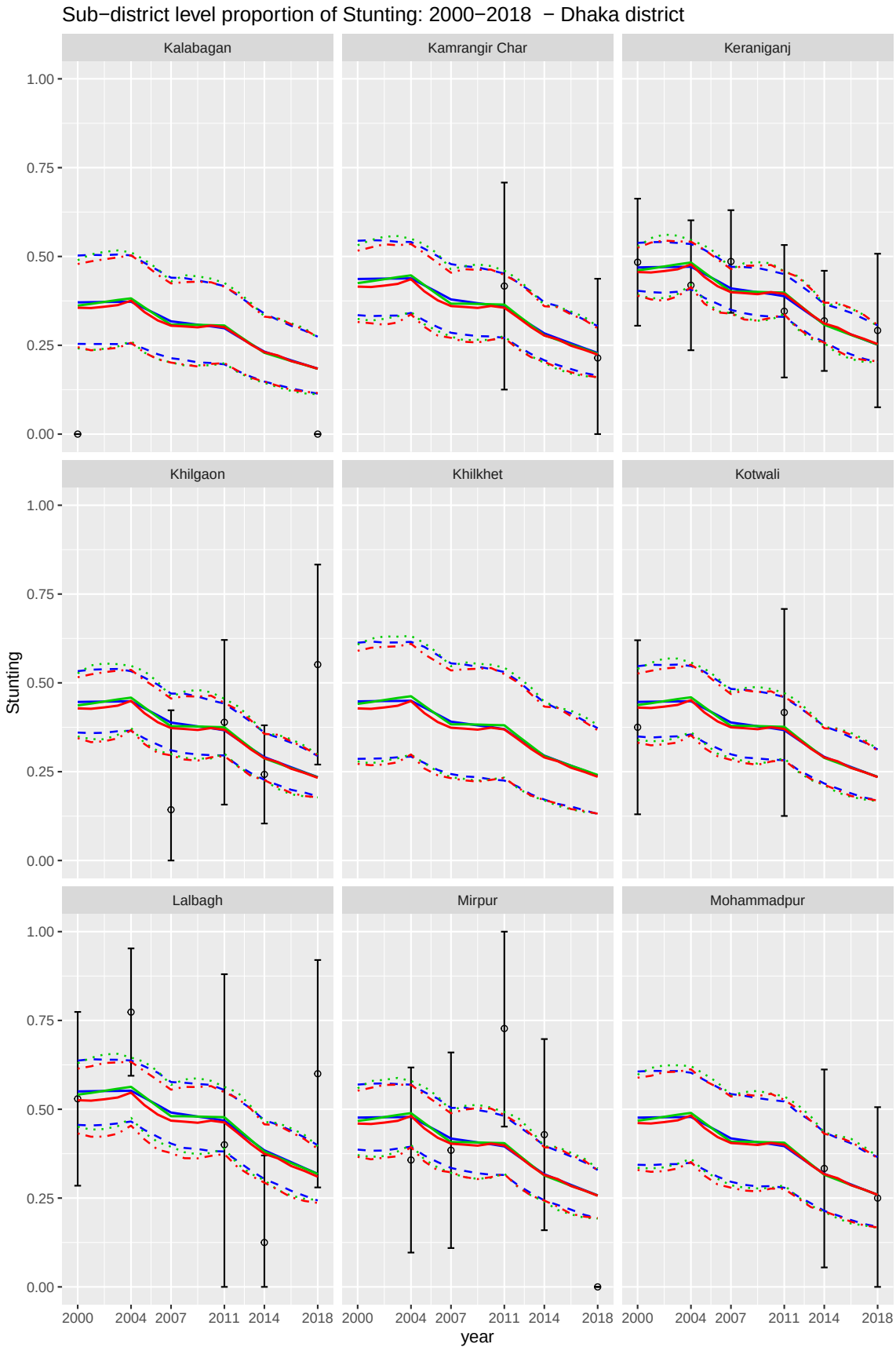


Figure S.4.70: Sub-district level trends of stunting in Dhaka district during 2000-2018 by DIR estimator (black error-bar line), MTS-1 model (blue line), MTS-2 model (green line) and MTS-3 model (red line) with 95% confidence band. Models are developed at sub-district level.

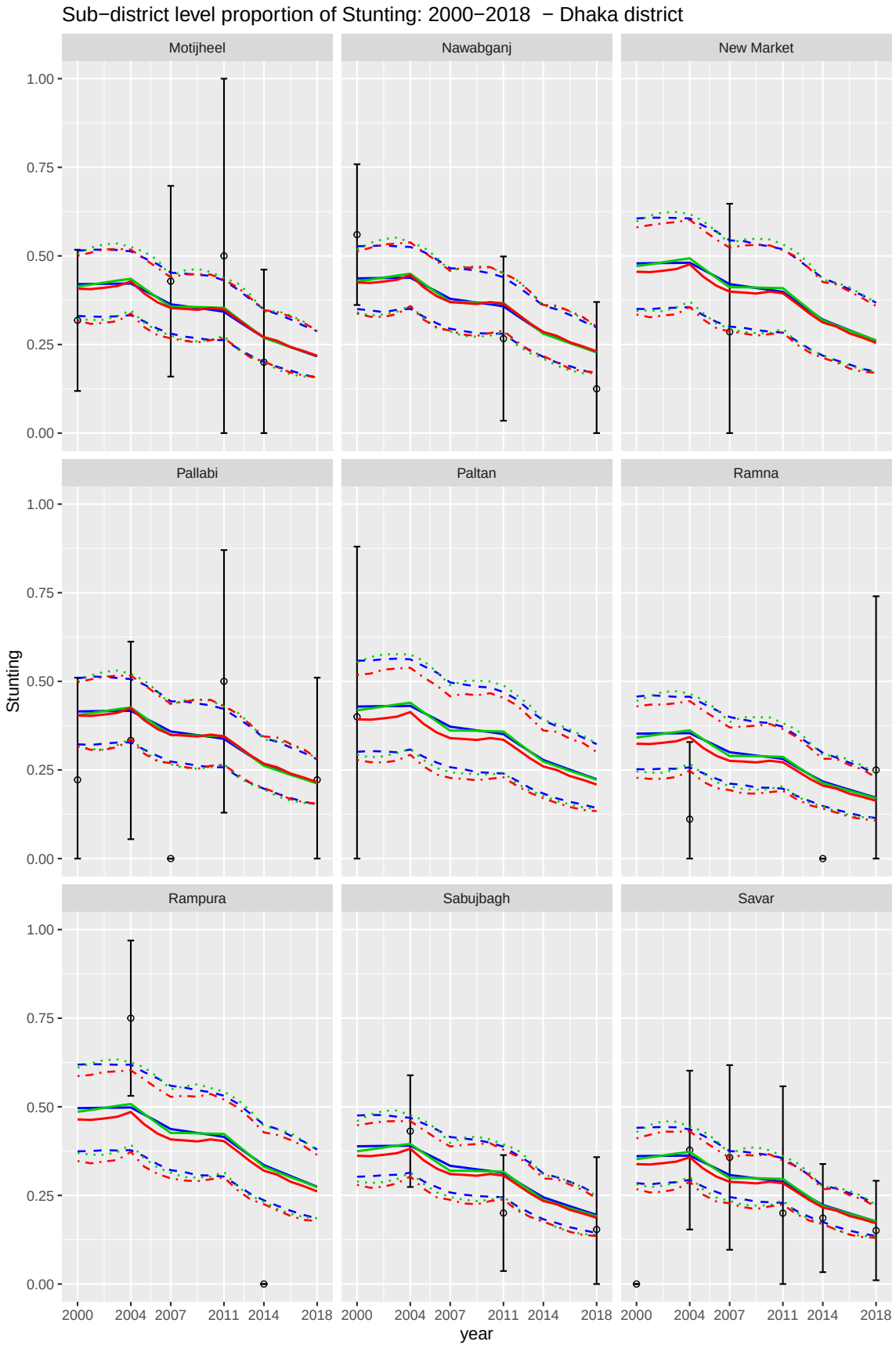


Figure S.4.71: Sub-district level trends of stunting in Dhaka district during 2000-2018 by DIR estimator (black error-bar line), MTS-1 model (blue line), MTS-2 model (green line) and MTS-3 model (red line) with 95% confidence band. Models are developed at sub-district level.

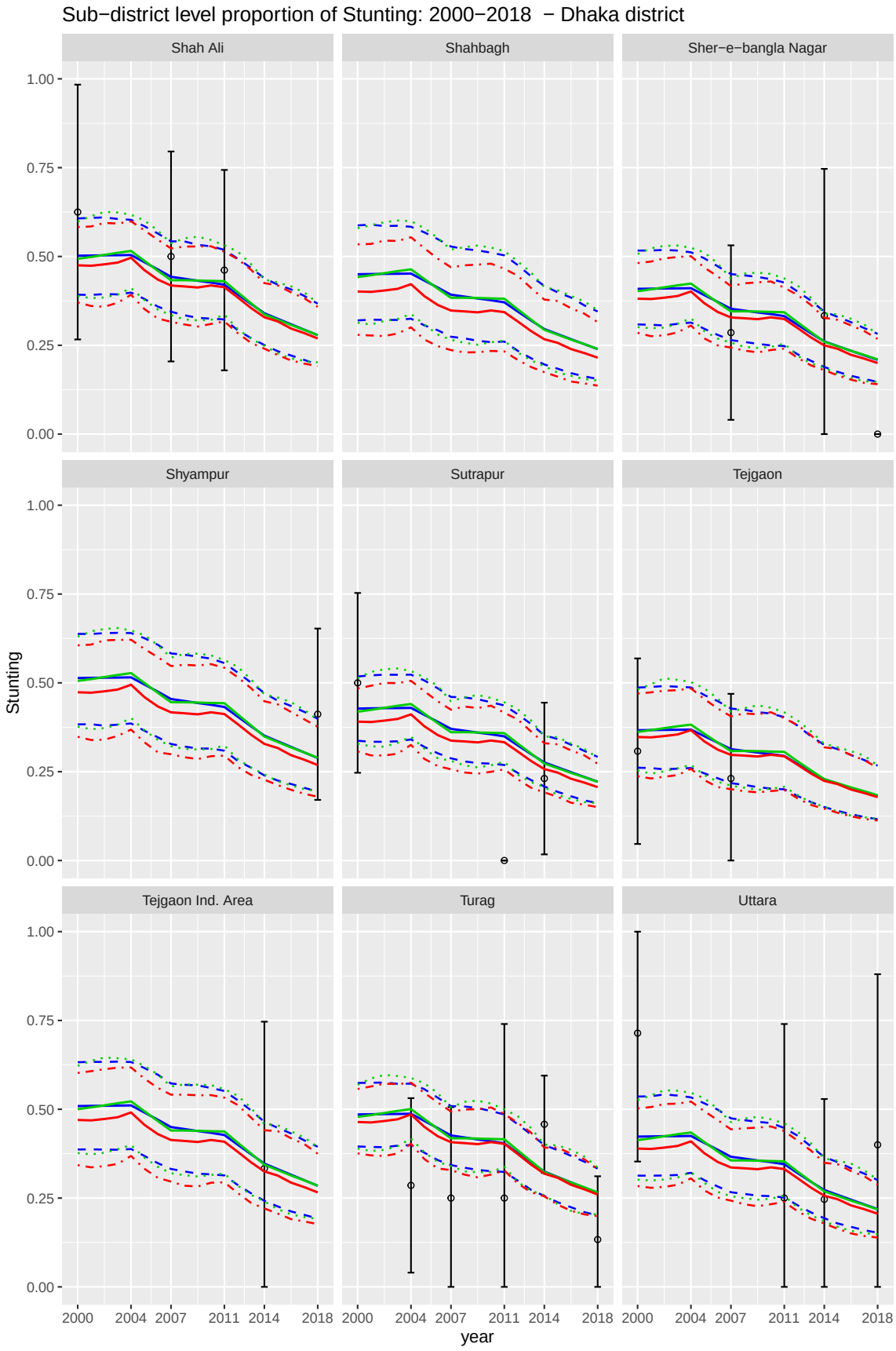


Figure S.4.72: Sub-district level trends of stunting in Dhaka district during 2000-2018 by DIR estimator (black error-bar line), MTS-1 model (blue line), MTS-2 model (green line) and MTS-3 model (red line) with 95% confidence band. Models are developed at sub-district level.

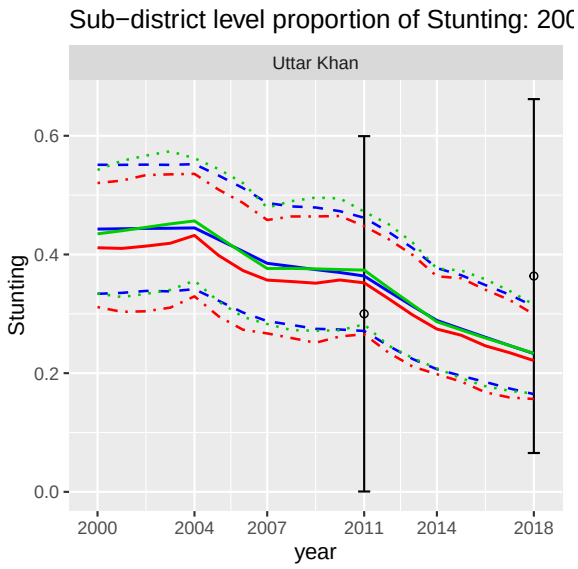


Figure S.4.73: Sub-district level trends of stunting in Dhaka district during 2000-2018 by DIR estimator (black error-bar line), MTS-1 model (blue line), MTS-2 model (green line) and MTS-3 model (red line) with 95% confidence band. Models are developed at sub-district level.

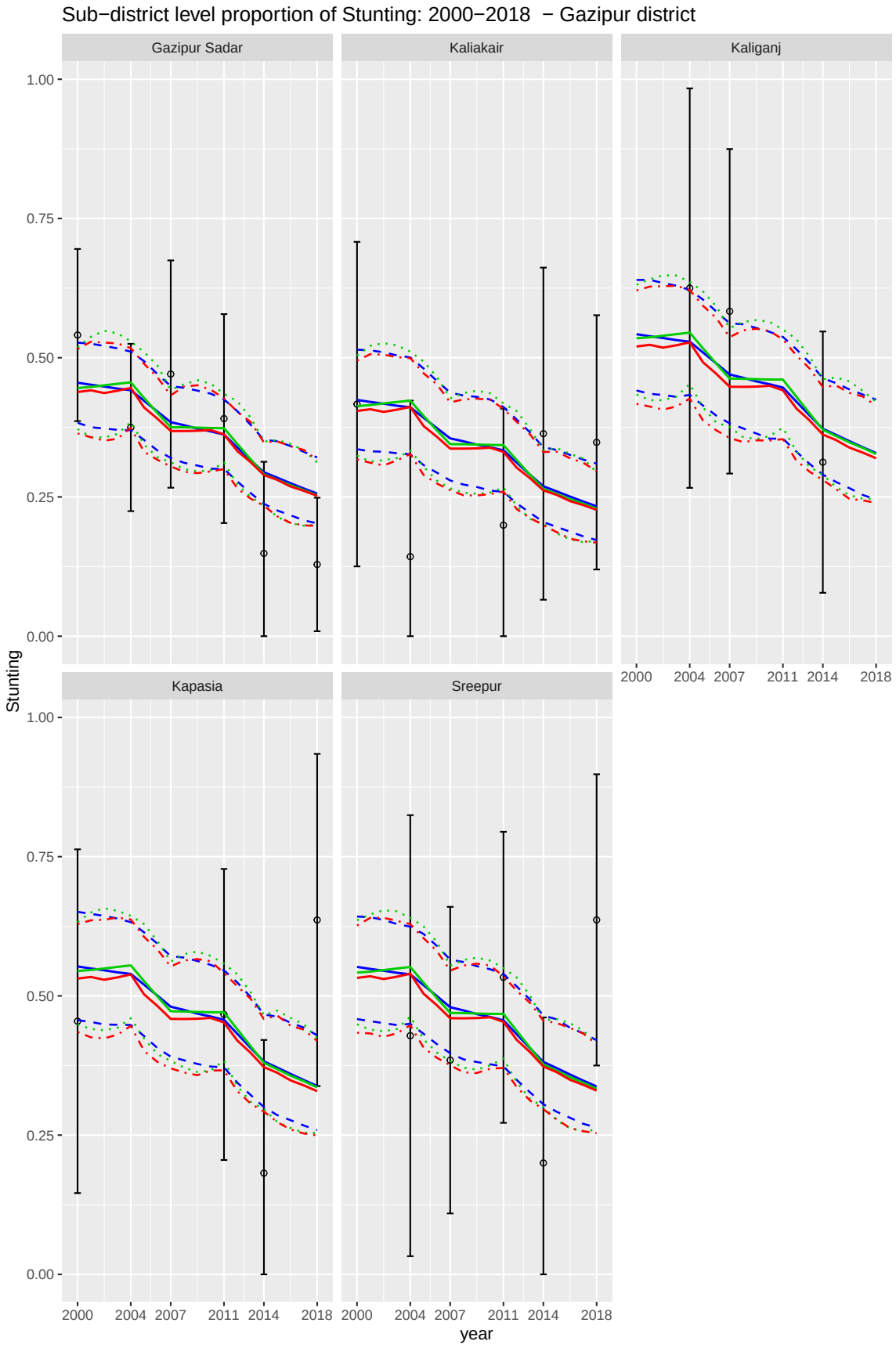


Figure S.4.74: Sub-district level trends of stunting in Gazipur district during 2000-2018 by DIR estimator (black error-bar line), MTS-1 model (blue line), MTS-2 model (green line) and MTS-3 model (red line) with 95% confidence band. Models are developed at sub-district level.

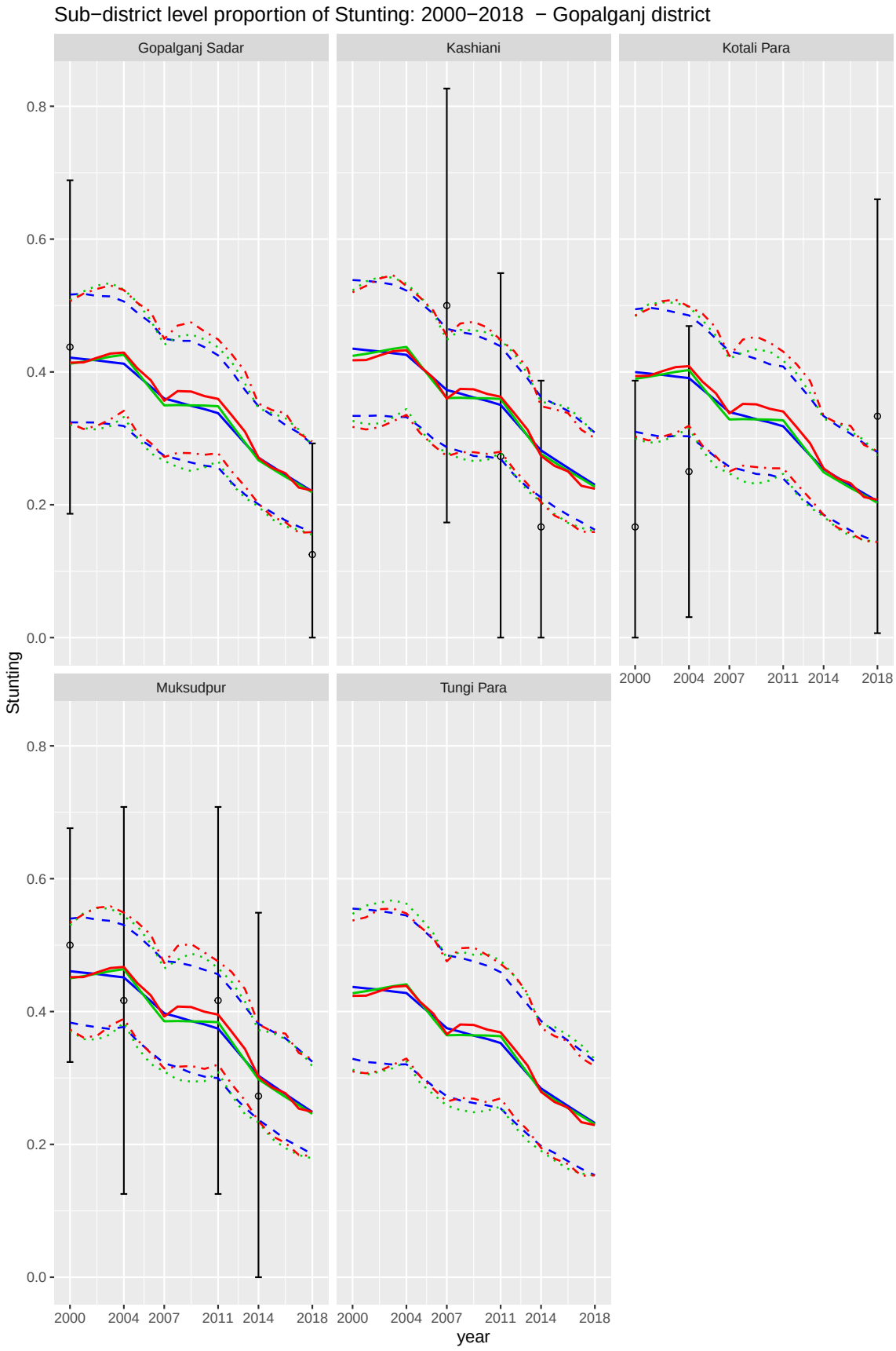


Figure S.4.75: Sub-district level trends of stunting in Gopalganj district during 2000-2018 by DIR estimator (black error-bar line), MTS-1 model (blue line), MTS-2 model (green line) and MTS-3 model (red line) with 95% confidence band. Models are developed at sub-district level.

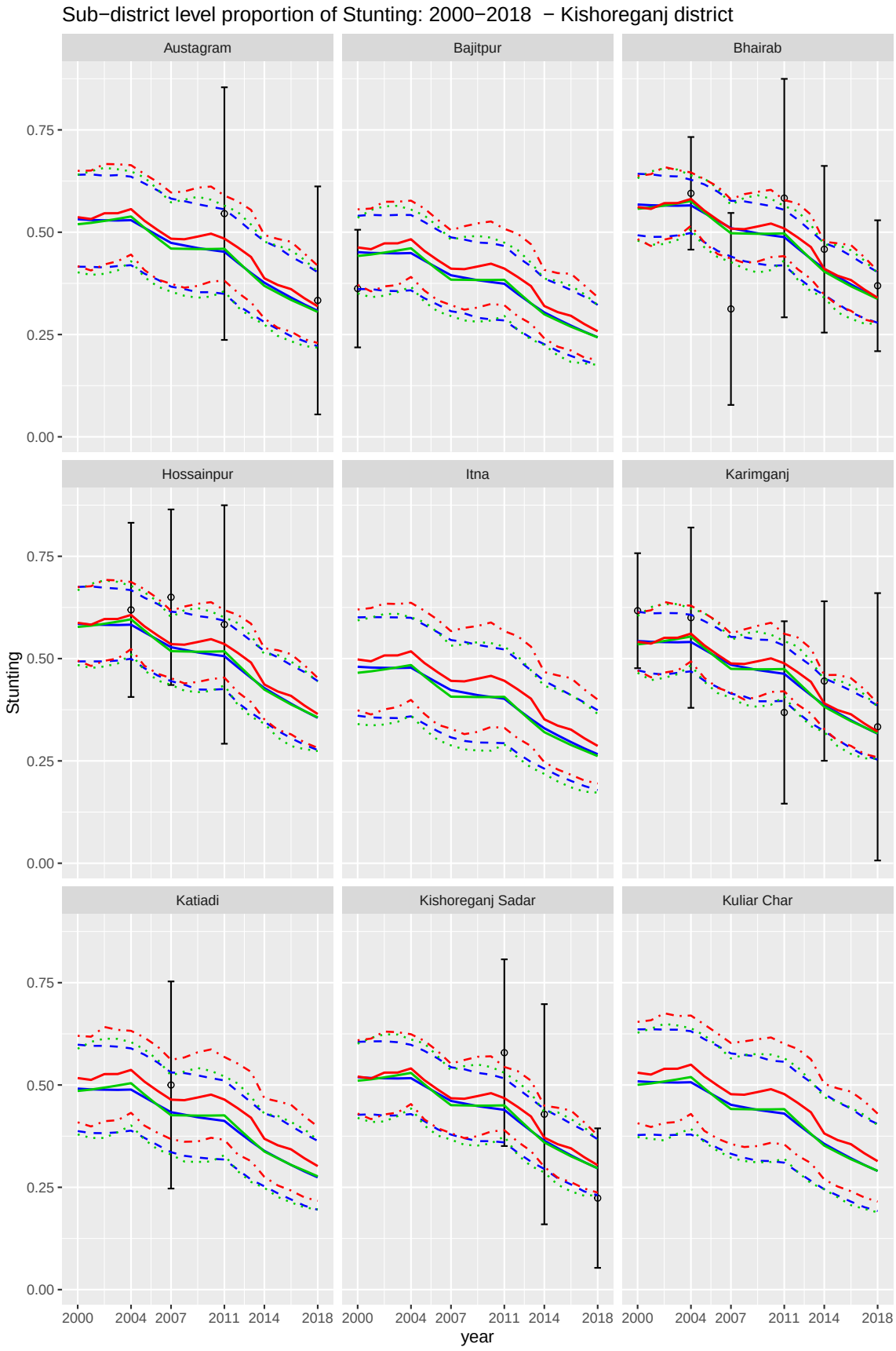


Figure S.4.76: Sub-district level trends of stunting in Kishoreganj district during 2000-2018 by DIR estimator (black error-bar line), MTS-1 model (blue line), MTS-2 model (green line) and MTS-3 model (red line) with 95% confidence band. Models are developed at sub-district level.



Figure S.4.77: Sub-district level trends of stunting in Kishoreganj district during 2000-2018 by DIR estimator (black error-bar line), MTS-1 model (blue line), MTS-2 model (green line) and MTS-3 model (red line) with 95% confidence band. Models are developed at sub-district level.

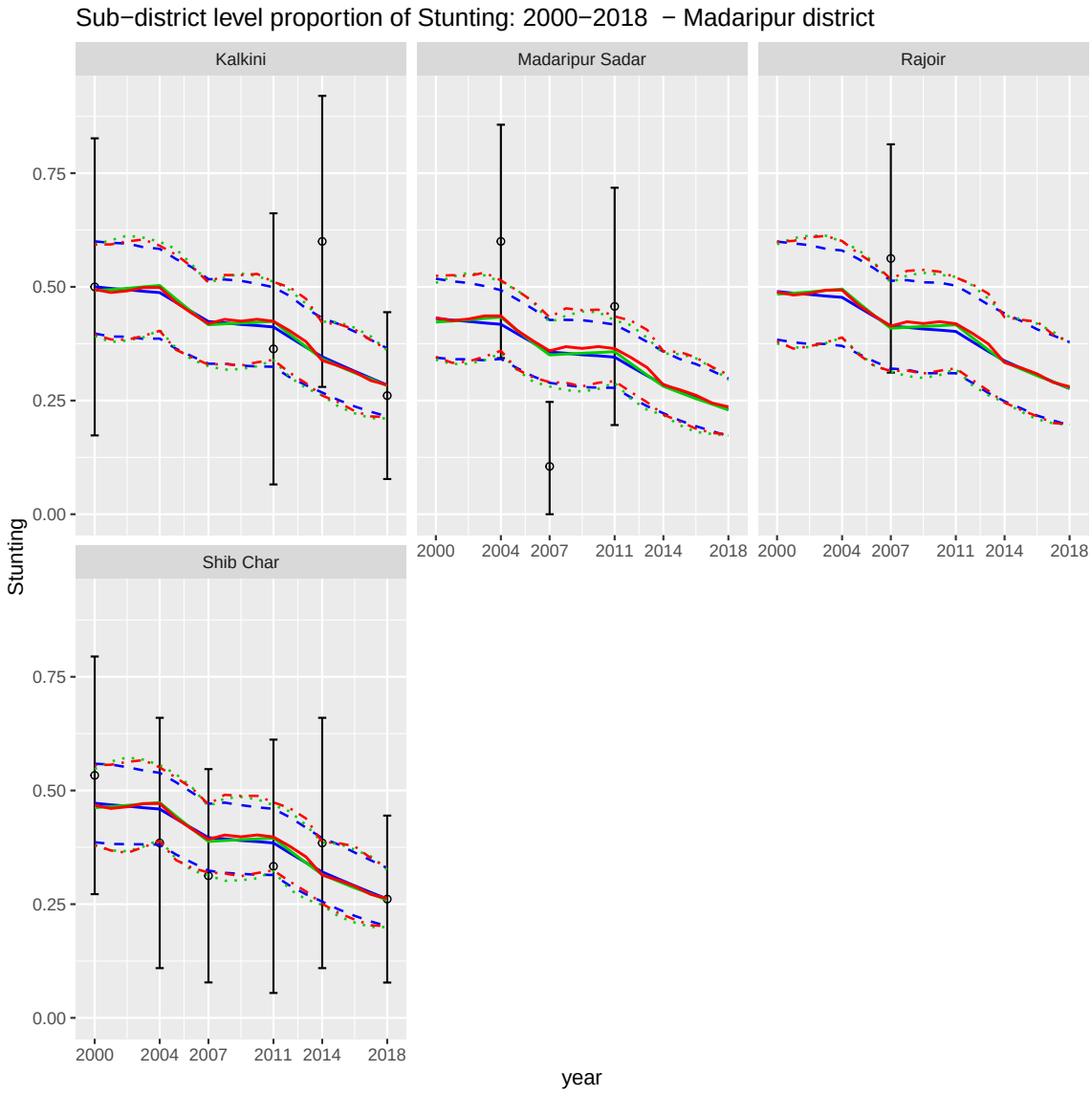


Figure S.4.78: Sub-district level trends of stunting in Madaripur district during 2000-2018 by DIR estimator (black error-bar line), MTS-1 model (blue line), MTS-2 model (green line) and MTS-3 model (red line) with 95% confidence band. Models are developed at sub-district level.

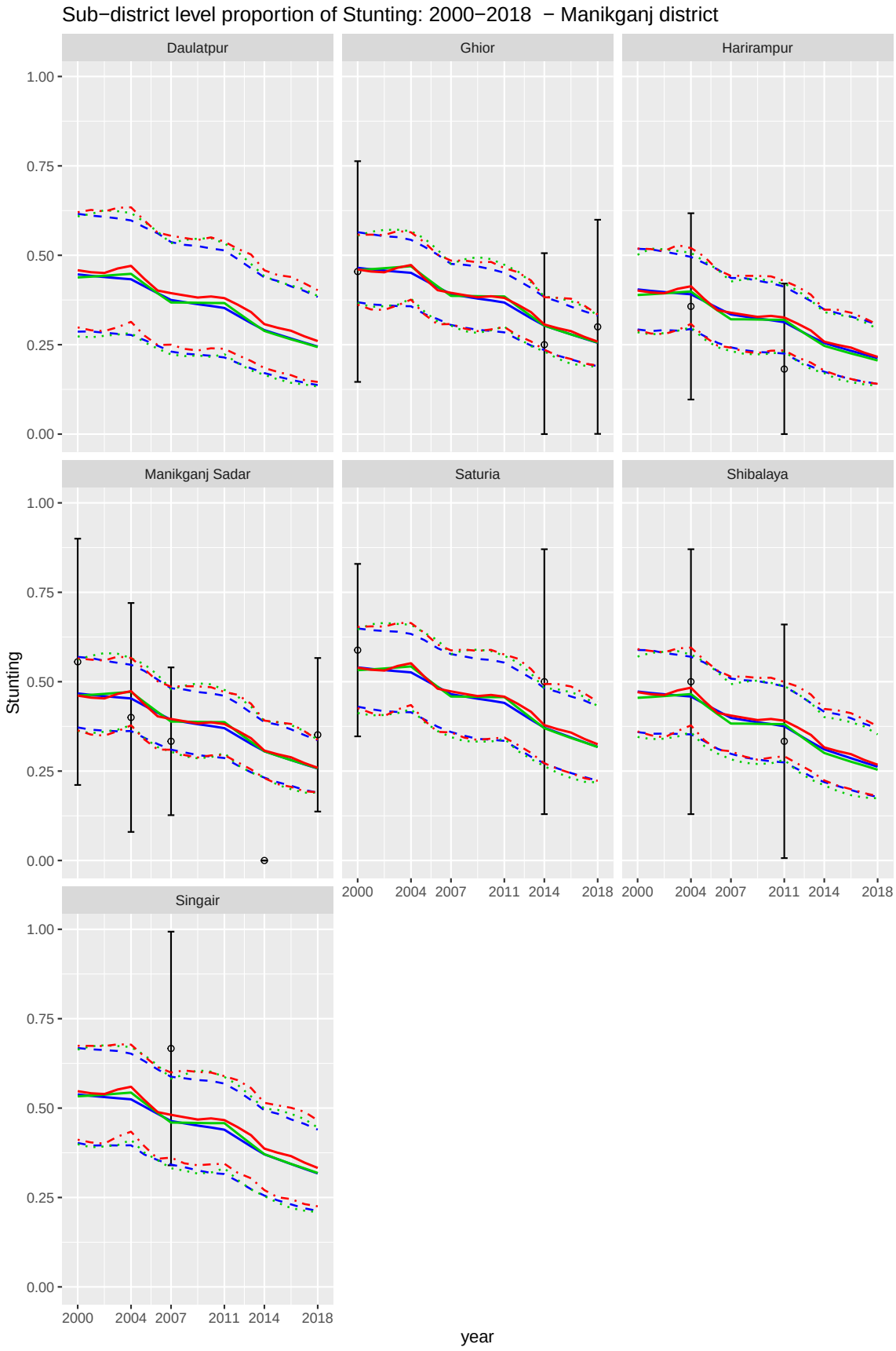


Figure S.4.79: Sub-district level trends of stunting in Manikganj district during 2000-2018 by DIR estimator (black error-bar line), MTS-1 model (blue line), MTS-2 model (green line) and MTS-3 model (red line) with 95% confidence band. Models are developed at sub-district level.

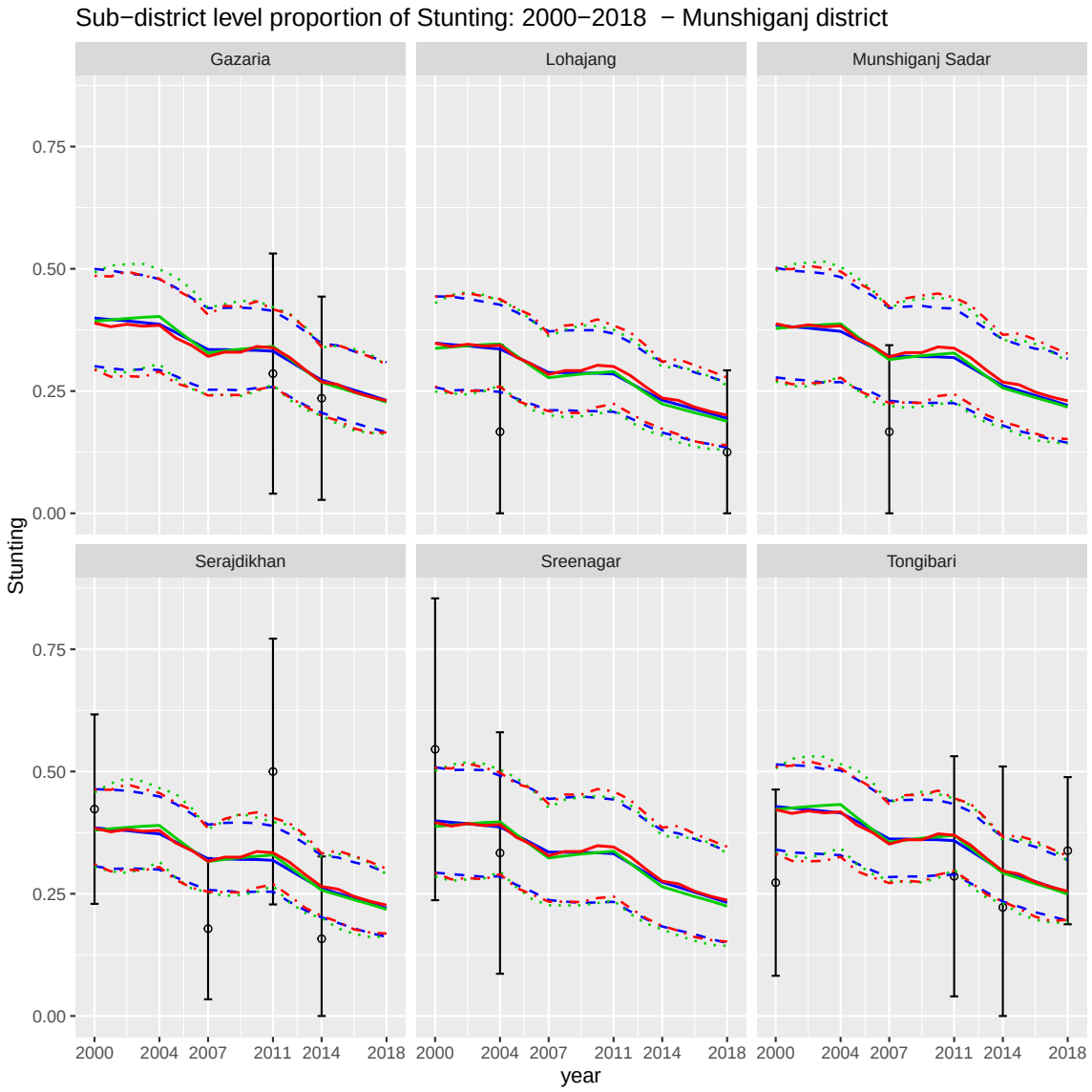


Figure S.4.80: Sub-district level trends of stunting in Munshiganj district during 2000-2018 by DIR estimator (black error-bar line), MTS-1 model (blue line), MTS-2 model (green line) and MTS-3 model (red line) with 95% confidence band. Models are developed at sub-district level.

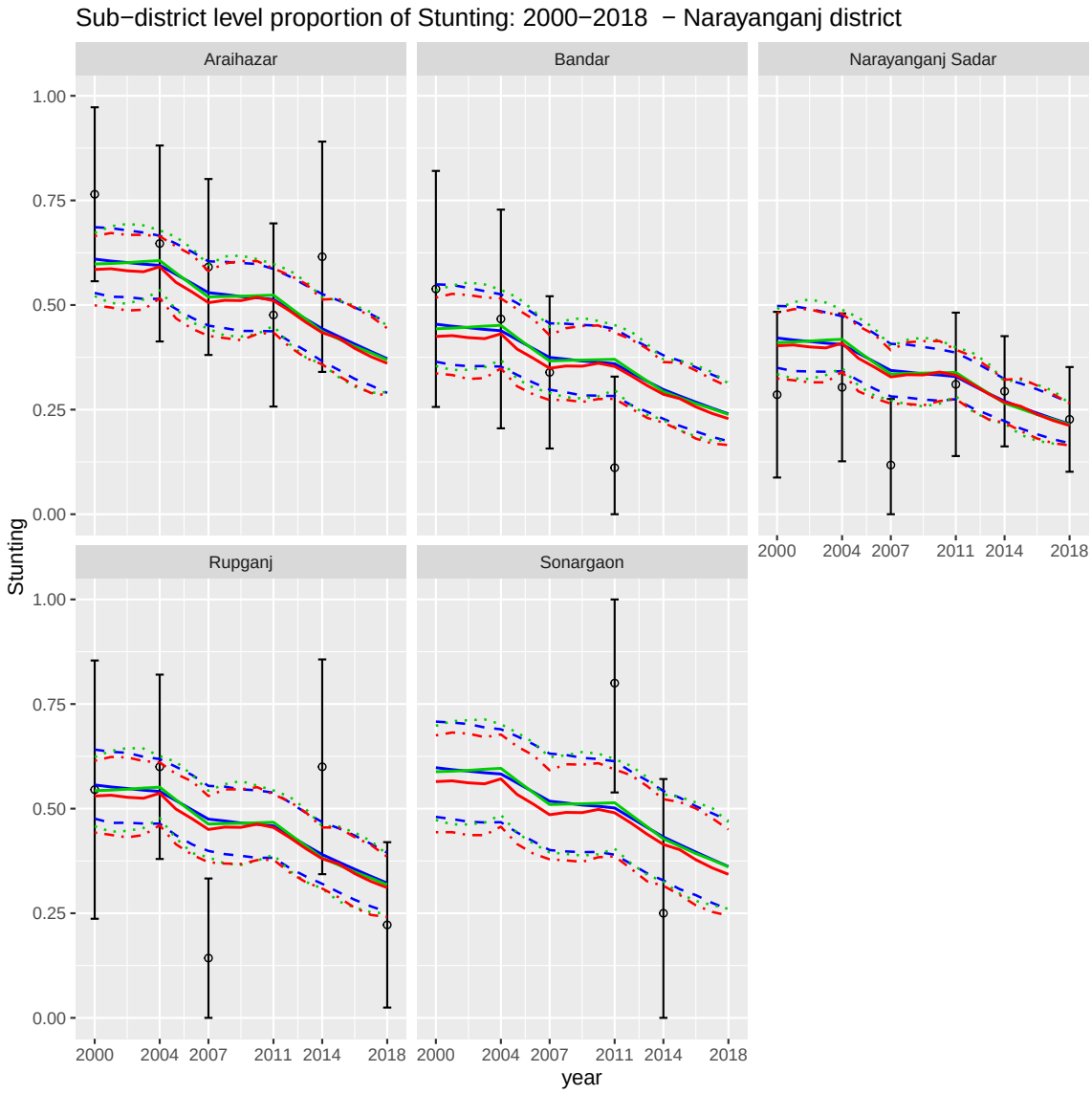


Figure S.4.81: Sub-district level trends of stunting in Narayanganj district during 2000-2018 by DIR estimator (black error-bar line), MTS-1 model (blue line), MTS-2 model (green line) and MTS-3 model (red line) with 95% confidence band. Models are developed at sub-district level.

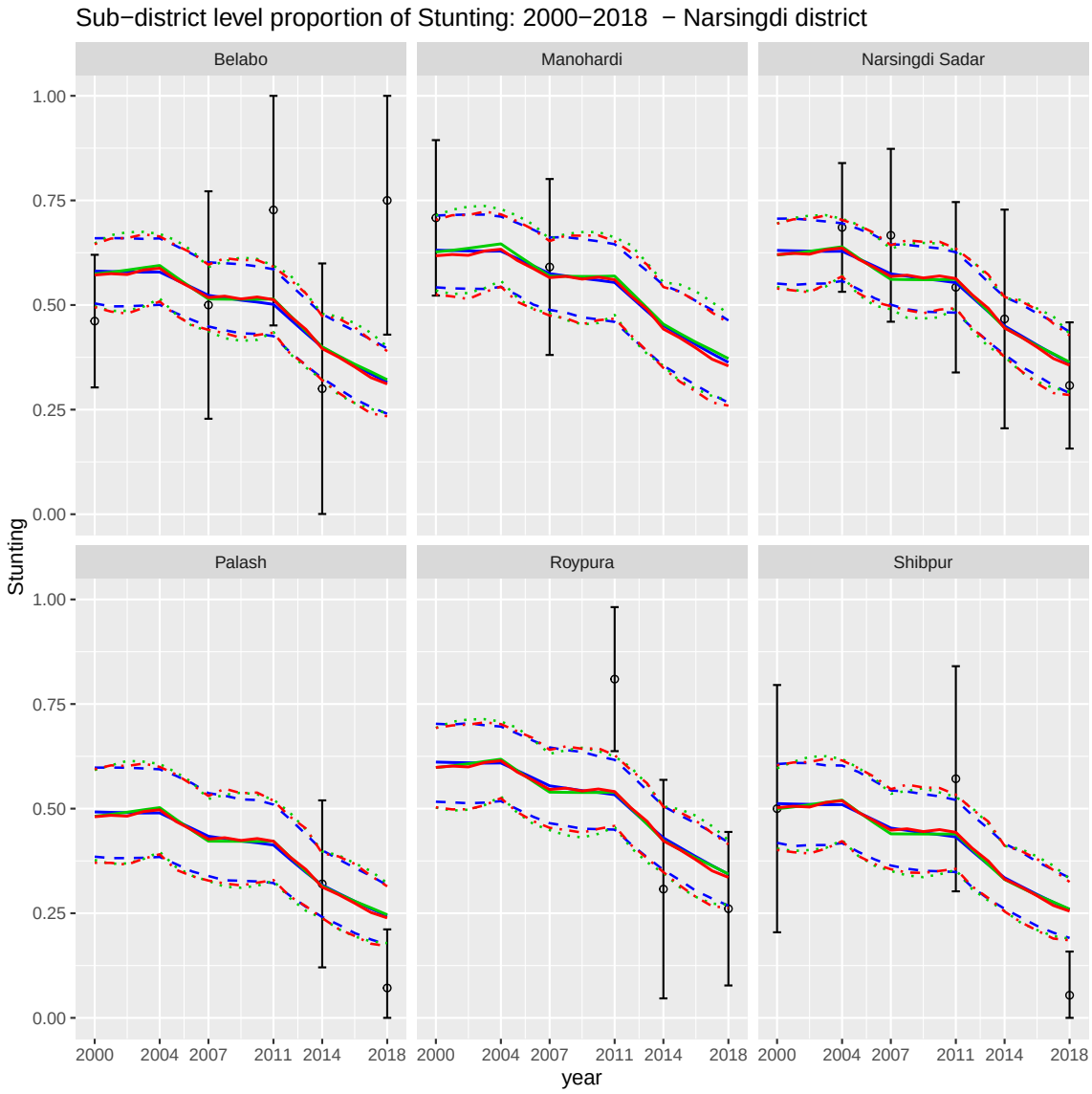


Figure S.4.82: Sub-district level trends of stunting in Narsingdi district during 2000-2018 by DIR estimator (black error-bar line), MTS-1 model (blue line), MTS-2 model (green line) and MTS-3 model (red line) with 95% confidence band. Models are developed at sub-district level.

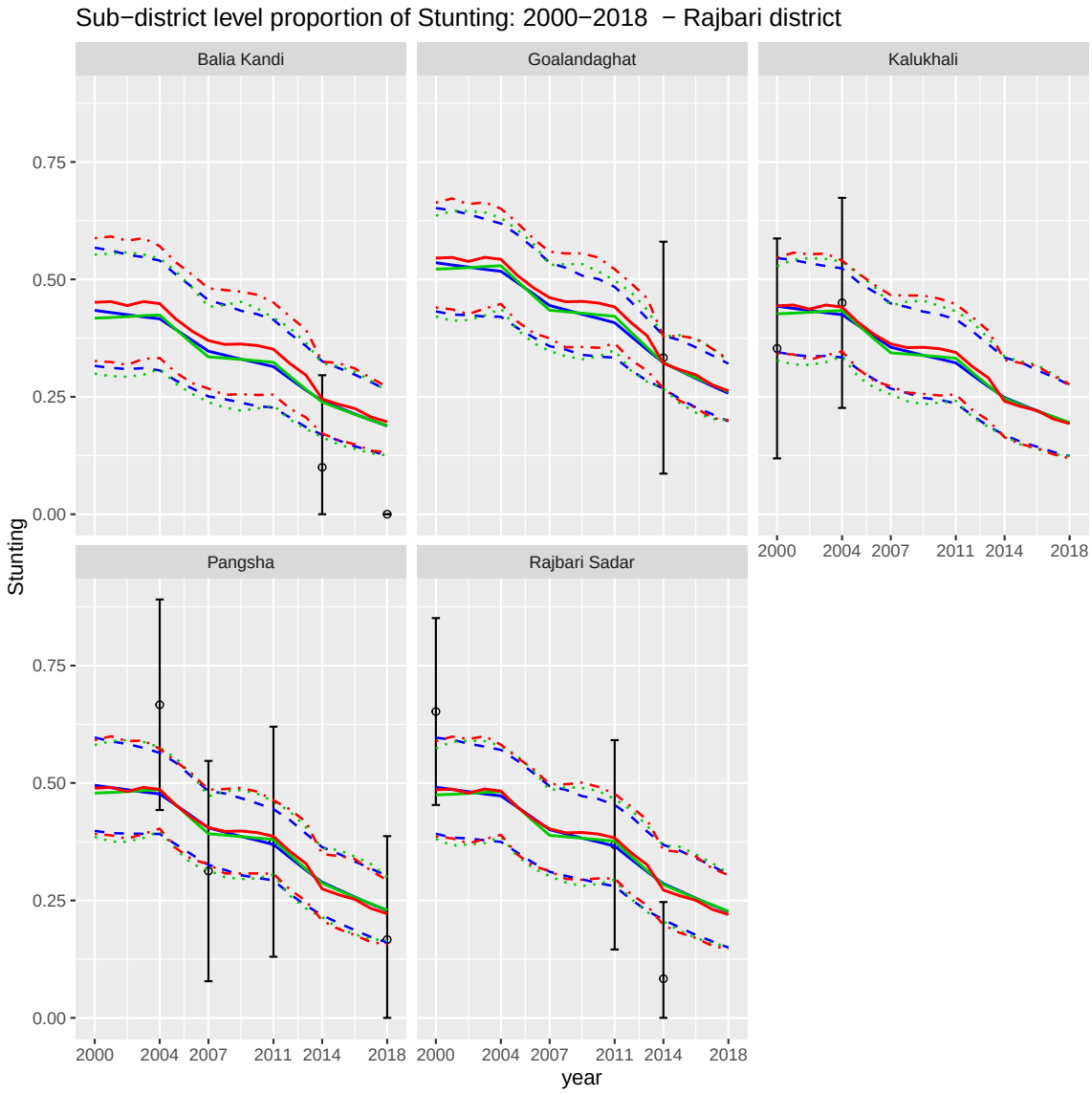


Figure S.4.83: Sub-district level trends of stunting in Rajbari district during 2000-2018 by DIR estimator (black error-bar line), MTS-1 model (blue line), MTS-2 model (green line) and MTS-3 model (red line) with 95% confidence band. Models are developed at sub-district level.

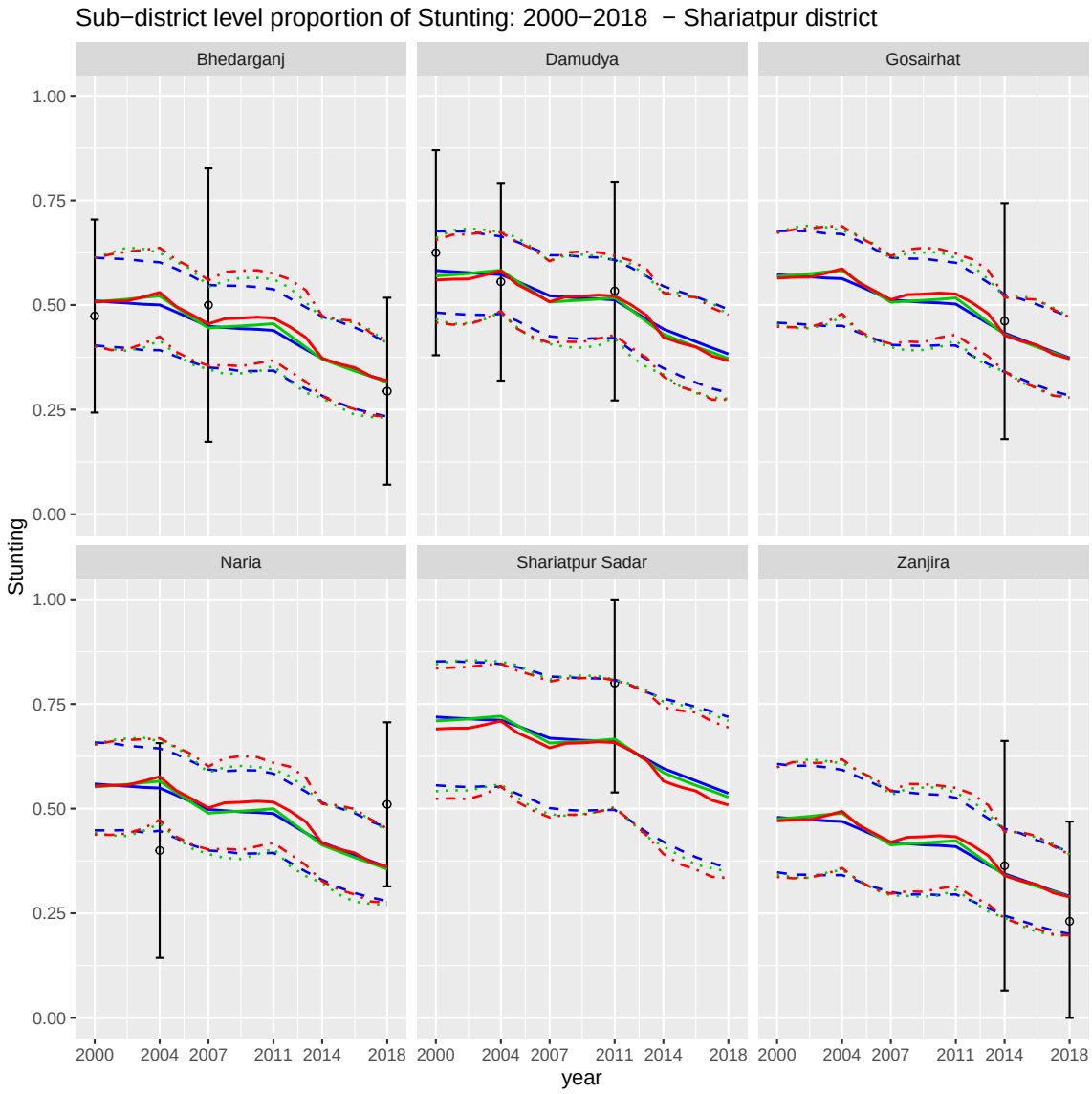


Figure S.4.84: Sub-district level trends of stunting in Shariatpur district during 2000-2018 by DIR estimator (black error-bar line), MTS-1 model (blue line), MTS-2 model (green line) and MTS-3 model (red line) with 95% confidence band. Models are developed at sub-district level.

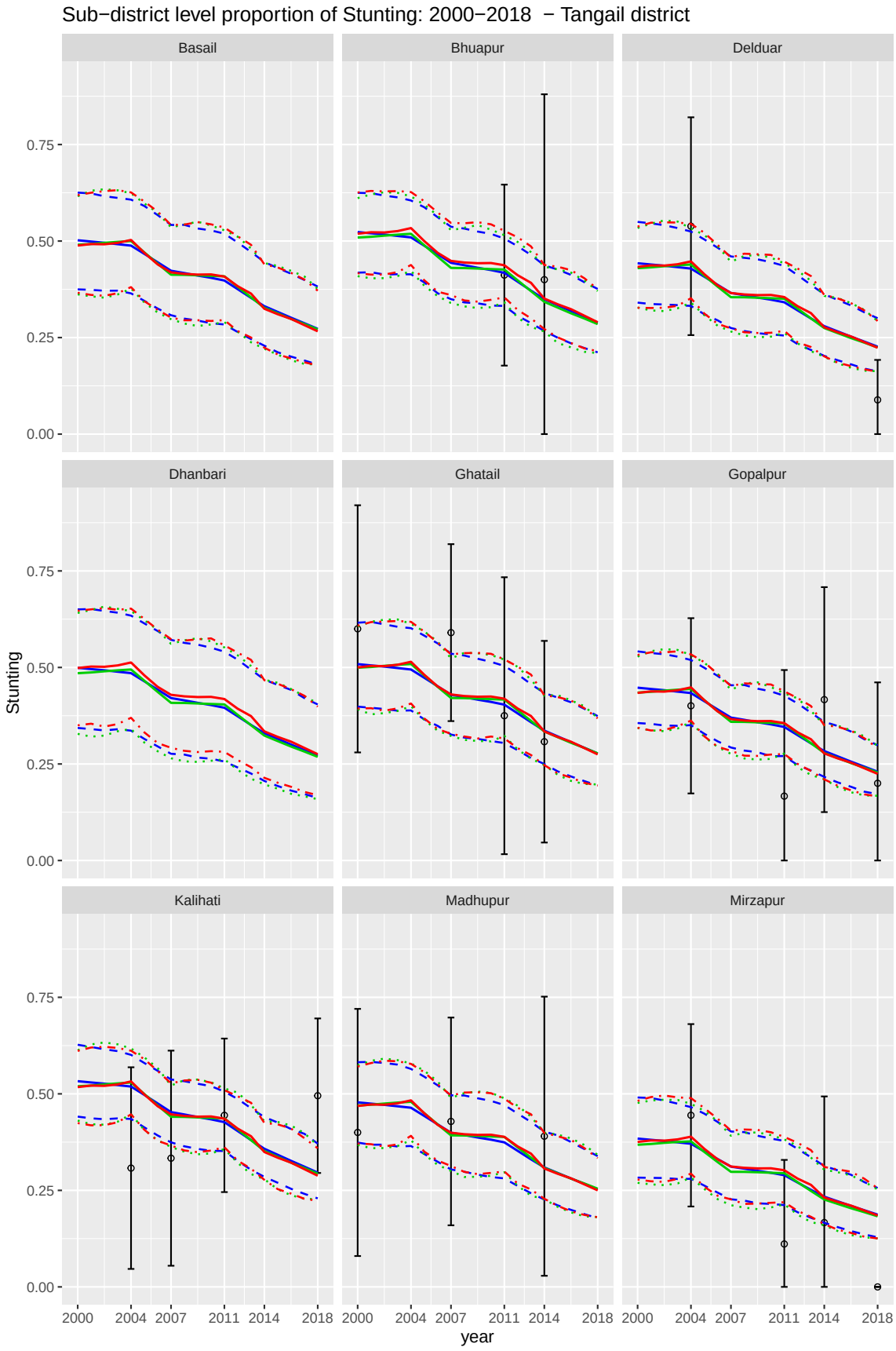


Figure S.4.85: Sub-district level trends of stunting in Tangail district during 2000-2018 by DIR estimator (black error-bar line), MTS-1 model (blue line), MTS-2 model (green line) and MTS-3 model (red line) with 95% confidence band. Models are developed at sub-district level.

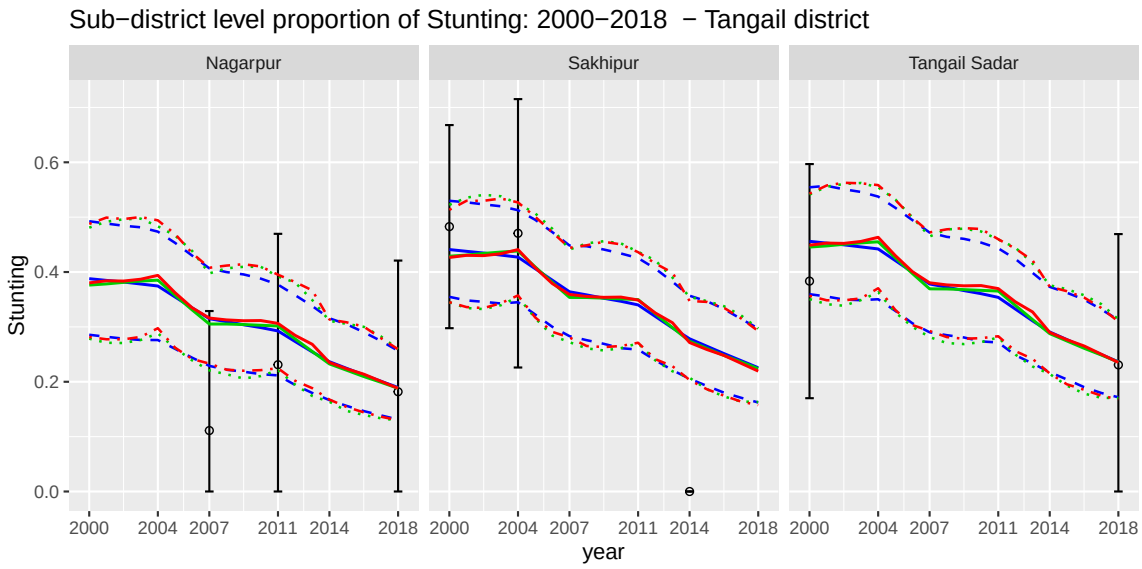


Figure S.4.86: Sub-district level trends of stunting in Tangail district during 2000-2018 by DIR estimator (black error-bar line), MTS-1 model (blue line), MTS-2 model (green line) and MTS-3 model (red line) with 95% confidence band. Models are developed at sub-district level.

S.4.4 Sub-district level trends: Khulna division

There are 10 districts and 64 sub-districts under Khulna division. The trends estimates of stunting for each of the sub-districts are shown under their respective districts in Figures from S.4.87 to S.4.95.

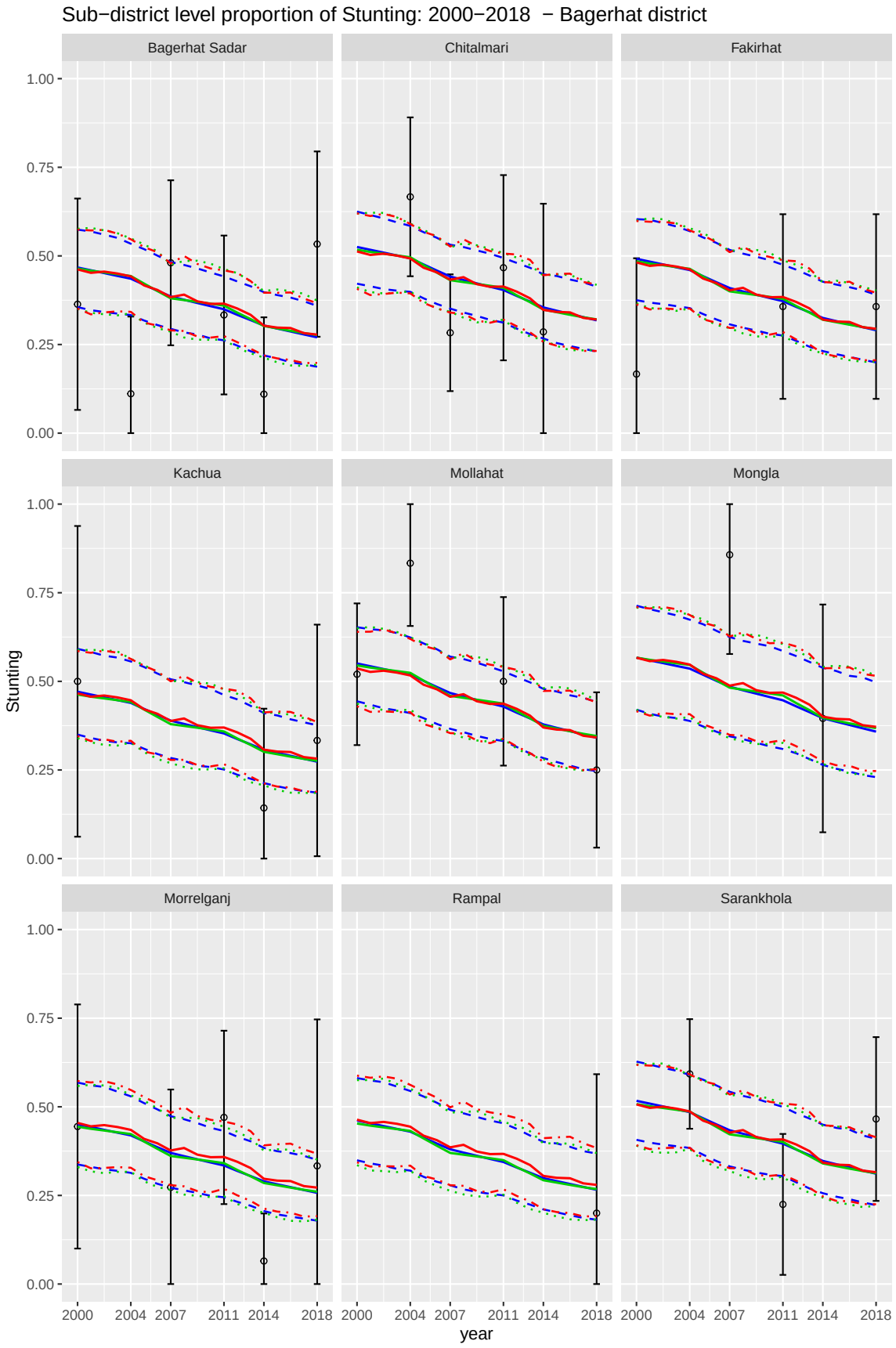


Figure S.4.87: Sub-district level trends of stunting in Bagerhat district during 2000-2018 by DIR estimator (black error-bar line), MTS-1 model (blue line), MTS-2 model (green line) and MTS-3 model (red line) with 95% confidence band. Models are developed at sub-district level.

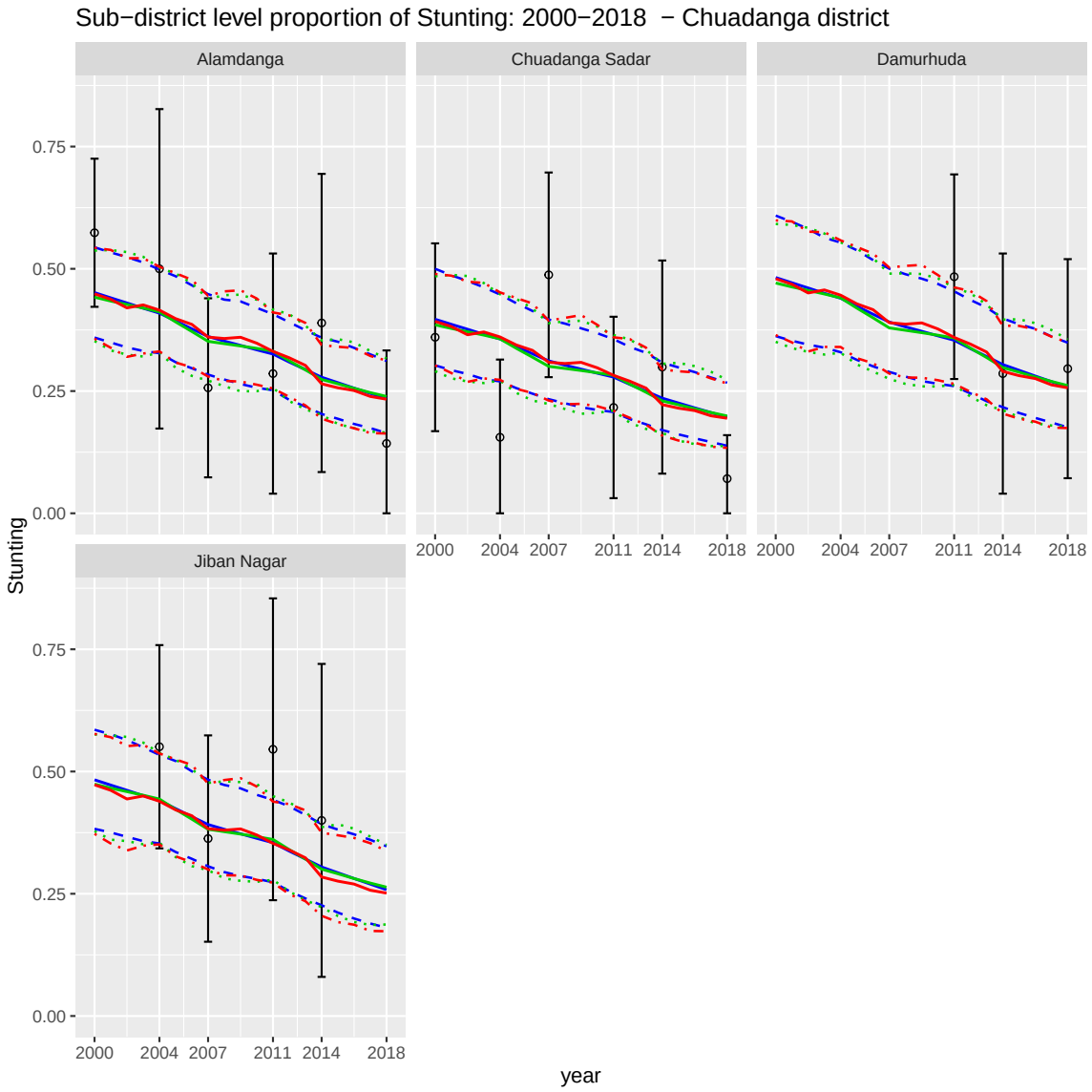


Figure S.4.88: Sub-district level trends of stunting in Chuadanga district during 2000-2018 by DIR estimator (black error-bar line), MTS-1 model (blue line), MTS-2 model (green line) and MTS-3 model (red line) with 95% confidence band. Models are developed at sub-district level.

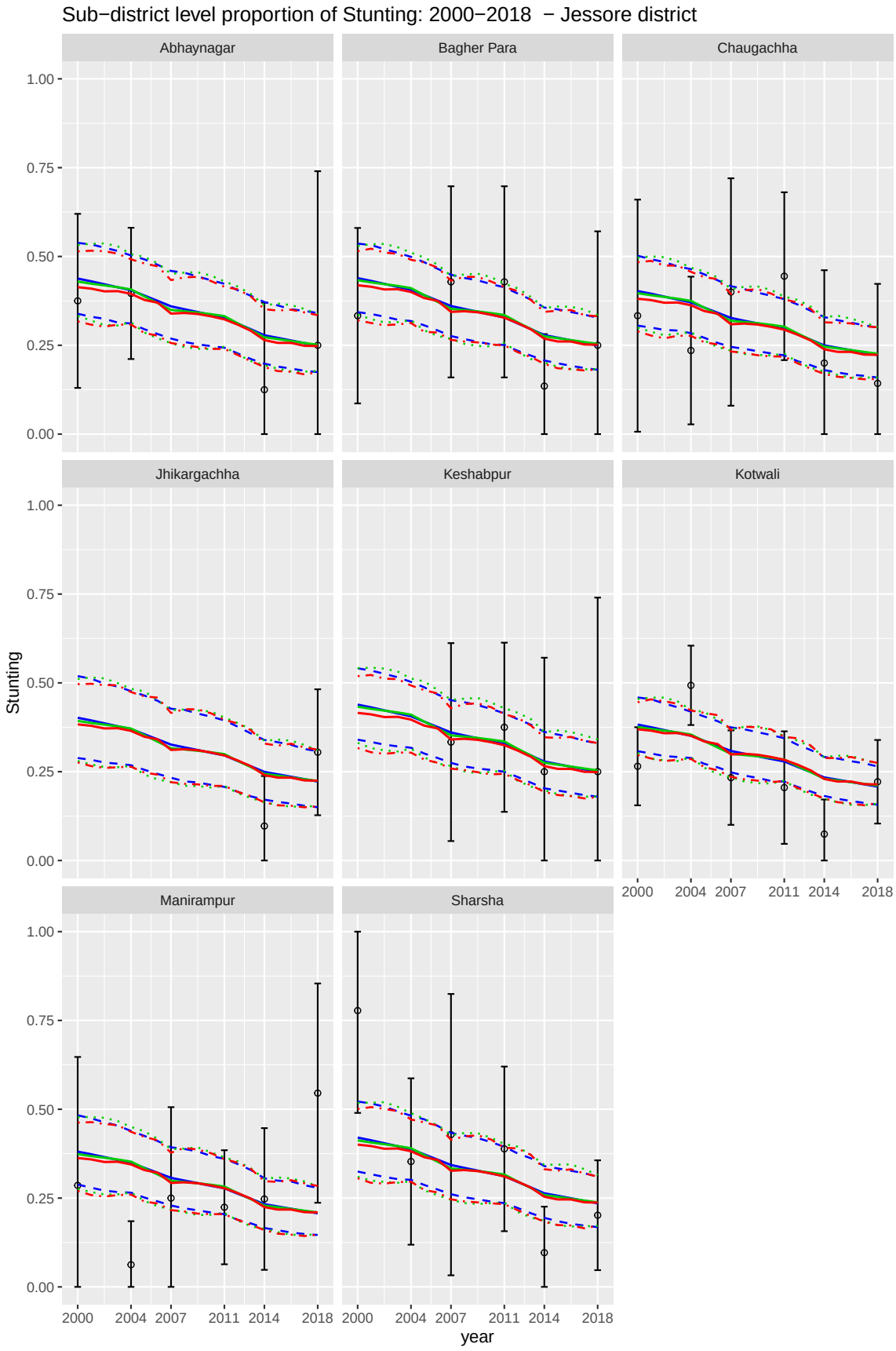


Figure S.4.89: Sub-district level trends of stunting in Jessore district during 2000-2018 by DIR estimator (black error-bar line), MTS-1 model (blue line), MTS-2 model (green line) and MTS-3 model (red line) with 95% confidence band. Models are developed at sub-district level.

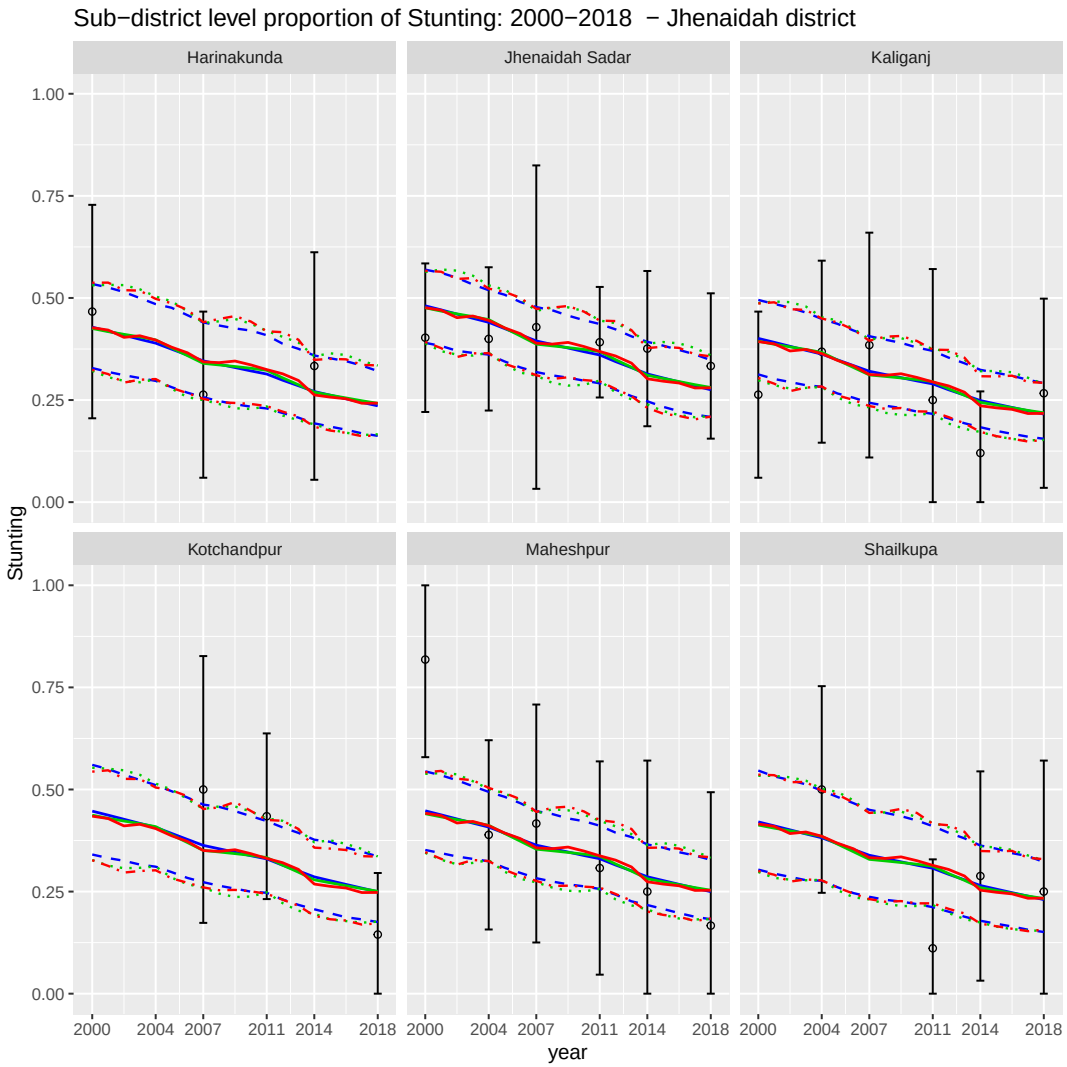


Figure S.4.90: Sub-district level trends of stunting in Jhenaidah district during 2000-2018 by DIR estimator (black error-bar line), MTS-1 model (blue line), MTS-2 model (green line) and MTS-3 model (red line) with 95% confidence band. Models are developed at sub-district level.

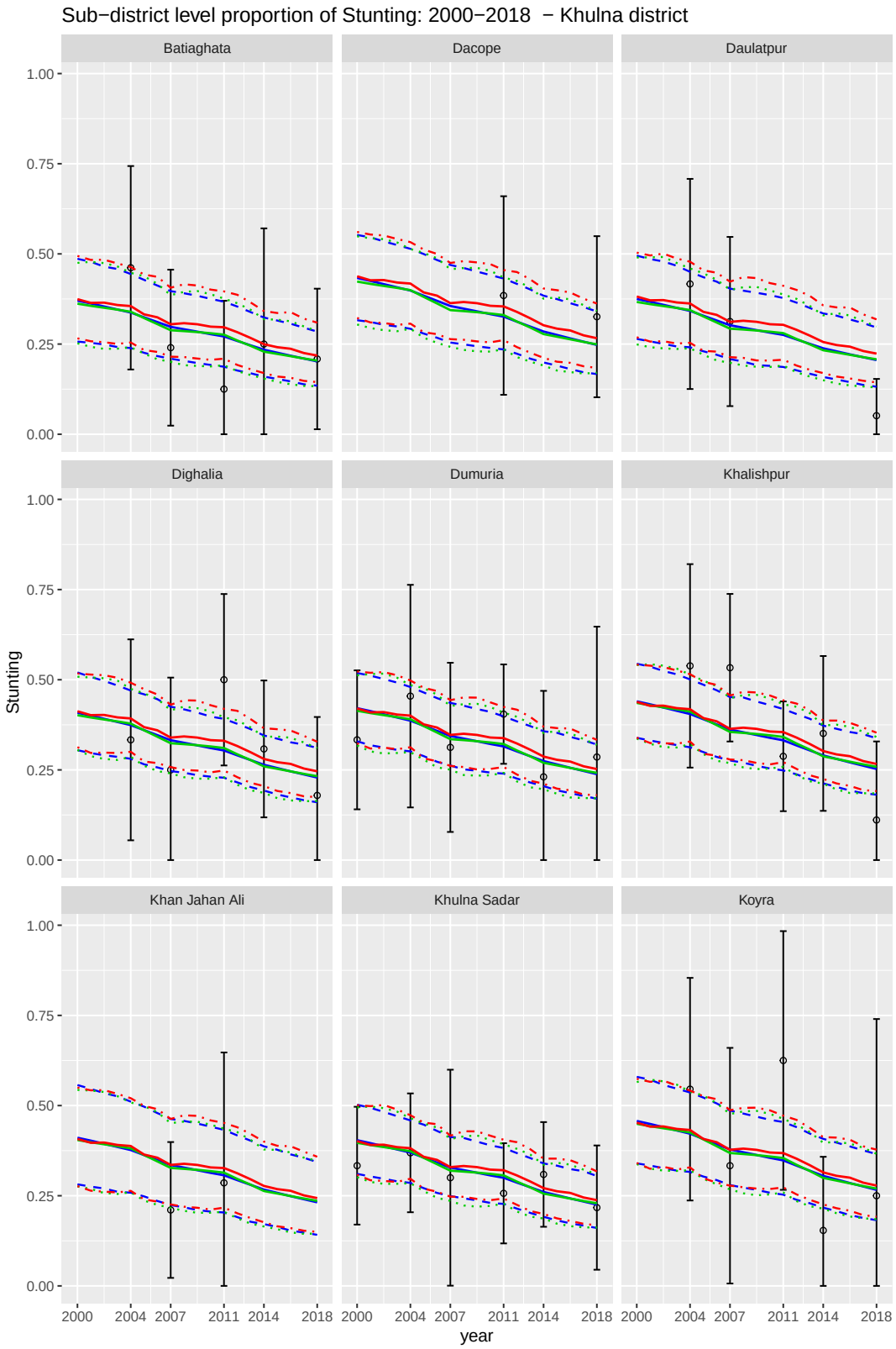


Figure S.4.91: Sub-district level trends of stunting in Khulna district during 2000-2018 by DIR estimator (black error-bar line), MTS-1 model (blue line), MTS-2 model (green line) and MTS-3 model (red line) with 95% confidence band. Models are developed at sub-district level.

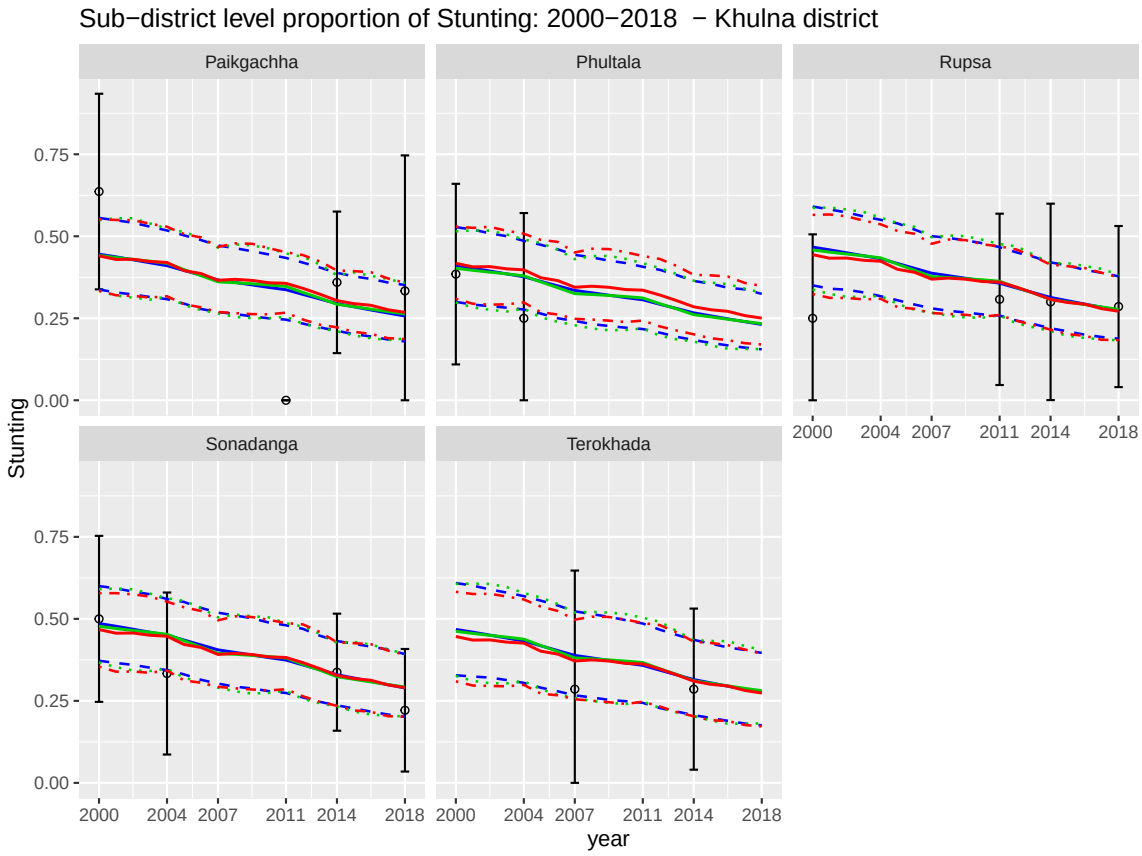


Figure S.4.92: Sub-district level trends of stunting in Khulna district during 2000-2018 by DIR estimator (black error-bar line), MTS-1 model (blue line), MTS-2 model (green line) and MTS-3 model (red line) with 95% confidence band. Models are developed at sub-district level.

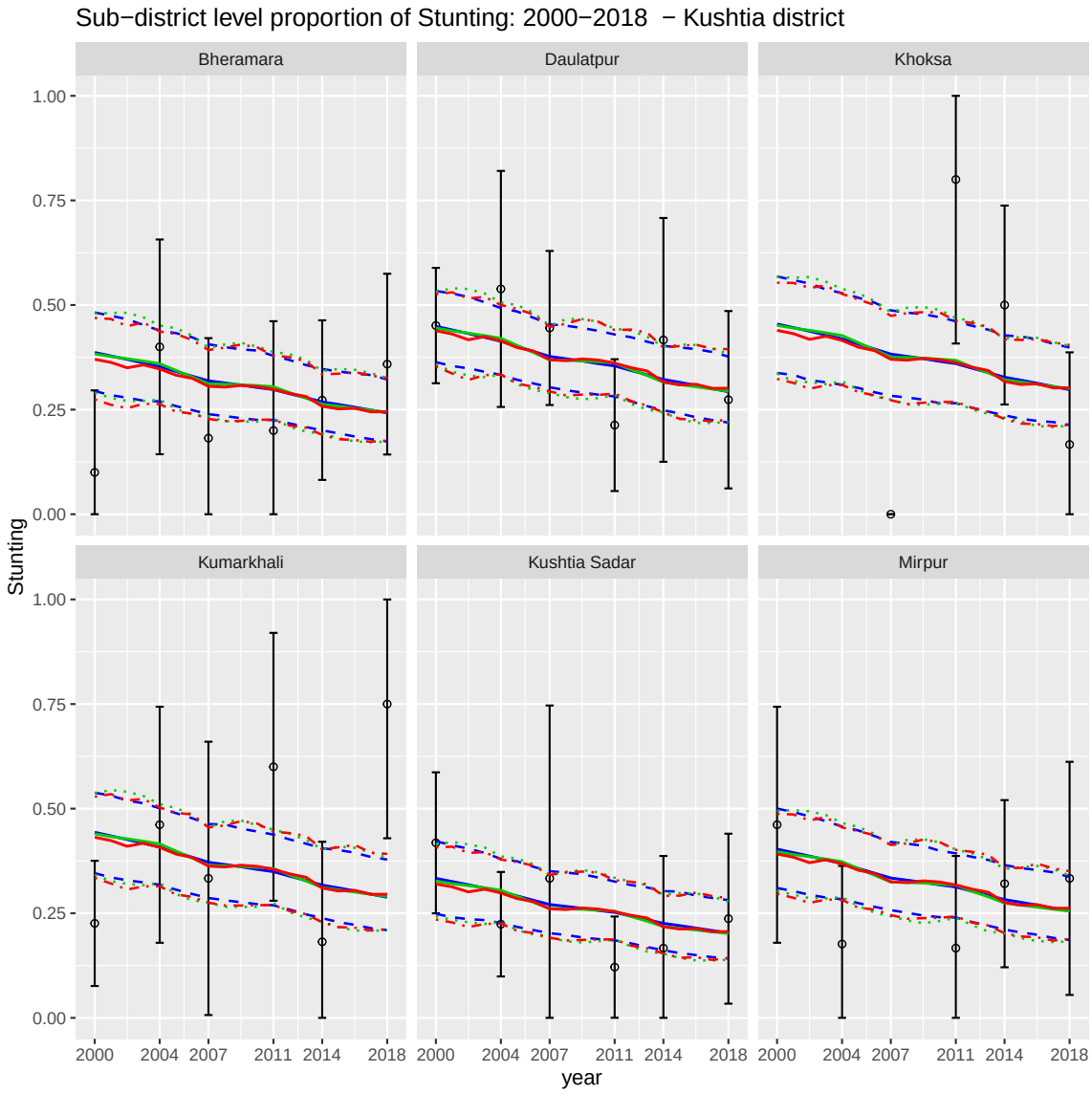


Figure S.4.93: Sub-district level trends of stunting in Kushtia district during 2000-2018 by DIR estimator (black error-bar line), MTS-1 model (blue line), MTS-2 model (green line) and MTS-3 model (red line) with 95% confidence band. Models are developed at sub-district level.

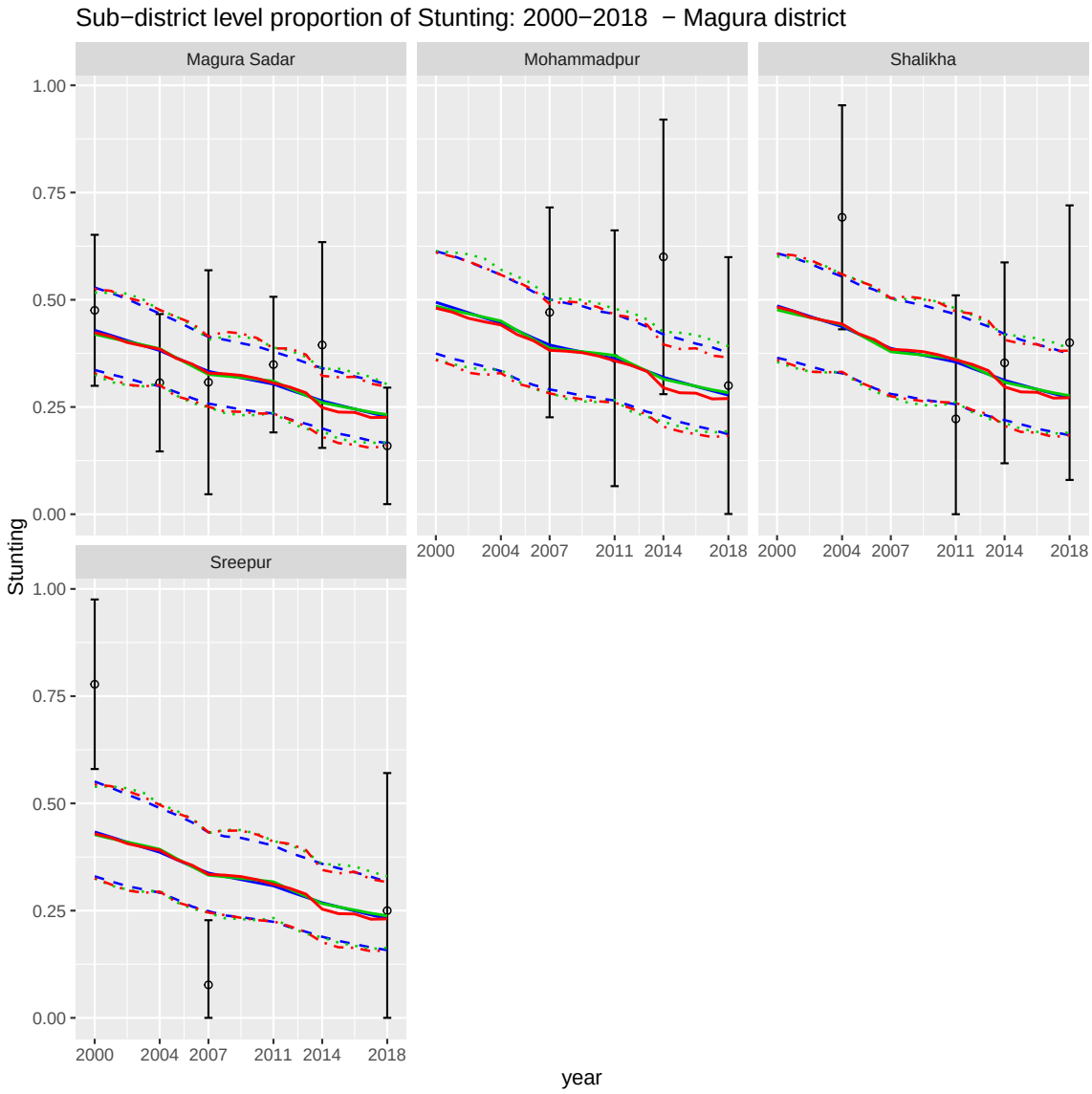


Figure S.4.94: Sub-district level trends of stunting in Magura district during 2000-2018 by DIR estimator (black error-bar line), MTS-1 model (blue line), MTS-2 model (green line) and MTS-3 model (red line) with 95% confidence band. Models are developed at sub-district level.

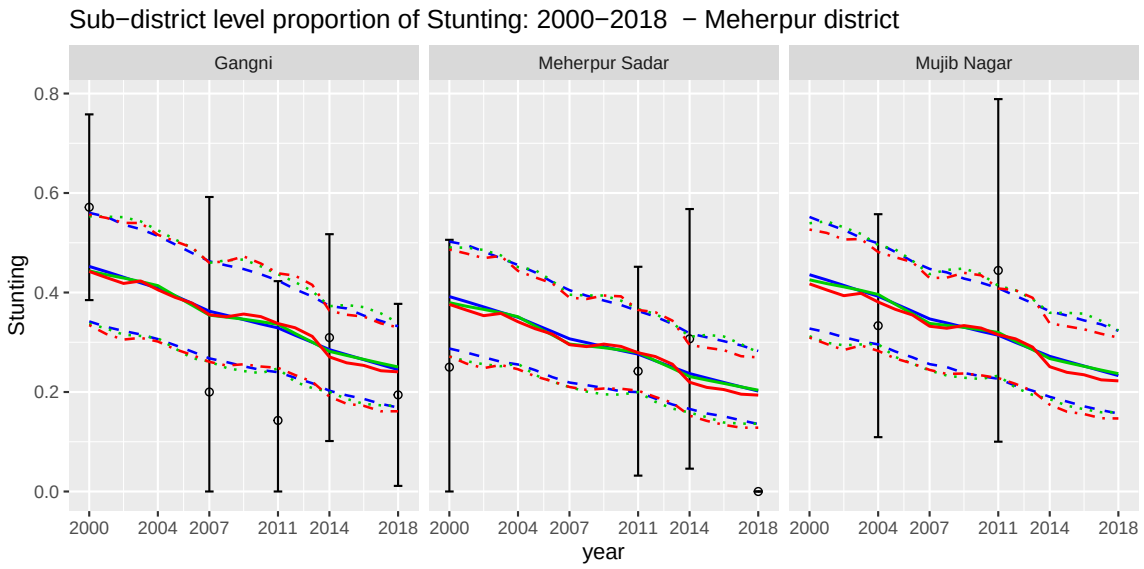


Figure S.4.95: Sub-district level trends of stunting in Meherpur district during 2000-2018 by DIR estimator (black error-bar line), MTS-1 model (blue line), MTS-2 model (green line) and MTS-3 model (red line) with 95% confidence band. Models are developed at sub-district level.

S.4.5 Sub-district level trends: Rajshahi division

There are 8 districts and 70 sub-districts under Rajshahi division. The trends estimates of stunting for each of the sub-districts are shown under their respective districts in Figures from S.4.96 to S.4.106.

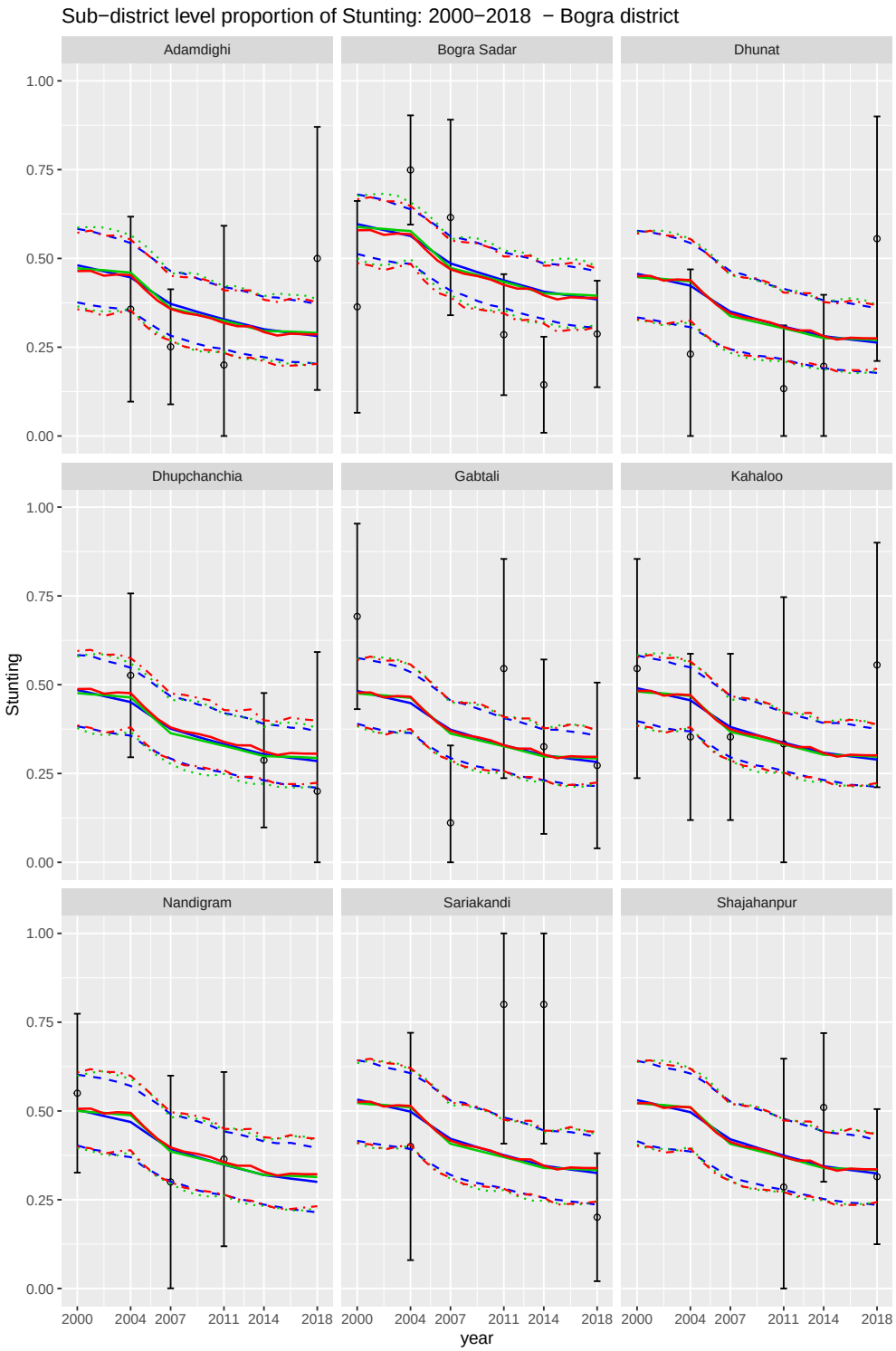


Figure S.4.96: Sub-district level trends of stunting in Bogra district during 2000-2018 by DIR estimator (black error-bar line), MTS-1 model (blue line), MTS-2 model (green line) and MTS-3 model (red line) with 95% confidence band. Models are developed at sub-district level.

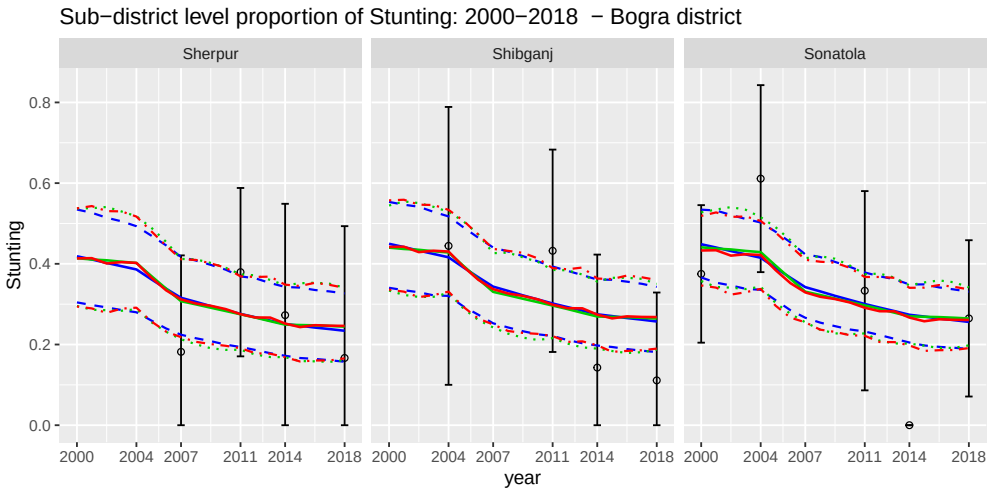


Figure S.4.97: Sub-district level trends of stunting in Bogra district during 2000-2018 by DIR estimator (black error-bar line), MTS-1 model (blue line), MTS-2 model (green line) and MTS-3 model (red line) with 95% confidence band. Models are developed at sub-district level.

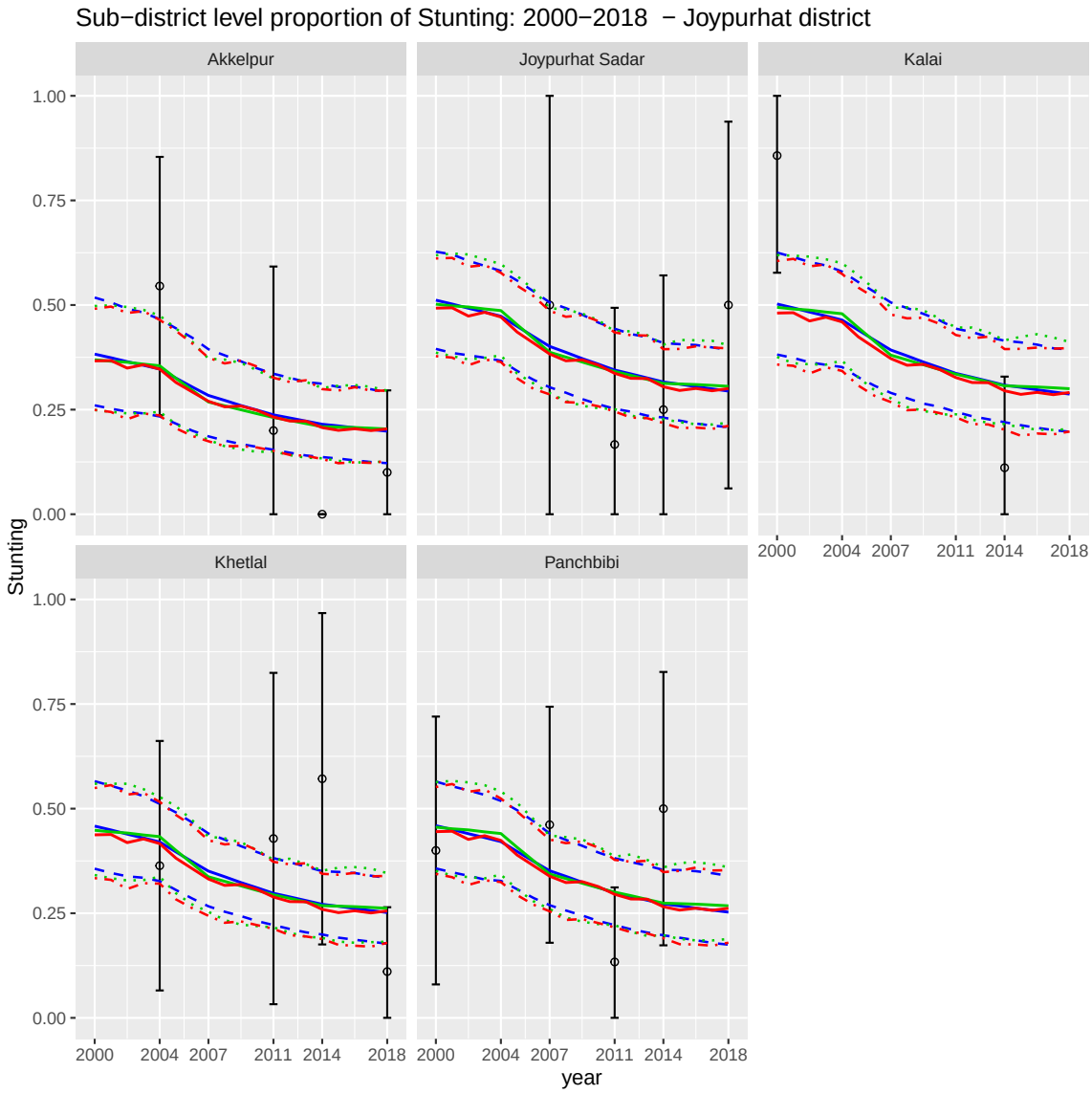


Figure S.4.98: Sub-district level trends of stunting in Joypurhat district during 2000-2018 by DIR estimator (black error-bar line), MTS-1 model (blue line), MTS-2 model (green line) and MTS-3 model (red line) with 95% confidence band. Models are developed at sub-district level.

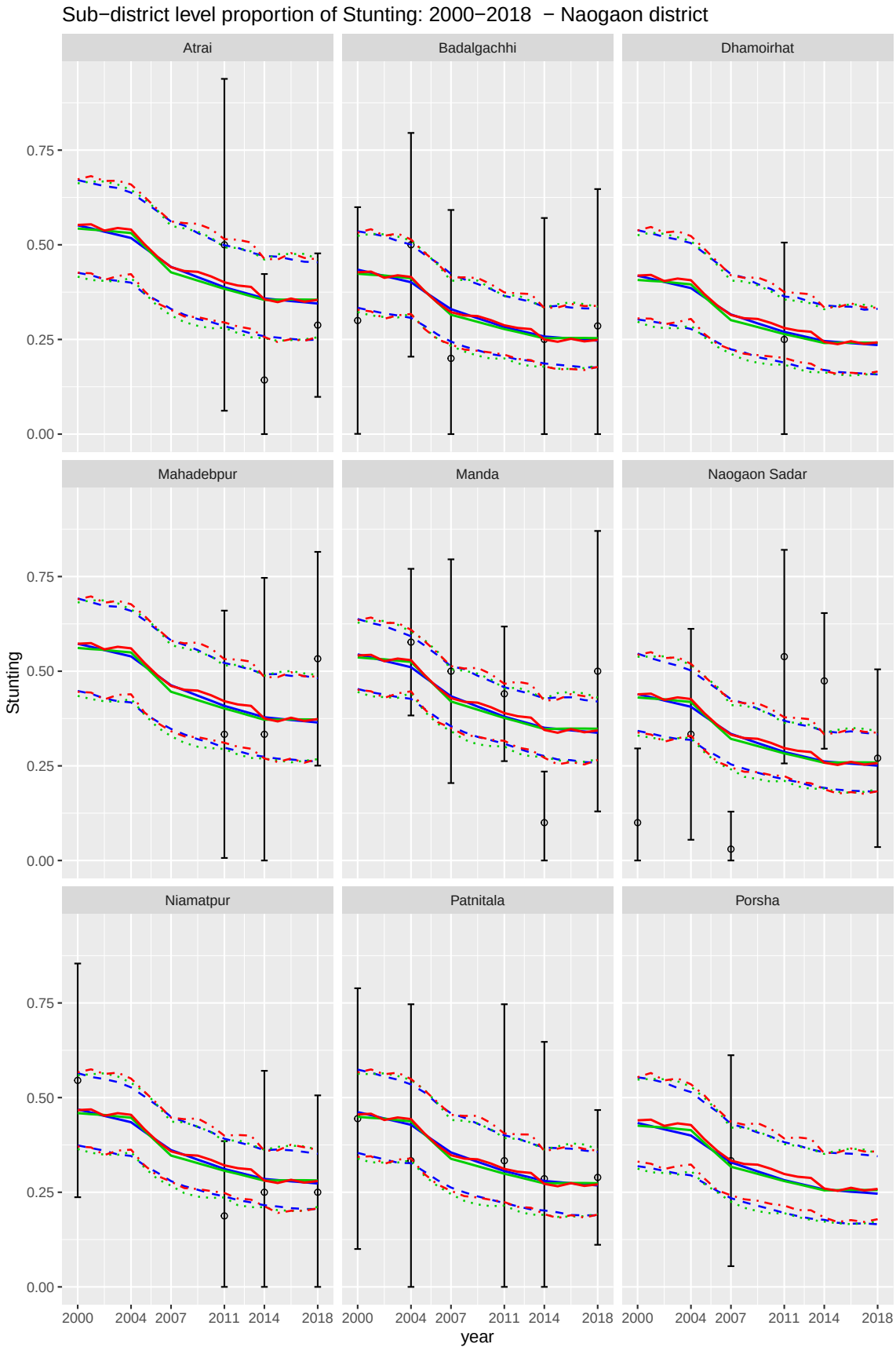


Figure S.4.99: Sub-district level trends of stunting in Naogaon district during 2000-2018 by DIR estimator (black error-bar line), MTS-1 model (blue line), MTS-2 model (green line) and MTS-3 model (red line) with 95% confidence band. Models are developed at sub-district level.

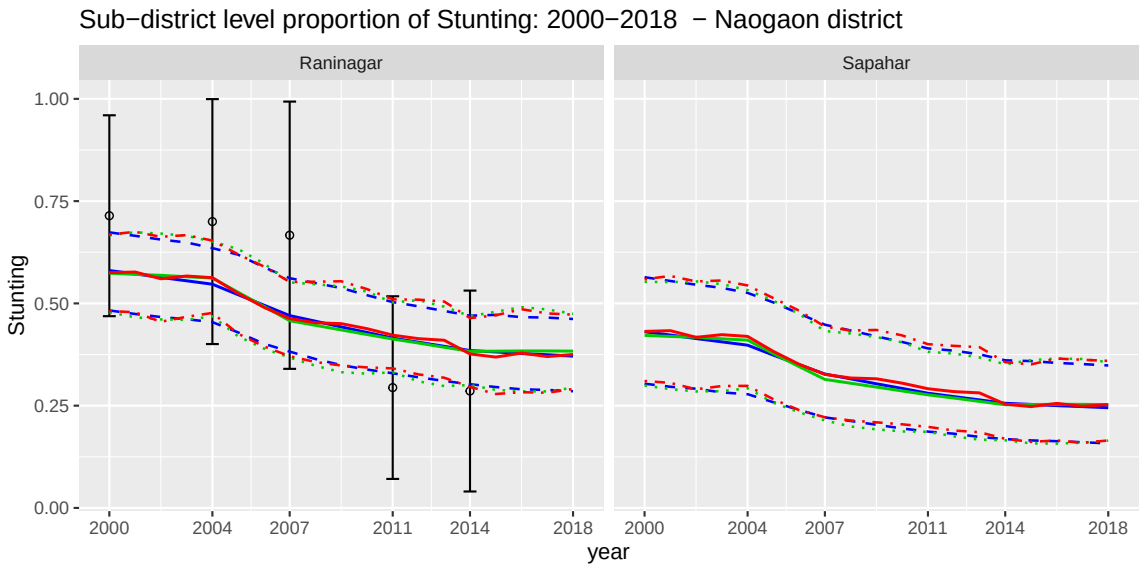


Figure S.4.100: Sub-district level trends of stunting in Naogaon district during 2000-2018 by DIR estimator (black error-bar line), MTS-1 model (blue line), MTS-2 model (green line) and MTS-3 model (red line) with 95% confidence band. Models are developed at sub-district level.

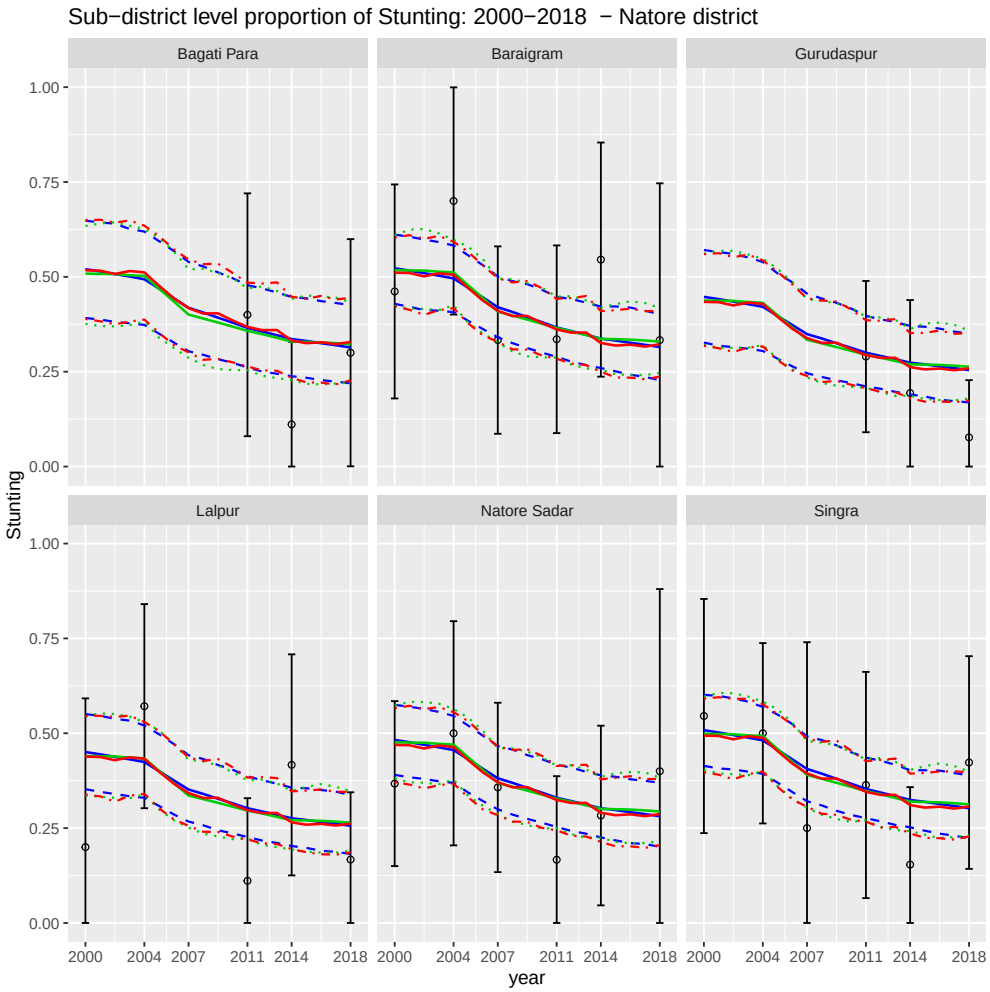


Figure S.4.101: Sub-district level trends of stunting in Natore district during 2000-2018 by DIR estimator (black error-bar line), MTS-1 model (blue line), MTS-2 model (green line) and MTS-3 model (red line) with 95% confidence band. Models are developed at sub-district level.

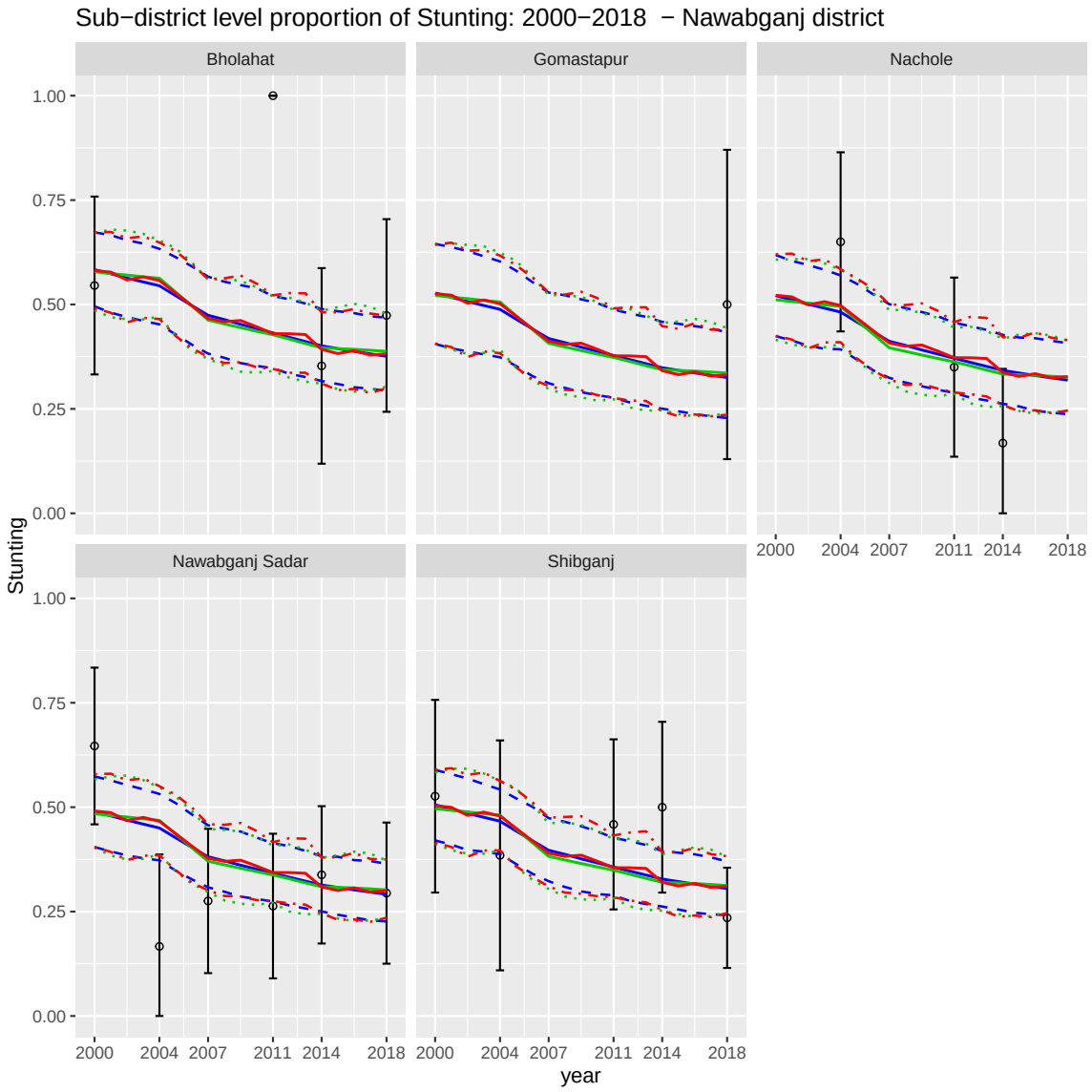


Figure S.4.102: Sub-district level trends of stunting in Nawabganj district during 2000-2018 by DIR estimator (black error-bar line), MTS-1 model (blue line), MTS-2 model (green line) and MTS-3 model (red line) with 95% confidence band. Models are developed at sub-district level.

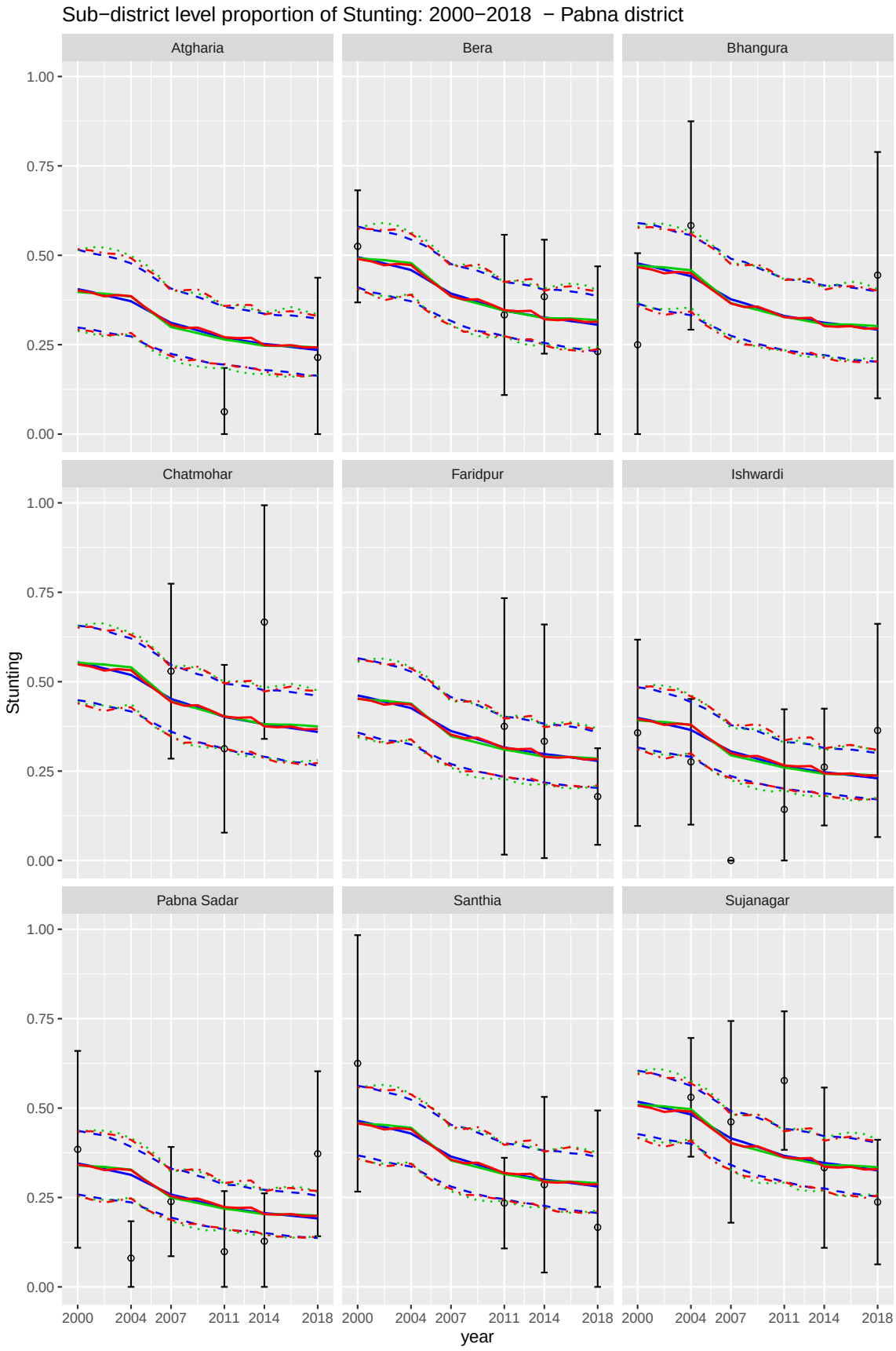


Figure S.4.103: Sub-district level trends of stunting in Pabna district during 2000-2018 by DIR estimator (black error-bar line), MTS-1 model (blue line), MTS-2 model (green line) and MTS-3 model (red line) with 95% confidence band. Models are developed at sub-district level.

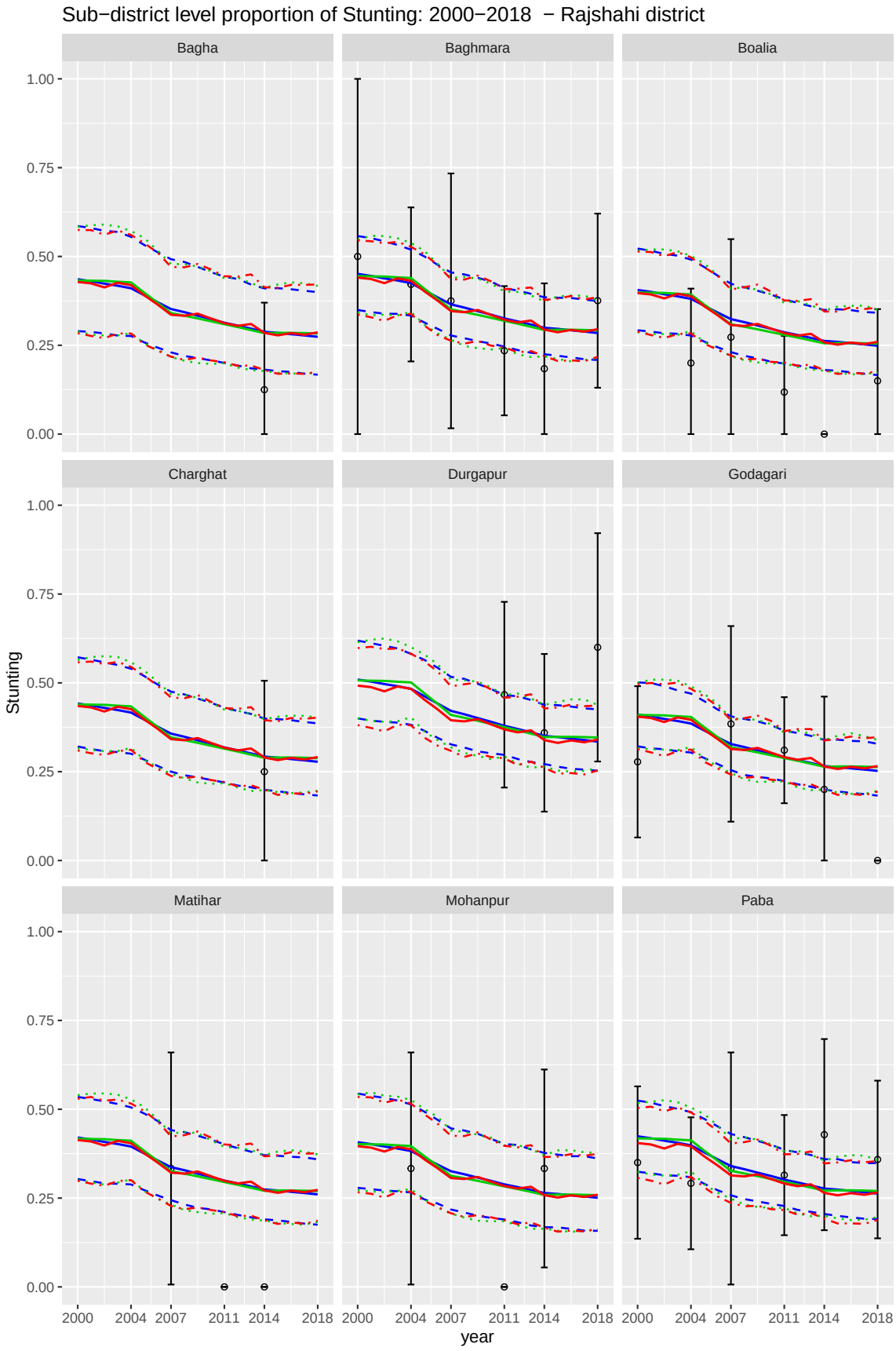


Figure S.4.104: Sub-district level trends of stunting in Rajshahi district during 2000-2018 by DIR estimator (black error-bar line), MTS-1 model (blue line), MTS-2 model (green line) and MTS-3 model (red line) with 95% confidence band. Models are developed at sub-district level.

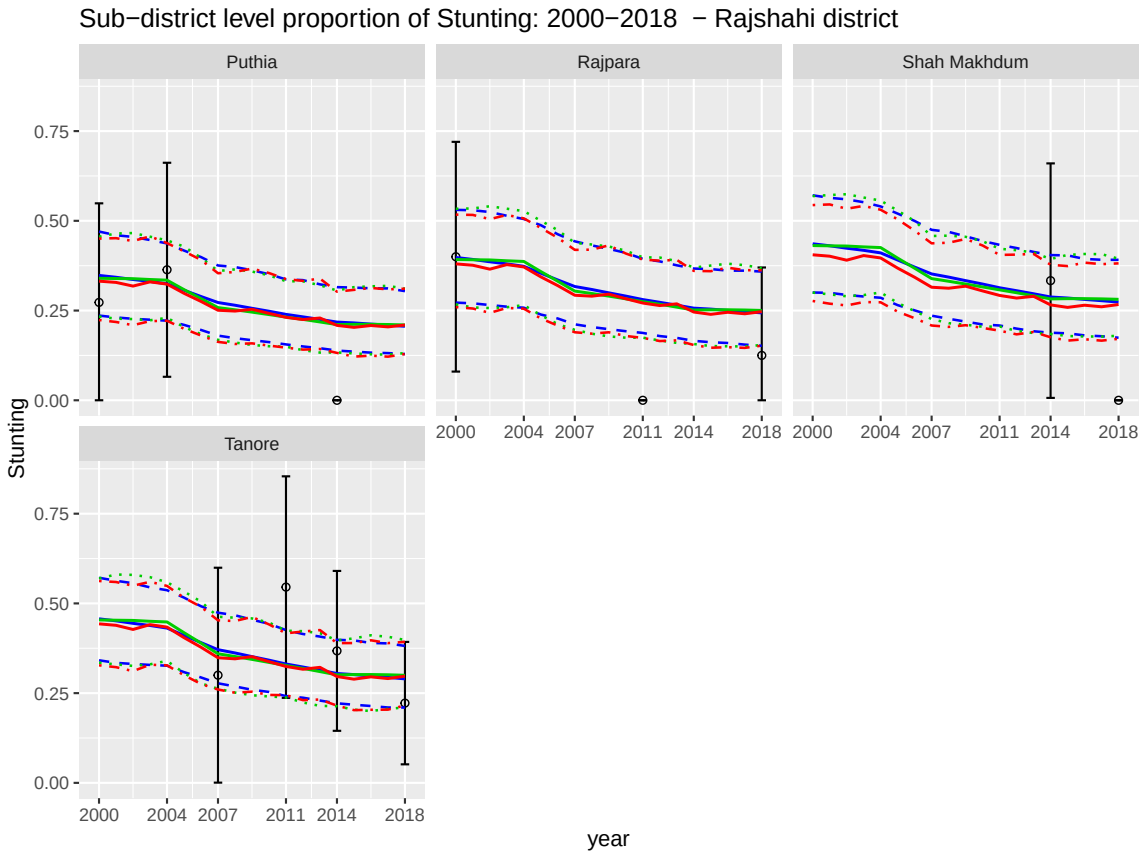


Figure S.4.105: Sub-district level trends of stunting in Rajshahi district during 2000-2018 by DIR estimator (black error-bar line), MTS-1 model (blue line), MTS-2 model (green line) and MTS-3 model (red line) with 95% confidence band. Models are developed at sub-district level.

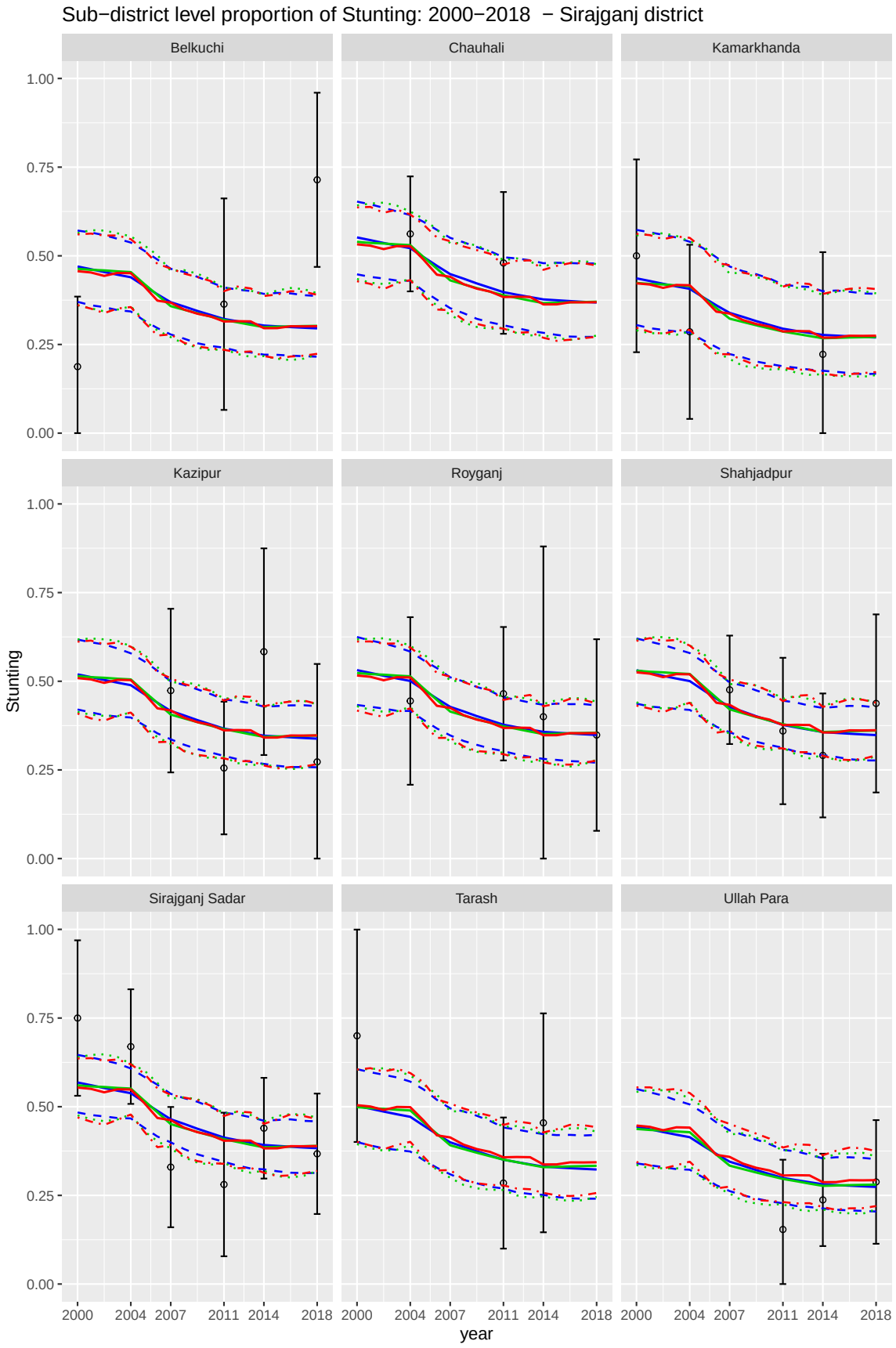


Figure S.4.106: Sub-district level trends of stunting in Sirajganj district during 2000-2018 by DIR estimator (black error-bar line), MTS-1 model (blue line), MTS-2 model (green line) and MTS-3 model (red line) with 95% confidence band. Models are developed at sub-district level.

S.4.6 Sub-district level trends: Rangpur division

There are 8 districts and 58 sub-districts under Rangpur division. The trends estimates of stunting for each of the sub-districts are shown under their respective districts in Figures from S.4.107 to S.4.115.

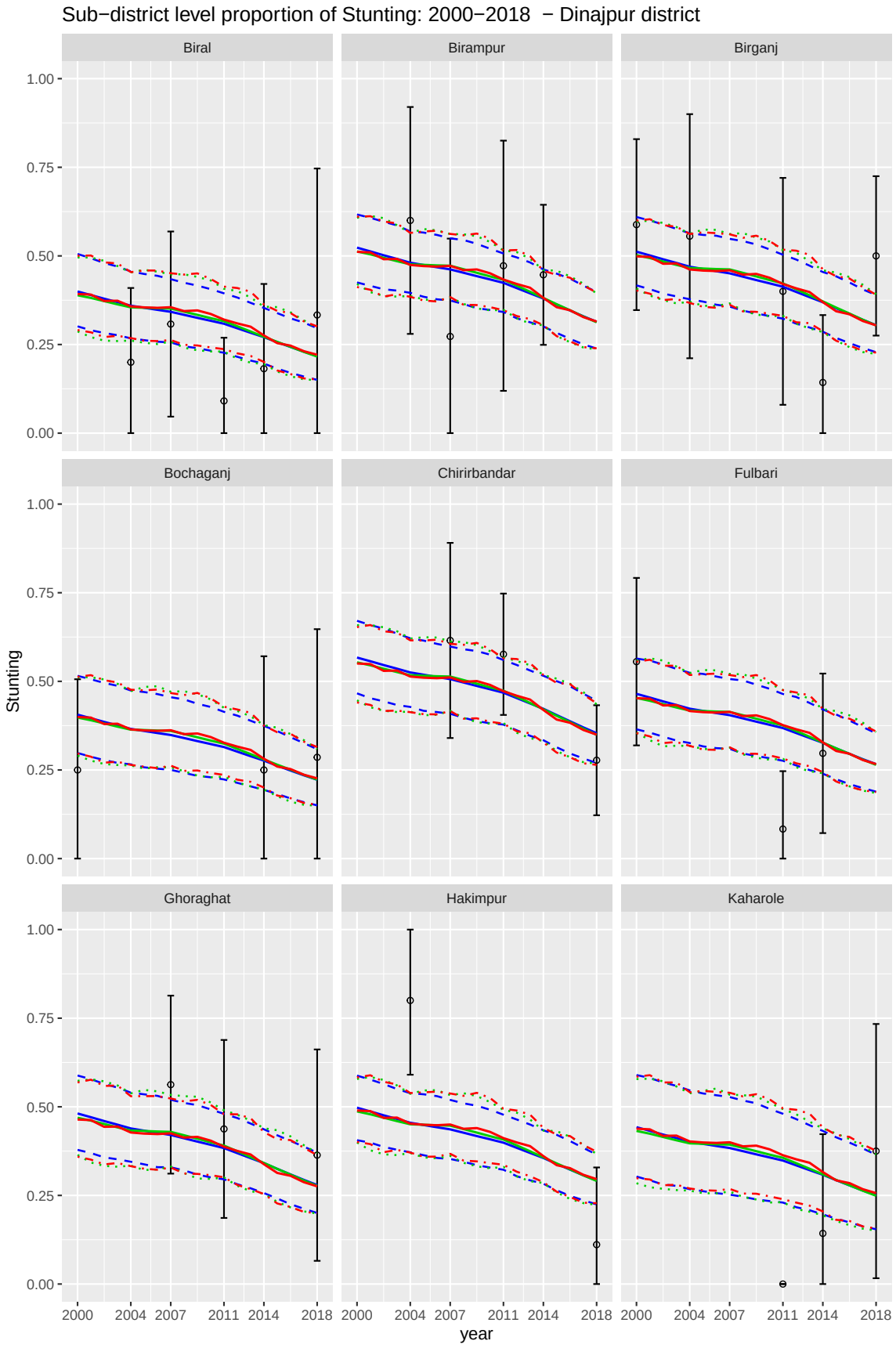


Figure S.4.107: Sub-district level trends of stunting in Dinajpur district during 2000-2018 by DIR estimator (black error-bar line), MTS-1 model (blue line), MTS-2 model (green line) and MTS-3 model (red line) with 95% confidence band. Models are developed at sub-district level.

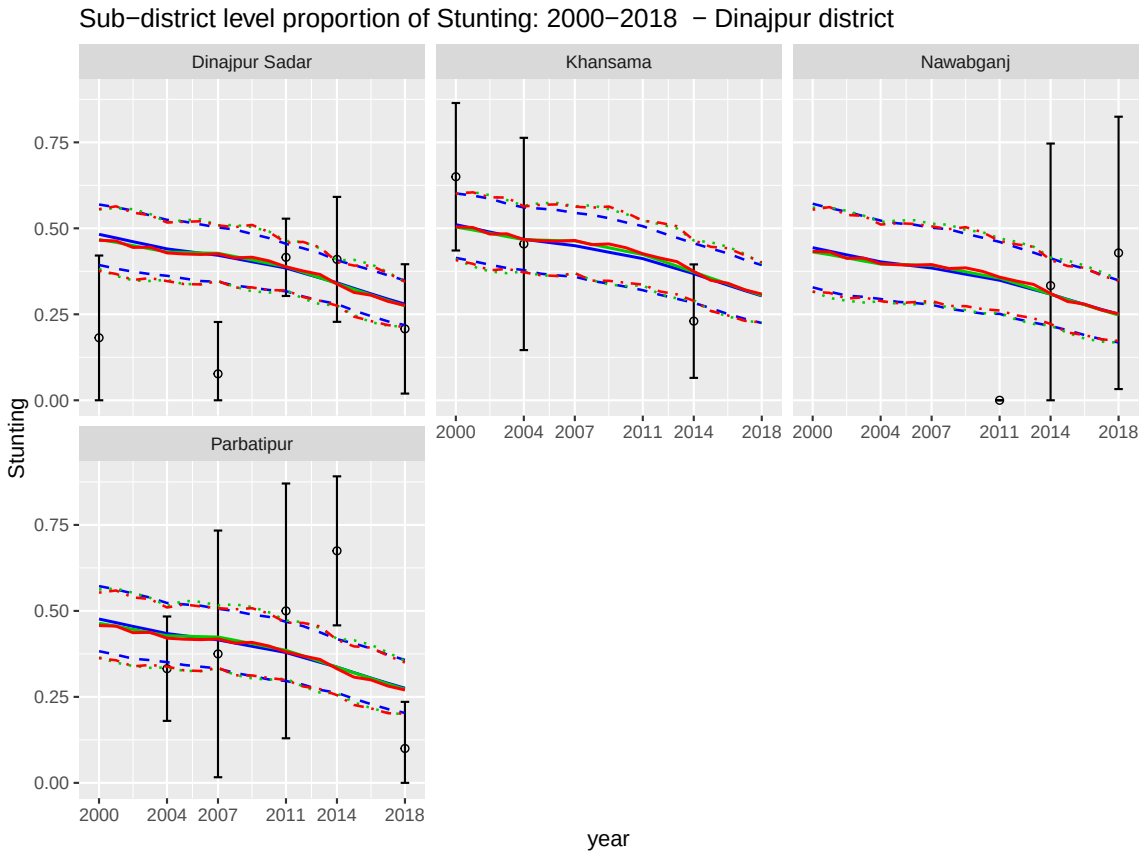


Figure S.4.108: Sub-district level trends of stunting in Dinajpur district during 2000-2018 by DIR estimator (black error-bar line), MTS-1 model (blue line), MTS-2 model (green line) and MTS-3 model (red line) with 95% confidence band. Models are developed at sub-district level.

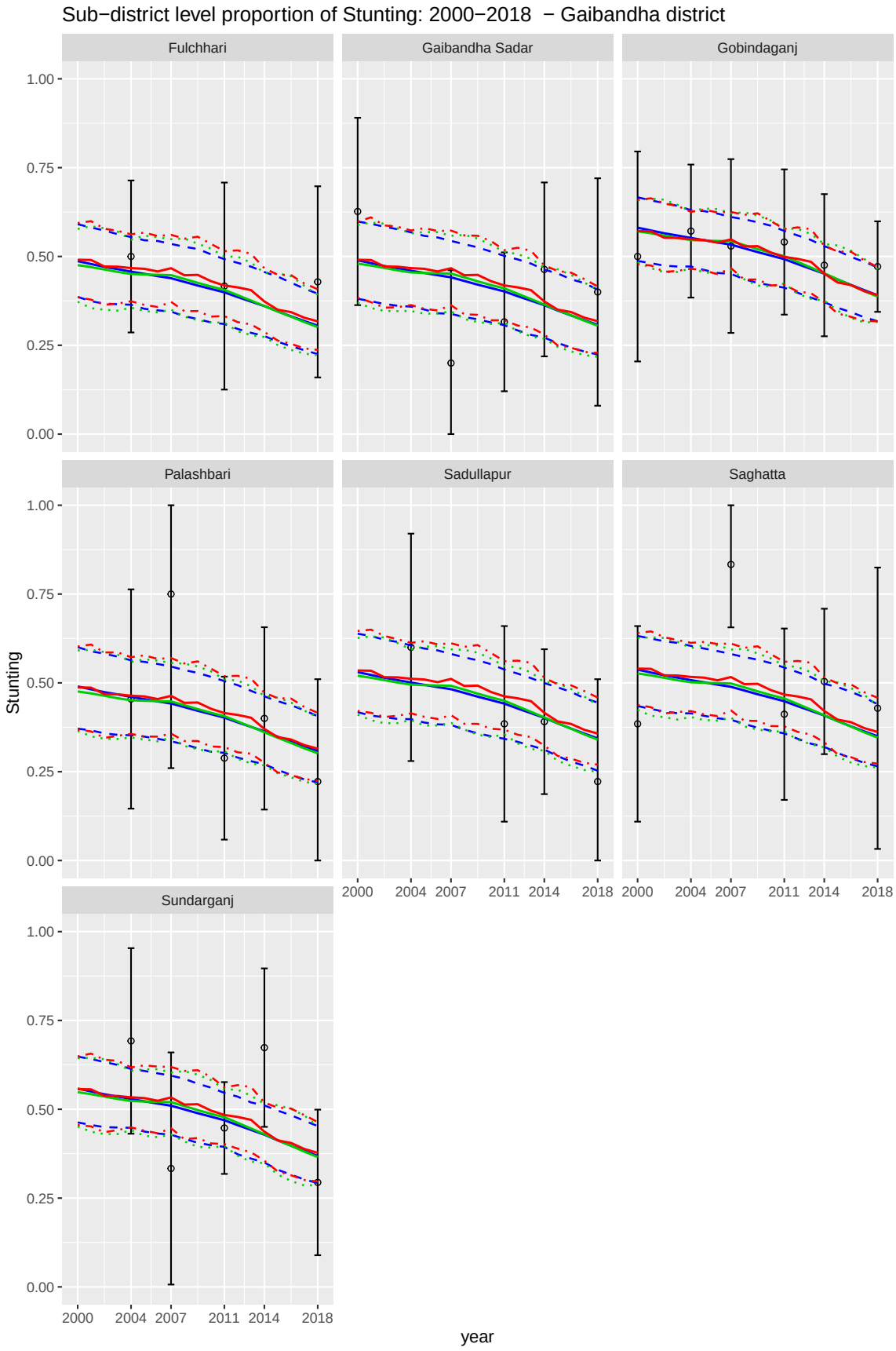


Figure S.4.109: Sub-district level trends of stunting in Gaibandha district during 2000-2018 by DIR estimator (black error-bar line), MTS-1 model (blue line), MTS-2 model (green line) and MTS-3 model (red line) with 95% confidence band. Models are developed at sub-district level.

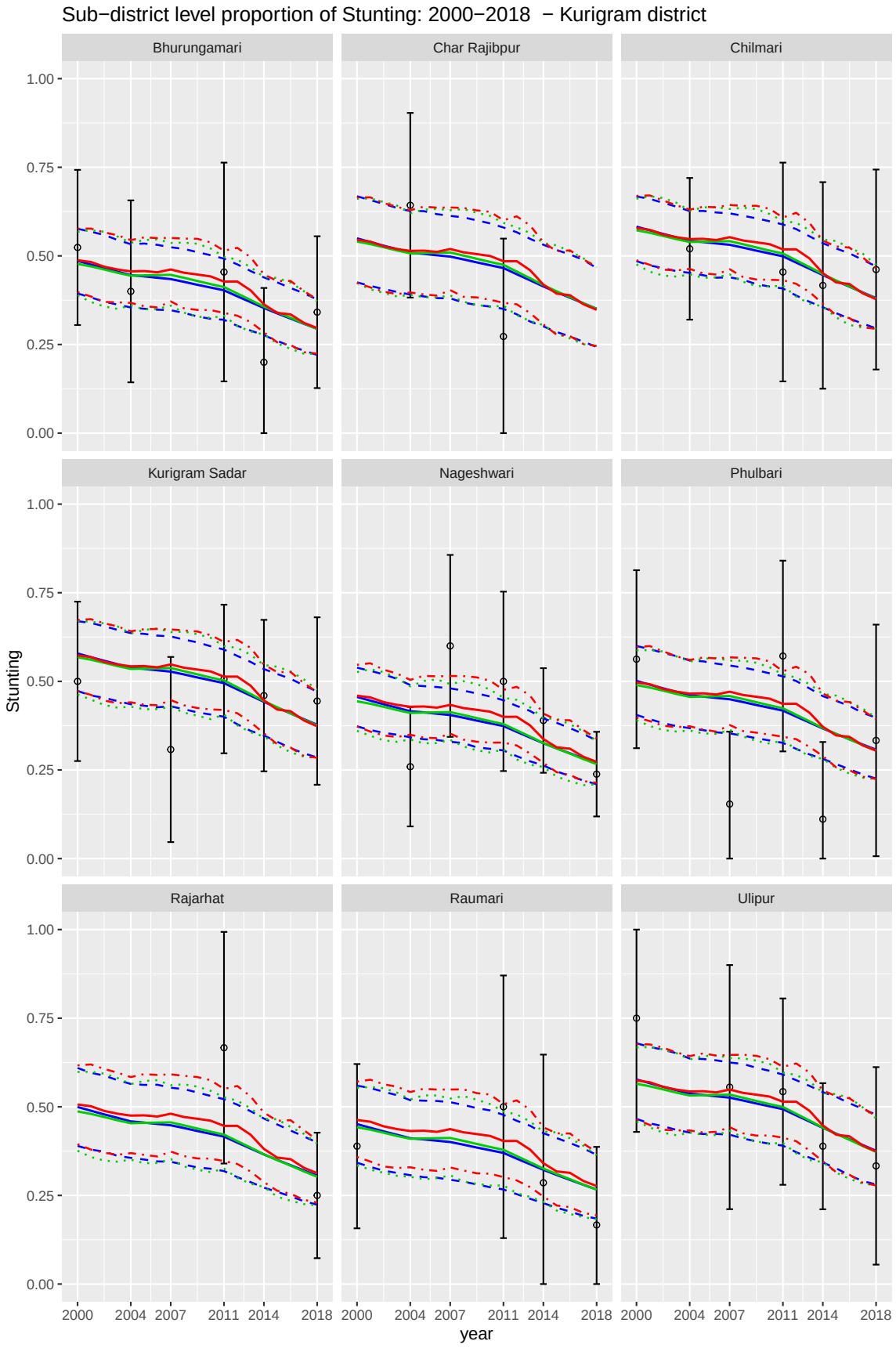


Figure S.4.110: Sub-district level trends of stunting in Kurigram district during 2000-2018 by DIR estimator (black error-bar line), MTS-1 model (blue line), MTS-2 model (green line) and MTS-3 model (red line) with 95% confidence band. Models are developed at sub-district level.

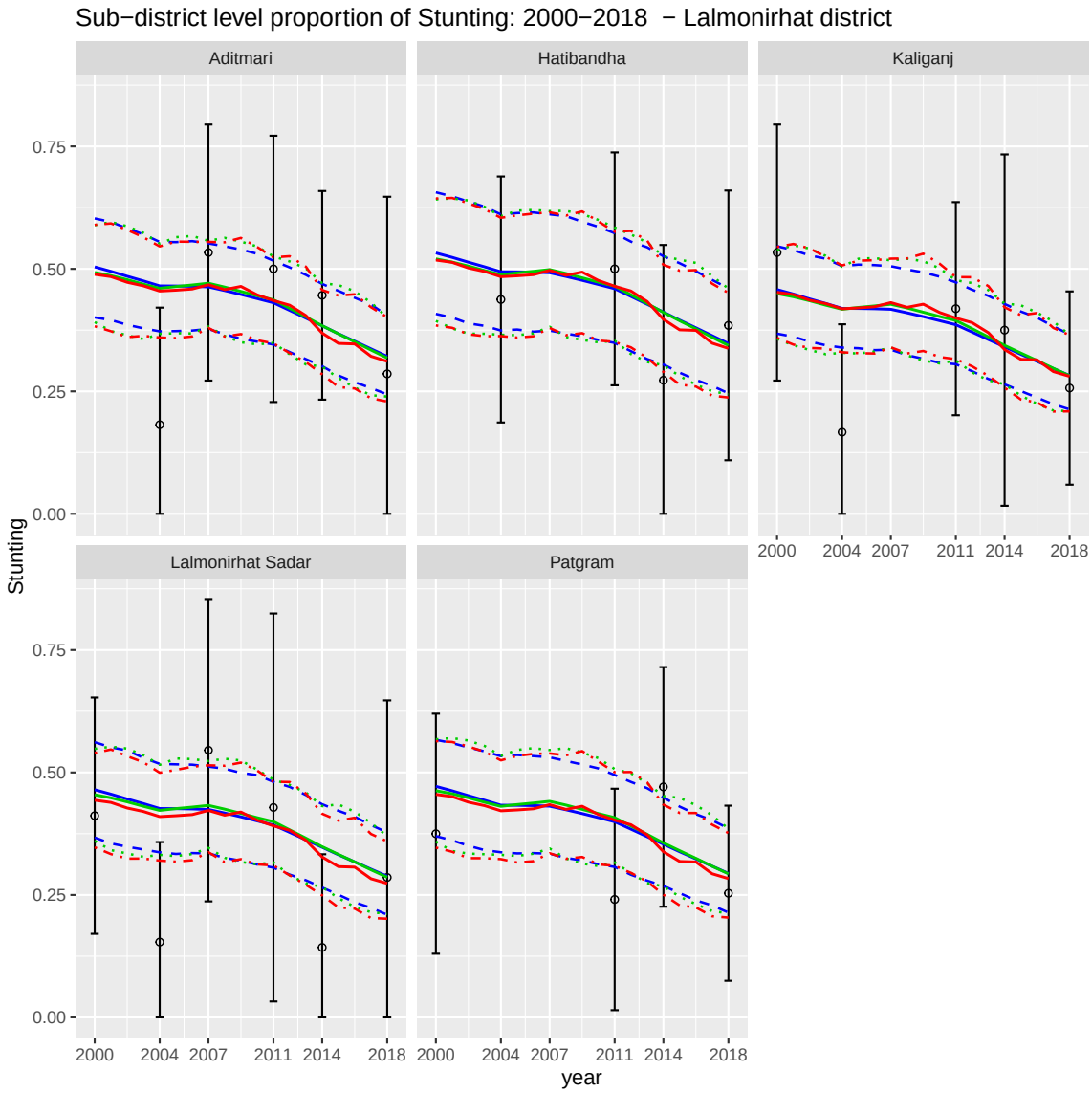


Figure S.4.111: Sub-district level trends of stunting in Lalmonirhat district during 2000-2018 by DIR estimator (black error-bar line), MTS-1 model (blue line), MTS-2 model (green line) and MTS-3 model (red line) with 95% confidence band. Models are developed at sub-district level.

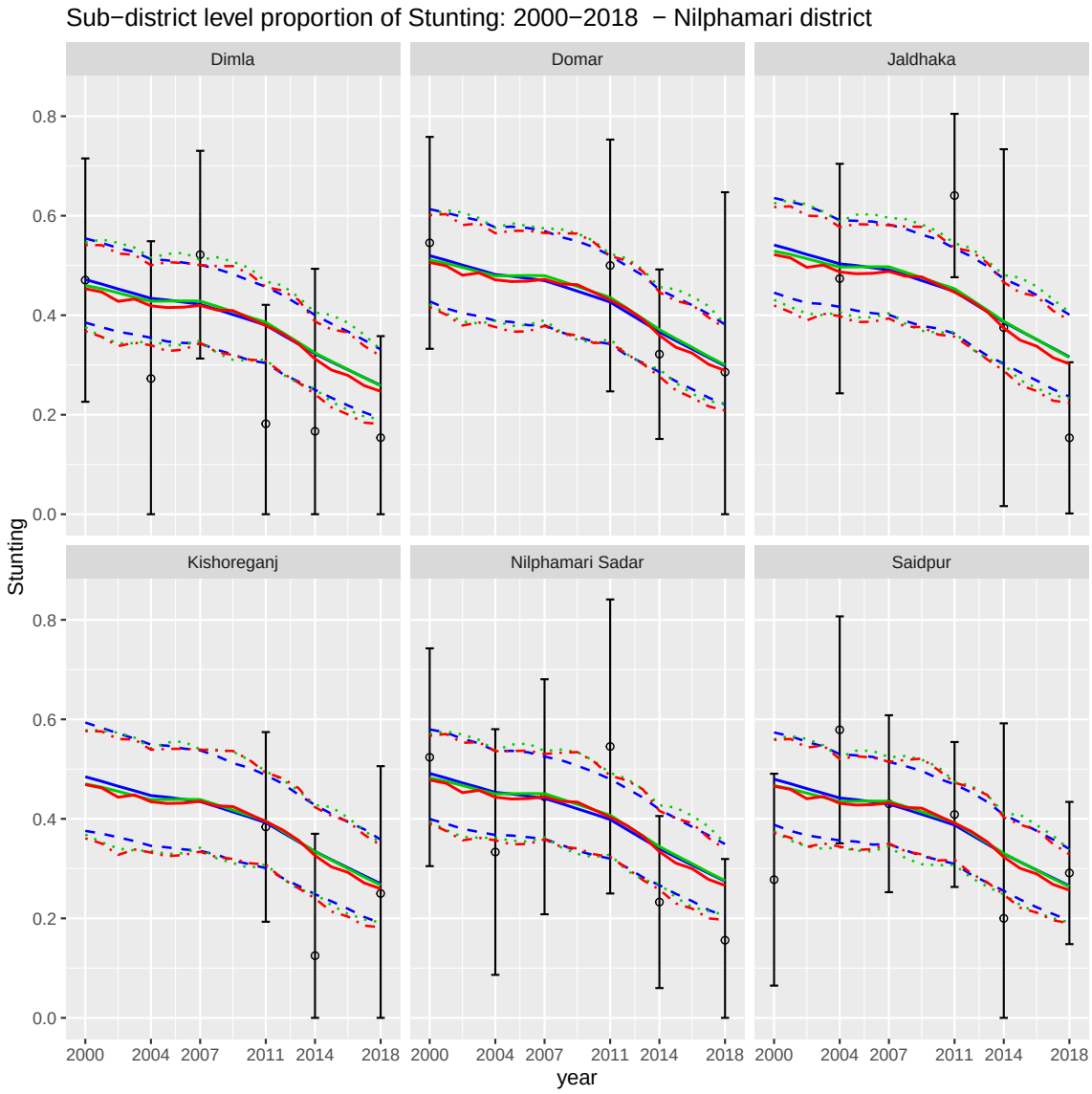


Figure S.4.112: Sub-district level trends of stunting in Nilphamari district during 2000-2018 by DIR estimator (black error-bar line), MTS-1 model (blue line), MTS-2 model (green line) and MTS-3 model (red line) with 95% confidence band. Models are developed at sub-district level.

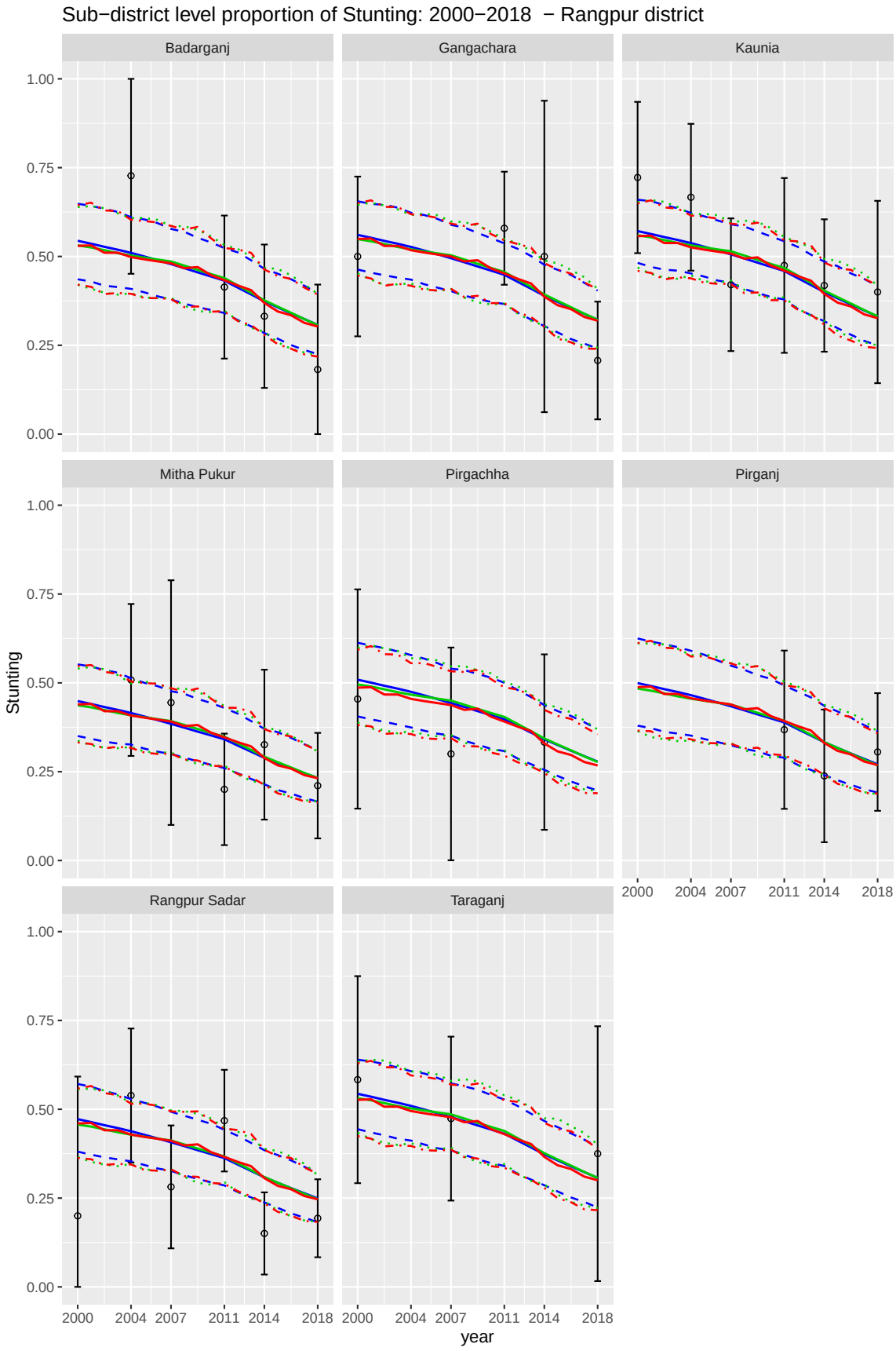


Figure S.4.113: Sub-district level trends of stunting in Rangpur district during 2000-2018 by DIR estimator (black error-bar line), MTS-1 model (blue line), MTS-2 model (green line) and MTS-3 model (red line) with 95% confidence band. Models are developed at sub-district level.

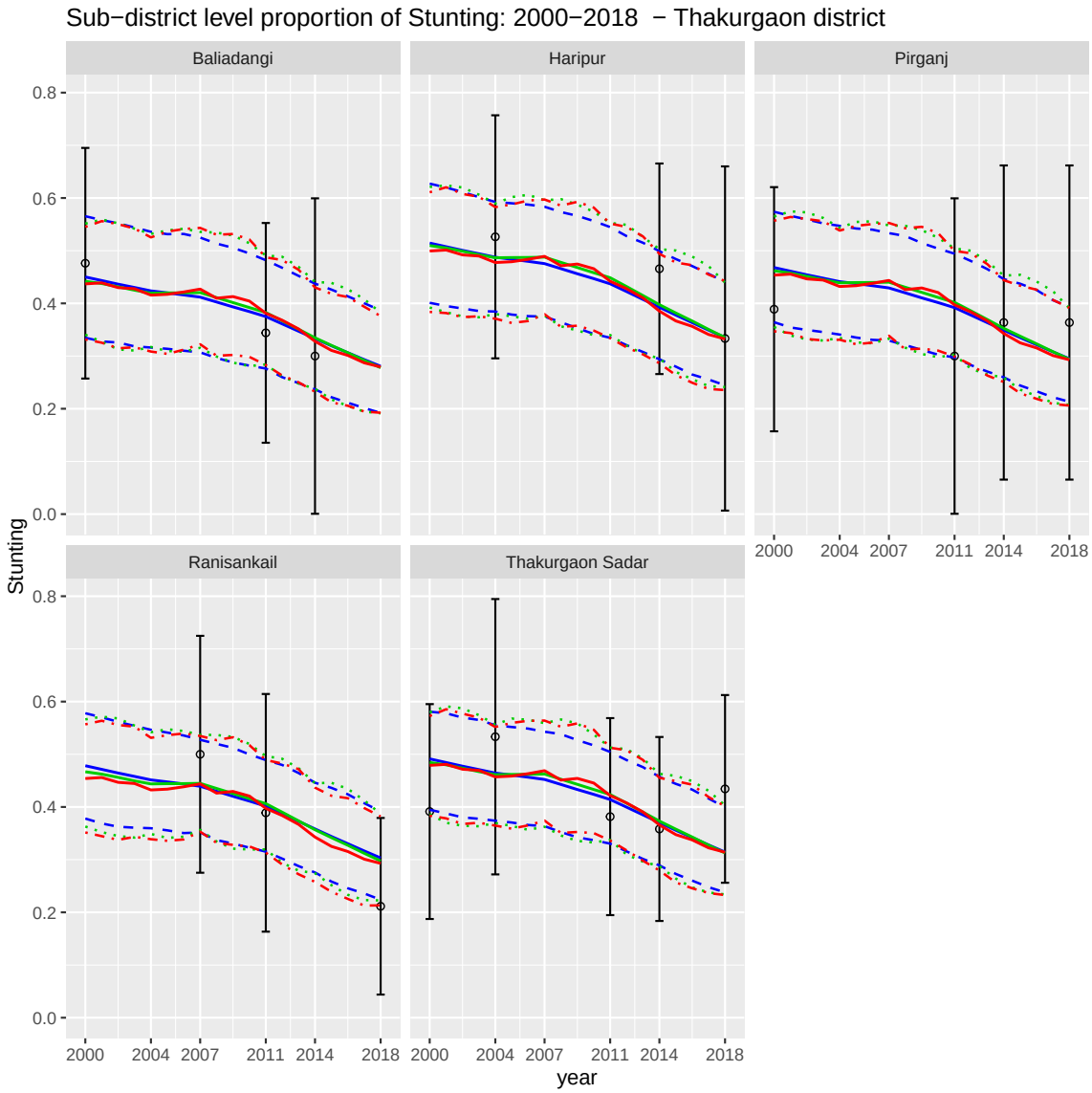


Figure S.4.114: Sub-district level trends of stunting in Thakurgaon district during 2000-2018 by DIR estimator (black error-bar line), MTS-1 model (blue line), MTS-2 model (green line) and MTS-3 model (red line) with 95% confidence band. Models are developed at sub-district level.

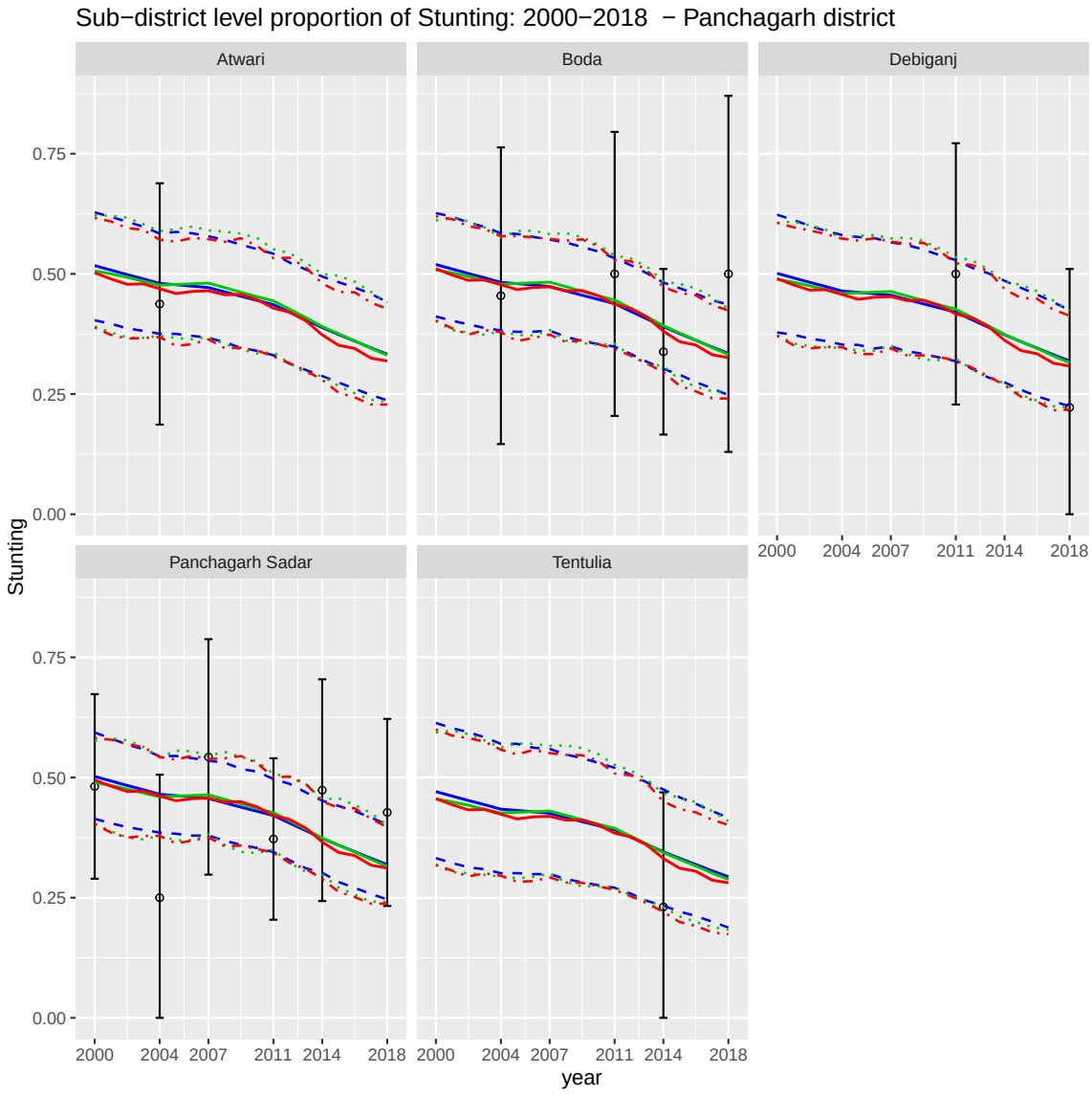


Figure S.4.115: Sub-district level trends of stunting in Panchagarh district during 2000-2018 by DIR estimator (black error-bar line), MTS-1 model (blue line), MTS-2 model (green line) and MTS-3 model (red line) with 95% confidence band. Models are developed at sub-district level.

S.4.7 Sub-district level trends: Mymensingh division

There are 4 districts (Mymensingh, Jamalpur, Sherpur and Netrakona) and 34 sub-districts under Mymensingh division. The trends estimates of stunting for each of the sub-districts are shown under their respective districts in Figures from S.4.116 to S.4.121.

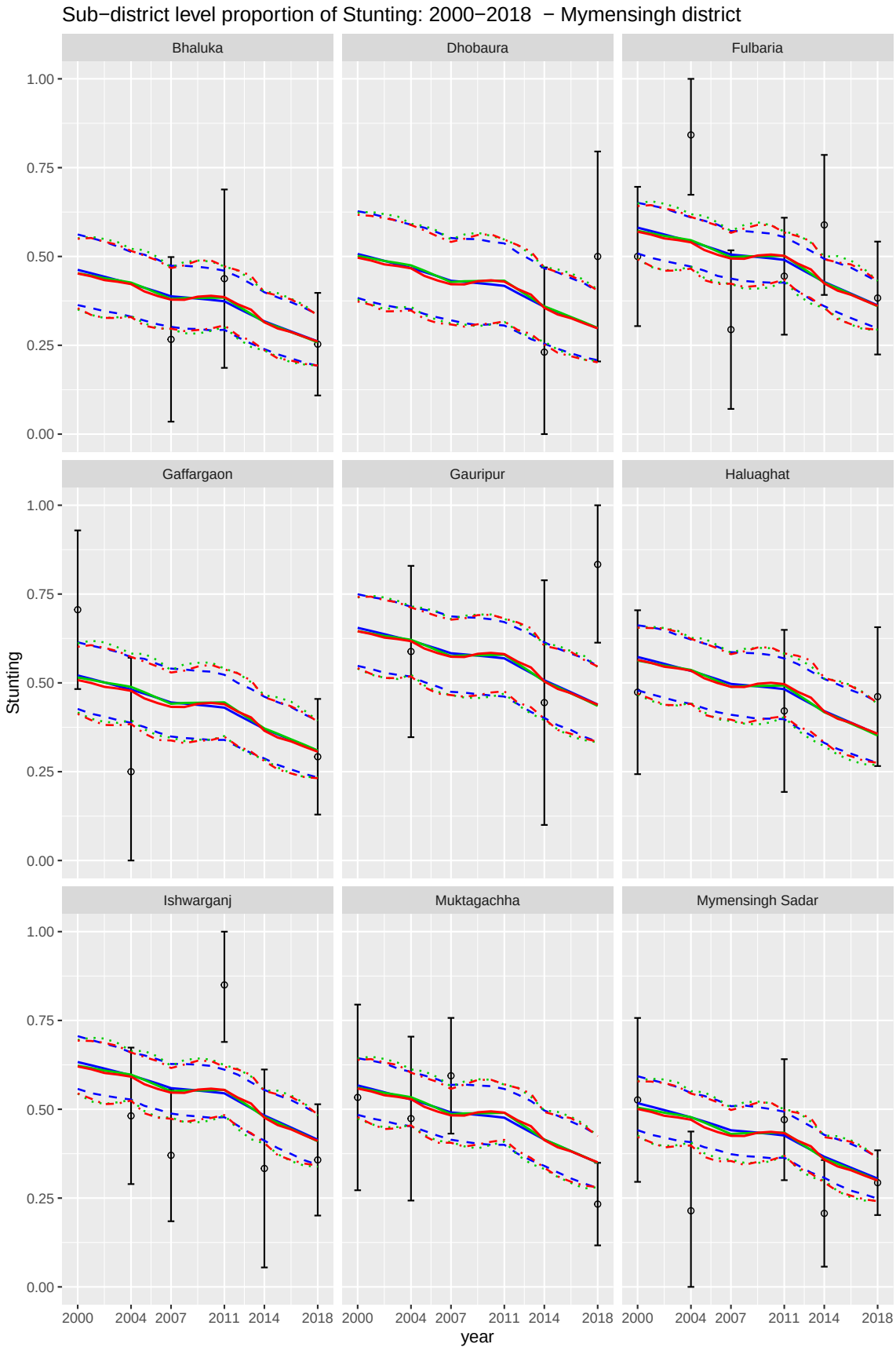


Figure S.4.116: Sub-district level trends of stunting in Mymensingh district during 2000-2018 by DIR estimator (black error-bar line), MTS-1 model (blue line), MTS-2 model (green line) and MTS-3 model (red line) with 95% confidence band. Models are developed at sub-district level.

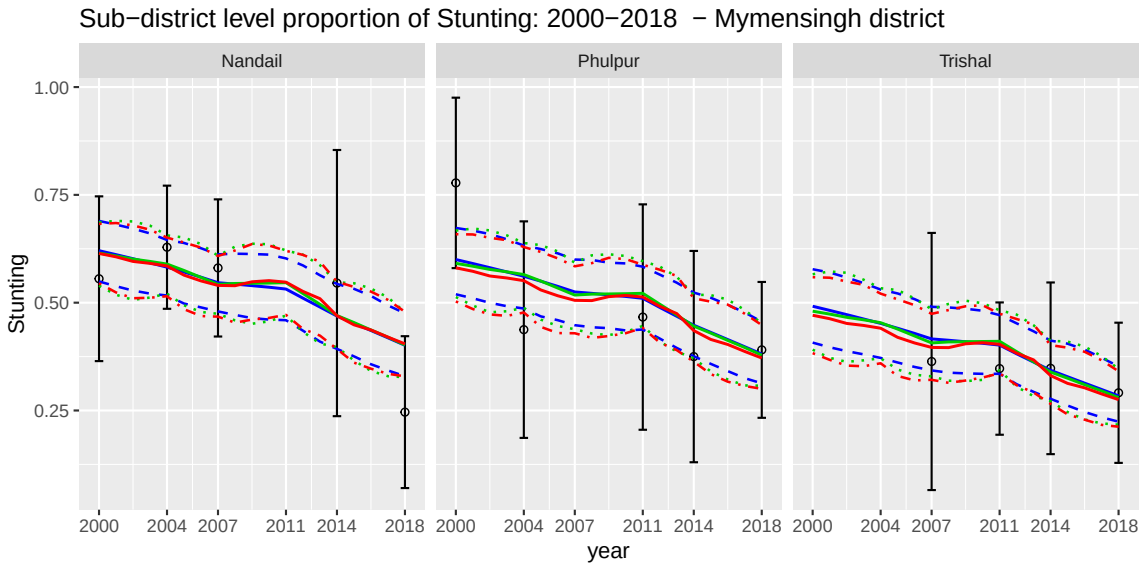


Figure S.4.117: Sub-district level trends of stunting in Mymensingh district during 2000-2018 by DIR estimator (black error-bar line), MTS-1 model (blue line), MTS-2 model (green line) and MTS-3 model (red line) with 95% confidence band. Models are developed at sub-district level.

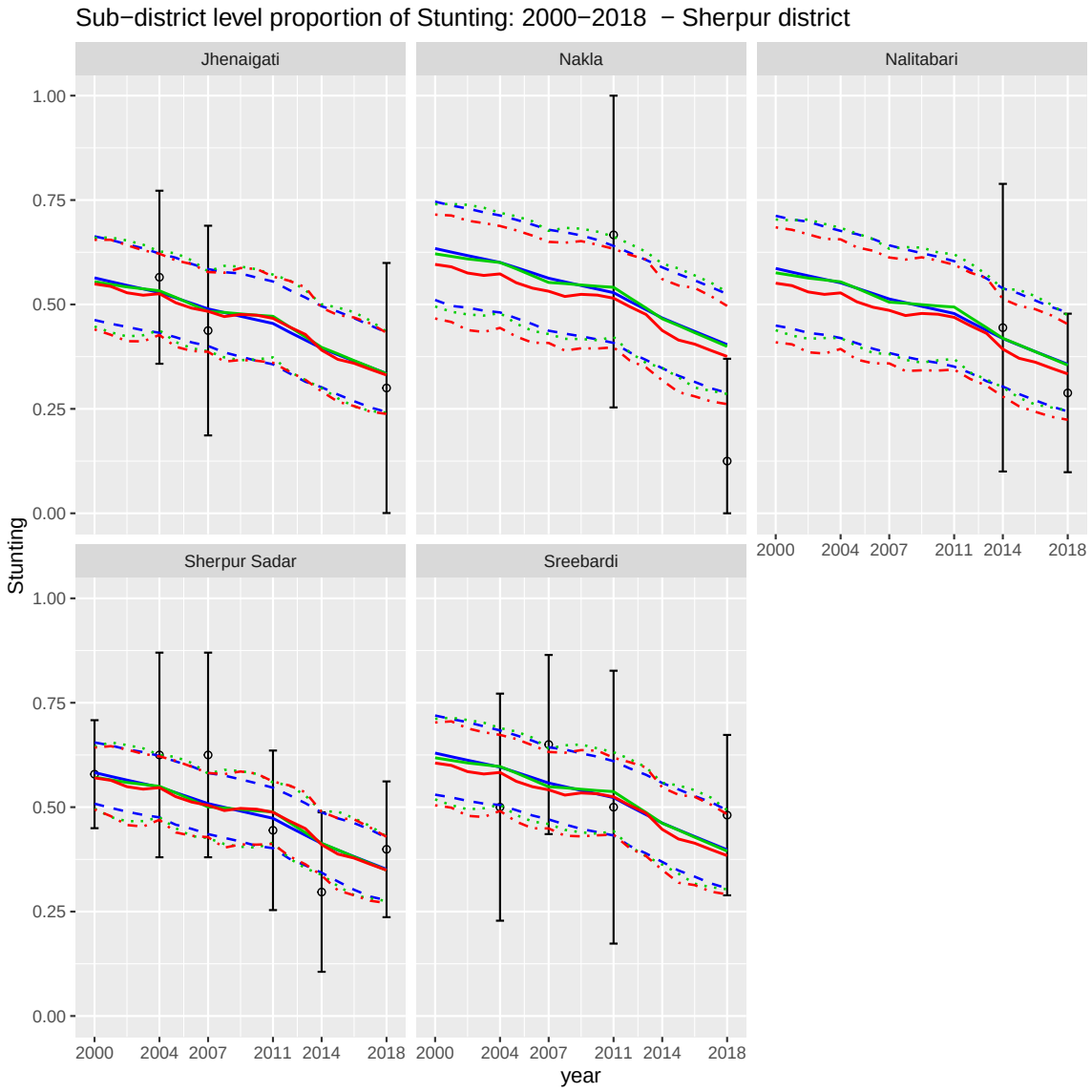


Figure S.4.118: Sub-district level trends of stunting in Sherpur district during 2000-2018 by DIR estimator (black error-bar line), MTS-1 model (blue line), MTS-2 model (green line) and MTS-3 model (red line) with 95% confidence band. Models are developed at sub-district level.

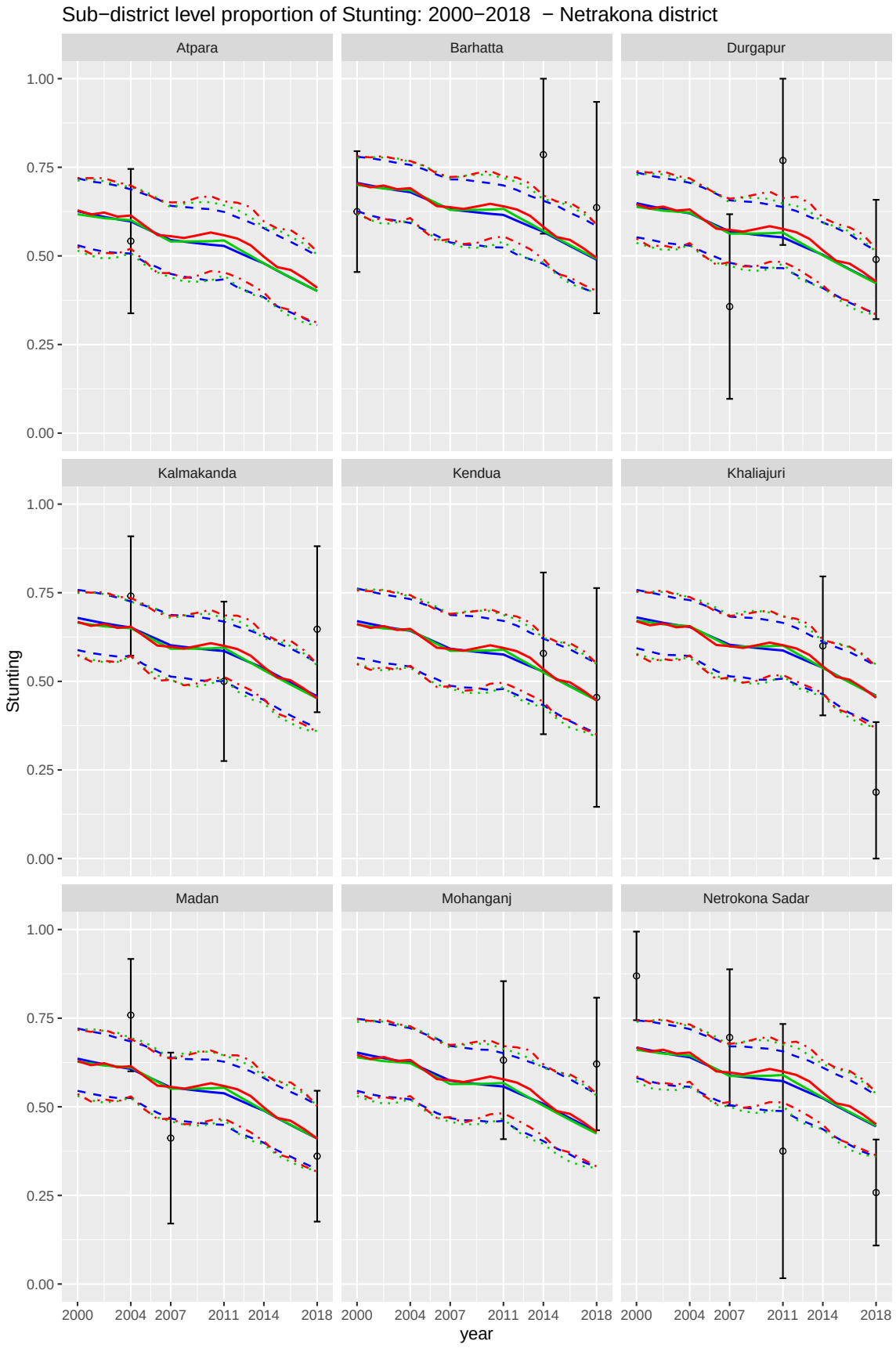


Figure S.4.119: Sub-district level trends of stunting in Netrakona district during 2000-2018 by DIR estimator (black error-bar line), MTS-1 model (blue line), MTS-2 model (green line) and MTS-3 model (red line) with 95% confidence band. Models are developed at sub-district level.

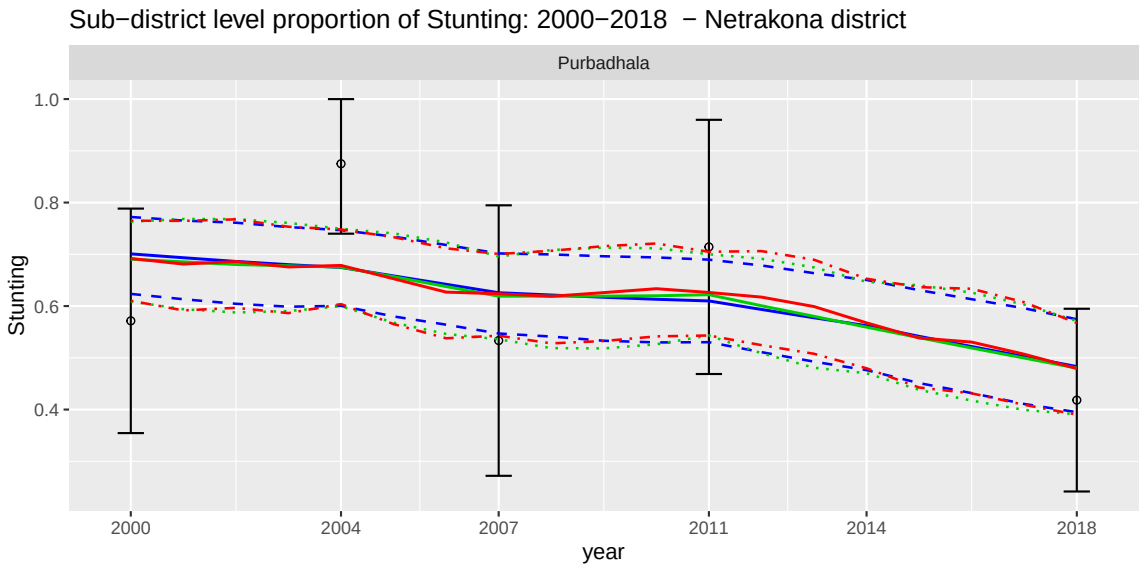


Figure S.4.120: Sub-district level trends of stunting in Netrakona district during 2000-2018 by DIR estimator (black error-bar line), MTS-1 model (blue line), MTS-2 model (green line) and MTS-3 model (red line) with 95% confidence band. Models are developed at sub-district level.

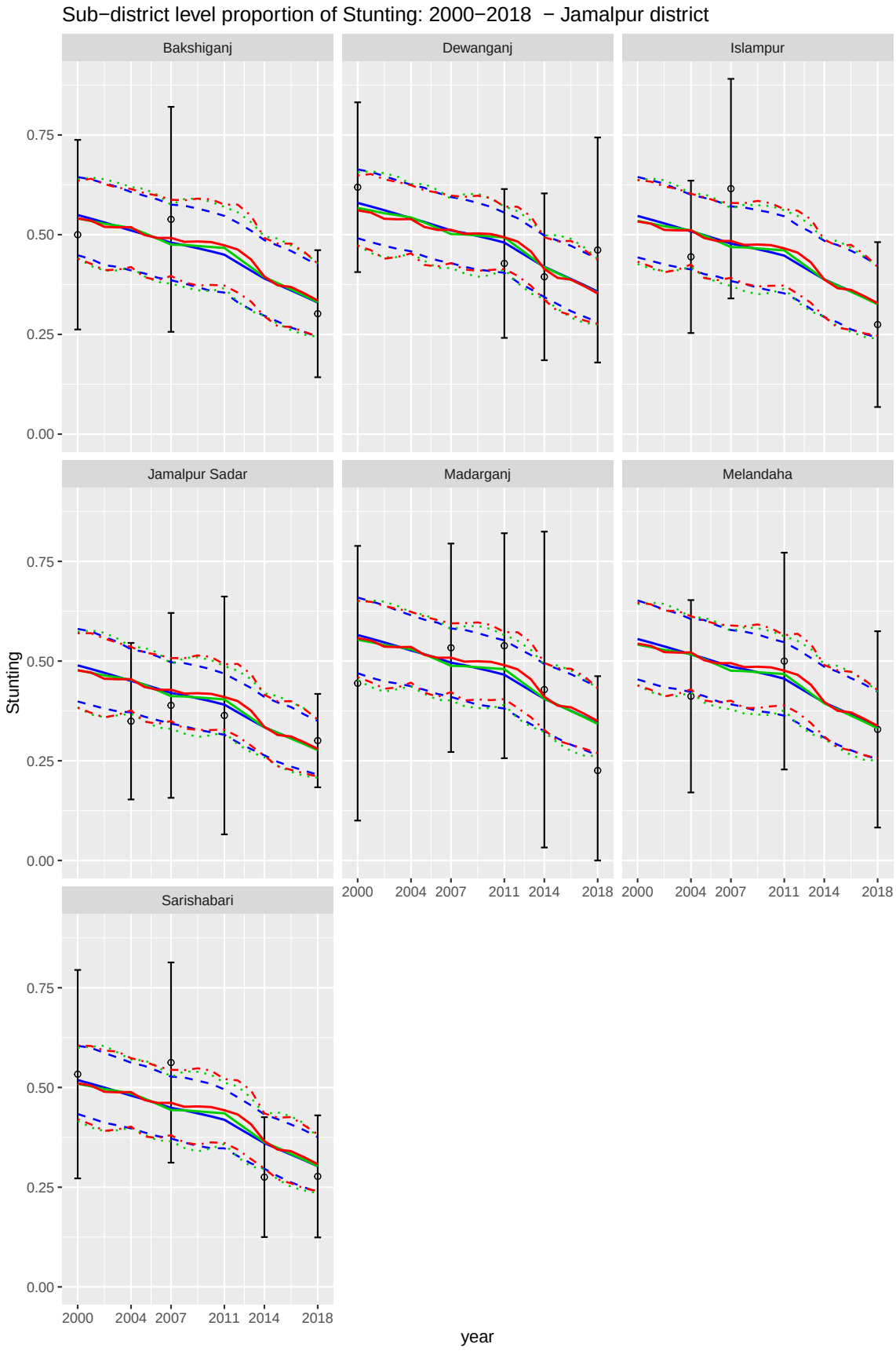


Figure S.4.121: Sub-district level trends of stunting in Jamalpur district during 2000-2018 by DIR estimator (black error-bar line), MTS-1 model (blue line), MTS-2 model (green line) and MTS-3 model (red line) with 95% confidence band. Models are developed at sub-district level.

S.4.8 Sub-district level trends: Sylhet division

There are 4 districts and 38 sub-districts under Sylhet division. The trends estimates of stunting for each of the sub-districts are shown under their respective districts in Figures from S.4.122 to S.4.127.

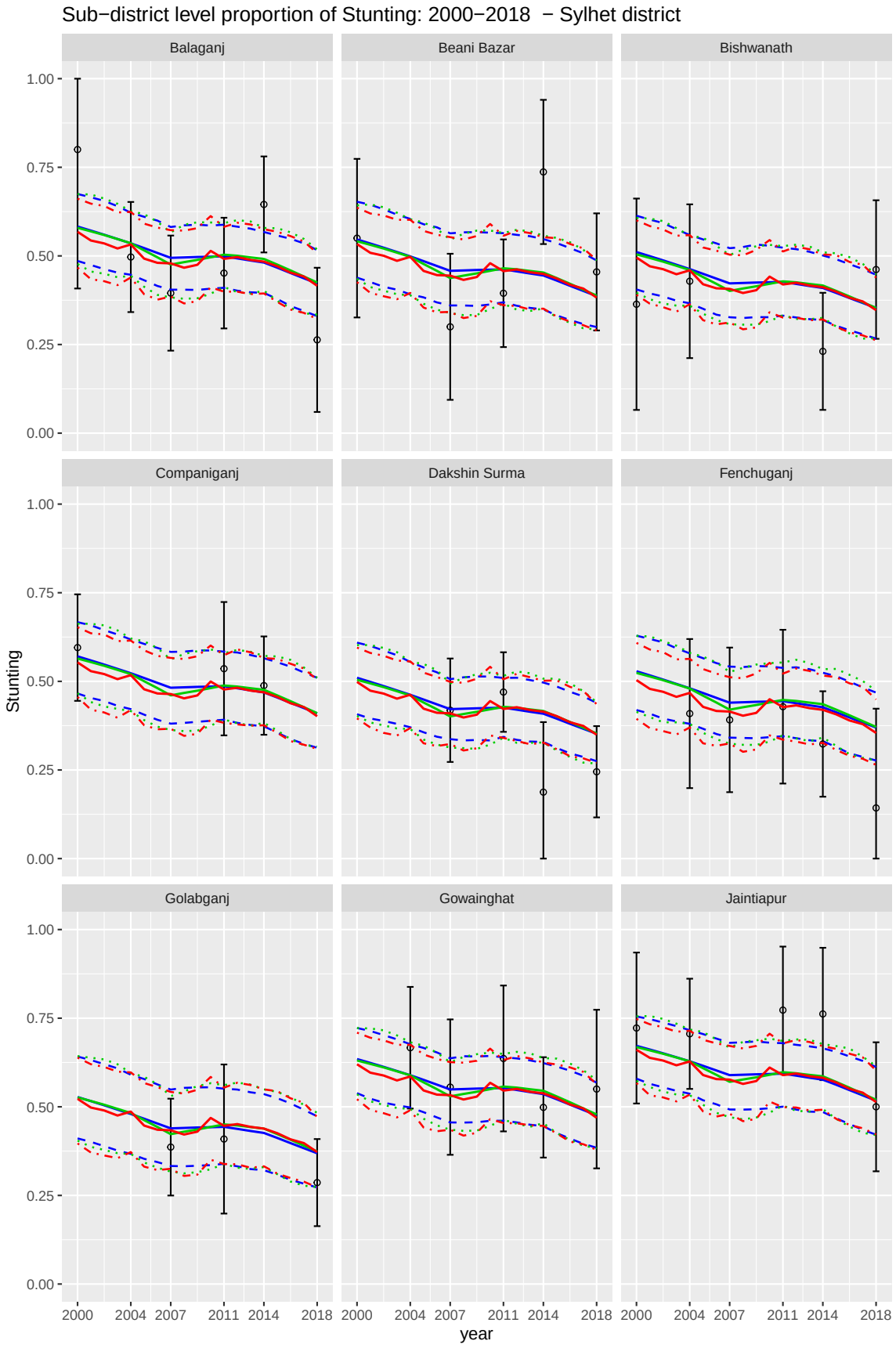


Figure S.4.122: Sub-district level trends of stunting in Sylhet district during 2000-2018 by DIR estimator (black error-bar line), MTS-1 model (blue line), MTS-2 model (green line) and MTS-3 model (red line) with 95% confidence band. Models are developed at sub-district level.

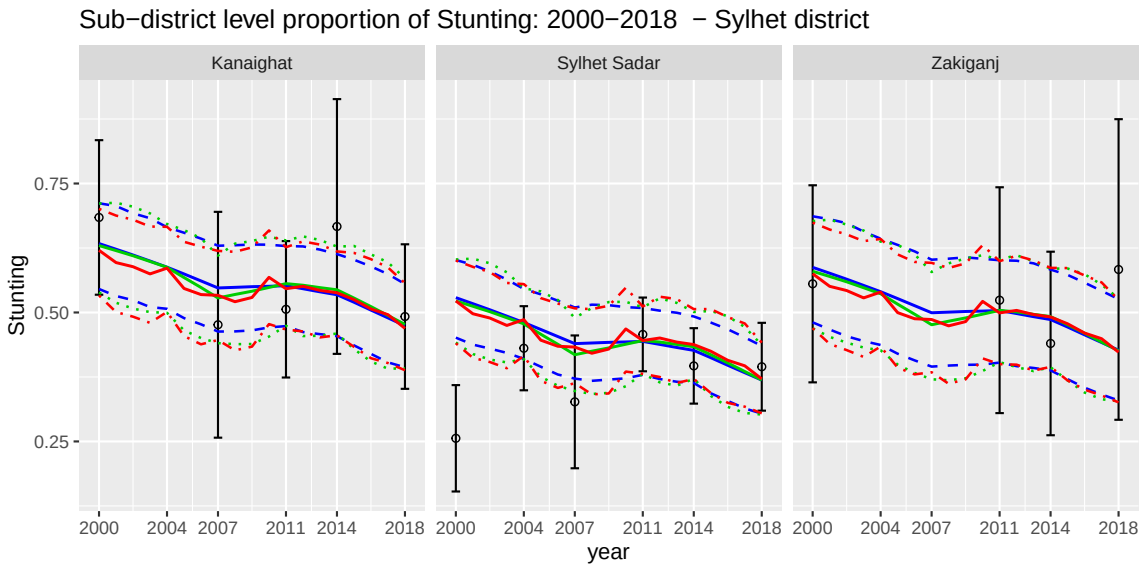


Figure S.4.123: Sub-district level trends of stunting in Sylhet district during 2000-2018 by DIR estimator (black error-bar line), MTS-1 model (blue line), MTS-2 model (green line) and MTS-3 model (red line) with 95% confidence band. Models are developed at sub-district level.

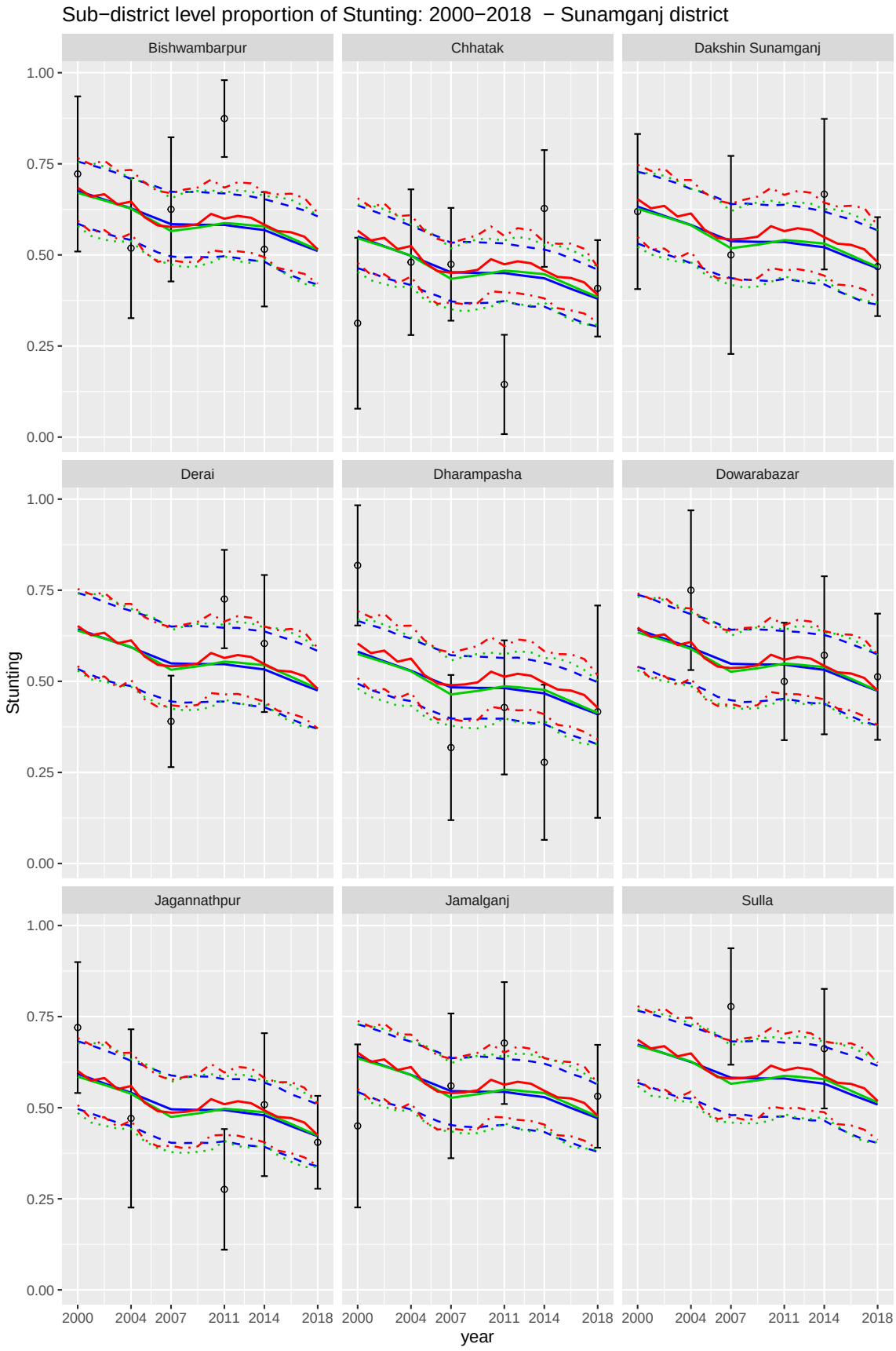


Figure S.4.124: Sub-district level trends of stunting in Sunamganj district during 2000-2018 by DIR estimator (black error-bar line), MTS-1 model (blue line), MTS-2 model (green line) and MTS-3 model (red line) with 95% confidence band. Models are developed at sub-district level.

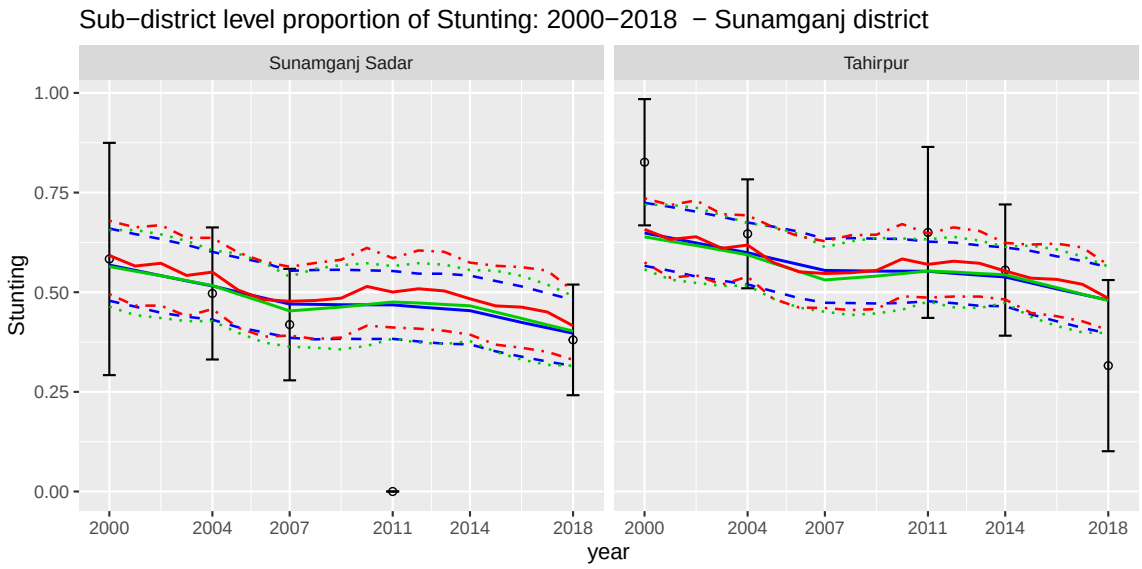


Figure S.4.125: Sub-district level trends of stunting in Sunamganj district during 2000-2018 by DIR estimator (black error-bar line), MTS-1 model (blue line), MTS-2 model (green line) and MTS-3 model (red line) with 95% confidence band. Models are developed at sub-district level.

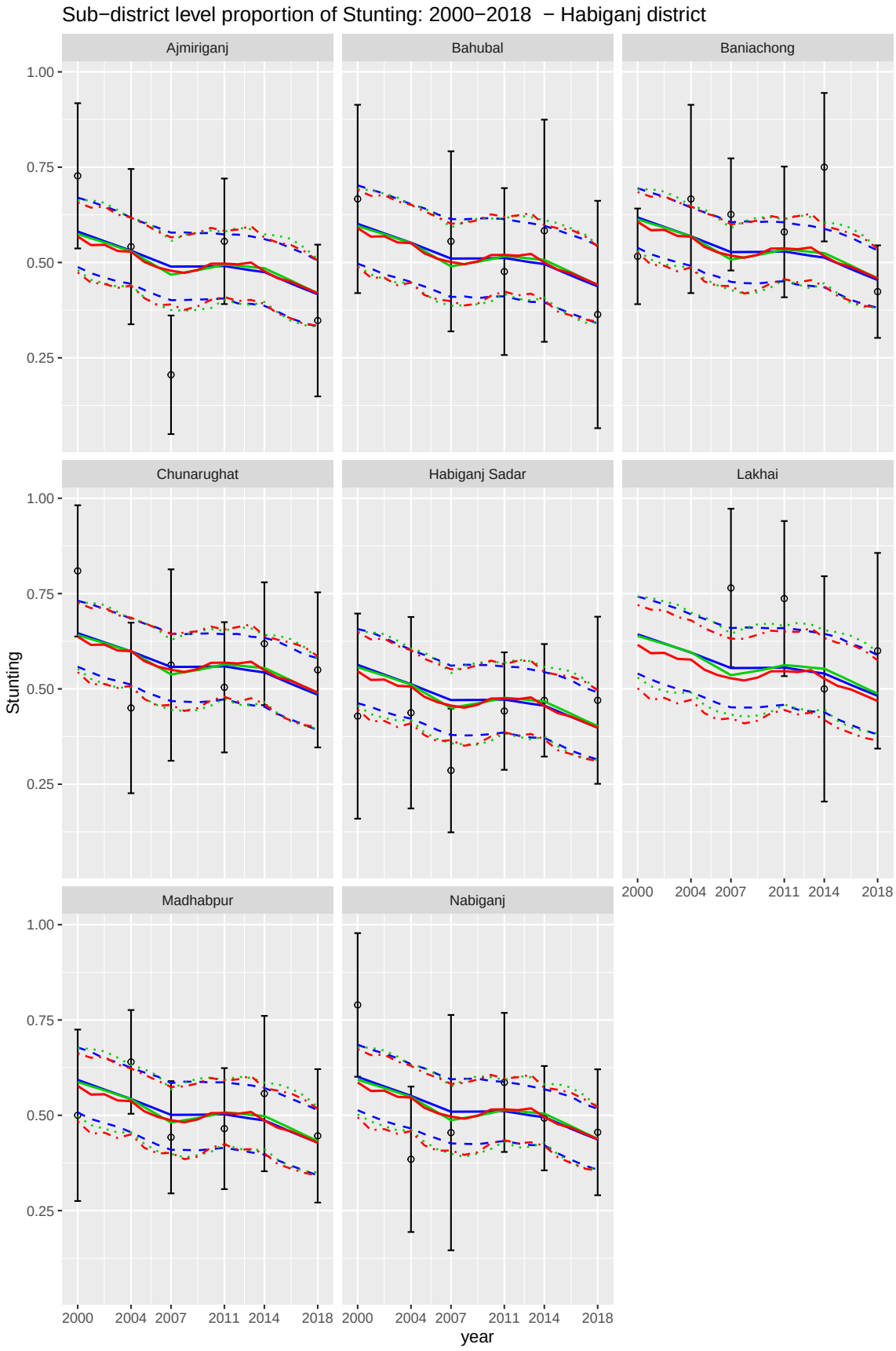


Figure S.4.126: Sub-district level trends of stunting in Habiganj district during 2000-2018 by DIR estimator (black error-bar line), MTS-1 model (blue line), MTS-2 model (green line) and MTS-3 model (red line) with 95% confidence band. Models are developed at sub-district level.

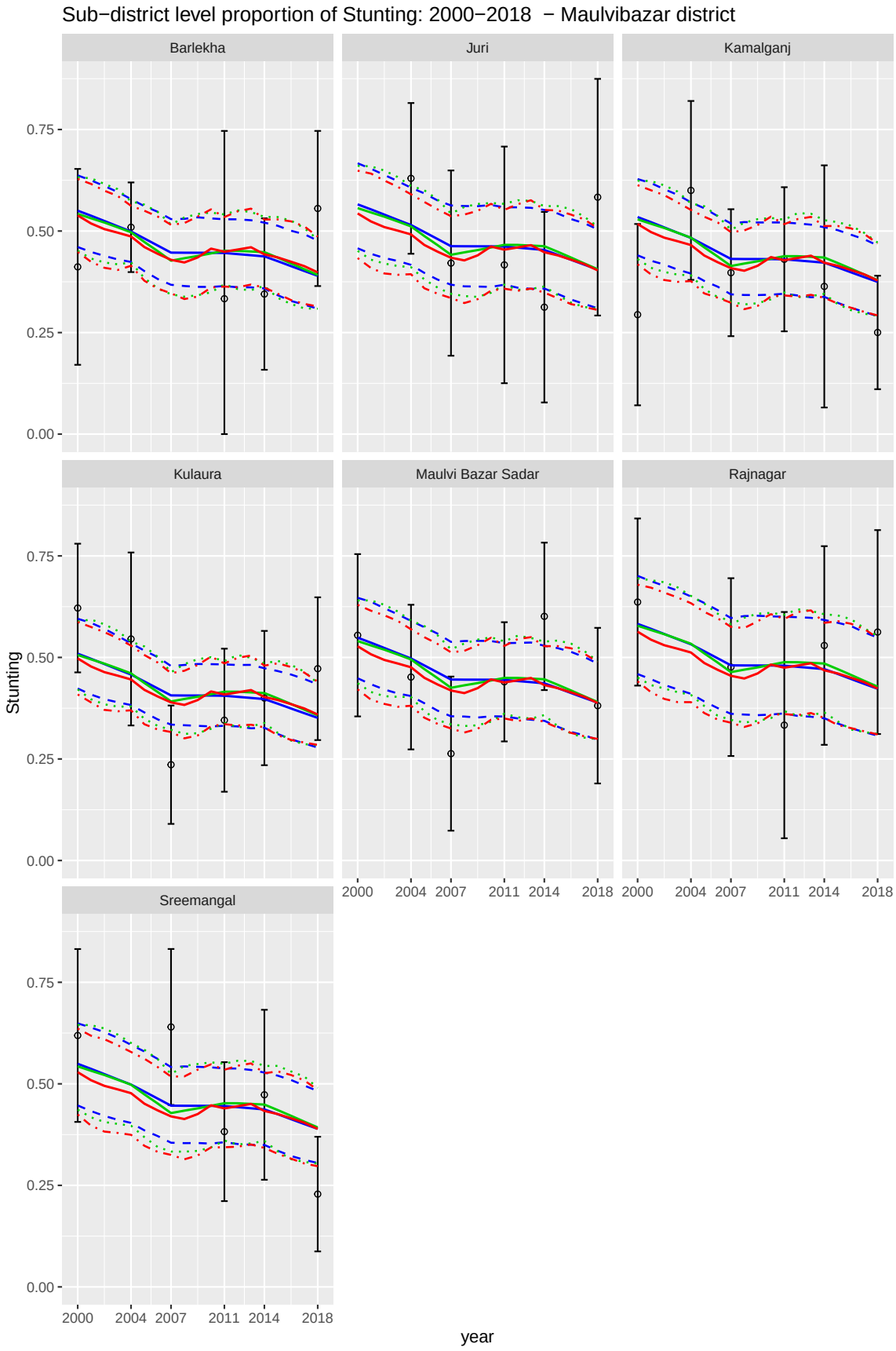


Figure S.4.127: Sub-district level trends of stunting in Maulvibazar district during 2000-2018 by DIR estimator (black error-bar line), MTS-1 model (blue line), MTS-2 model (green line) and MTS-3 model (red line) with 95% confidence band. Models are developed at sub-district level.

S.5 Posterior Predictive Check

The idea behind posterior predictive checking is that a good model fit will enable us to generate data that resemble the observed data. For examining predictive performance of the fitted models, we compared observed data to simulated data from the posterior predictive distribution following (Gabry et al., 2019) through utilization of the `R` package **bayesplot** (Gabry et al., 2022). It is recommended to compare graphical plots, such as the distribution of observed data and simulated data, looking for any systematic differences which could indicate potential failings of the model (Gelman et al., 2013). In this regard, the kernel density estimate of the observed stunting prevalence (dark curves) is plotted with 2000 corresponding density estimates for simulated stunting prevalence (thin, lighter curves) drawn from the posterior predictive distribution (using the values from one chain only) at four levels: (i) detailed level (sub-district) at which the model is fitted, (ii) district level, (iii) division level, and (vi) national levels over the six survey time points. The posterior predictive check plots are given for all the six models illustrated in the main manuscript in Figures S.5.128 to S.5.133. The density plots suggest that the simulated values are exactly following the density of observed stunting prevalence at the higher aggregation levels as expected and provides reasonably smoothed trends at the sub-district level at which level direct estimates are noisy and inconsistent.

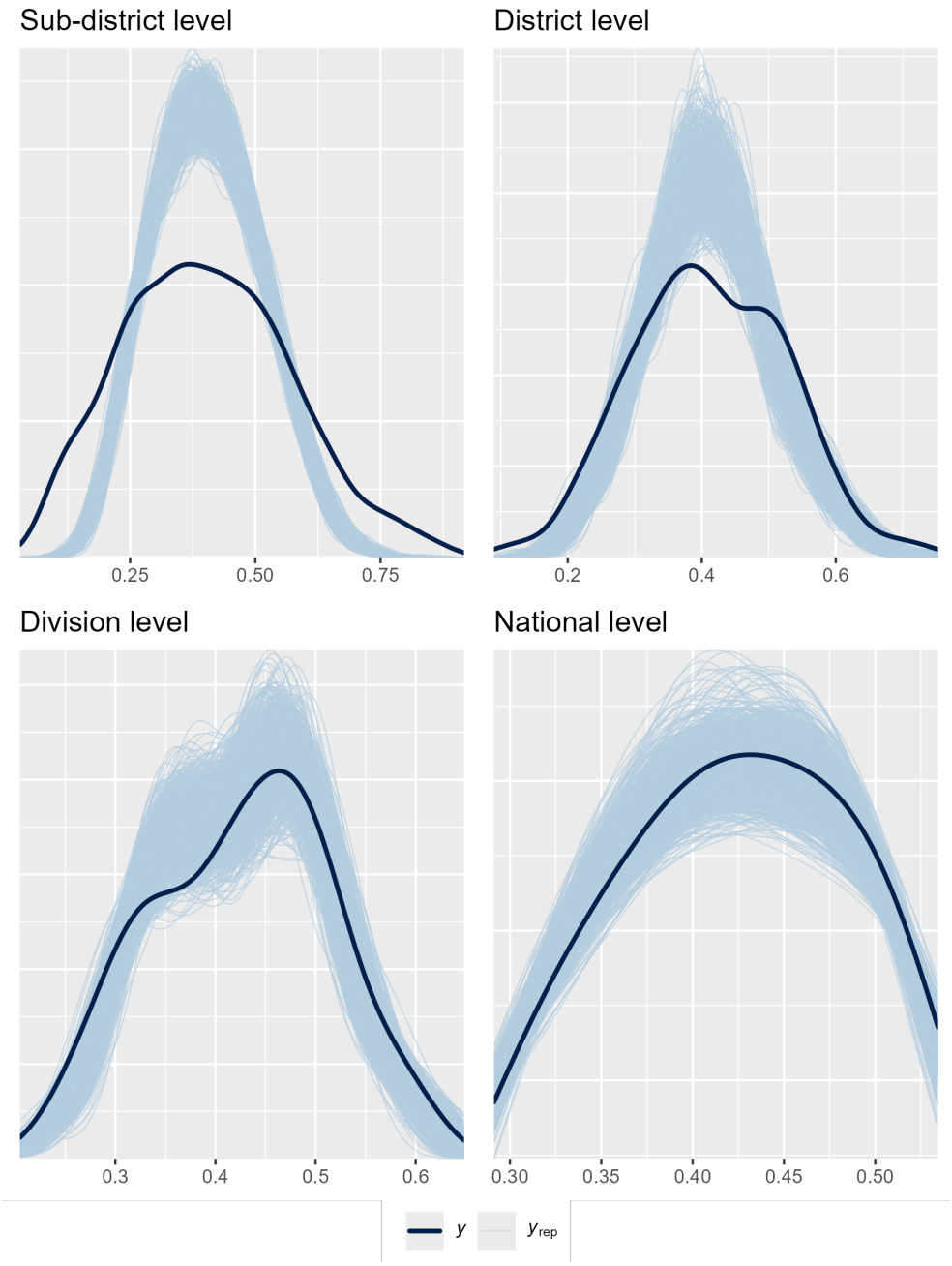


Figure S.5.128: Posterior predictive check of the model-based trend estimates at the sub-district, district, division and national level. The thin lines present Kernel densities of 2000 simulated stuntunting prevalence draws from the posterior distributions based on model M1 with structured random effects at the sub-district level. The thick lines shows the Kernel density of direct estimates obtained from the survey data.

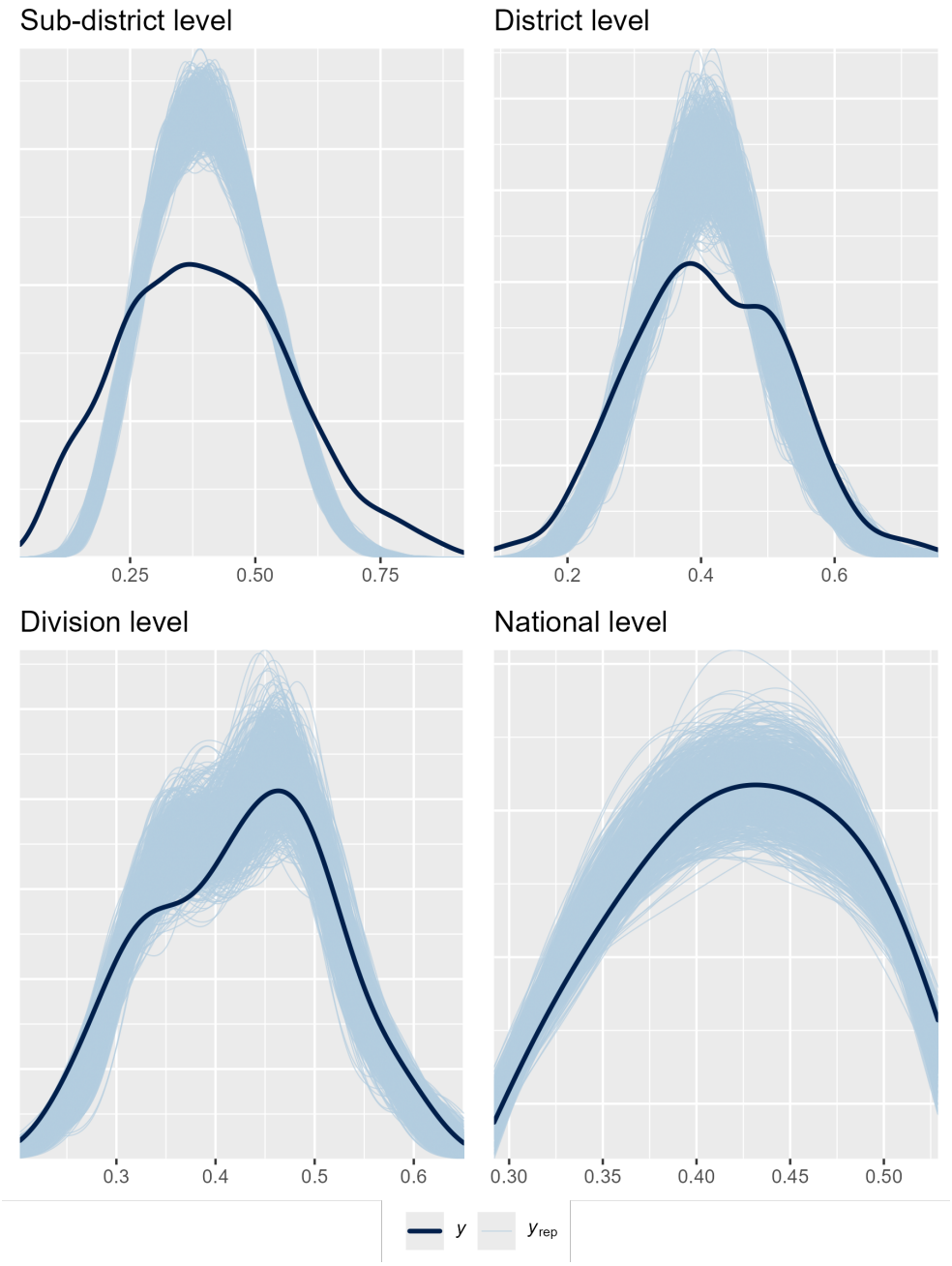


Figure S.5.129: Posterior predictive check of the model-based trend estimates at the sub-district, district, division and national level. The thin lines present Kernel densities of 2000 simulated stuntunting prevalence draws from the posterior distributions based on model M1 with unstructured random effects at the sub-district level. The thick lines shows the Kernel density of direct estimates obtained from the survey data.

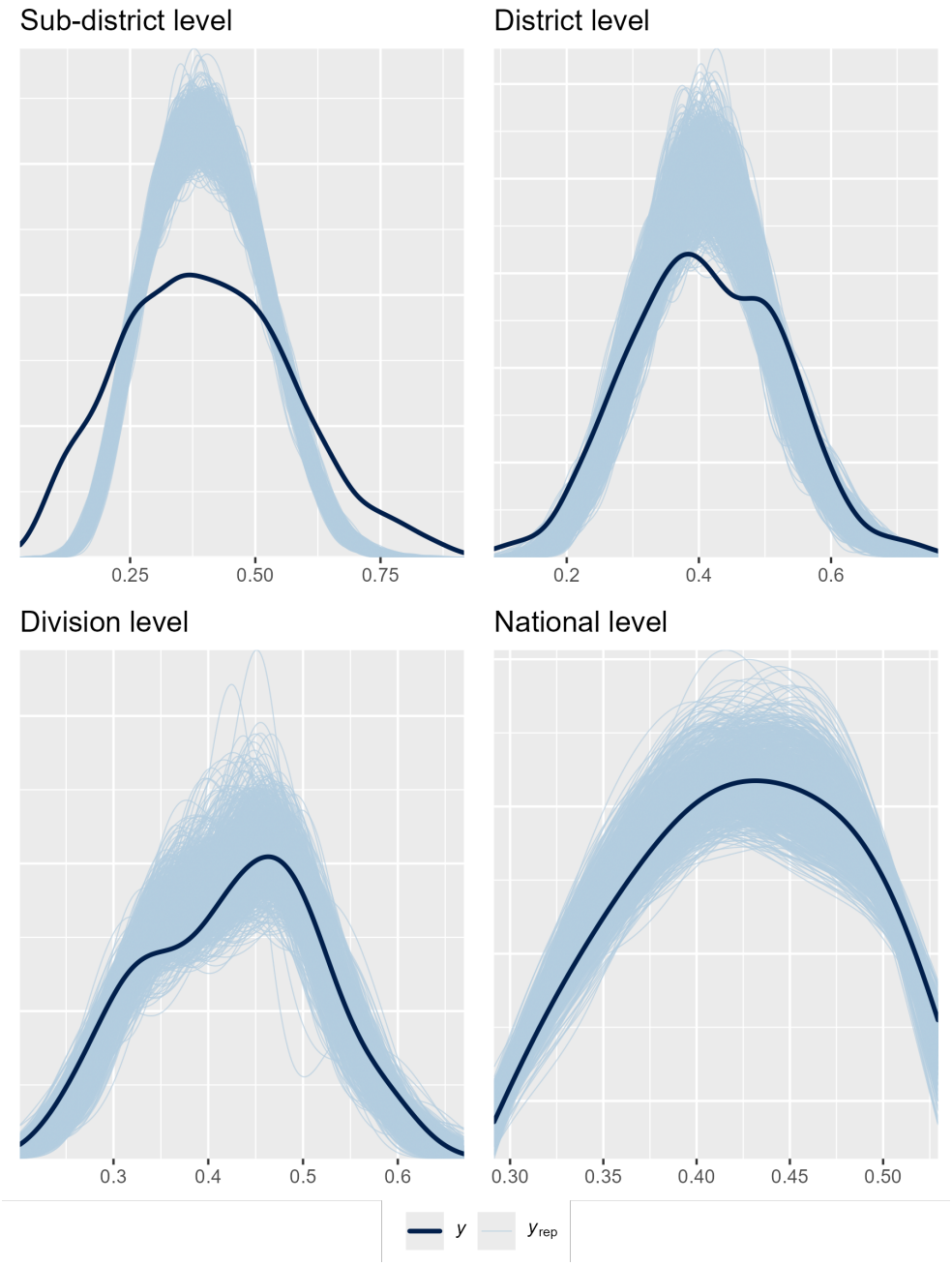


Figure S.5.130: Posterior predictive check of the model-based trend estimates at the sub-district, district, division and national level. The thin lines present Kernel densities of 2000 simulated stunting prevalence draws from the posterior distributions based on model M2 with structured random effects at the sub-district level. The thick lines shows the Kernel density of direct estimates obtained from the survey data.

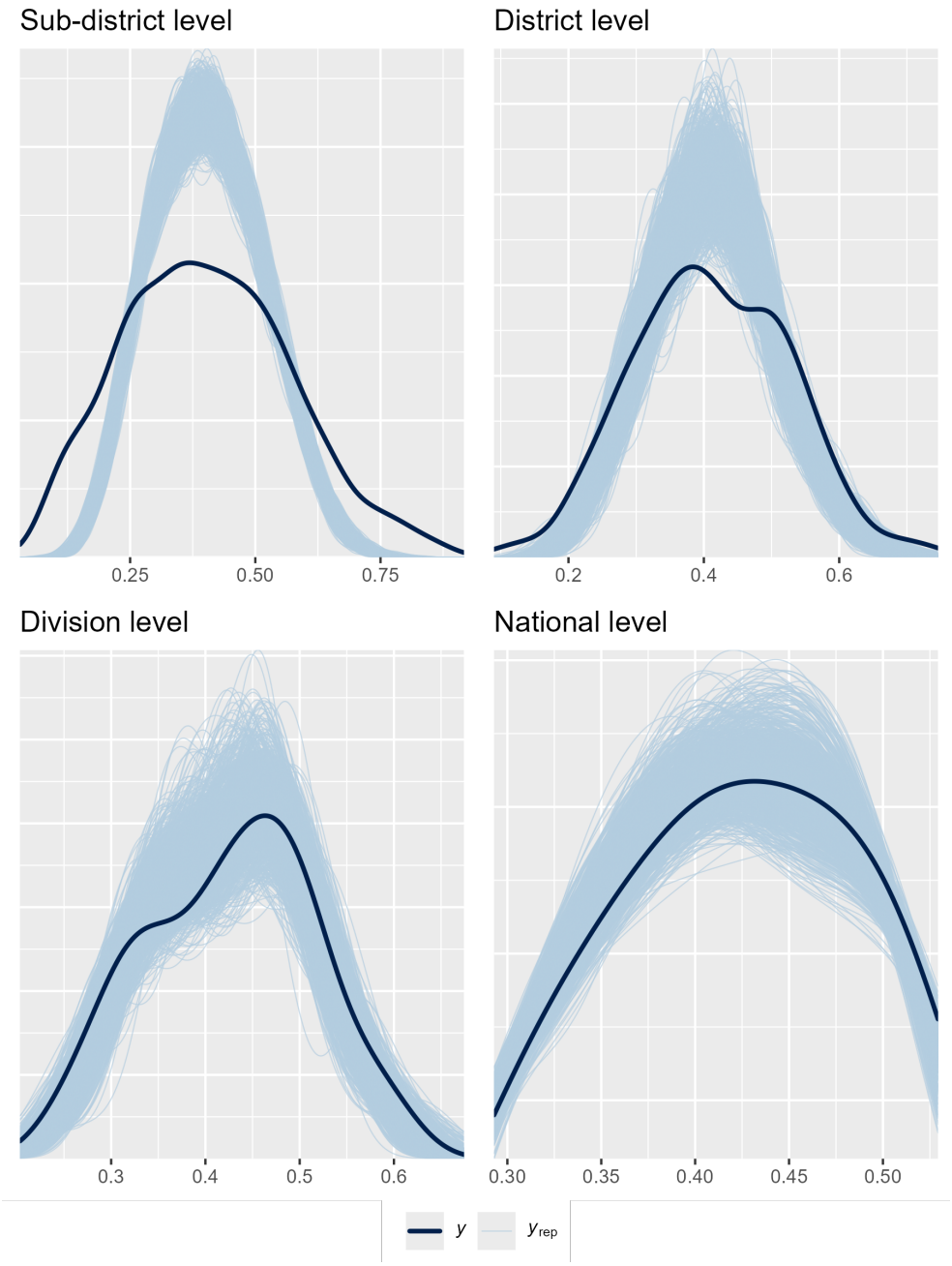


Figure S.5.131: Posterior predictive check of the model-based trend estimates at the sub-district, district, division and national level. The thin lines present Kernel densities of 2000 simulated stunting prevalence draws from the posterior distributions based on model M2 with unstructured random effects at the sub-district level. The thick lines shows the Kernel density of direct estimates obtained from the survey data.

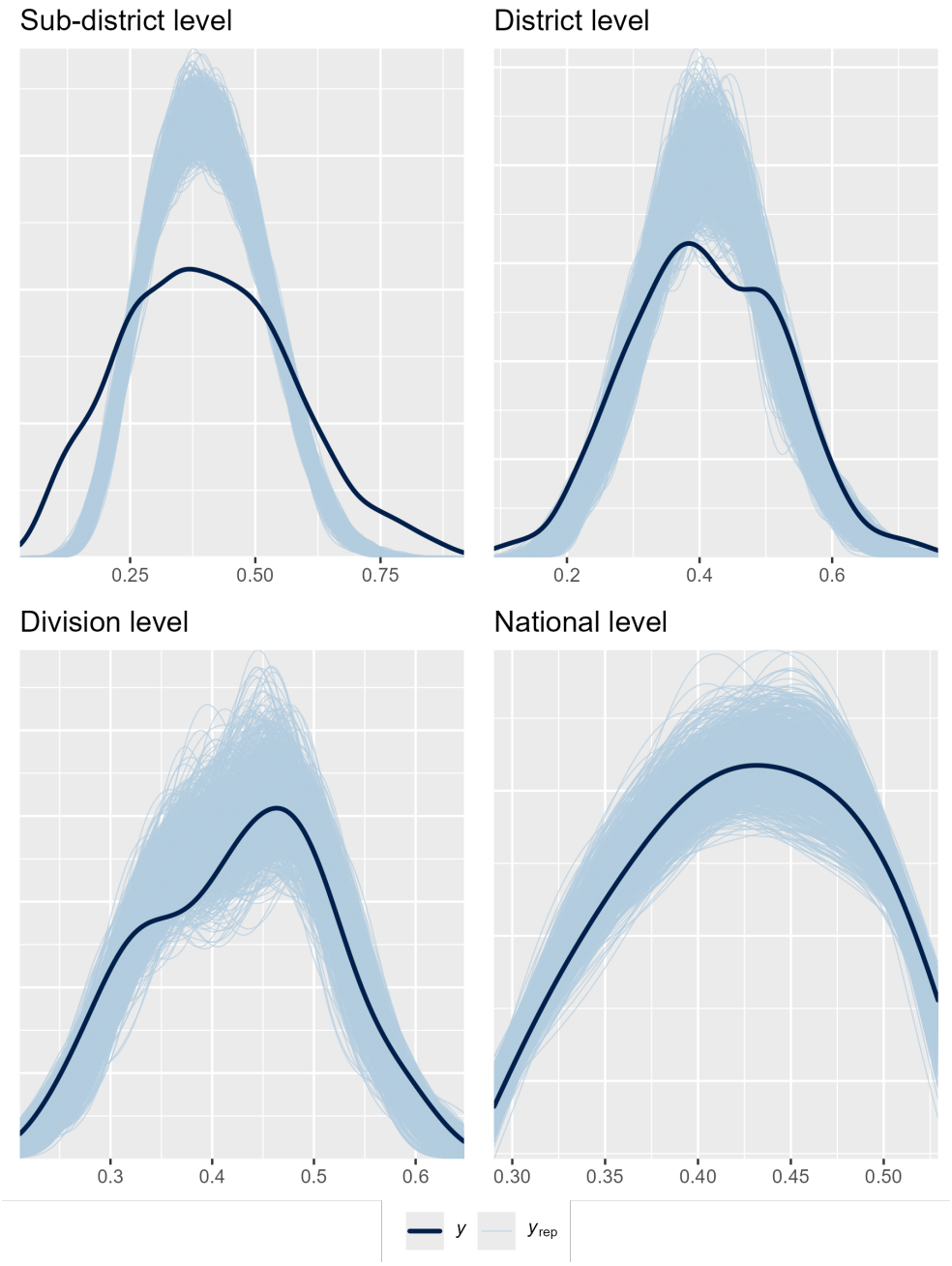


Figure S.5.132: Posterior predictive check of the model-based trend estimates at the sub-district, district, division and national level. The thin lines present Kernel densities of 2000 simulated stunting prevalence draws from the posterior distributions based on model M3 with structured random effects at the sub-district level. The thick lines shows the Kernel density of direct estimates obtained from the survey data.

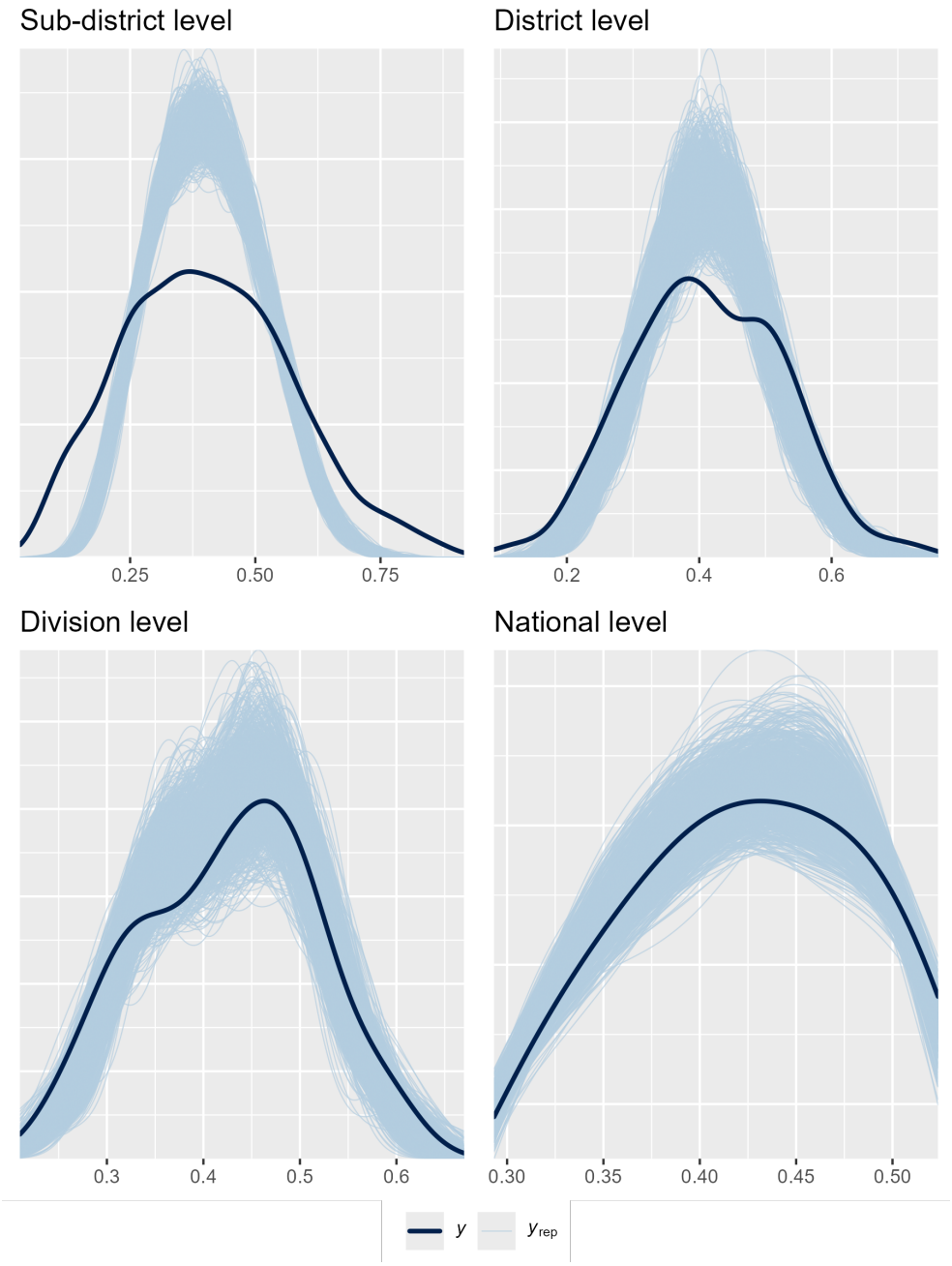


Figure S.5.133: Posterior predictive check of the model-based trend estimates at the sub-district, district, division and national level. The thin lines present Kernel densities of 2000 simulated stunting prevalence draws from the posterior distributions based on model M3 with unstructured random effects at the sub-district level. The thick lines shows the Kernel density of direct estimates obtained from the survey data.

S.6 Comparison of Binomial and Gaussian based time-series models

Since the time-series model can be developed assuming the proportion of stunted children follow a Gaussian distribution, we developed a Gaussian based model and then compare with the finally selected binomial model. For developing the Gaussian based time-series model, we followed the steps illustrated in Das et al. (2023) to create the model inputs. Then the same fixed and random effects components are used to develop a Gaussian based multilevel time-series model.

Since a large number of sub-districts have a few children, the estimated stunting level is too sparse with many zeros and ones. Consequently, the standard errors are also not available. In such case the GVF model has been applied to estimate their smoothed standard errors. Finally, the pairs of direct estimates and their smoothed standard errors are used as model inputs to develop the time-series model. Since modelling of stunting on original scale may provide negative estimates particularly the simulated values, we developed time-series models using both on square-root and original scale to understand how they behave. For comparison purpose, we plotted results for the finally selected binomial model MTS-3 (red lines in Figure S.6.134), Gaussian model on original scale denoted as MTS-4 (green lines in Figure S.6.134) and Gaussian model on square-root scale denoted as MTS-5 (blue lines in Figure S.6.134) .

At the national level, the trends explicitly show the Gaussian based models failed to provide reasonable trends (Figure S.6.134). The square-root based model shows overestimation, while the original scale model shows underestimation. Division level trends shown in Figures S.6.135 and S.6.135 indicate that Dhaka and Chittagong divisions are mostly affected due to having many sub-districts with a few children. The district level trends shown in S.6.137 and S.6.138 Figures by these models also show the very similar differences.

A few sub-districts from Dhaka and Chittagong districts are plotted in Figures S.6.139 and S.6.140. Since the sub-district level direct estimates are sparse and also based on a few observation when available, it is very tough to assess the models. Though the differences among the three models relatively less compared to the higher aggregation levels, the pattern remains same as the district and division levels.

The difference between the binomial and Gaussian based models are mainly due to sparse data, particularly when the outcome variable is proportion. To understand and examine this issue, we developed such models at the district level using seven rounds of BDHS and two rounds of Bangladesh Multiple Indicator Cluster Surveys in 2012 and 2019 (Das et al., 2022). The number of observation are comparatively reasonable to have a proportion and their standard errors at the district level (see Table S.1.2). So the comparison of these district levels shown in Figures S.6.141 and S.6.142 indicate that both models perform in the similar manner. This investigation indicates that the binomial based models can perform when the data are too sparse but the Gaussian model fails due to inability of accounting for zero or one proportions.

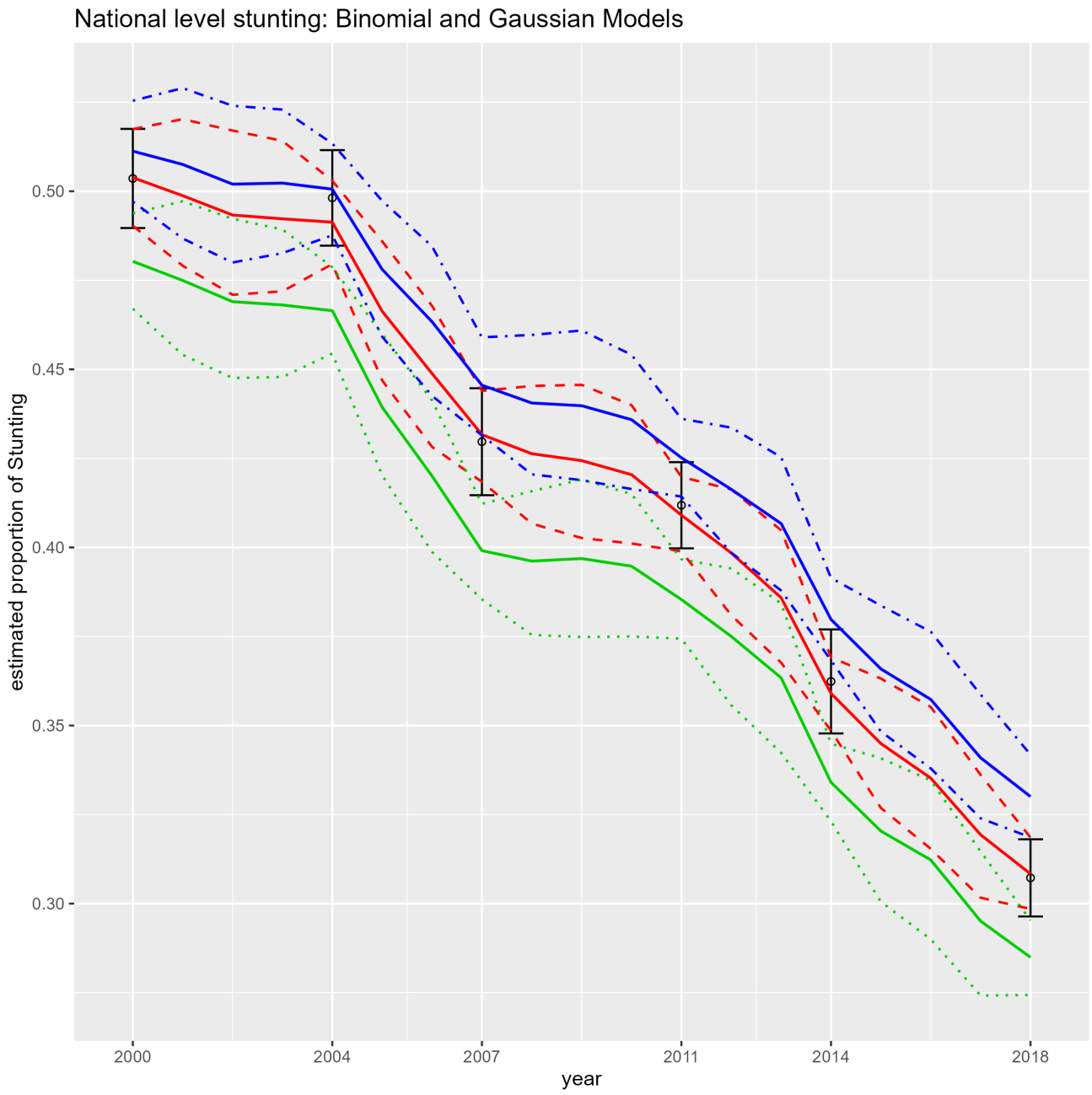


Figure S.6.134: Comparison of binomial and Gaussian based multilevel time-series models developed at the sub-district level. National level trends of stunting in Bangladesh during 2000-2018 by DIR estimator (black error-bar line), binomial based MTS-3 model (red line), Gaussian based MTS-4 model on original scale (green line) and Gaussian based MTS-5 model (red line) on square-root scale with their 95% confidence bands. Models are developed at sub-district level.

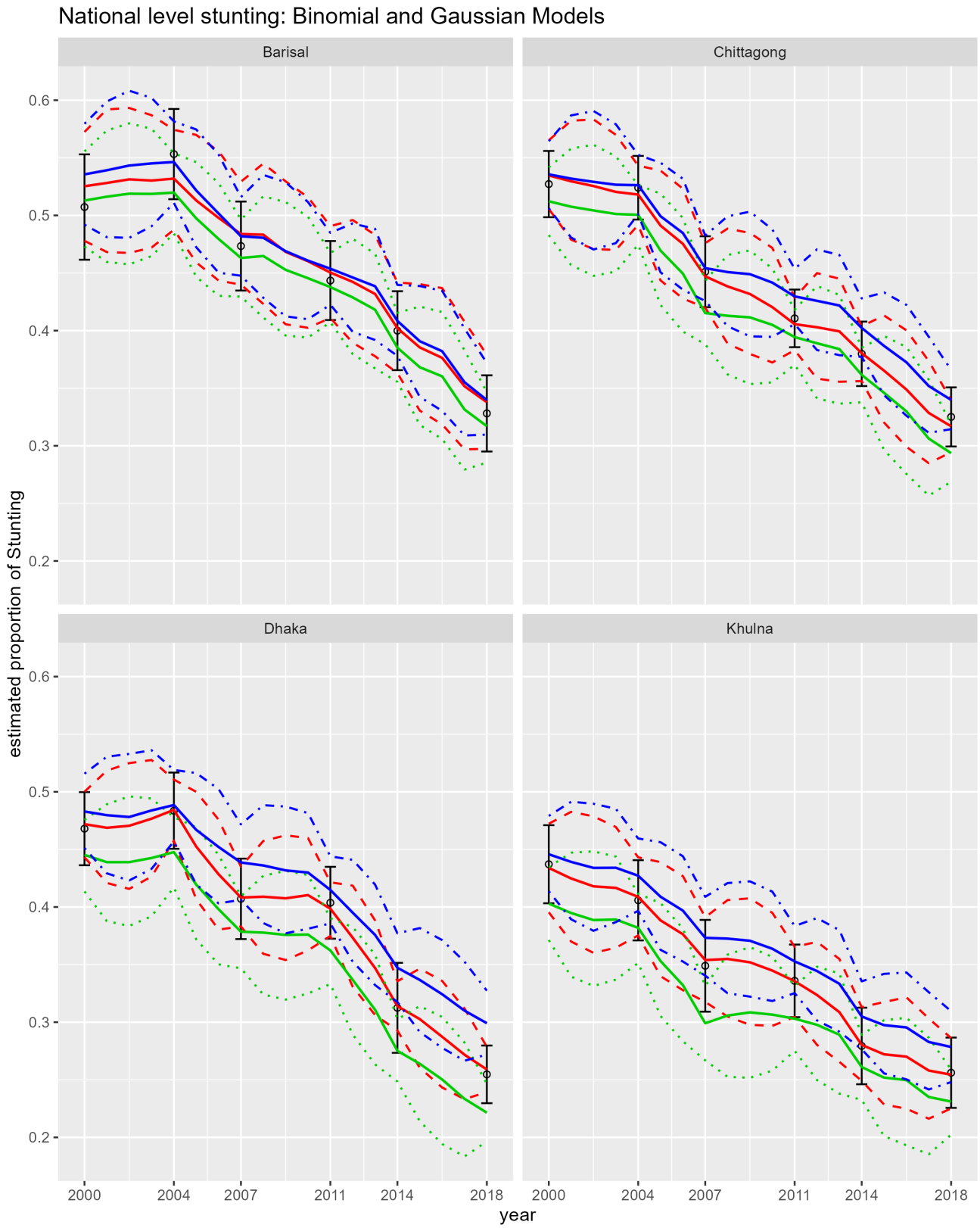


Figure S.6.135: Comparison of binomial and Gaussian based multilevel time-series models developed at the sub-district level. Trends of stunting for Barisal, Chittagong, Dhaka and Khulna divisions during 2000-2018 by DIR estimator (black error-bar line), binomial based MTS-3 model (red line), Gaussian based MTS-4 model on original scale (green line) and Gaussian based MTS-5 model (red line) on square-root scale with their 95% confidence bands. Models are developed at sub-district level.

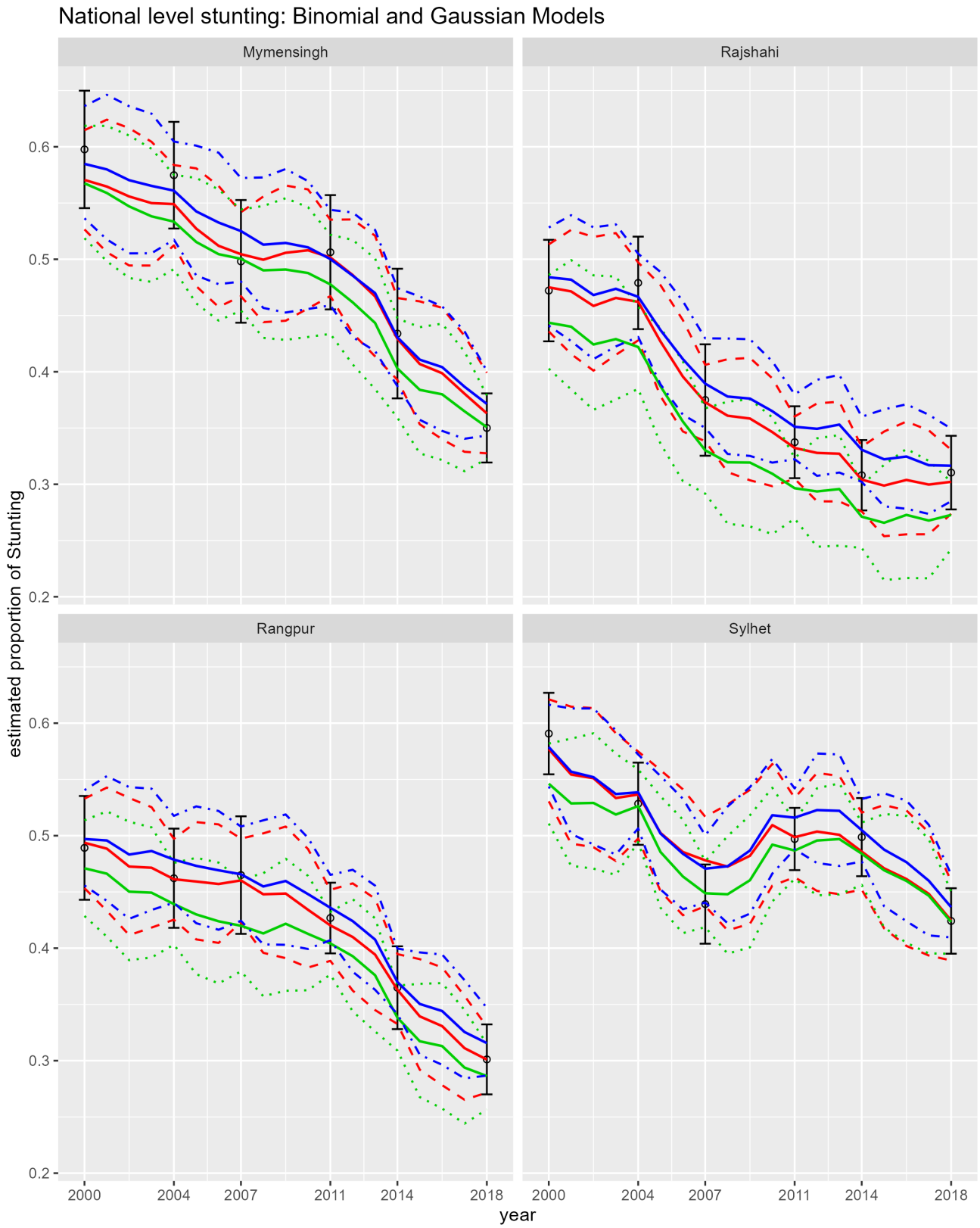


Figure S.6.136: Comparison of binomial and Gaussian based multilevel time-series models developed at the sub-district level. Trends of stunting for Mymensingh, Rajshahi, Rangpur and Sylhet divisions during 2000-2018 by DIR estimator (black error-bar line), binomial based MTS-3 model (red line), Gaussian based MTS-4 model on original scale (green line) and Gaussian based MTS-5 model (red line) on square-root scale with their 95% confidence bands. Models are developed at sub-district level.

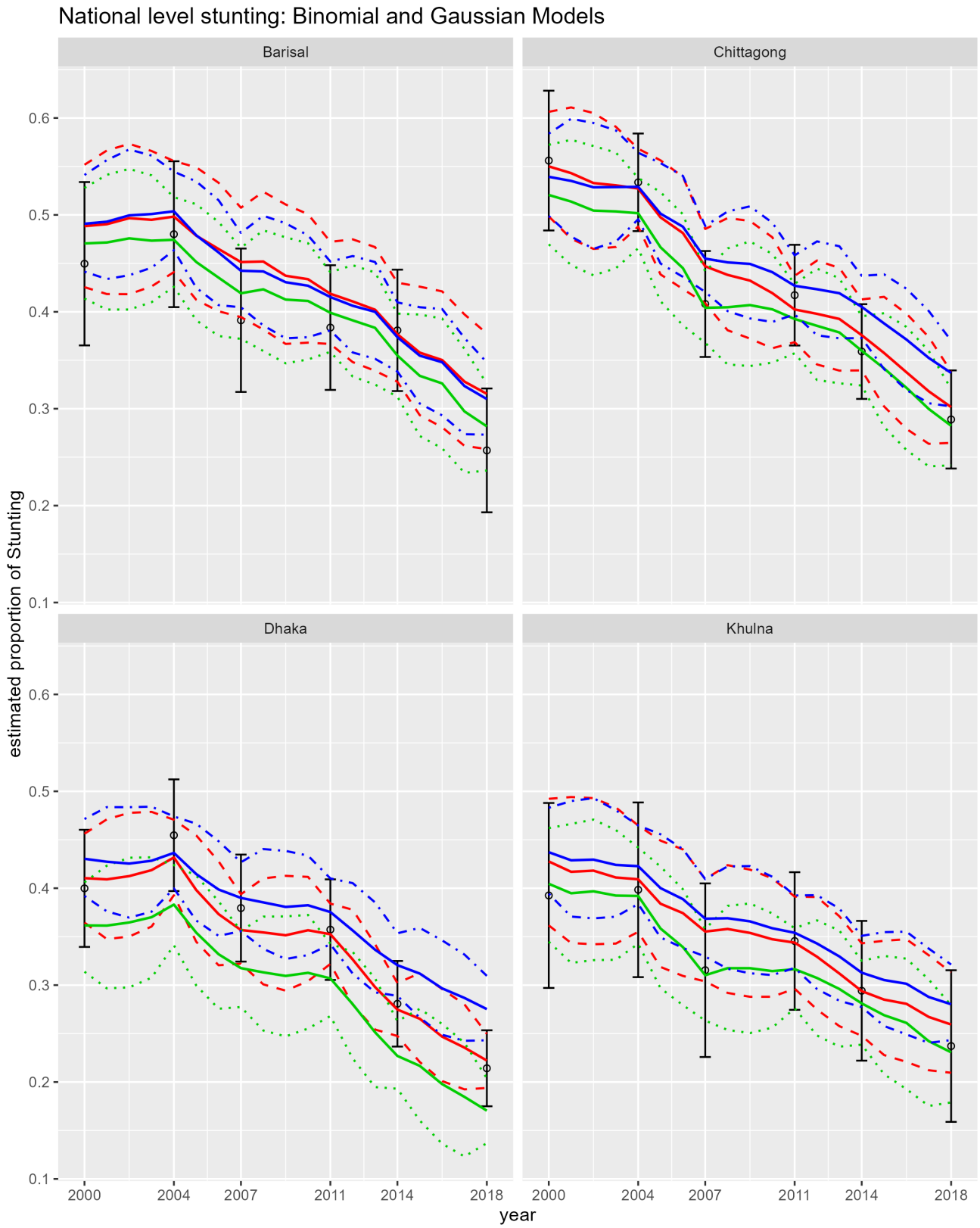


Figure S.6.137: Comparison of binomial and Gaussian based multilevel time-series models developed at the sub-district level. Trends of stunting for Barisal, Chittagong, Dhaka and Khulna districts during 2000-2018 by DIR estimator (black error-bar line), binomial based MTS-3 model (red line), Gaussian based MTS-4 model on original scale (green line) and Gaussian based MTS-5 model (red line) on square-root scale with their 95% confidence bands. Models are developed at sub-district level.

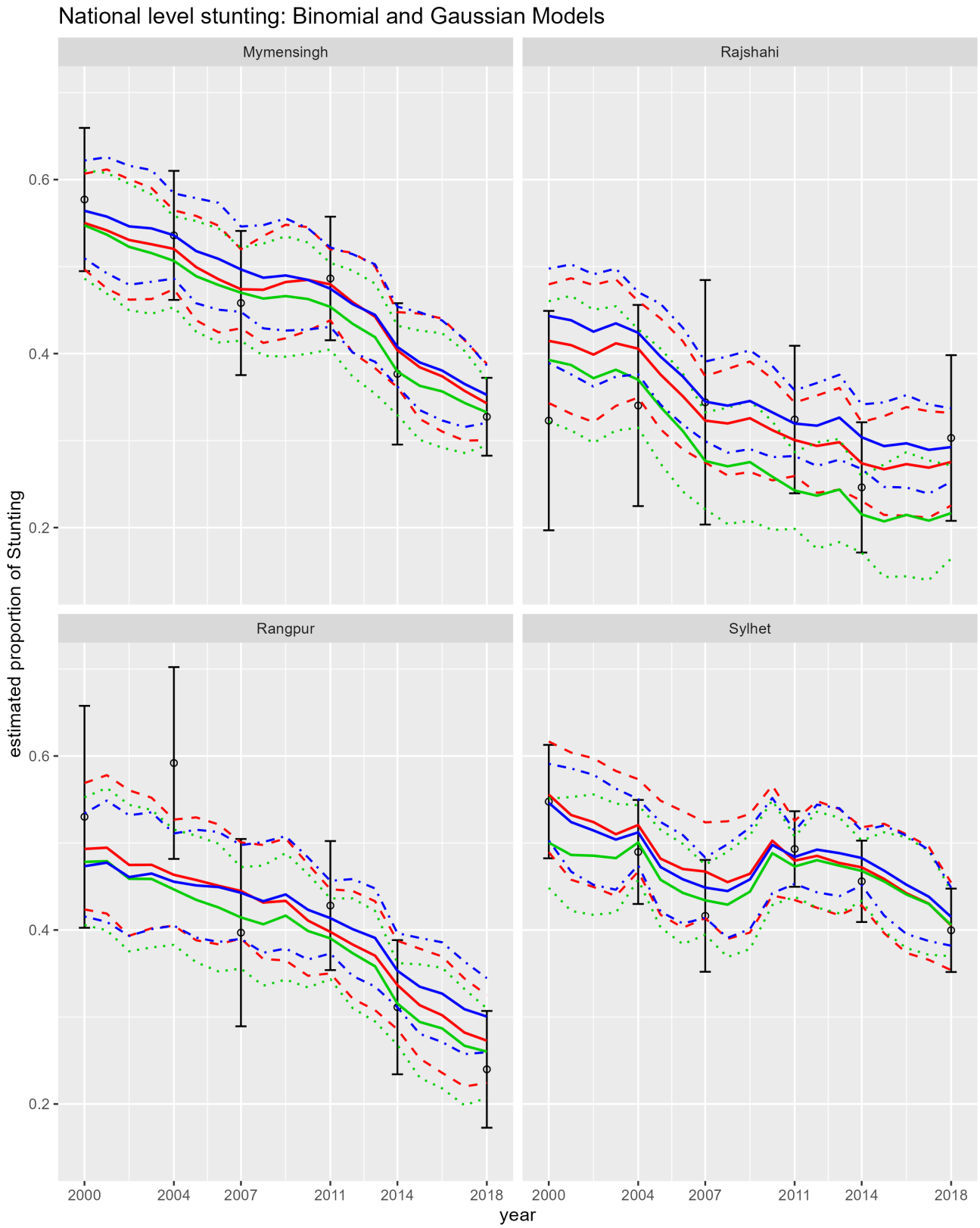


Figure S.6.138: Comparison of binomial and Gaussian based multilevel time-series models developed at the sub-district level. Trends of stunting for Mymensingh, Rajshahi, Rangpur and Sylhet districts during 2000-2018 by DIR estimator (black error-bar line), binomial based MTS-3 model (red line), Gaussian based MTS-4 model on original scale (green line) and Gaussian based MTS-5 model (red line) on square-root scale with their 95% confidence bands. Models are developed at sub-district level.

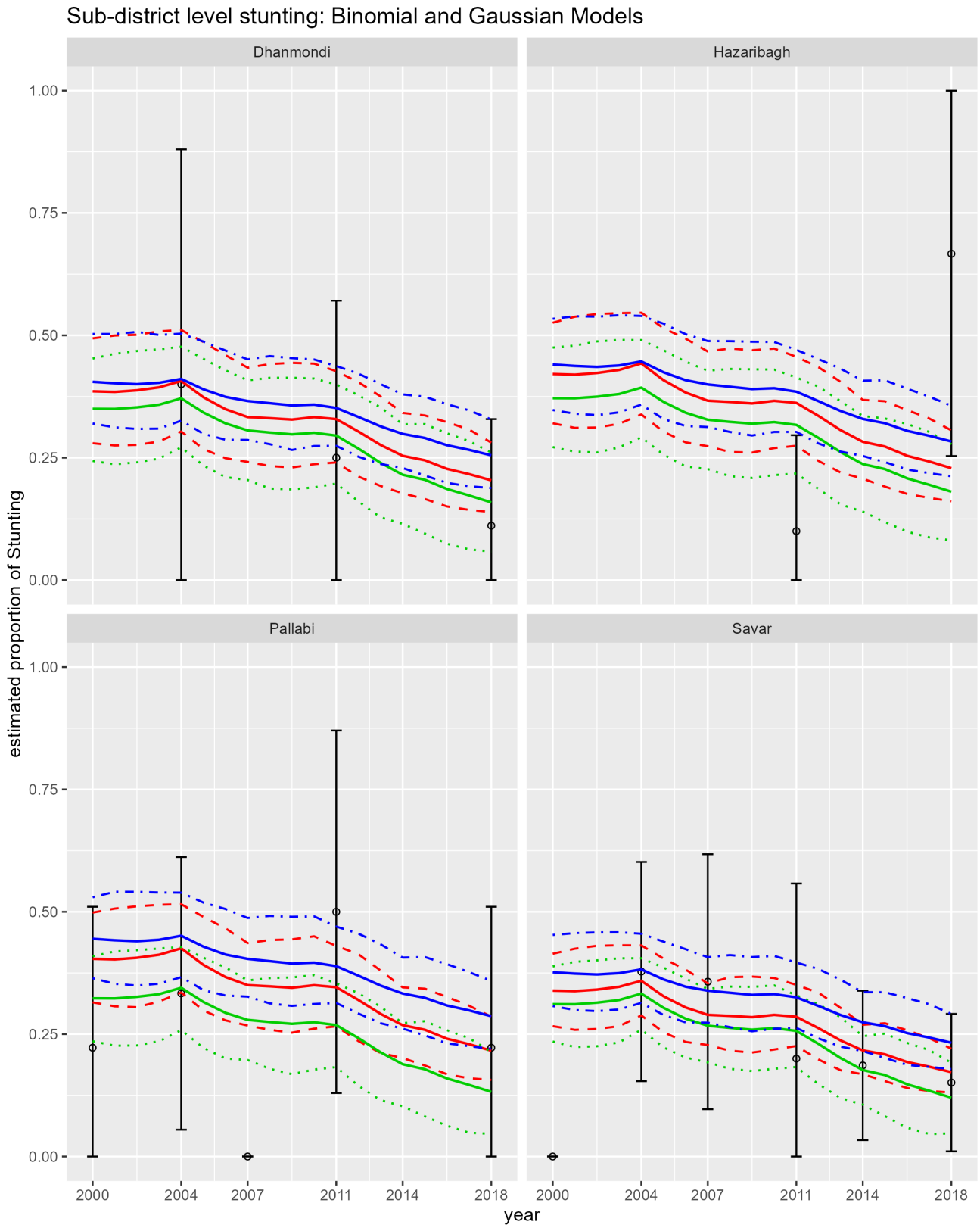


Figure S.6.139: Comparison of binomial and Gaussian based multilevel time-series models developed at the sub-district level. Sub-district level trends of stunting for four sub-districts under Dhaka district during 2000-2018 by DIR estimator (black error-bar line), binomial based MTS-3 model (red line), Gaussian based MTS-4 model on original scale (green line) and Gaussian based MTS-5 model (red line) on square-root scale with their 95% confidence bands. Models are developed at sub-district level.

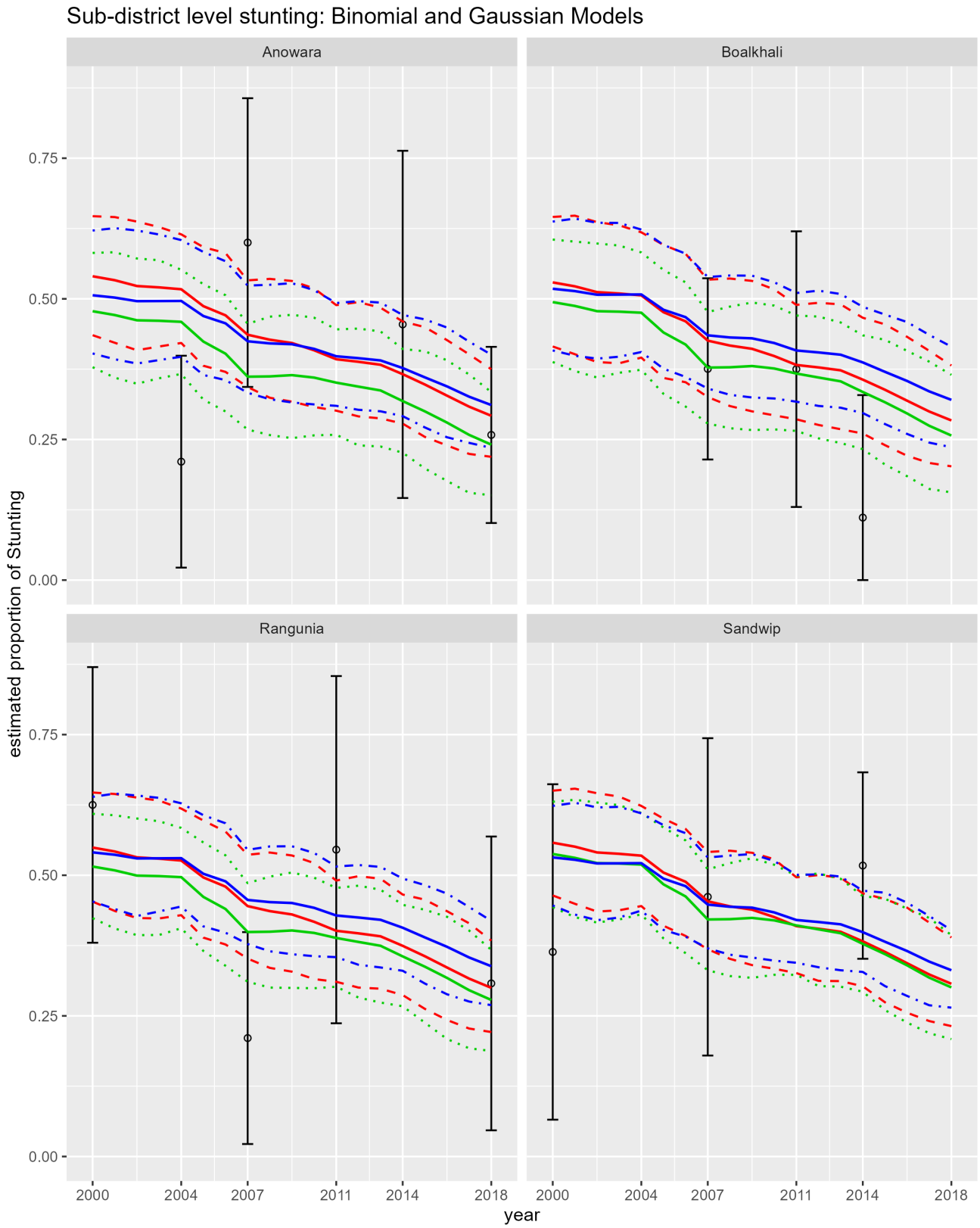


Figure S.6.140: Comparison of binomial and Gaussian based multilevel time-series models developed at the sub-district level. Sub-district level trends of stunting for four sub-districts under Chittagong district during 2000-2018 by DIR estimator (black error-bar line), binomial based MTS-3 model (red line), Gaussian based MTS-4 model on original scale (green line) and Gaussian based MTS-5 model (red line) on square-root scale with their 95% confidence bands. Models are developed at sub-district level.

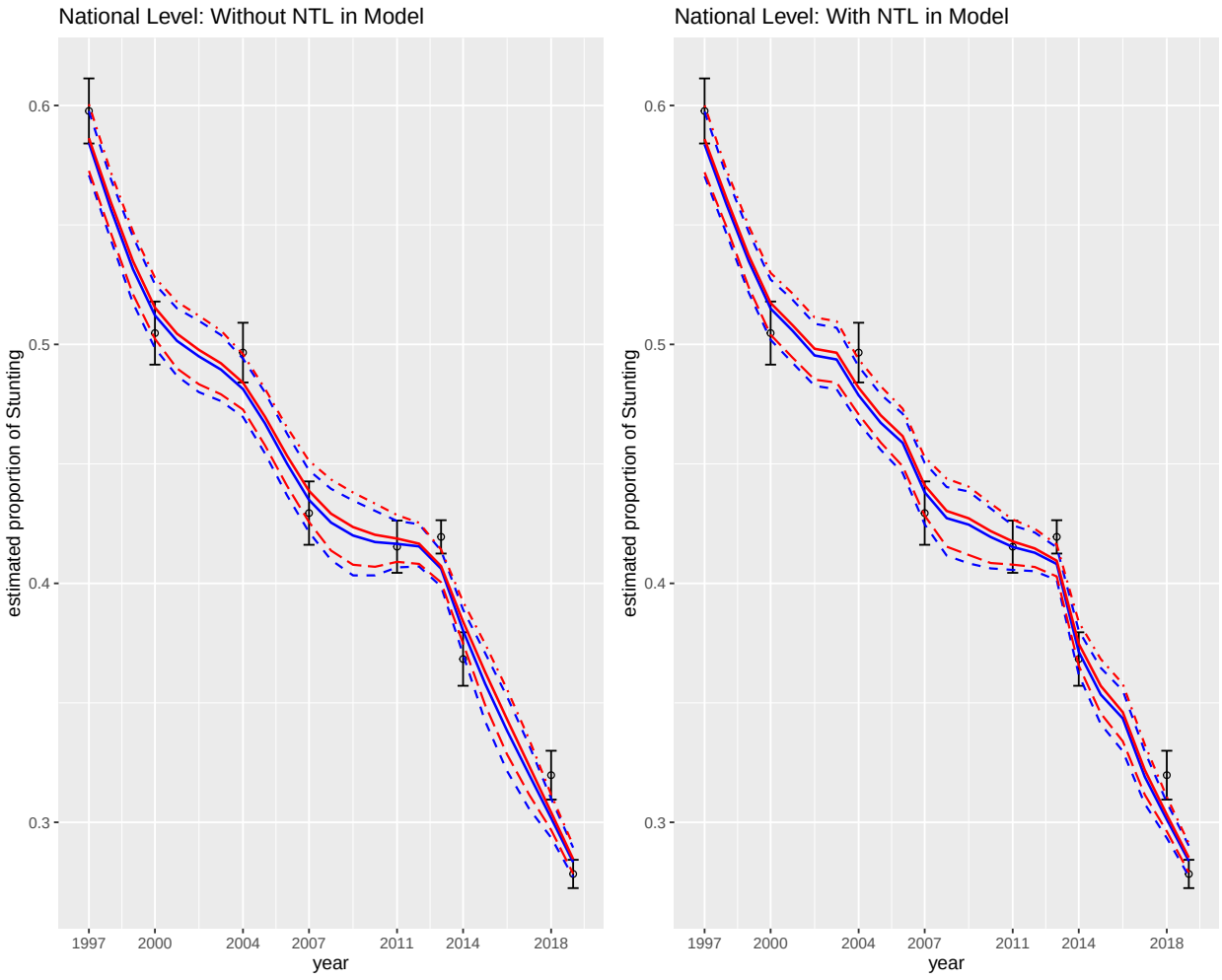


Figure S.6.141: Comparison of binomial and Gaussian based multilevel time-series models developed at the district level. National level trends of stunting during 1997-2019 by DIR estimator (black error-bar line), binomial based model (red line) and Gaussian based model on original scale (blue line) with their 95% confidence bands.

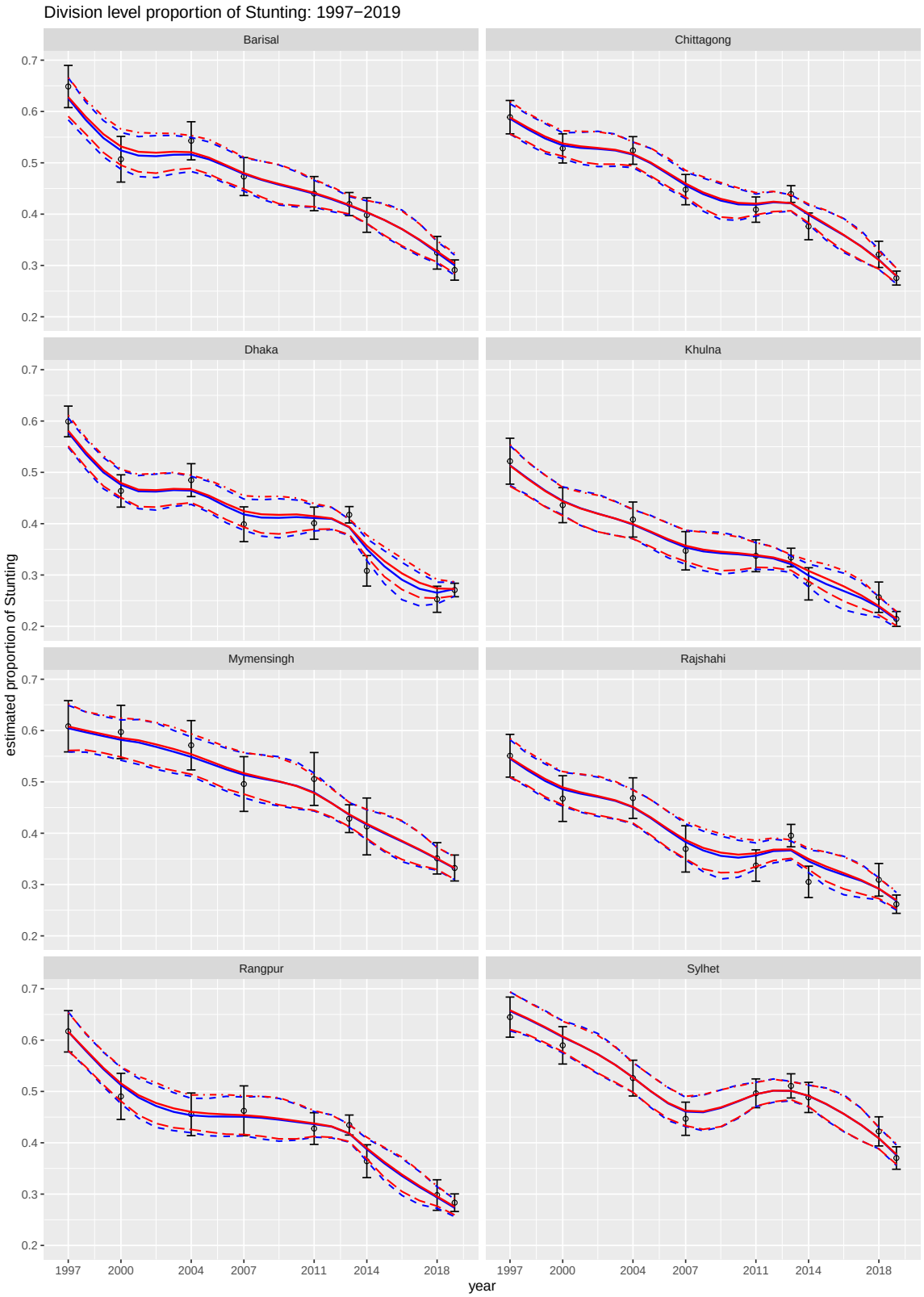


Figure S.6.142: Comparison of binomial and Gaussian based multilevel time-series models developed at the district level. Division level trends of stunting during 1997-2019 by DIR estimator (black error-bar line), binomial based model (red line) and Gaussian based model on original scale (blue line) with their 95% confidence bands.

References

Das, S., B. Baffour, S. A. Basher, P. Godwin, A. Richardson, and S. Rashid (November, 2022). Trend estimation of child undernutrition indicator at micro-level administrative units in Bangladesh using remote-sensed night-time lights data. 22nd Australian Population Association Conference 2022.

Das, S., B. Baffour, and A. Richardson (2023). Trends in chronic childhood undernutrition in bangladesh for small domains. *Population Studies*, 1–19.

Du, L., Q. Tian, T. Yu, Q. Meng, T. Jancso, P. Udvardy, and Y. Huang (2013). A comprehensive drought monitoring method integrating modis and trmm data. *International Journal of Applied Earth Observation and Geoinformation 23*, 245–253.

Gabry, J., T. Mahr, P.-C. Bürkner, M. Modrák, M. Barrett, F. Weber, E. C. Sroka, and A. Vehtari (2022). *bayesplot: Plotting for Bayesian Models*. R package version 1.9.0.

Gabry, J., D. Simpson, A. Vehtari, M. Betancourt, and A. Gelman (2019). Visualization in Bayesian workflow. *Journal of the Royal Statistical Society A 182*, 389–402.

Gelman, A., J. B. Carlin, H. S. Stern, D. B. Dunson, A. Vehtari, and D. B. Rubin (2013). *Bayesian data analysis*. Chapman and Hall/CRC. Third edition.

Jain, S. K., R. Keshri, A. Goswami, A. Sarkar, and A. Chaudhry (2009). Identification of drought-vulnerable areas using noaa avhrr data. *International Journal of Remote Sensing 30*(10), 2653–2668.

Kogan, F. N. (1995). Droughts of the late 1980s in the united states as derived from noaa polar-orbiting satellite data. *Bulletin of the American Meteorological Society 76*(5), 655–668.

NIPORT and ICF (2020). Bangladesh Demographic and Health Survey 2017-18. Technical report, National Institute of Population Research and Training (NIPORT), and ICF.